Contract Number: 622177

Deliverable D3.1

Synthesis report on relevant monitoring technologies for repository

Work Package 3, Task 1

Project Acronym	Modern2020
Project Title	Development and Demonstration of Monitoring Strategies and Technologies for Geological Disposal
Start date of project	01/06/2015
Duration	48 Months
Lead Beneficiary	AMBERG
Contributor(s)	*AMBERG, NRG, VTT, ANDRA, ETH Zurich and IRSN*
Contractual Delivery Date	May 2019
Actual Delivery Date	27/07/2019
Reporting period 3:	01/06/2018 to 31/05/2019
Version	2

Project co-funded by the European Commission under the Euratom Research and Training Programme on Nuclear Energy within the Horizon 2020 Framework Programme		
Dissemination Level		
PU	Public	X
PP	Restricted to other programme participants (including the Commission Services)	
RE	Restricted to a group specified by the partners of the Modern2020 project	
CO	Confidential, only for partners of the Modern2020 project and EC	

History chart			
Type of revision	Document name	Partner	Date
First set-up	*Modern2020_WP3_D3.1_Final Report_v0.docx*	AMBERG	24.12.2018
Chapter T3.5	*Modern2020_WP_D3.1_Final Report_V1_T3.5.docx*	AMBERG	16.01.2019
Chapter T3.6	*Modern2020_WP_D3.1_Final Report_V1_T3.6.docx*	AMBERG	17.01.2019
Revised Chapter T3.6	*Modern2020_WP_D3.1_Final Report_V1_T3.6.docx*	IRSN	18.01.2019
Revised Chapter T3.2	*Modern2020_WP_D3.1_Final Report_V1_T3.2docx*	NRG	27.03.2019
Revised Chapter T3.5	*Modern2020_WP_D3.1_Final Report_V1_T3.5.docx*	ETH Zurich	28.03.2019
Revised Chapter T3.3	*Modern2020_WP_D3.1_Final Report_V1_T3.3.docx*	VTT	25.06.2019
Revised Chapter T3.4	*Modern2020_WP_D3.1_Final Report_V1_T3.4.docx*	Andra	28.06.2019
Final version	*Modern2020_WP3_D3.1_Final Report_vf.docx*	AMBERG	27.07.2019

Abstract

Monitoring was identified in previous MoDeRn project ([1]) as a multi-purpose tool –including many objectives and activities-for a radioactive waste management programme. Besides, it helped to recognise several limitations of the available technology that should be improved. The following project, Modern2020, were 21 partners out of 30 were involved in several R&D activities to overcome such limitations (WP3), has provided very good results regarding wireless data transmission through engineered barriers with different frequencies and distances, alternative power sources focused on wireless sensor units, development of new in-situ sensors tailored to geological disposal including different types of FO solutions, the improvement of non-invasive monitoring based on geophysical techniques, and the development of a methodology for qualifying the components of the monitoring system. Although the progress was excellent, further perfections are foreseen, such as qualifying of obtained solutions for wireless transmission, integration and verification of the energy sourcing parts to improve the energy efficiency, the long-term reliability of FO based sensors, etc. This report gives an overview of the research carried out in WP3 of the European project Modern2020 and of the challenges that remain to accomplish the monitoring of the future nuclear waste repository. A more detailed description of the results can be found in Modern2020 deliverables D3.2, D3.3, D3.4, D3.5 and D3.6.

Table of content

List of Figures

List of Tables

Glossary

ADC	Analog-to-Digital Converter
AISG	Antenna interface standards group
BPSK	Binary Phase Shift Keying
CCA	Circuit-Card Assembly
DFT	Discreet Fourier Transformation
EBS	Engineered Barrier System
ERT	Electric Resistance Tomography
FFT	Fast Fourier Transformation
GBM	Granular Bentonite-sand Mixture
HFW	High Frequency Wireless
HLW	High-Level Waste
LF	Low Frequency
ISM	Industrial, Scientific and Medication
LNA	Low Noise Amplifier
LTRBM	Long-Term Rock Buffer Monitoring demonstrator
LVDT	Linear Variable Displacement Transducer
MB	Main borehole
MF	Medium frequency
PA	Power Amplifier
QPSK	Quaternary Phase Shift Keying
R&D	Research and Development
RF	Radio frequency
SD	Secure Digital memory card
SDR	Software-Defined Radio
TTE	Through-the-Earth
UPS	Uninterruptible Power Supply
URL	Underground Research Laboratory
VLF	Very low frequency
WMO	Waste Management Organisation
WP	Work Package
WSU	Wireless Sensor Unit
WTB	Wireless Testing Bench

1 Introduction

1.1 Modern2020 project structure

The EU H2020 project Modern2020, as a continuation of the former MoDeRn project [1], deals with the Development and Demonstration of Monitoring Strategies and Technologies for Geological Disposal and is jointly funded by the Euratom research and training programme 2014-2018 and European nuclear waste management organisations (WMOs). The Project is running from June 2015 to May 2019, and a total of 29 WMOs and research and consultancy organisations from 12 countries are participating.

The overall aim of the Modern2020 Project is to provide the means for developing and implementing an effective and efficient repository monitoring programme, taking into account requirements of specific national programmes on geological disposal.

The Project is divided in six Work Packages (WPs):

- WP1: Coordination and project management.
- WP2: Monitoring programme design basis, monitoring strategies and decision making. This WP aims to define the requirements of monitoring systems in terms of the parameters to be monitored in repository monitoring programmes with explicit links to the safety case and the wider scientific programme (see below).
- WP3: Research and development of relevant monitoring technologies, including wireless data transmission systems, new sensors, and geophysical methods. This WP will also assess the readiness levels of relevant technologies and will establish a common methodology for qualifying the elements of the monitoring system intended for repository use.
- WP4: Demonstration of implementing monitoring programmes, and related technologies and systems in repository-like conditions. The intended demonstrators, each one addressing a range of monitoring-related objectives, are the Full-scale in situ System Test in Finland, the Highly-Active (HA) Industrial Pilot Experiment in France, the Long-Term Rock Buffer Monitoring (LTRBM) Experiment in France, and the Full-scale Emplacement (FE) Experiment in Switzerland. An assessment and synthesis of several other tests and demonstrators will also be undertaken.
- WP5: Effectively engaging local citizen stakeholders in research and development (R&D) and research, development and demonstration (RD&D) on monitoring for geological disposal.
- WP6: Communication and dissemination, including an international conference, a training school, and the Modern2020 Synthesis Report.

1.2 Background: state of art on Monitoring Technology-MoDeRn Project (2009-2013)

Work on technology has the ambition of moving the state-of-the-art in innovative repository monitoring techniques from the proof of feasibility stage to the technology development and demonstration phase.

An important effort has been made to elaborate a state of art on Monitoring technology in previous MoDeRn Project (2009-2013) in a comprehensive way (see Modern D2.2.2).

The Modern D2.2.2 document serves as the basis to elaborate a framework programme for developing suitable technologies for the geological disposal purposes.

1.3 Objectives of WP3

During the previous MoDeRn Project (2009-2013), monitoring was identified as a tool capable of encompassing many different objectives and activities within a radioactive waste management programme. However, the focus was clearly set on repository monitoring, in particular the monitoring of the near field to check the assumptions in the long-term safety case and to support decision making. MoDeRn provided a first boost for the development and analysis of the capabilities of monitoring technologies for nuclear waste repository in different fields such as: existing measurement probes and methods, data transmission capabilities and energy supply options.

Research and development made in MoDeRn demonstrated that technologies are available for monitoring the near-field but with evident limitations, which need to be addressed before repository monitoring commences. These include the adaptation of the technologies to specific monitoring objectives, host rocks and repository concepts, for the monitoring of specific parameters, and improvement of the long-term performance.

As a result, these gaps in the existing technology were identified and prioritized [1] as the main objectives for Modern2020 project:

- To improve wireless monitoring technology including the combination of high-frequency and low-frequency systems, task 3.2.
- To research on alternative power supplies, task 3.3.
- To develop new sensors based on optical fibre, low-intrusive techniques including sensors to monitor water content and water chemistry, pH and irradiation, task 3.4.
- To refine and further improve the most promising geophysical methods for non-intrusive monitoring, task 3.5.
- To establish a common methodology for qualifying the components of the monitoring system, task 3.6

1.4 Scope of this report

This deliverable represents the final technical report of the Modern2020 project's WP3, Research and development of relevant monitoring technologies. It was done as conclusion of Task 3.1, *Readiness level of monitoring technologies* and synthetizes the progress achieved by all partners contributing to the WP3 R&D activities. This report aims to support the evaluation of the readiness level of all the investigated technologies (tasks 3.2 to 3.6). It presents the innovative technical sheet use during the interaction with the public stakeholders.

The report integrates contributions from Amberg, NRG, VTT, Andra, ETH Zurich and IRSN and is prepared and compiled by Amberg.

1.5 Structure of this report

The reminder of this report is set out as follows:

- Chapter 2: shows the management structure to coordinate the R&D activities in the Modern2020 project
- Chapter 3 provides a synthesis of the activities performed and the results gathered for each research line.
- Chapter 4: studies the Technology Readiness Levels
- Chapter 5 summarises the overall results and conclusions.
- Appendixes are included in Chapter 6 and references in Chapter 7.

2 WP3 Management structure

The activities addressed to improve the technical feasibility of the repository monitoring were very challenging and complex. Up to 21 of the 29 partners of the project were involved in the different tasks and up to 44% of the overall resources were devoted to this mission. The amount of work and the number of participants made necessary to implement a specific organisation and procedures to guarantee an efficient development (see Figure 1).

As shown in Figure 1, six main tasks were run in parallel to acomplish the objectives identified at the project start-up. Task 3.2 to 3.6 were directly linked with the listed objectives (section 2). Task 3.1 was a transversal one devoted to coordinate all activities both from the technical point of view and the required reporting. Besides, Task 3.1 was in charge of doing the required coordination and communication with remaining WPs of the project and finally, of providing the final report including an evaluation of the readiness level of all the investigated technologies.

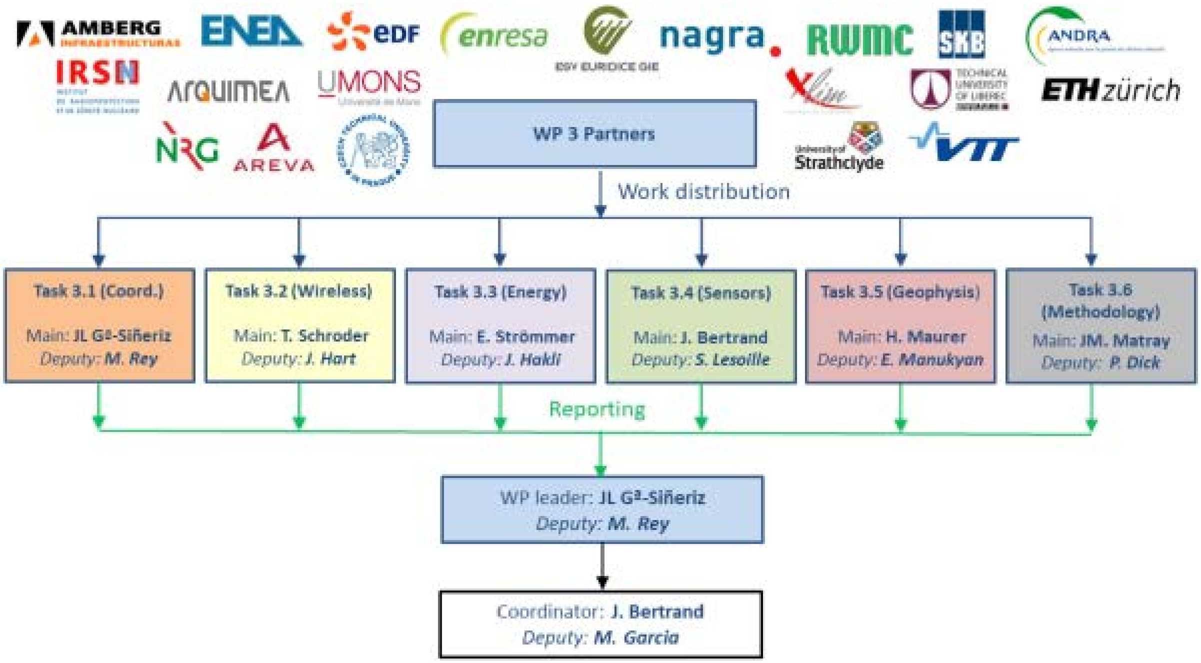

Figure 1. Organization chart of WP3 showing all the involved partners and distribution of work

3 Status of Monitoring Technologies

3.1 Wireless data transmission systems

3.1.1 Introduction: principles and current status

Modern2020's Task 3.2, which is further elaborated in this chapter, is related to wireless data transmission systems that allow the transmission of monitoring data over engineered and natural barriers without the use of wires: wired solution may impair the safety function of the barriers. The barriers of interest could be anything from the concrete buffer of a supercontainer design, a borehole plug, sealings of disposal sections or a shaft sealing, i.e. wireless solutions are necessary that can bridge distances between less than a meter up to several hundred meters. While wireless communication is nowadays used in many industrial and consumer applications, the specific challenge for the application of wireless techniques in repository monitoring lies in the strong attenuation of high-frequency radio waves by the host rock or components of the engineered barrier system (EBS).

Generally, it can be distinguished between short range (up to 10 m) and medium to long range wireless techniques (>10 m to several hundreds of meters). An important performance figure for wireless solutions is their energy need, certainly for the long distance. The current research initiatives in WP3.2 are directed to understand and develop the energy efficiency further by extending and improving the energy efficiency of existing solutions. Different options for the supply of power are addressed in Chapter 3.2.

Task 3.2 is divided into three subtasks, with different scopes:

- **Subtask 1** is related to improvements of existing short range (tens of meters) wireless systems based on high or medium frequencies
- **Subtask 2** is related to improvements of existing long range (hundreds of meters) wireless systems based on low frequencies
- **Subtask 3** is related to the integration of wireless systems with sensors or other wireless systems to provide complete solutions.

In the next sections, the principles and current status of wireless data transmission are presented, and the contributions to these three subtasks are summarized.

3.1.1.1 Principles of wireless data transmission

While the receiver antenna's efficiency is increasing with frequency, higher frequencies can also result in an increasing attenuation of magnetic fields during propagation through the EBS or host rock. The optimum transmission frequency is thus dependent on the transmission frequency and the electrical conductivity of the medium [2], 7.1.1, and to provide an optimum solution for each application case, interactions with the medium need to be understood.

A simple concept that allows making first estimations on the principal relevance of interactions with the geologic medium is the so-called *skin depth* that defines the distance, at which a signal is attenuated by a factor of $1/e$, equivalent to 8.7 dB ([3], [4], 7.1.1). The skin depth for a good conducting medium in the absence of paramagnetic materials can be calculated by

$$\delta[m] = \frac{1}{\sqrt{\pi \cdot f \cdot \sigma \cdot \mu_0}}$$

With

μ_0 permeability constant ($1.257 \cdot 10^{-6}$ V·s/A·m)

The electrical conductivity σ of geological media can vary to a large extent, from µS/m to mS/m range for crystalline rock, and mS/m to S/m range for argillaceous rock [5] , 7.1.1. The water-filled porosity of the geological media or EBS component has an important influence on the conductivity, as well as the pore water composition. The electric conductivity of fresh water is about 10 mS/m to 1 S/m, and the conductivity of saline water can be as high as 1 – 10 S/m. Table 1 gives some example values for the skin depth at different frequencies and electrical conductivities.

Table 1. Skin depth as function of electrical conductivity and transmission frequency

Skin depth δ [m]						
	Electrical conductivity σ [mS/m]					
	1	5	10	50	100	1000
1000 Hz	503	225	159	71	50	16
2500 Hz	318	142	101	45	32	10
5000 Hz	225	101	71	32	23	7

Because for lower frequencies an electric antenna is too inefficient, most contributions to this task make use of magnetic fields generated by a *magnetic loop antenna*.

3.1.1.2 Current status of wireless technologies in repository monitoring

A general overview on the state-of-the-art of wireless systems and its main applications is given in [6]. Table 2 summarizes successful data transmission experiments in URLs under conditions relevant for underground disposal of radioactive waste. In addition to the data transmission experiments, a number of long range signal transmission experiments has been performed, e.g. experiments by MISL who performed measurements through 225 m of Boom Clay and saturated sandy aquifer at the HADES URL [6], 7.1.1 and through 80 m of granite and 100 - 250 m of access tunnel at the Grimsel URL [6], or by Andra who demonstrated signal transmission through 275 m of limestone and shales at the Tournemire URL and over 300 m in a surface-surface configuration at the Tournemire URL and the Andra URL.

Table 2. Overview on current experiments on wireless data transmission in URLs

Distance	Transmission mode	Frequency	Host rock/barrier (location)	Organization
0.1 m	Resonant cavity antenna	2.4GHz	Concrete buffer	EURIDICE
4 m	Electric dipole antenna	169 MHz	Bentonite/shotcrete (Grimsel URL)	AITEMIN
4 - 6 m	λ/4 loop antenna	2.2 MHz	(Partially) saturated bentonite (Tournemire URL)	Arquimea
5 - 10 m	Magnetic loop antenna	8.5 kHz	(Partially) saturated bentonite (Tournemire URL)	Andra
23 m	Magnetic loop antenna	125 kHz	Granite + Air (Espoo research hall)	VTT
25 m	Magnetic loop antenna	8.5 kHz	Sedimentary rock (Meuse/Haute Marne URL)	RWMC/Andra
30 m	Magnetic loop antenna	4.0 kHz	(Partially) saturated bentonite (Tournemire URL)	Amberg
30 m	Magnetic loop antenna	575 Hz	Bentonite/shotcrete (Grimsel URL)	MISL
225 m	Magnetic loop antenna	1.8 kHz.	Boom Clay & saturated sandy aquifer (Hades URL)	NRG
250 m	Magnetic loop antenna/relay system	8.5 kHz	Sedimentary rock (Horonobe URL)	RWMC
275 m	Magnetic loop antenna	8.7 kHz	Limestone & Shale (Tournemire URL)	NRG

Since high frequencies lead to high signal attenuation when transmitting through a (partially) saturated barrier, all current wireless techniques, except for very short distances (<1 m) make use of the very low frequency (VLF) to – medium frequency (MF) range (4 KHz to 2.2 MHz).

For long range data transmission, frequencies below 10 kHz are used, although under unsaturated conditions as present in e.g. the Tournemire URL, higher transmission frequencies may be applied as well.

In summary, in MoDeRn, Modern2020 and few other occasions, successful data transmission has been demonstrated under realistic conditions on distances between less than a meter and about 300 m, and six of the application cases in Table 2 that are developed in Modern2020 are summarized in the next chapters. Experiments were performed in relevant environments, in order to account for interactions with the host rock or EBS of interest. The overall performances achieved by the different data transmission systems (data rate, energy need) will be presented in the next chapters, and are summarized in the overall conclusions.

3.1.2 Short range systems

3.1.2.1 Implementation of a Wireless Testing Bench (WTB)

A Wireless Testing Bench (WTB) was implemented by Aitemin, ENRESA and IRSN in 2016 in IRSN's Underground Research Laboratory (URL) in Tournemire in the South of France (Aveyron) to provide the possibility of evaluating signal transmission parameters from different wireless technologies for data transmission (short- and long-range radio) under representative in situ conditions. A brief description of the Tournemire site is given in Section 3.1.4.3.

The WTB is composed of:

- A main horizontal borehole (MB) measuring 60 cm in diameter and 10.13 m in length (Figure 2)
- A bentonite buffer at the rear end of the MB, measuring 4.52 m in length. It is divided in two segments by a cemented resin plate in between:
  - A 2.3 m long segment at the rear end of the MB, filled with a Granular Bentonite-sand Mixture (GBM – 75 % sand and 25% bentonite), with a dry density of 1.34 g/cm^3.
  - A 2.19 m long segment at the front end filled with 13 layers of highly compacted blocks made of a MX80 bentonite/sand mixture in a ratio of 60/40, and one layer made of pure bentonite blocks.
- An artificial hydration system composed of three circular shaped sections of geotextile hydration mats, to accelerate buffer saturation.
- A 2.58 m long cement plug confining the bentonite buffer.
- Three perpendicular access boreholes, located respectively at the rear end, middle section and front end of the buffer, to insert wireless units into the buffer.

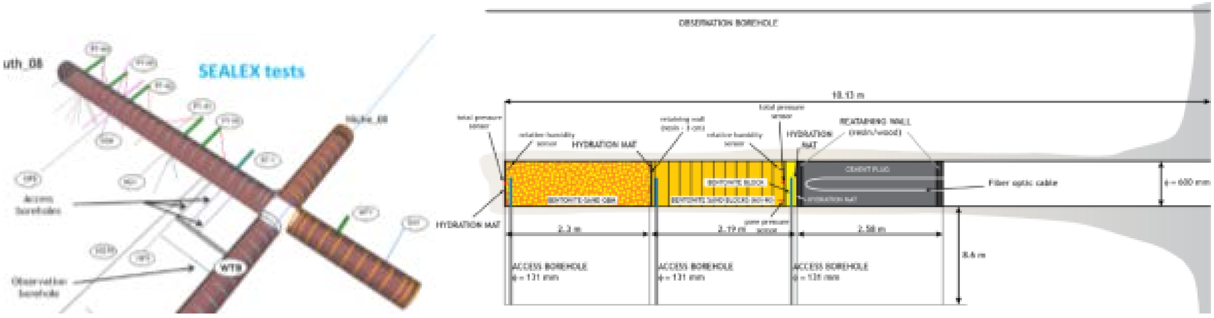

Figure 2. Location and layout of WTB facility

The buffer and the cement plug are instrumented with wired sensors so to measure: total pressure, pore pressure and relative humidity in the buffer; and displacement, deformation and temperature at the cement plug. Water inflow is measured too.

Tests have been carried out in the WTB by Arquimea, Amberg and Andra, as described in this chapter and in section 3.1.4.1.

3.1.2.2 Data transmission at 2.2 MHz

Experimental set-up & testing

The first series of tests was performed in the WTB facility during 2015 before the installation of the buffer material ("clean site") to assess the optimum frequency range. Measurements were done by placing a transmitter and a receptor node at different depths in the rear and front access boreholes, respectively. Based on the analysis of the results a frequency band around 1.8 MHz was initially selected.

After the selection of the frequency band, Arquimea designed a new wireless communication module *ad-hoc* based on the technology used in AISG standard compliant on and off keying modem transceiver working at 2.2 MHz).

The new developed transceiver was first tested in Arquimea installations, by transmitting through air with several antenna types and amplifiers. Those components providing the best results regarding both transmission power and low consumption were selected.

Then a first campaign of tests was performed in the WTB at Tournemire during June 2017, when the buffer material was already in place, to confirm the results obtained through air by combining antennas and amplifiers. The transmitter was placed at different depths into the three access boreholes, and the receiver was placed in the mouth of the main borehole. It was possible to establish a radio link between access boreholes, but not from one access borehole to the mouth of the main borehole through the buffer. As a result, a "T" λ/4 antenna was selected, it was stated the need to use an intermediate node to act as a repeater, and to redesign the amplification stage.

After implementing the changes, a second test campaign was performed in Tournemire between end of 2017 and beginning of 2018, to evaluate the influence of the buffer hydration on the transmission parameters. For this campaign, a transmitter was buried in the bentonite buffer (Figure 3), emitting 2.2 MHz. As receiver, a software-defined radio (SDR) connected to a PC took several samples daily during the beginning of the hydration period.

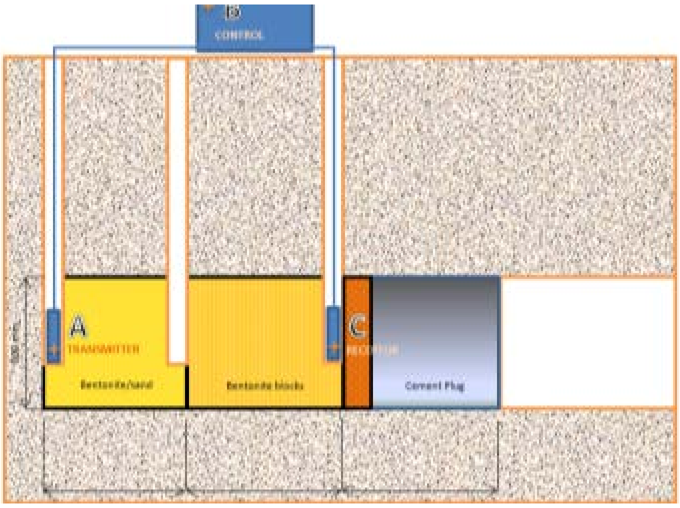

Figure 3. Test configuration at WTB during hydration phase

It was found that during the first month, the hydration did not influence the transmission between nodes in an appreciable way, with differences below 5 dB.

Final design

Results from the second test campaign were used to validate the design of the prototype to be installed at LTRBM, with two modifications:

- Instead of using two antennas with different impedances for transmitting and receiving, to reduce the node dimensions it was decided to share one single antenna for both functions, with an impedance adaptor.
- Instead of using an air core, the antenna features a nylon core, to withstand the external pressure without affecting the transmission frequency, as nylon is inert in this sense (Figure 4).

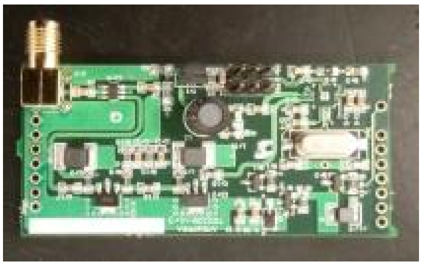 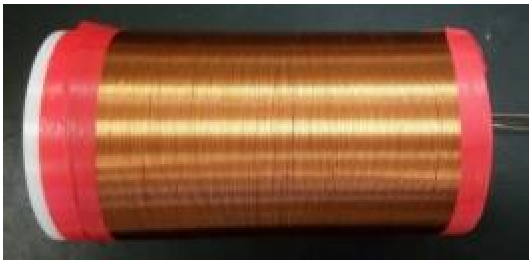

Figure 4. Final RF module (left) and final antenna configuration with nylon core (right)

Energy consumption is around 1.8 J per data transmission, with a current of 400 mA, and a consumption of 0.001 mA in inactive mode, so the total system consumption is determined by the number and type of sensors connected to the WSU.

Conclusion

A new improved WSU system has been developed for testing in the LTRBM demonstrator. It is versatile and can be produced at a reasonable price. The main challenges involved understanding the transmission attenuation physics, the limitation on power availability and the integration of the device. Potential improvements could be focused on size reduction, fabrication procedure and energy management optimisation.

3.1.2.3 Data transmission at 125 kHz

VTT Technical Research Centre of Finland Ltd has developed short to medium range wireless sensor data communication based on magnetic inductive coupling between two coils, which has been already tested for obtaining sensor data wirelessly at 125 kHz from inside bioleaching heaps of nickel ore. The system has been adapted for the engineered barrier materials used inside radioactive waste repositories with novel hardware for enhanced capabilities. The objective of VTT's contribution to Modern2020 was to develop an optimal approach to solve the short distance underground communication problem with state-of-the-art low cost commercial technology based on magnetic inductive coupling between the transmitter and receiver coils.

The operating frequency of 125 kHz was chosen as a compromise to have low electrical losses with reasonable coupling and to have a reasonable bandwidth available for frequency modulated signals (~1-2 kHz). As an Industrial, Scientific and Medication (ISM) frequency band it is free to use for wireless sensor data transfer, and electrical components are also readily available.

To achieve a longer transmission range, new methods were needed to overcome the distance and frequency induced limitations. The hardware was developed with carefully chosen and matched low noise preamplifiers and high-performance AD-converters together with three tone frequency modulation method and Fourier transform mathematics.

Developed Hardware

The setup used a 3 m x 3 m loop antenna in the transmitter side and a two-stage low noise amplifier was matched to the receiving coil impedance at 125 kHz with a capacitor. The receiving coil is a five-turn rectangular loop antenna of 3 m x 3 m in dimension and with 0.45 mm wire diameter. The self-resonance frequency of the coil is about 530 kHz and the unloaded Q-value approximately 44. After the amplifiers the signal is multiplied with two analogue multipliers in quadrature phase. Afterwards the signal is filtered with low pass filters, and then an AD-conversion is performed, and data is collected to the internal double-buffered storage of the processor with interrupt-controlled hardware and direct DMA-transfer all the way to the final storage in the system controller, Raspberry Pi 3. Figure 5 shows the hardware of the current reception setup.

Transmitter side modulation is accomplished by phase modulation of the 125 kHz carrier. A three tone modulation is used (bit zero tone, bit one tone and end-of-bit tone). Modulation is performed as a linear ramp of phase. Phase is shifted from 0° to 180° in one tone by delaying the start of a new cycle of the carrier by one clock pulse in the transmitting microcontroller. The value of the bit is determined by the rate at which the phase changes. The base-band signal is in the 1 kHz range with tones of a few tens of Hertz. Bit length in time is in the order of one second.

Measuring the frequency components of the signal instead of the amplitude, which is commonly used in FM radios, is one way to improve signal to noise ratio, as it offers several orders of magnitude higher dynamic range than amplitude measurements. In low power transmission and reception of weak signals, however, large modulation depths may be a problem if the signal has a small bandwidth due to the relatively high Q-value of the receiving coil. This issue can be solved by using phase modulation, which is close to frequency modulation. In the current study frequency shift keying (FSK) with small modulation depth was used.

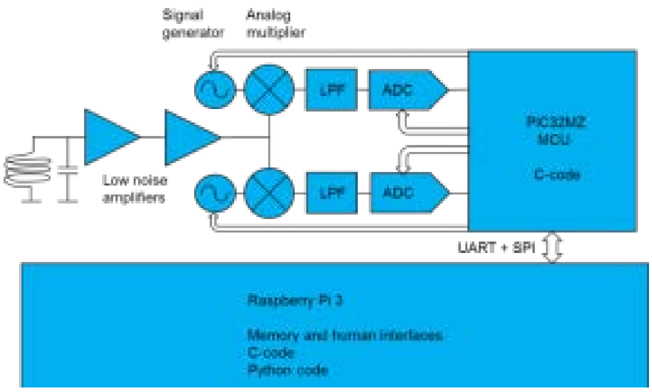

Figure 5. Block diagram of the receiver electronics. The receiver coil in the final setup is tuned in series with the capacitor

A Fourier transform of the gathered data is used for decoding the received signal into spectral frequency and tone components, further enhancing the signal-to-noise ratio. In the tests, the whole 10 kHz wide bin structure was used for the Fourier transform.

The transfer path was demonstrated in VTT's Otaniemi Research Hall I in Espoo, Finland, in November 2017. A transmission distance of 23 m including 15 m of rock was achieved there. In the Otaniemi demonstration the available space together with the metallic structures restricted the transmission range.

Results

Underground data transmission over a distance of 23 m including 15 m of rock has been achieved with a frequency of 125 kHz and a data rate of about 1 bit/s. The demonstration was held in VTT's Otaniemi Research Hall I in Espoo, Finland, in November 2017. From the received data it could be seen that a practically error-free transmission was achieved.

Conclusion

Underground data transmission has been demonstrated over a distance of 23 m including 15 m of rock at a frequency of 125 kHz. The signal was transmitted essentially by the magnetic field coupling between transmitter and receiver coils, which is not much affected by non-metallic materials within the path. The power supply energy during transmission was 1.02 W. Energy consumed per bit was approximately 1 Ws. However, a reasonable distance of 7.3 m would still be achievable with a much smaller bit energy of 1 mWs.

The low data rate is the result of the extremely challenging radio link conditions, operating near the noise limit and needing to integrate for a longer time to receive and correctly detect the transmitted bits. This is not a significant disadvantage, not even combined with the low duty cycle, because the quantities to be monitored only change very slowly.

The developed technology is still at a demonstrational stage, having a distance to go into a prototype and a mature product. One of the problems to be solved is the automatic tuning of the antennas, as once buried the surrounding materials and metal parts will change their delicate tuning.

3.1.2.4 Data transmission at 4 kHz

Low frequency digital magnetic induction technology, so called wireless 'Through-the-Earth' or TTE, penetrates concrete, rock and other obstructions enabling communications and position determination with commercial equipment in some of the most difficult environments in the world, including: mines, caves, subways, utility tunnels, buildings, and parking garages. The objective of the work performed by Amberg was to adapt this kind of equipment to the requirements of the Modern2020 project, integrate it into a WSU, and test it under realistic conditions to asses if it could offer a valid approach for the future use in underground repository monitoring.

General set-up

The operational requirements imposed for the equipment adaptation were as follows: maximum TTE transmitter diameter of 10 cm; receiver at 10 m to 20 m (minimum) through solid rock, clay formations (argillite) and sealing materials (concrete, bentonite plugs); sensor control and power supply provided by the transmitter; low duty data transmission (one or two transmissions per day); and target lifespan of 10 years for transmitter battery.

A preliminary layout of the desired data transmission system is given by Figure 6 and the different blocks are described hereafter.

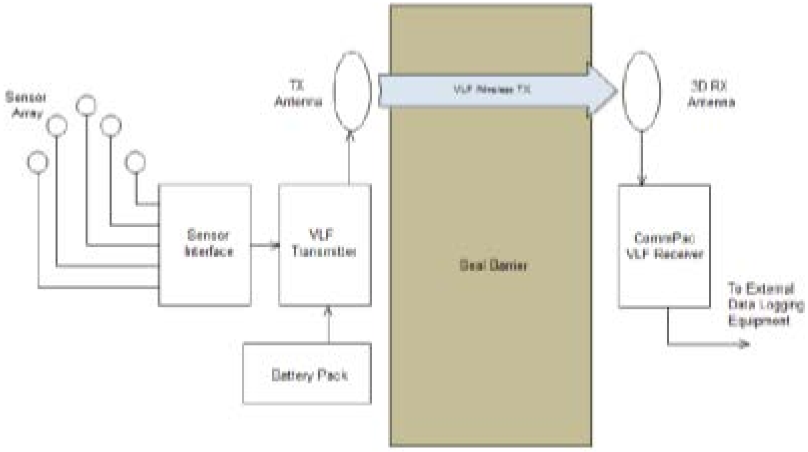

Figure 6. Preliminary layout for TTE data transmission system

The WSU allows to link a number of sensors from different manufacturers, each one with its own excitation requirement and output type (analog voltage, 0-20 mA current loop, etc.), and powered and controlled (if required) by a Sensor Interface Circuit-Card Assembly.

The transmitter antenna features a ferrite core with dimensions 19 cm x 8 cm and fits into a 9 cm diameter tube, and as receiver antenna a standard production antenna was housed in a waterproof enclosure and connected to the VLF receiver through cable and MIL connector. Each sensor's reading is converted to a standard number format and integrated into a 16 bytes data packet together with a Sensor ID and CRC bits, resulting in a full data payload of 96 bytes (768 bits) for the sensor array. The last two payloads will be always stored in the MCU non-volatile memory and will be transmitted along with the current payload so to provide transmission redundancy. The resulting total payload of 300 bytes can be transmitted over the VLF link in less than two seconds.

The TX antenna, electronics and battery of the WSU are all sealed into a single tube. The new ferrite core antenna is much smaller than air cored loop, so the length and diameter of the tube has been greatly reduced to 69 cm and 89 mm respectively. The new enclosure has a volume of 4050 cm^3.

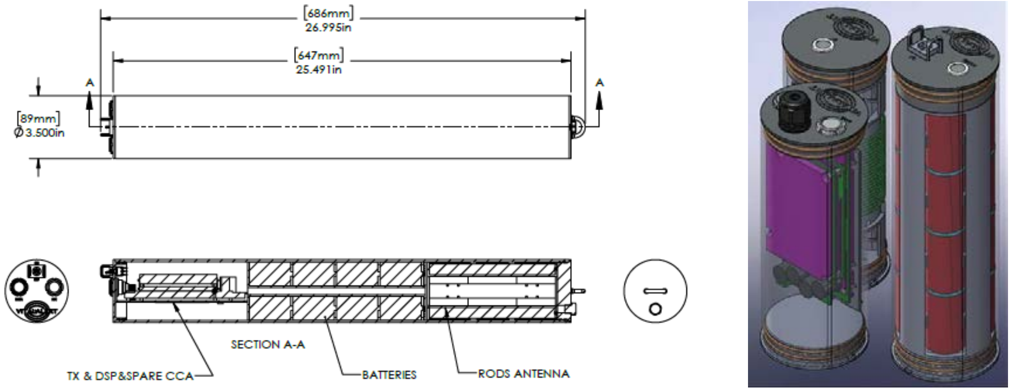

Figure 7. Proposed designs: borehole deployment (left) and repository deployment (right)

Energy budget analysis

When the transmitter is started up from sleep mode, several operations must take place: DSP processor boot; transmission of clock synchronisation frames; enabling and reading of sensors; and creation and transmission of data payload. The total time for these operations is 37 seconds.

The power consumption while the transmitter is on is 9.3 W, so the energy consumed per transmission is 96 mWh. The total energy consumed per day is therefore 107 mWh, or ~ 39.3 Wh. per year.

To provide more than 10 years operation, the power supply must have a capacity of at least 393 Wh. For this application a primary battery is required that also has a very low self-discharge rate. The best battery technology for this application is Lithium Thionyl Chloride (Li-$SOCl_2$), which is available in different commercial cell sizes with a nominal voltage of 3.6 V. A battery comprising 8 cells supplies an output voltage of 28.8V, which is at the upper range for the transmitter, where efficiency is at the highest. The main trade off in this technology is between discharge rate and current output capability (see also [10] 7.1.1).

Experimental work

A prototype of the TTE system was first tested in March 2018 at Mina Escuela Bierzo (FSB), a former underground coal mine in Leon (Spain) currently used for staff training on civil underground works. The equipment (Figure 8, top) was tested in three different scenarios: (1) two quasi-parallel galleries that diverge at an angle of 60º; (2) two opposite ends of a gallery, currently under excavation, which will meet in the middle, separated by 23 m of rock at the time of the testing and (3) two parallel galleries separated by 30 m of rock. Results for scenario (1) were 25 and 26 dB signal relative to noise level for a distance of 25 m, while for scenario (2) the signal ranged from 25 to 29 dB and for (3) the signal was 25-26 dB.

The second testing was carried out at the WTB of Tournemire in April 2018, with the same prototype (see specifications above). The test results over a distance of up to 10 m were better than expected; in fact the test using the access boreholes oversaturated the receiver input (signal too strong when both the transmitter and the receiver were located inside the boreholes, Figure 8, bottom left). It was then decided to install the transmitter in the access boreholes and the receiver along the access gallery that leads to SEALEX gallery (Figure 8, bottom right) to take signal measurements in the readable range. Results were similar to those gathered at FSB, and the maximum range achieved with this arrangement was 30 m.

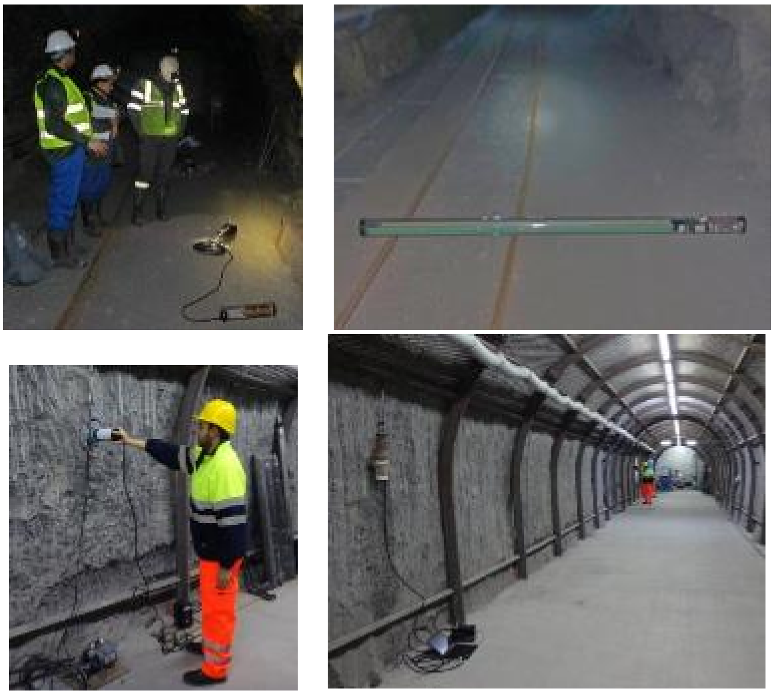

Figure 8. Field testing: FSB on top, with receiver (left) and transmitter (right), and WTB below, with borehole testing (left) and gallery testing (right)

Conclusions

Results show that the TTE equipment used is suitable to transmit data over distances of up to 30 m under conditions similar to those expected in a future repository. The signal was transmitted by the magnetic field coupling between transmitter and receiver coils. A frequency of 4 kHz was used and the data rate was 1600 bit/s with an energy efficiency of approximately 1 mWs/bit.

However, there is room for much more improvement, as described above, and the same approach could be applied to longer transmission ranges, by just changing the antenna. The operating range expected in the low noise repository environment, based on an RX level of 30 dBpT, is 30 m for a 90 x 200 mm ferrite core and can be extended to 60 m with a 1 m antenna and four loops, and up to 200 m with a 10 m diameter antenna and one loop.

The power consumption of the transmitter can be reduced, extending the battery life, by reducing the range, the number of sensors, or re-designing the internal electronics of the WSU. Taken together, these changes would reduce the TX power consumption to ~ 4 W, which would greatly extend the battery life.

While VLF radio equipment is generally more immune to the effects of ionizing radiation than high frequency RF devices, the transmitter hardware will also need to be hardened to prevent damages. These design changes may be incorporated together with the low power design changes discussed above.

3.1.2.5 Discussion and conclusions

To demonstrate the technological feasibility of underground wireless data transmission, VTT, Arquimea and Amberg have developed different short range solutions. As the wireless system capability to transmit across the repository materials and components decreases with increasing frequency, three schemes were planned and implemented: Arquimea has improved the existing prototype from MoDeRn Project by using a new short loop antenna and lower frequencies, achieving a distance of 4 m in partially saturated bentonite at 2.2 MHz. VTT, on its side, has focused on a frequency of 125 kHz, and demonstrated that they can bridge a distance of 23 m including 15 m of granite, at a data rate of 1 bit/s. Finally, Amberg has provided a solution based on low frequencies by using Through-the-Earth commercial technology, achieving a distance of 30 m with a frequency of 4 kHz.

Furthermore, IRSN has implemented the WTB in the Tournemire Laboratory to provide an environment for testing and develop communications systems under relevant conditions, where WSUs from Arquimea, Amberg and Andra have been tested. The systems of Arquimea and Andra were also used within the LTRBM (Modern2020 WP4.3).

In all the studies, understanding of the general principles and applicable technology of short range underground data transmission have been obtained and demonstrated, reaching different states of maturity. The problems that arise concern engineering, not basic physics as the general theory of wireless transmission applies to the underground environment, taking into account the electromagnetic properties of the associated natural and engineering materials in the transmission path. Therefore, to bring the underground short range wireless technologies into products and practical industrial applications, not basic research but engineering development is needed, including a multidisciplinary approach (radio frequency circuit technology, electronics, antennas, mechanics and applied electromagnetics).

The real application case may differ from the demonstration environment in some important aspects, as signal attenuation, or even complete blocking, from metallic objects (reinforcements, nets, full metal enclosures, etc.). Therefore, to ensure successful communications it is necessary to test the system in the actual environment during repository construction.

3.1.3 Long range systems

3.1.3.1 Single-staged long range data transmission system (Andra)

In the French project for a deep underground radioactive waste repository (Cigéo project), monitoring tools and transmission ways need to be as discrete as possible. Several types of wireless transmission systems have been developed. The current strategy for Andra is to use only low frequency transmission (i.e. about 10 kHz) to transmit through the host rocks and repository cells seals, and to adapt it to each different cell design (High Level and Intermediate Level - Long Live Radioactive waste cells) and to the different sensor configurations, as miniaturized wireless transmitters connected to one or two sensors in monitoring boreholes near HLW repository cells, or all-in-one wireless transmitters connected to several sensors inside an IL-LLW repository cell (Figure 9, left).

An alternative option to the medium range wireless configuration is considered for Cigéo: a wireless data transmission from the repository level directly to the ground surface over more than 500 m of rock (Figure 9, right). This system would be especially suitable for monitoring of structural health after the foreseen complete closure of Cigéo site at the end of the operational phase. As part of Modern2020, Andra performed several tests on long range transmission that are summarized in this section.

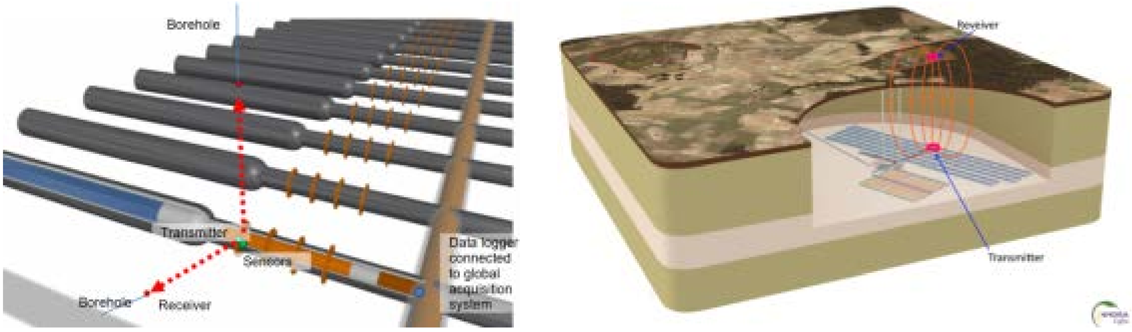

Figure 9. Medium and long range wireless configuration

A large antenna of 3.75 m by 3.75 m and with a transmission power of 200-300 W has been designed to transmit a signal at 8533 Hz over hundreds of meters (Figure 10). A modulated data signal was broadcasted in the Tournemire URL. The test was focused on the signal strength, so no real data were transmitted.

Figure 10. Large antenna for long range wireless transmission in the Tournemire URL

In spring 2015, two long distance transmission test campaigns were performed in Andra's URL, with the large antenna transmitter on the ground surface and a receiver on the surface at a certain distance, and with a receiver placed at the surface and the transmitter located in a borehole of the underground URL.

The set-up succeeded to transmit wirelessly a modulated signal in a coplanar surface-surface configuration up to 310 m, but not further. A transmission between URL and surface (500 m) could not be established, which is consistent with the former. Two main reasons can explain this: the noise level due to buildings and human activities nearby, which was high but not excessive, and the signal attenuation due to the geological properties of the rock, for which there is not very precise information.

In order to consolidate the results obtained in Andra's URL, three test campaigns were performed to test the long distance transmission devices in the Tournemire URL in summer 2017, and wireless signal transmission was achieved for each campaign:

- Campaign A: transmission test from the subsurface gallery to top of the mountain.

  This is the most relevant configuration with respect to the objective of wireless transmission from the Cigéo gallery to the surface. A transmission through 270 m of rock was achieved, providing a signal strength about four times higher than the EM noise level on the top of the mountain. This demonstrates also that the transmission from the gallery of Andra's URL to the ground surface cannot be achieved with the current set-up, due to higher EM noise level and greater distance.
- Campaign B: surface-surface transmission test on the mountain plateau.

  Results of the surface-surface test above Andra's URL were confirmed: the transmission range was limited to 300 meters, although in Tournemire, with lower EM noise level, it should have worked theoretically at a distance of 500 m.
- Campaign C: transmission test from the mountain plateau to the subsurface gallery.

  Wireless transmission was successful over a distance from 270 m to 290 m with the receiver in several locations in the tunnel: the received signal strength was two times higher than the noise level in the gallery. The tunnel is a former railway tunnel, and the rails evened the signal.

Conclusions

The use of a larger antenna has permitted to extend the previous range of wireless transmission devices from tenths of meters to hundreds of meters. It demonstrates also that the transmitted signal is weakly attenuated by the rocks and strongly deviated by metallic parts such as rails. Nevertheless, the developed system was not able to transmit data from the Andra's URL to the ground surface. As it is hardly possible to reduce the environmental EM noise level or increase the size of the antenna, the best option to achieve a transmission over 500 meters of distance under the given conditions will be to increase the power put in the antenna. However, this would probably bring safety issues. The use of relay seems more adequate at this stage of developments.

3.1.3.2 Field characterizations at Tournemire for long range data transmission (NRG)

NRG developed a long range wireless data transmission system and demonstrated data transmission through 225 m of overburden in the HADES underground research facility at Mol, Belgium [2], 7.1.1. As part of the LTRBM demonstrator (Modern2020 work package 4.3), NRG is responsible for the wireless data transmission from the Tournemire tunnel to the surface plateau on top of the tunnel. The low water table and type of host rock is expected to result in comparable low electrical conductivity that allows using higher (and more efficient) transmission frequencies for long range data transmission than e.g. applied in the HADES URL in Mol [2], 7.1.1. In this section, the general set-up is discussed, and measurement results are presented.

Low frequency data transmission makes use of a magnetic field that is induced by forcing a current through a loop antenna. Its value is a function of such current, the loop area and the number of turns of the loop. In a conducting half-space [8], 7.1.1, magnetic field propagation at the surface can be estimated as a function of such field, frequency, axial and radial distance to the transmitter and electric and magnetic parameters of the medium. Based on this models, field characterization measurements where performed and an overall data transmission set-up was developed, optimized for the specific conditions at the Tournemire site.

Experimental set-up

The set-up used for signal and data transmission experiments consists of a signal source providing the test signals, a battery based coil driver supplying about 60 mW to the transmitter antenna, a (tuned) transmitter antenna placed in the northern part of the tunnel, a (tuned) receiver antenna situated at the surface 275 m on top of the transmitter, a preamplifier for the receiver antenna, an analog-to-digital converter (ADC), and a (software) demodulator and decoder (Figure 11).

Figure 11. Antennae used: receiver antennas (left) and transmitter antenna (right)

Several antennae were used in order to perform a variety of measurements, including calibration, measurements of 2D noise and signal attenuation, and data and signal transmission. For the latter, antennas with a diameter of 2.25 m and between 3 and 7 turns were used.

The receiver was based on the design used in Mol [2], 7.1.1, adapted to the higher frequency range considered in Tournemire (5 - 9 kHz) and featured an additional ultra-low-noise input stage to increase sensitivity.

Field measurements in Tournemire

Two field measurement campaigns were performed by NRG in Tournemire:

- in the first campaign in July 2017, site characterization measurements were performed with the following objectives: to quantify the sensitivity of the updated receiver set-up in field; to characterize vertical and radial interferences and background noise levels; to characterize magnetic field propagation; and to identify potential impact of the rails on it.
- in the second campaign in April 2018, data transmission modes were tested. Main focus was to study the specific interactions of local interference with the transmitted data stream, and to test different transmission modes (BPSK and QPSK) and data rates (30 - 100 sym/s).

Results

In the first campaign, site characterization measurements have been performed. Interferences from the electric network in vertical direction in Tournemire were found to be much lower than in Mol. Interferences in the north-south direction (perpendicular to the power line) are in a comparable order of magnitude as in the vertical direction, while in the east-west direction (parallel) are generally lower.

A higher sensitivity of the improved receiver was observed. The vertical background noise between the harmonics is estimated to be about 3 to 7 fT/√Hz for the most favourable channels, higher than in the Netherlands, and in between the peaks it consists mainly of bursts, rather than random Gaussian noise, which has to be taken into account when evaluating the necessary power for data transmission.

Only a weak frequency-dependent attenuation by the overburden was found, implying an effective electrical conductivity of 1 mS/m or less. However, a frequency-independent overall attenuation by a factor of three was found as well (Figure 12).

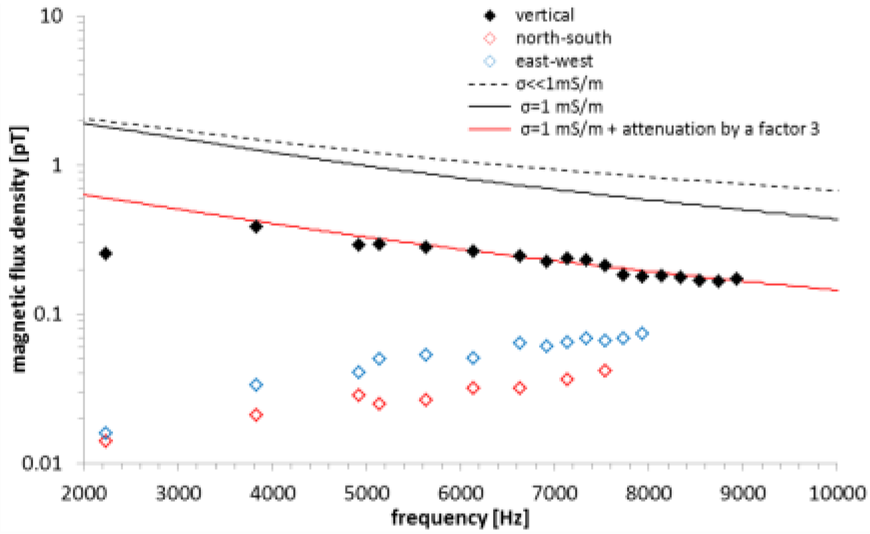

Figure 12. Frequency-dependent signal attenuation of the vertical and radial fields at Tournemire (diamonds), and model calculations for several electric conductivities (lines)

From radial field strengths it can be concluded that the presence of the rails in the tunnel does not favour overall signal propagation but has an adverse effect on propagation behaviour of the vertical field. The frequency range of 8 - 9 kHz is identified as most suitable for data transmission. Alternatively, a range with low background noise was found between 6.0 and 6.5 kHz.

In the second campaign, data transmission experiments have been performed using a critical, low power level of the transmitter (60 mW), to study the effect of the specific local interferences on the transmission performance. At the used power level, data transmission has been achieved at a transmission frequency of 8723 Hz, although with errors, (bit error rate $\pm$0.1%), especially at higher data rates (>60 sym/s).

In preparation of the intended demonstration of a combined wireless solution in Modern2020 Task 4.3, additional analyses will be performed on the recorded data transmissions from the second measurement campaign in Tournemire. Based on the outcomes, the most suitable demodulation schemes will be implemented, and the necessary power level will be determined that allows to transmit data with a sufficient low bit error rate ($\ll$0.1%).

Conclusion

The measured attenuation of a magnetic field in the 5 - 9 kHz range due to interactions with the overburden is low in Tournemire, best estimation is an effective electrical conductivity of <1 mS/m. The presence of rails in the tunnel attenuates the field by about a factor of three, equivalent to an increase of the transmission distance to 400 m. Data transmission has been demonstrated successfully at a low power level (60 mW), although a flawless data transmission (bit error rate $\ll$0.1%) will require either better demodulation techniques or higher power levels. However, it is expected that data transmission over 275 m of overburden is possible with an antenna power of less than 5 mW/bit of transmitted data.

3.1.3.3 Multi-staged long range data transmission system

Concept of the wireless relay system

Since 2002, RWMC is working on wireless data transmission systems, based on electromagnetic waves with frequencies of several kHz, as part of their monitoring system developed to avoid detrimental effects on the quality and performance of the seals in a geological repository [9], [10], 7.1.1. In order to enable monitoring in a limited space such as inside buffer materials or the near-field environment, and to enable receiving the monitoring data on the surface, a miniaturized transmitter has been developed [11], 7.1.1, as well as middle-range and long-range transmission antennas [12] in a collaborative study with Andra.

The miniaturized transmitter can be used for the monitoring system, including wireless relay system. It measures 60 mm in diameter and 240 mm in length and can withstand up to 40 °C and 10 MPa. It can transmit data over 25 m at 8.5 kHz during approximately 10 years at a rate of 1 transmission per week.

General set-up

A long distance wireless relay system has been developed by using the long-range transmission antenna, and a transmission test through 250 m has been successfully carried out at the Horonobe URL using an external power source [9]. However, the large power supply necessary for long-distance transmission by underground wireless transmitters and relay devices [13] is a limiting factor. To reduce power consumption, a multi-stage relay system has been proposed to shorten the transmission distance between devices, and redundancy has been also improved by introducing a multi-route relay system to secure alternative transmission routes in case of malfunction (see Figure 13). Power consumption is reduced by combining data from more than 10 transmitters in a relay.

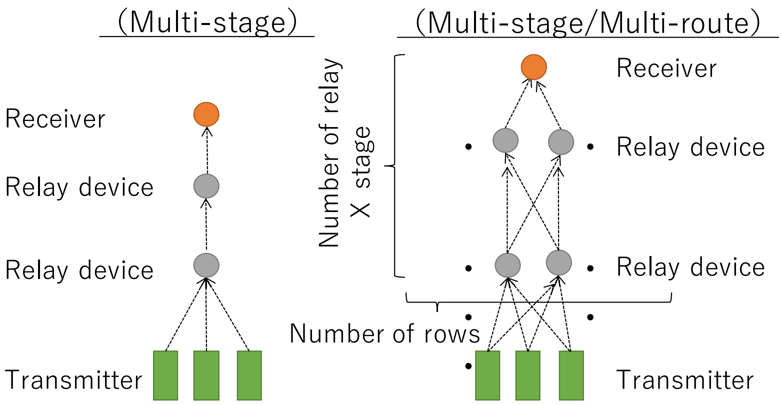

Figure 13. Conceptual diagram of a multi-hopping data relay. The figure on the right side shows rerouting of the data transmission in case of a malfunction of the relay device. Modified from [16]

The relay system can reduce the power consumption when one transmitter is connected to a relay only. However, the power consumption can increase when the relay device manages several transmitters due to the increase of waiting time to receive a complete set of data from all transmitter nodes, which can be up to 70 % of the overall power consumption. Therefore, the power consumption has been reduced from 123 mA to 4 mA by using a low consumption activation code (GOLAY code; [15], 7.1.1) that optimizes the receiving circuit usage state.

In a next step, antennas, power supplies, and a container to protect the whole relay device were designed and manufactured (Figure 14 left). The relay device measures 216 mm in diameter and 565 mm in length and can withstand up to 5 MPa. It can transmit data from 10 transmitters over 100 m at 8.5 kHz during approximately 10 years at a rate of 1 transmission per week.

Experimental work

Transmission tests over a distance up to 95 m were carried out at the surface. All measured signal strengths were above the noise level and on or above the theoretical attenuation line, confirming that the stable transmission was secured [16], 7.1.1. The maximum transmission distance was constrained by the experimental facility.

Furthermore, to secure transmission redundancy in case of malfunction, data rerouting tests were carried out in laboratory using three relay devices over a distance of several meters with the following sequence (see Figure 14 right):

Step 1: Transmitter 1, 2 → relay device 1 → relay device 2 → receiver
Step 2: Malfunction of relay device 2
Step 3: Instruction signal from receiver manually sent to relay device 3 to send data to the receiver
Step 4: Transmitter 1, 2 → relay device 1 → relay device 3 → receiver

As result, data from the transmitter were successfully delivered to the receiver even when the data was rerouted from the relay device 2 to 3.

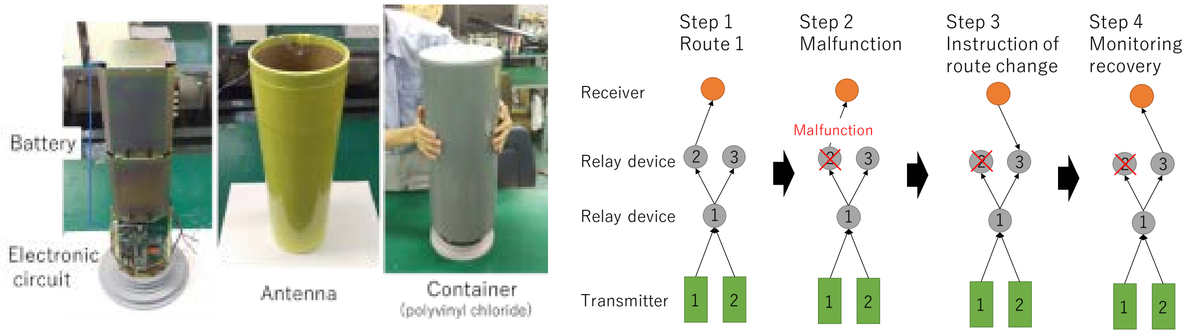

Figure 14. Relay device for the multi-stage / multi-route relay system [19] (left) and conceptual diagram of route change in the case of device malfunction. Modified from [16] (right)

Finally, to validate the durability of the relay system and to evaluate early infant mortality failure rates, an endurance test with the configuration in Figure 14 has been performed in laboratory during 6 months over a distance of several meters. More than 4,000 transmissions have been done without loss of data, which is much more than the 510 planned ones over 10 years at a rate of 1 transmission per week.

Conclusion

RWMC has developed and tested an underground wireless relay system (multi-stage/multi-route relay system) during the Modern2020 project, enabling relay of data sent from miniaturized wireless transmitters to the surface with redundancy by introducing a function to change the transmission route in case some of the devices fail.

3.1.3.4 Discussion & Conclusions

Adaption and testing of three existing long range systems has been successfully performed, and data transmission over a distance of 275 m has been achieved with as little as 5 mWs per bit of transmitted data.

There are at least two principal options to send monitoring data from transmitter(s) with sensors from an underground disposal facility to the surface as described above: the direct transmission over long distances, or the use of multistage relay systems. These systems may have advantages and drawbacks as indicated in Table 3.

Table 3. Comparison of two-types of transmission system for long-distance

Type of transmission system	Advantages	Drawbacks
Long-range transmission system	• Simple system eases installation • Small number of units reduces probability of malfunction	• Large antenna requires large space • Large power consumption requires large-capacity power source(s) • No redundancy if single-route is used
Multi-stage/multi-route relay system	• Relatively smaller antennas required • Reduced power consumption enables use of conventional battery (for about 10 years) • Multi-route secures redundancy	• Complicated installation • Large number of units increases probability of malfunction

Taking into account the experiments feedbacks, it would be more convenient to use relay systems at the beginning of the repository life. The long-range transmission with unique transmitter including a large antenna is an option that should be considered afterwards in the future of the repository life.

3.1.4 Integration of short range wireless techniques with sensors and long range wireless systems

3.1.4.1 Wireless vibrating wire sensor

In the Wireless Test Bench (WTB) of the Tournemire URL (see Chapter 3.1.2.1), Andra has taken part at an experiment with a short-range wireless transmission system in July 2018. This system is the result of a RWMC-Andra collaboration and has been realized by the SAKATA Denki Company.

General set-up

The system comprises: a miniaturized transmitter with antenna, battery, data logger, sensor interface connected to a vibrating wire, a portable receiver unit and a needle indicator for the wireless signal level (Figure 15).

Figure 15. Miniaturized transmitter and vibrating wire extensometer (left) – Portable Receiver connected to the needle indicator (right)

The aim of the test is to verify that the wireless system can transmit sensors data from behind the cell plug of an ILL radiative cell to the entrance of the cell. Hence the test configuration consists of putting the transmitter connected to the sensor consecutively in the three access boreholes of the WTB and to analyse the signal received by the receiver on the other side of the bentonite plug (i.e. at the entrance of WTB borehole), thus testing three distances of transmission from 5 to 10 meters.

Results and conclusions

In order to receive the sensors data, the signal strength at the receiver end must be higher than the ambient electromagnetic noise (EM noise), which was the case at the transmission frequency of 8.5 kHz as the noise level was low. Therefore, all data transmissions were successful. The transmitter consumes a power of 0.55 W during transmission, which takes approximatively 20 seconds for ten timestamped measurements.

The transmitted data recorded on the receiver was loaded on a computer as a table containing date, voltage of the transmitter battery and sensor data, including natural frequency of the vibrating wire extensometer for strain measurements and electrical resistivity for temperature measurements. Data were consistent with the conditions of the experiment.

The wireless transmission system successfully passed the test at the longest distance of the test bench. Besides, it seems to have also a margin to be able to transmit data 5 m further.

3.1.4.2 Wireless fiber optics sensor

As part of Modern2020, EURIDICE evaluates the option to link a new developed fiber optic sensor with a wireless data transmission system that allows monitoring inside a supercontainer waste package design for the disposal of high level radwaste as considered in the Belgian research programme.

In the current concept, the Belgian waste disposal programme considers the packaging of the high-level radioactive waste (both spent nuclear fuel assemblies as well as canisters with vitrified waste) in a so-called supercontainer (Figure 16).

The actual waste is first packaged in a thick-walled (few cm) steel overpack, which is covered by a cement-based buffer of about 0.7 m thickness. This buffer has several safety functions, such as radiation shielding and corrosion control of the overpack. The supercontainer is manufactured in a surface facility, and integrates a lot of EBS materials, which together with the radiation shielding further reduces the complexity of the underground installation works.

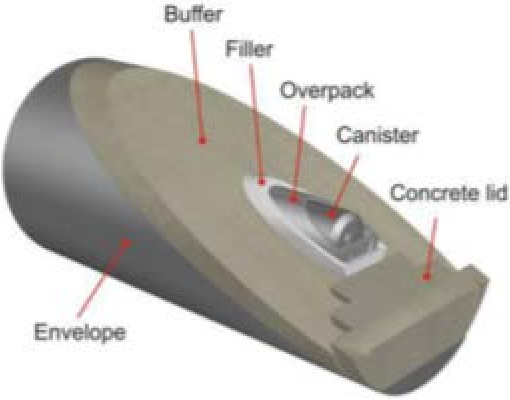

Figure 16. Cross-section of a supercontainer with a cement-based buffer as main component

Monitoring the condition of a supercontainer could be a relevant part of its quality assessment. Although no formal parameter screening has been performed yet, strain, pH, and presence of hydrogen could be relevant parameters to monitor the hardening of young concrete, so to detect the formation of cracks, and the chemical buffering, so to detect unexpected corrosion processes. Within Modern2020's WP3.4, some sensors to monitor these parameters have been developed by the University of Mons.

For the implementation of this monitoring, a wireless (or contactless) method is recommended for both safety and reliability reasons: the absence of signal cables is essential to guarantee the buffer integrity and besides the vulnerability of cables at the exit point is avoided, as well as the need of cable manipulation (connection and disconnection) close to the waste in a long term monitoring.

The idea is then to install a wireless interrogator within the cement-based buffer, at a sufficient depth so that its integrity is not compromised (at least 10 cm).

General set-up

After consultation with their subcontractor Com&Sens, EURIDICE decided to aim for a demonstration of a wireless readout of the *mINT* fiber interrogator. The *mINT* device is a miniaturized version of a readout for Fiber Bragg Grating (FBG) Sensors developed in the frame of the EC SMARTFIBER project (2010-2014; [19]). A prototype of the *mINT* device, with a diameter of 10 cm and a thickness of less than 1 cm (to affect the structure as little as possible) is shown in Figure 17, left. For the *mINT* interrogator itself, a 'proof of principle' version (without the miniaturisation) was assembled (Figure 17 right). It has an optical bandwith of 50 nm, up to 8 input channels and 5 to 10 sensors per channel with a resolution of 2.5 pm. The power consumption is 5 W, and the readout frequency 1 kHz

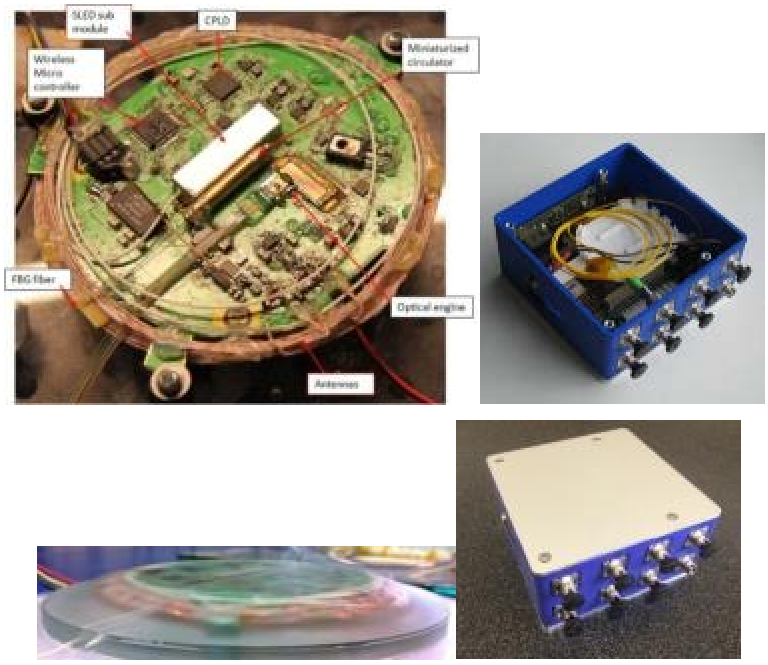

Figure 17. First *mINT* prototype (left) and current *mINT* demonstrator (45x150x150 mm³) (right)

This version of the *mINT* to a wireless transmitter was linked with an external, commercially available wireless LAN transmitter connected to the *mINT* through its USB interface, but it did not work due to software incompatibility. Therefore, a second approach used a Raspberry Pi Zero W device, with the '*VirtualHere CloudHub'* software installed. The receiving device consisted of a laptop, running the *VirtualHere* client to connect to the *mINT* device, and the *mINT* readout software itself.

This study focused on demonstrating the general feasibility of wireless measurements using the *mINT* interrogator, but the set-up was not optimised for low-power and the transferred data could be reduced too with better hardware processing. In addition, the entire USB communication with the *mINT* device had to be transferred over the wireless connection, increasing such transferred data significantly. The wireless data transfer uses IEEE 802.11 b/g/n wireless LAN on the 2.4 GHz band, with the corresponding transmission protocols (DSSS for IEEE 802.11b and OFDM for 802.11 g/n).

Experimental results

In practical in-house testing using 802.11n, the achieved transmission rates with line of sight at 20 m distance were in excess of 30 Mbit/s. The wireless performance is directly linked to the WiFi characteristics, as the technical solution used (*VirtualHere CloudHub*) creates its own WiFi network. This resulted in measurement rates that depend on the distances and obstacles, being sufficient to achieve more than one measurement per second through a concrete building wall at 20 m distance, or more than 50 FBG measurements per second at distances of 10 cm or less. If the control software for the *mINT* device would be running at an embedded PC, there would be no need to send the USB communication overhead wirelessly along with the processed data, thus reducing the energy needs.

A 75 Wh powerbank allowed for about 12 to 25 hours of continuous measurement, with a power consumption between 3 W and 6 W depending on the *mINT* light source intensity, or longer times for discontinuous measurement (e.g. 1500 days with one measurement/day).

A particular design feature of the original *mINT* prototype was wireless energy transmission to power the interrogator (through inductive coupling at 125 kHz). With limited distances in mind, this could also be considered (a possible implementation is then the wireless charging of the embedded battery).

Conclusions

The results indicate that it is feasible to monitor FBGs using a *mINT* device combined with a wireless link and a compact battery to transmit measurements from inside the supercontainer, especially if the required data rate is limited. With an appropriate size battery, it should be possible to monitor stand alone for several years. For very long term monitoring, it will become an economical and practical decision between very large batteries or other power sources without recharging, and a smaller battery that is intermittently topped up using wireless charging.

3.1.4.3 Combined short- and long range wireless data transmission

In a combined effort, Amberg, Arquimea, IRSN, ENRESA and NRG have evaluated the possibility to provide an integrated solution that links sensor nodes situated in a disposal cell behind a safety relevant barrier (seal) to the surface by a combination of wireless technologies for short and long distance data transmission.

Description of the Tournemire Site

IRSN has been carrying out its own research at the Tournemire Underground Research Laboratory (URL) in southern France (Aveyron) for the last 30 years. Located in a former railway tunnel built over 120 years ago, the Tournemire URL provides access to a shale formation that has geological characteristics similar to the site chosen by Andra. The research carried out at Tournemire enables IRSN to examine certain processes that play an especially important role in ensuring the long-term safety of a geological repository.

Excavated at the end of the 19th century, the old Tournemire railway tunnel is 1,885 m long. It thus offers a unique opportunity to observe 125 years of disturbances generated by an underground engineering structure excavated in a shale formation. The URL itself is located in a central part of the massif (Figure 18 left). It is made up of the former tunnel, six drifts which are 285 m in length in total, and over 400 boreholes excavated since 1988, which lead in different directions from either the tunnel or the drifts Figure 18 right).

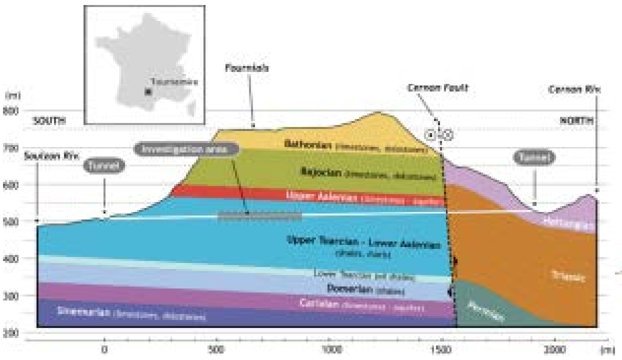

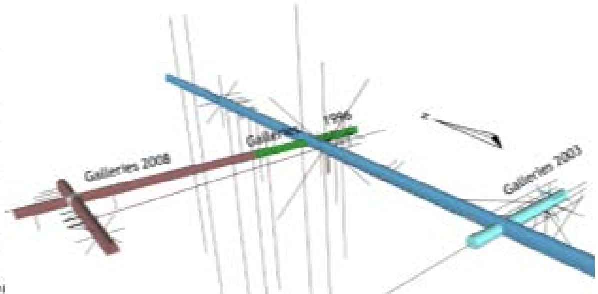

Figure 18. General geological cross-section along the Tournemire tunnel (left) and 3D diagram of the investigation area (right)

A range of measuring equipment and observation techniques are deployed in the URL to analyse the shale and its behaviour, detect faults using geophysical methods, the water it contains and the rate at which it moves through the formation, as well as disturbances likely to affect this type of rock if it is used for disposal. More recently, the URL has been used to assess the performance of sealing components that may be used in a disposal facility.

The Long-Term Rock Buffer Monitoring (LTRBM) is one of the field demonstrators in WP4 of the Modern2020 project. It was installed in summer 2018. Initially, LTRBM was intended to host part of the new monitoring devices developed in WP3 (mainly wireless devices including long term power supply solutions and new sensors) to assess the real performance of the suggested solutions under realistic conditions. The layout is given in Figure 19 right, and has the following specifications:

- A main horizontal borehole (MB) parallel to the gallery *South_08* measuring 60 cm in diameter and up to 10 m in length
- A bentonite-sand buffer (highly compacted bentonite-sand blocks and granular material based on bentonite pellets) confined by means of a low-pH concrete plug lid. Its length and composition are decided according to the operational conditions needed for the prototypes. Natural sodic Wyoming bentonite MX-80 type is used, and the ratio 60/40 of bentonite/sand could be adjusted as well depending on IRSN's scoping calculations on hydration times and hydromechanical evolution.
- An artificial hydration system, composed of several hydration mats, to accelerate buffer saturation.

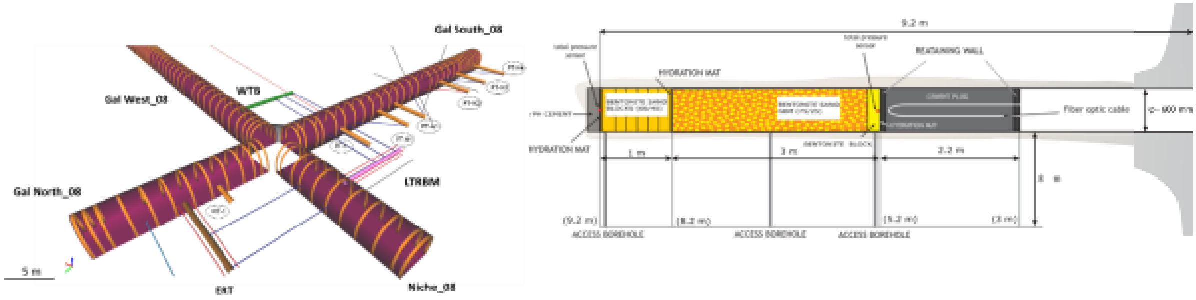

Figure 19. Location of LTRBM in the Tournemire URL (left) and proposed layout (right)

Short range data transmission

As part of the combined demonstration in Modern2020's Task 4.3, Arquimea is responsible for the wireless data transmission from the buffered section of the LTRBM to the gallery. Arquimea developed a short range wireless data transmission system based on the prototype used for the tests performed in the WTB that demonstrated transmission through 4 m of bentonite buffer (Chapter 3.1.2.1). The set-up consists of three of those wireless sensor units (WSUs; see Figure 20) with the following sensors payload: 2 new psychrometers developed by Arquimea under Task 3.4 (relative humidity from 95% to 99.96%); 1 analogue pore pressure transducer (0-10 bar); 1 digital capacitive type hygrometer (0% to 100% relative humidity); and temperature measurements (-40°C to 125 °C).

Figure 20. Wireless node in preparation for LTRBM (left), final WSU (right)

Two of the WSUs (WSU1 and WSU2) will be installed inside the buffered section of the LTRBM, and will link to the third one (Master WSU) installed outside the borehole (see Figure 21). WSU2 can act as a repeater for WSU1 if direct transmission from this one is not possible, and the parallel borehole could be used as well to insert the Master WSU to bring it closer to the buried nodes if necessary.

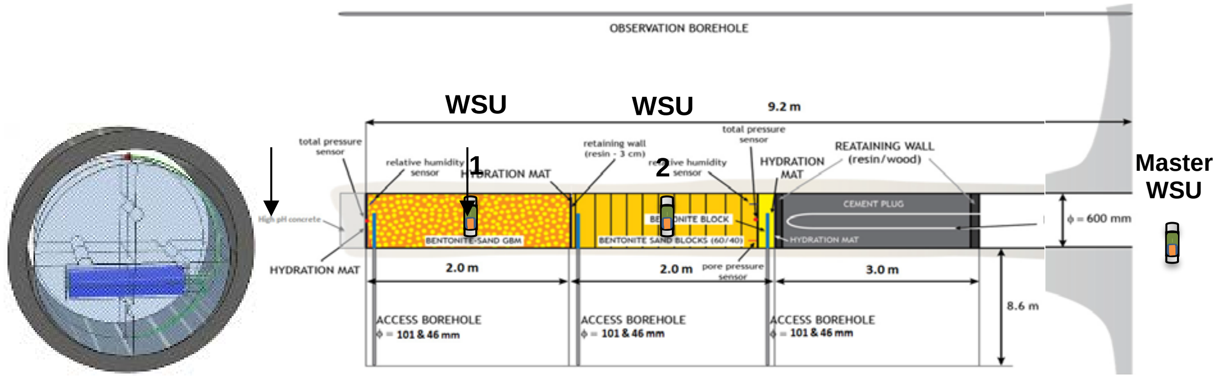

Figure 21. Drawing of WSU in the block buffer of the LTRBM (left) and conceptual layout (right)

The Master WSU will be on listen mode by default, powered by an UPS, and will be in charge of time synchronization and data recording readable by serial command from the SEALEX computer, as it will be connected to the Data Acquisition System (DAS).

Measuring and transmitting data twice a day with the sensor configuration chosen for the LTRBM configuration results in an approximate total daily consumption of 18 mWh per node and an estimated lifetime of its battery of 4 to 5 years.

Long range data transmission

The long distance transmitter is placed in the main tunnel north of the test facility, where there is no additional mechanical support. This also avoids large interferences from a high voltage power line on top of the main facility. For the experiments, it was decided to locate the receiver antenna right on top of the transmitter antenna in a coaxial position, resulting in a transmission distance of about 275 m (Figure 22). Site characterization measurements were performed (see Section 3.1.3.2), resulting in an optimized set-up for the final demonstration to be performed in WP4.3 of Modern2020 [ref to D4.3].

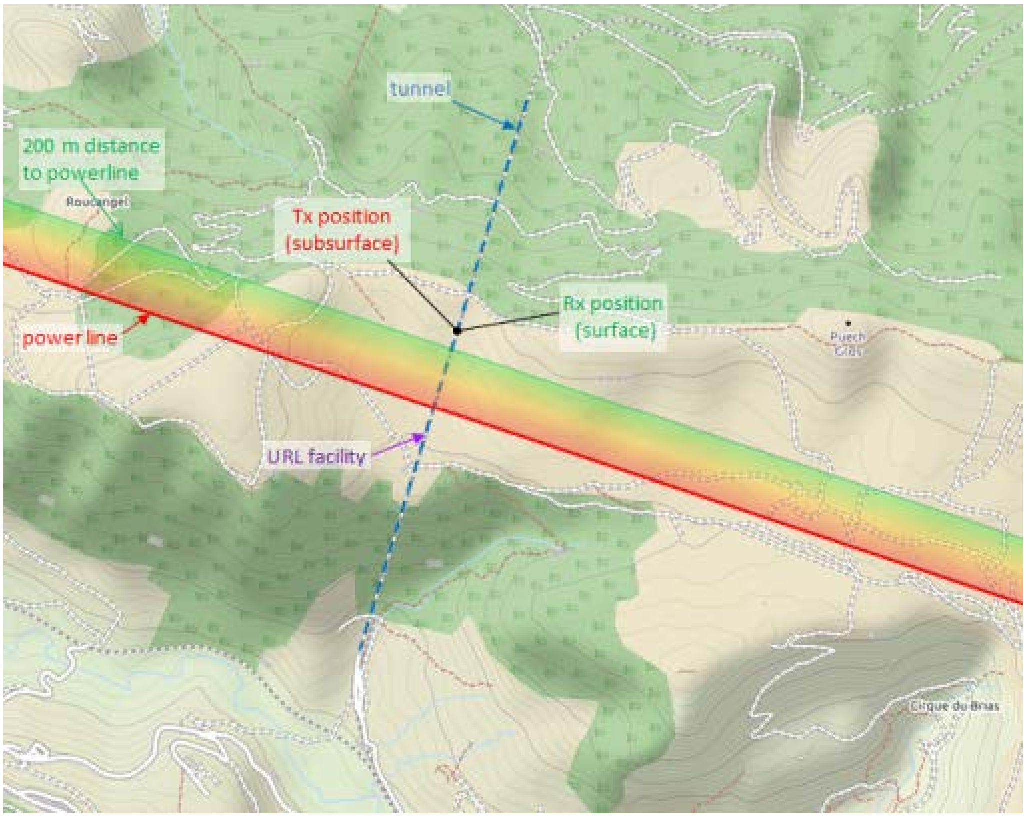

Figure 22. Top-down view on the Tournemire URL. Background map © OpenStreetMap contributors (*www.opendatacommons.org/licenses/odbl*)

Data acquisition and data link between short and long range transmission systems

Figure 23 provides an overview of the overall set-up and data flow in the LTRBM demonstrator: Monitoring data obtained twice a day by the WSUs buried in the LTRBM are transmitted wirelessly to a Master WSU that records the incoming data. The collected data of all WSUs is send via a wired link to a central Data Acquisition System (DAS), which stores the data of all wired and wireless sensors located in the LTRBM, and allows to distribute them further via several wired and wireless routes. The long range subsurface transmitter requests data from the DAS via a wired interface (RS-485) and transmits these wirelessly to the surface.

The LTRBM Data Acquisition System is integrated in the new Tournemire DAS, composed of linked OMNIALOG data loggers. Data are transferred every 30 minutes to a server/database, and a web-software allows data visualisation and downloading. Real time data is available through direct LAN Ethernet, USB and RS232 connection to the data logger.

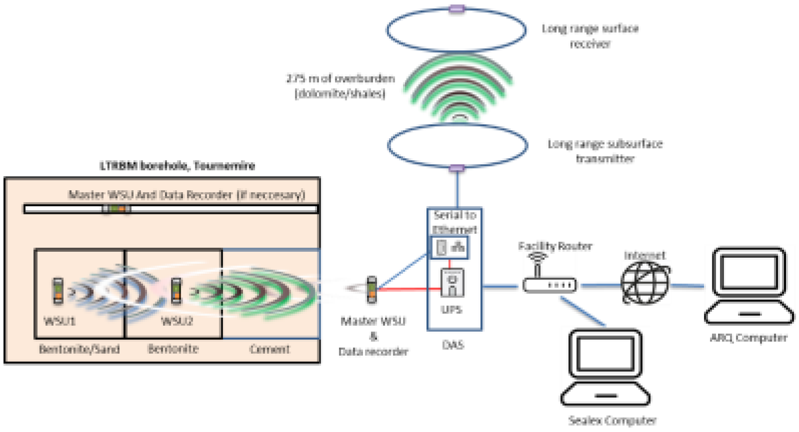

Figure 23. Overall set-up of the wireless data transmission chain out of the LTRBM borehole to the surface

3.1.4.4 Discussion and conclusions

Within Task 3.2, Andra successfully tested a wireless vibrating sensor in the WTB with a miniaturized transmitter over distances of 5 to 10 m. EURIDICE linked their *mINT* fiber optic sensors with a commercial wireless LAN transmitter and demonstrated data transmission through the air and a concrete building wall with high data rates (>600 kbit/s). Furthermore, a basic set-up and technology was developed and tested to demonstrate a combined solution that allows to monitor in a disposal cell behind a safety relevant barrier, and to transmit the data wirelessly in two stages, through the plug and through 275 m of overburden, to the surface. The combined solution consists of four contributions:

- The LTRBM borehole that has been prepared and constructed at the Tournemire URL by Amberg under the supervision of IRSN.
- A wireless sensor node developed and successfully tested by Arquimea that allows to monitor inside the borehole and to transmit the data to a receiver node placed outside the borehole.
- A data acquisition system (DAS), set-up by IRSN and operated by Amberg that collects and stores all data from the wireless sensor node and other (wired) sensors in the LTBRM.
- A long range data transmission system by NRG that successfully transmits data stored in the DAS from the tunnel through 275 m of overburden to the surface.

The demonstration of the overall transmission chain is part of Modern2020s WP4.3.

3.1.5 Overall conclusions on wireless data transmission systems

Wireless data transmission technologies are used in an increasing number of industrial and consumer applications. Today, wireless technologies that transmit all kinds of data through the air are an abundant part of everyday life. The success of these technologies is related to their robustness and priceeffectiveness. In the previous chapters, several solutions for wireless data transmission have been presented, developed as part of the Modern2020 project. These contributions focussed on the transmission of data through solid media: unlike for the transmission in air, high frequencies are considerably attenuated in solid materials. Consequently, distances of more than a meter require specific solutions that are not available on the market today: much lower frequencies are applied than in other established applications, with communication often taking place in a more unfavourable, noisy part of the frequency spectrum. In addition, low frequencies cannot be efficiently generated by electric dipole antennas as used in the vast majority of applications. Therefore, many contributions in this report had to apply another, rather uncommon technique: the generation of magnetic fields by loop antennas.

Within the Modern2020 and previous MoDeRn project, major steps has been achieved in understanding, designing and demonstrating specific solutions that allow transmitting data through components of the EBS or the host rock. Different technological solutions covering transmission distances between 0.1 and more than 275 m have been developed and tested, covering a variety of application situations, disposal concepts, and host rocks. A greater understanding of the underlying technical and physical principles has been achieved, and the provided solutions have been tested under realistic conditions, e.g. in the Tournemire Wireless Testing Bench (WTB), from the Tournemire tunnel to the surface plateau, or in the VTT underground laboratory. The performance of the developed technologies depends on a number of factors which, if carefully implemented, allow transmitting data over distances of 275 m through the underground with less than 5 mWs/bit of transmitted data, or over 4 m or more of a (partially) saturated barrier with less than 1 mWs/bit.

With respect to short range data transmission over distances larger than 1 m, several options are available, operating at frequencies between 4 kHz and 2.2 MHz. Each one of these technologies has its own advantages, and for all these technologies, successful data transmission through solid media has been demonstrated. Therefore, a variety of options and transmission frequencies for various application cases of interest are available on the short range with solutions reaching different states of maturity.

Regarding long range data transmission, the experience gained in Tournemire URL, the Hades URL and the Andra URL raises confidence that transmission can be achieved over distances larger than 300 m as well. This is necessary because disposal facilities are usually situated at larger depths than URLs. However, the energy necessary to transmit data can rise up to the 6th power of the distance[1], and one may wonder if transmission distances of 500 m or more are feasible at all. Bigger antennas, in the order of 20 m of diameter could perform on those distances as the tested ones have performed over distances in the order of 275 m.

Another solution presented to reduce the energy needs consists of transmitting data in several stages from the disposal facility to the surface with sequential relays. Attenuation through non-homogeneous media and interferences at low frequencies must be taken into account too, requiring specific solutions.

In Modern2020, also far-going integration of wireless technologies has been achieved, resulting in two WSU's, two specific combination sensors (fiber optics and vibrating wire sensor) with a wireless transmitter, and an integrated approach that evaluated the possibility to offer an overall transmission chain that allows transmitting data measured in the LTRBM demonstrator of Modern2020's WP4.3 to the surface on top of the Tournemire URL. Three of the wireless technologies developed in WP3.2 will be demonstrated as part of WP4.3.

Finally, although wireless data transmission is a promising technology for repository monitoring and major progresses have been achieved in Modern 2020, additional research is necessary to bring this technology to a readiness level that allows its application in disposal facilities:

- Long-term reliability is a key-topic, as maintenance of the components will be difficult or even impossible, and they will be placed in a harsh environment.

[1] This is an (often) used, conservative estimation

- Energy efficiency is another key-topic, particularly for long range data transmission systems, where it can be a limiting factor for the amount of data transmitted, but also in the short range, as it can determine the choice of wireless systems in competition with others as fiber optics.
- Other topics that require further research regarding wireless solutions are: combination of wireless systems with long-term power supply sources; potential interactions of transmitter antennas with magnetic permeable materials in a repository (steel, etc.); demonstration over distances longer than 500 m (typical repository depth); and dealing with large (man-made and natural) interferences in the 1 - 10 kHz range, which can strongly limit the overall performance, and automatic tuning of the antennas for 125 kHz data transmission technology.

3.2 Alternative power supply sources

3.2.1 Energy sourcing concepts of wireless sensor units for repository monitoring

Four alternative energy sourcing concepts for wireless repository monitoring sensors were investigated: energy harvesting on thermal gradients, wireless energy transfer, wireless communication add-on and miniaturized nuclear generator.

The considered power sources are not able to provide continuous power to the sensors, so the usual procedure is to operate in cycles, keeping the power consuming parts in sleep mode –unpowered or in extremely low consumption- until they start their activity period and returning them to the sleep mode.

The energy management (EM) is crucial for the overall functionality of the system, as it optimizes the energy acquisition from the power source and produces stable supply voltages to the power consuming parts.

3.2.1.1 Energy harvesting on low thermal gradients

NRG performed a feasibility study on the ability to use decay heat of High Level Waste (HLW) containers to power wireless sensors units (WSUs) in a geological disposal facility. *Thermoelectric Generators* (TEGs) are widely applied to convert high temperature gradients into electric energy. The research focused in the feasibility to harvest thermal energy from very small temperature gradients (<2°C), and to quantify the performance and efficiency of the different subcomponents of the energy harvesting system under disposal conditions.

3.2.1.1.1 Concept description

After the disposal of the containers in the geological disposal, heat is produced in the waste containers due to the radioactive decay of the HLW, diffusing through the engineered barrier system (EBS) into the host rock and causing the increase of temperatures. A temperature gradient will settle throughout the system. As time progresses, the decay heat will decrease, and the temperatures as well as the temperature gradients will settle, finally to the ambient values before the disposal. The heat flow can be converted into electrical power with a *Thermoelectric Generator* (TEG), which consists of one or several couples of semiconducting materials, based in the so-called *Seebeck effect* that occurs in metals and semiconductors.

At small temperature gradients, the little voltages generated by a TEG cannot be directly used to power WSUs: they have to be boosted up to higher voltage levels as required by sensor electronics. Furthermore, to provide sufficient energy to perform a measurement cycle, the small amounts of available power need to be accumulated and stored over longer periods. The electronic circuit that performs the voltage boosting, power conditioning and storage is shortly indicated as ‘*energy management device*’ (EMD). The combination of a TEG-module and the EMD is indicated in this report as ‘*Thermoelectric harvester’* (TEH).

3.2.1.2 Feasibility analysis

3.2.1.2.1 Thermal analysis

A thermal analysis was performed by NRG to the generic Dutch OPERA disposal concept in Boom Clay [20]. In this concept, the HLW consists mainly of vitrified, reprocessed waste and the heat produced is due to the radioactive decay of the fission products contained in the glass. The main contributors to the heat output during the first hundreds of years are ^{90}Sr and ^{137}Cs.

Directly after reprocessing, the thermal power output of the container is a few thousands watts. However, due to the long interim storage of at least 100 years in the Netherlands, at the moment of disposal, the power output will decrease to less than 200 W. After 200 years, i.e. 100 years of interim storage and 100 years of subsurface disposal, the thermal output is about 40 W per CSD-V canister.

The evolution of the temperature gradients between different positions in a disposal gallery for vitrified waste: over the supercontainer buffer, over the backfill, over the gallery support, and in the first meter of Boom Clay was studied. The conclusion was that, in order to provide energy over a relevant period of time, the TEH must be able to operate at temperature gradients of 2˚C or less.

3.2.1.2.2 TEH performance requirements

Many different types of TEGs are available on the market and used for cooling purposes, with limitations in their specifications. Commercial EMDs require at least 20 mV to operate, leading to a preliminary requirement for the TEG to provide about 100 mV/˚C in order to be able to harvest at low temperature gradients (< 0.5 ˚C). To estimate and optimize the overall performance of the TEH solution, detailed measurements were necessary to quantify the TEG and its interaction with the EMD.

3.2.1.2.3 Experimental set-up

A thermoelectric test bench was set-up to characterize the relevant performance parameters at very low temperature gradients (Figure 24), with Resistance temperature detectors (RTDs) above and below the TEG to quantify the heat gradient over the TEG element. Two additional RTDs were installed to verify a homogeneous heat spreading over the TEG for the experimental conditions applied.

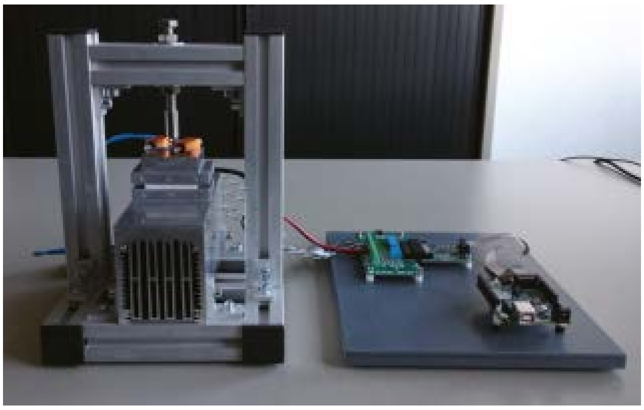

Figure 24. Thermoelectric test bench

The output voltages of two different TEGs were measured, without load and with a constant load of 3.3 Ω, measuring. Output voltages U_{TEG} of respectively 110 and 66 mV/˚C were found in the temperature gradient range of interest. With the load resistor, the output voltage drops to 28 and 43 mV/˚C, respectively.

For the studied TEGs, the voltage and power that is supplied to the EMD can be plotted as a function of the temperature difference from a combination of measured voltage-temperature relation and the measured input resistance. Figure 25 shows that a temperature difference of about 0.5 ˚C results in a voltage U_{TEG} of about 27 mV, and about 50 to 100 μW is supplied to the EMD.

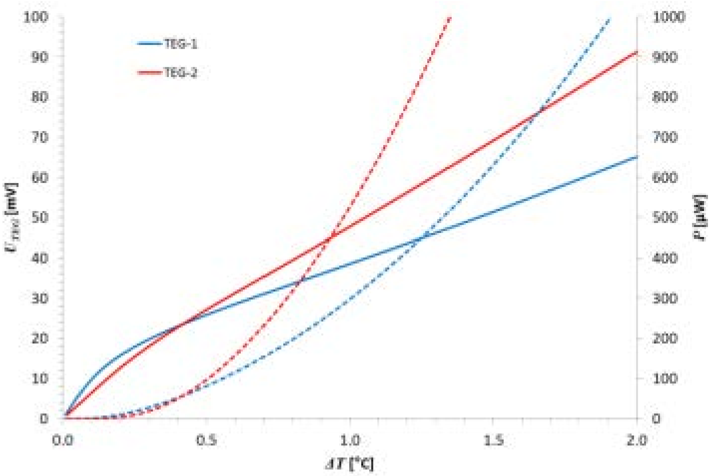

Figure 25. Estimated output voltage (solid line) and resulting power input (dashed line) of two TEGs into the energy management device

On basis of the characterization of the TEGs and the EMD, a performance analysis for two application examples was performed. The parameters considered were voltages of TEF and EMD, consumption, conversion efficiencies and thermal losses due to heat conduction in the TEH.

Several positions for the TEH are considered for the example case of the OPERA disposal concept, two design requirements being applied:

- the TEH should not alter the overall heat flow of the supercontainer & disposal cell: therefore, the overall thermal conductivity of the TEH must match with the thermal conductivity of the EBS component where the TEH has to be placed in.
- the TEH should not bridge more than one EBS component: two positions were analysed (TEH inside the backfill and inside the gallery lining.

In general, the results of this study show the principal feasibility to used decay heat of HLW containers to supply reasonable amounts of power to repository monitoring WSUs. The considered TEH designs are able to provide power of a relevant period of time, under very low temperature gradients as expected in a disposal situation after 100 years of interim storage. The efficiency of the TEG decreases linearly with the temperature gradient, and is generally low for the gradient range of interest (< 2 °C).

The quantitative outcomes showed that temperature gradient of less than 0.5 °C can be harvested, and converted to about 10 μW of electrical power. Limiting factors are the minimum input voltage of the harvester electronics, its efficiency and self-power consumption.

3.2.1.3 Wireless energy transfer

The wireless energy transfer by inductive coupling between loop antennas was studied with the construction of two different systems, for high and low electrical conductivity of the host rock. A generic feasibility analysis was performed, with the performance estimation of inductive energy transfer systems without medium interaction.

The purpose of this inspection is to highlight principal features of the inductive energy transfer, to set a baseline to the target power transfer performance, and to improve the understanding of the relation between the performance and the design parameters.

3.2.1.3.1 Feasibility analysis without medium interaction

The feasibility analysis is based on a simplified system model of a typical inductive energy transfer system with operating range longer than the antenna dimensions (long-range inductive energy transfer system). The system consists of a RF power transmitter and a wireless RF power receiver in the wireless sensor unit (WSU), located behind a geological or engineered barrier.

The received power has to charge the energy storage and cover the self-discharge of the energy storage, the self-power consumption of the energy management and the sleep mode current of the sensor and communication payload that typically are totally a few microwatts or more. For this reason, 10 μW is considered as the minimum reasonable received DC power level.

The total power transfer efficiency for the given system was calculated, by the characterisation of the different components by their parameters.

Finally, the power transfer performance was calculated (DC-to-DC power transfer efficiency and the received DC power with optimal tuning) with different diameters of the power transmitter antennae and variation of the axial distances between the antennae, assuming no attenuation by the intermediate materials such as rock or repository plug. The results indicate that transferring wirelessly a reasonable power level (10 μW or more) over 10 m distance is possible e.g. by transmitter antenna diameters of 2 m or more, receiver antenna diameters of 0.15 m or more, and transmitter power level of 100 W or more. Increasing the received power via improved link efficiency is possible by raising these design parameters, especially the receiver antenna diameter. The received power can also be increased by raising the transmitter power level, but this is limited by the fact that the transmitter antenna dissipates a big majority of the RF power generated by the inverter (P_{INV}), which can cause overheating of the transmitter antenna.

3.2.1.3.2 Wireless energy transfer pilot with communication add-on through low electric conductivity host rock

VTT designed and prototyped a pilot system for the verification and performance evaluation of the wireless energy transfer through low electric conductivity host rock (bedrock). It also features wireless data uplink for reading telemetry data messages from the sensor and wireless data downlink for sending telecommand messages to the sensor ("all wireless in one"). The operation of the wireless interface between the reader and the sensor is based on inductive coupling between the antennas and 125 kHz carrier frequency. The data modulation method (both data uplink and downlink) is carrier on/off keying (OOK). TDM (time division multiplexing) scheme between the powering, data uplink and data downlink is applied, for which the sensor electronics involves an energy storage (e.g. a capacitor or a rechargeable battery) with associated control circuits (energy management) for accumulating energy during powering periods, during which the sensor and communication payload are held in the sleep mode.

There are two possible antennae configurations: co-axial antenna, which can be applied e.g. for wireless interconnection through the repository plug or through the wall between the repository and an adjacent maintenance tunnel and co-planar antenna, which provides shorter operation range but can be also applied e.g. around the repository plug if the plug contains metallic enforcements that prevents the operation through the plug.

The wireless energy and data transfer performance of the pilot system was first tested in co-axial antenna configuration through the air at 10 m wireless distance and after in a bedrock cave, with a total distance between the antennas was about 8 m (7 m of rock). There were some metallic structures close to the antennas such as the staircase close to the reader antenna and a big metallic box close to the sensor antenna.

In conclusion, wireless inductive energy transfer by using LF frequencies such as 125 kHz is a valid concept for powering repository-monitoring sensors through bedrock. The field attenuation caused by 7 m thick bedrock wall is minor and lower than the measurement accuracy of the pilot test set-up in general. A better power level could be obtained by the modification of the distance, increase of sensor antenna diameter and improvement of the antenna.

3.2.1.3.3 Wireless energy transfer trough materials with high electric conductivity

NRG performed a feasibility study on the ability to transfer energy wirelessly through the host rock or components of the engineered barrier system (EBS) into a disposal cell by magnetic induction techniques. The focus of this contribution was to analyse the feasibility of wireless energy transfer by magnetic induction over larger distances through saturated media such as argillaceous host rocks or (partially) saturated EBS components that can be characterized as electrical 'good conductors', and to quantify the performance.

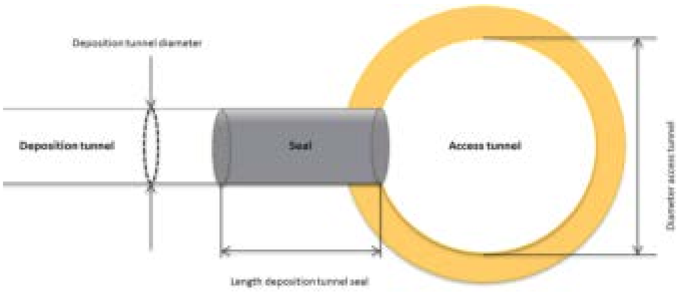

Figure 26. General outline of a deposition tunnel, separated by a seal from the access tunnel

The experiments in previous chapter were performed through electrical low conducting media (air and granite), and this is the opposite situation. The evaluation of the conductivity is made according to the distance at which a magnetic field is attenuated due to interactions with the medium (skin depth), considering permittivity and permeability values. The experiments were all made in the absence of magnetic permeable materials.

Argillaceous rocks with relevant water content are considered as good conductors, while rock salt, granite or other crystalline rocks can be assumed to behave over a wide frequency range as poor conductors.

Field experiments

For the wireless energy transfer experiments though conductive media, the set-up consisted of a programmable signal generator, a power inverter, a tuned transmitter antenna, a tuned receiver antenna and a load resistance (Figure 27). The mobile, battery powered inverter provides high currents to the inductive load of the transmitter antenna. A coplanar configuration was used, with the antennas situated directly on the ground. For the comparison with coaxial configuration, some corrections were needed.

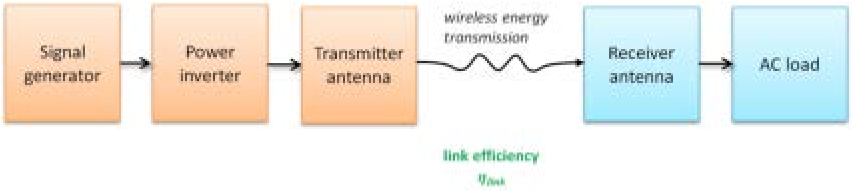

Figure 27. Set-up of the wireless energy transfer system.

Several experiments were performed in order to substantiate the interactions of the antennas with the environment. While large antennas are general favourable for high link efficiencies, a larger antenna might result in radiation resistances that affect the overall performance.

Figure 28 shows the effect of different heights and saturation degrees on the frequency dependent impedance of the loop antenna. Besides the wire resistance of 0.44 Ω, an additional resistance of 0.31 Ω was determined at the resonance frequency in the wet grassland. The effect of the conductive media is expected to be even larger when the antenna is covered on all sides.

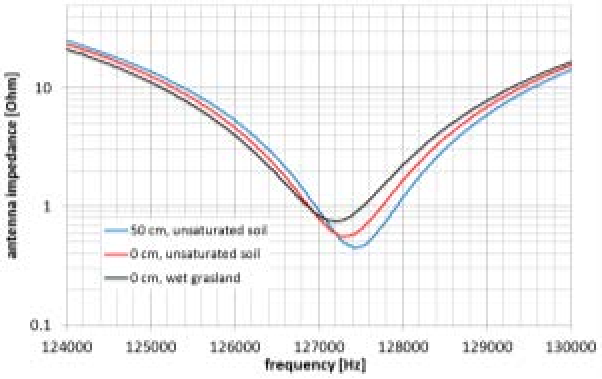

Figure 28. Field measurement of the receiver antenna's impedance at two heights above an unsaturated soil and on top of wet grassland

Wireless energy transfer experiments were performed for a coplanar for different load resistances and wireless distances of a receiver coil located on top of an unsaturated sandy soil and in a wet grassland, using the same experimental set-up, including the antenna tuning. On the shortest wireless distance (5 m), the measured power is comparable to the unsaturated situation. However, with increasing wireless distance, increasing attenuation is observed in the wet grassland, compared to the unsaturated situation.

It was demonstrated that wireless energy transfer is also feasible through highly conductive media, but needs some additional considerations regarding electrical conductivity and other factors to allow optimum transfer efficiencies.

In conclusion, wireless inductive energy transfer by using LF frequencies can be envisaged as a promising concept for powering repository monitoring sensors in general. However, reasonable power levels by inductive energy transfer require remarkably higher coupling between the antennas than usually required for proper signal-to-noise ratio for wireless inductive data transfer. In practice, this means shorter operation range and/or a need to apply bigger antenna diameters compared to data transfer systems.

The wireless transmission of energy over distances typical for sealing constructions as projected in typical disposal facility designs for radioactive waste (about 5 - 15 m, Appendix 2) is considered feasible. It was shown that the general concepts used for wireless energy transfer over short distances (smaller than the antenna radius) can be applied on longer distances reasonably well.

3.2.1.4 Miniature nuclear generators

ORANO (previously AREVA) studied nuclear batteries –also called Radio Isotopic Power Systems (RPS)- as an alternative power sourcing for wireless repository monitoring sensors.

For the past decades, the dominant RPS technology has been the radioisotope thermoelectric generator (RTG), which converts the decay heat of the radioisotopes into electricity through the Seebeck effect. These devices are widely used, with limitations mainly to space and nuclear environments.

RTG could also be a solution to provide autonomous power supply within a geological deep disposal of nuclear waste for monitoring and data transmission (including wireless) over a long period of time an option for areas of the repository where neither energy harvesting nor wireless energy transfer are possible.

An exhaustive state of the art study was carried on the possibilities offered by nuclear batteries and possible technical limitations of such a technology due to the physical conditions related to geological disposal. In addition, the work has involved a demonstration of the possibilities and technical limitations of an RTG type power supply inside intermediate level long lived (ILLL) waste vaults. This work is based on a preliminary design and thermal modelling of the RTG.

The aim of the state-of-art study was to perform an overview of miniaturized nuclear generator technologies in order to find the most suitable of them to develop an electrical power generator taking into account the constraints of geological lifetime disposal. The analysis is driven by the specifications (limit in vault concrete temperature, geometrical constraints) and environmental conditions provided by Andra [20], 7.1.2.

Among the technologies for converting the nuclear radiation energy to electricity, the thermoelectric conversion appears to be the most mature at the moment.

3.2.1.4.1 RTG design for geological disposal

Overall RPS performance is usually assessed from conversion system efficiency and specific power values. Conversion system efficiency is quite low, so a sufficient amount of heat production will be necessary, while it could be limited when copping specifications related to geological disposal. For the design of RTG for geological disposal applications with electric power levels of several watts, and according to the specific power value of the material used for heat production, quantities of kg or several hundred grams must be considered.

The isotope material should consider the type of radiation, the half-life of the isotope, the decay energy of the radiation, the cost of the isotope or the possible other radiation forms emitted by the isotope influencing shielding designs for nuclear safety purpose. These criteria limit appropriate materials to radionuclides with half-lives from 15 to 100 years that decay by alpha-particle emission over 99% of the time, of which only five exist.

Considering application to geological disposal monitoring, the equipment must also be robust, economically acceptable and consistent with regulations.

Among the materials considered, ^{241}Am is the preferred selection due to its specific thermal power and the possibility of extraction from stockpiles of transuranic waste, the bi-product of nuclear fission reactors. ^{241}Am is actually a weaker power source, however its greater half-life ensures a long term energy production as requiring for monitoring geological disposal.

The order of magnitude to feed an RTG of 5We and following the assumptions of 5 % conversion system efficiency, a radioisotope source of at least 100 Wth (thermal wattage) is required. This corresponds to about 100 cm^3 or about 1 kg of Am_2O_3.

The conversion efficiency of a TEG is extremely sensitive to temperature difference and to thermoelectric materials itself. For disposal application, due to a lower difference in temperature between cold and hot sides, lower efficiency could be a disadvantage.

AREVA has studied and proven the concept of using Mg_2Si-HMS (Higher Manganese Silicide) type TEG in order to improve the efficiency of the system. The conclusion of this study told that the thermoelectric performance of the material is confirmed by thermal model and the correlated experiment. One obstacle to using this material into the RTG for deep disposal will be its availability and the difficulty of its production process.

Another possibility could be to investigate new materials. Bismuth Telluride (BiTe) is commonly applied in terrestrial commercial applications and Bi_2Te_3 is available in a variety of commercial standard units and operates most efficiently with a cold-side temperature of around 320 K. Combined with the availability of standard commercial modules and relatively low cost, this makes Bi_2Te_3 a suitable selection.

In conclusion and regarding the RTG design for a geological disposal facility, the recommendation could be to use Bi_2Te_3 even if the maximum temperature is limited to 250 °C, because it is a well-known material with a mature and cost-effective production process.

3.2.1.4.2 Modelling

A thermal modelling analysis was performed to check compliance with specifications regarding geological disposal monitoring and to verify the feasibility of a 241 Am based RTG inside a vault while respecting a thermal criterion on the concrete. Different simplified designs were tested, and the numerical model considered the geological layer and the concrete of the disposal vault (6 ILLL waste containers).

A reference case was considered and the temperature gradient between the hot and cold side of the cooling plates was studied, including the impact of the concrete thermal conductivity, the length of cooling plates, the thickness of cooling plates and the thickness of the insulation material have been evaluated. The thermal criterion on the concrete was always met.

The numerical modelling showed that it is possible to evacuate the heat released by an RTG delivering an electrical power of 5 We inside a geological underground disposal facility, while respecting the thermal criterion on the concrete.

3.2.1.4.3 Economic aspects and potential commercialization

RTGs are considered a potential solution to the autonomous power supply in a deep geological disposal, in which neither energy harvesting nor wireless energy transfer are manageable. The purpose of the project is to pave the way for the feasibility demonstration of such an application. Beside the technical feasibility, future commercialization is an additional issue. Industrial and commercial development of ^{241}Am based RTGs will be derived from the actual needs, as well as from the standard drivers and optimizations. Building a RTG prototype for monitoring operations within geological disposal seems to be a realistic objective.

3.2.1.5 Energy storage

An energy storage technology analysis was performed by Arquimea to obtain a suitable solution that matches together the limited and sometimes intermittent supply capability of the power sources and the power consumption of the sensor and communication payload that usually is variable in time. Due to the intermittent working conditions of the wireless sensor unit (WSU), this typically requires rechargeable, intermediate energy storage as previously explained dealing with the WSU concepts for repository monitoring in general.

The requirements of the WSUs for repository monitoring considered are limited to the ones that are relevant for the energy storage subsystem, and will vary depending on the monitoring concept and applied power source of the WSU. A reference WSU, with selected numerical values with a reference scenario was selected, these values being the most representative ones.

The reference WSU is based on the Arquimea wireless system that was installed at LTRBM demonstrator. The system is composed by two buried WSUs with two new types of psychrometers, one pore pressure transductor and one capacitive relative humidity sensor. A third unit was placed in the gallery and will collect data from the buried ones.

The environmental requirements include the temperature range: 25 ºC - 45 ºC, humidity range: 50-100 % and maximum estimated radiation exposure conditions of 12 Mrads (20 years). The expected operating lifetime is between 20 to 50 years, the so called end of life of the WSU is the moment when the WSU is not able to provide any useful monitoring information. The sensor payload and the communication parts of the WSU are powered by a DC supply voltage, being the needed voltage level 3.00 to 3.63 V.

The operating conditions considered for a buried WSU consists of successive operation cycles, each of which involves a long-lasting sleeping period and a short activity cycle. During the activity cycles, the WSU will perform the measurements and transmit the data twice a day (every 12 hours). The WSU remains in sleep mode with extremely low power consumption between the activity cycles.

The energy supply the WSU will need to provide will depend on the number and type of sensors as well as of the time between the measurements or activity cycles in general.

The estimated energy consumption of the reference WSU during each 12 hours' operation cycle is 9.26 mWh (33.3 J) that can be divided into a base consumption of 0.15 J to cover the stand-by current and 33.15 J consumed by the 2 minutes activity cycle. The maximum instantaneous power demanded for the system is due to the data transmission (3600 mW).

In terms of energy, the demand of the reference WSU (33.3 J during 12 h) can be compared to the power output capacity of the thermal energy harvesting and wireless energy transfer systems presented in previous chapters. The distance wireless energy transfer is 10 m through host rock with low conductivity (0.05 mW).

3.2.1.5.1 Energy storage technologies

From the different requirements for energy storage, it is possible to outline: ultra-low power availability from harvesting source, long operating lifetime in years and peak current consumption of the payload. The combination of these requirements makes that any direct solution from the current commercial state-of-the-art cannot be directly used.

The available technologies for energy storage applied to low power energy harvesting analysed were: batteries, supercapacitors/electrostatic double-layer capacitors (EDLC) and electrochemical pseudocapacitors and hybrid capacitors devices.

<u>Rechargeable batteries</u>: based on galvanic cells that store energy in chemical form and are able to convert this to electrical energy on demand, typically by means of an electrochemical oxidation/reduction. They are widely used in wireless applications and have the advantage of providing a nearly constant voltage during most of the charge cycle.

Two technologies were considered: NiMH and Li-based. The first one do not suffer the loss of energy capacity due to repeated shallow recharge (memory effect) but require complex charging circuits that can provide high current pulses. NiMH batteries can be charged directly connected to an energy source, and do not need complex pulse charging circuits; the memory effect can be solved.

The big drawback of rechargeable batteries –that makes them non-applicable for the repository monitoring WSUs- is their short lifetime, limitation of high pulse current limitation, temperature efficiency and depth of discharge.

In conclusion, conventional batteries would be an appropriate solution during the initial years of the WSU, but the degradation of the batteries due to aging will reduce their lifetime and makes them not suitable for their use in geological disposals.

<u>Supercapacitors</u>: large capacity electrolytic capacitors that can be used as energy storage devices. They are based in two electrodes (positive and negative), a separator between them and a electrolyte filling the curves and porosities of the electrodes and the separator. Compared to the batteries, their main advantage is their capability of supplying high current pulses, consequence of their fast charge and discharge capabilities and low equivalent series resistance (ESR). Their large cycle life is also an advantage, although they do suffer from aging due to temperature and operating voltage ([34], [36]). The self-discharge [21], 7.1.2 of the supercapacitors must also be considered, as they can lose their energy very rapidly due to the parasitic leakage current that makes the capacitor to lose its charge without load. This parameter is dependent on the operational voltage and temperature and it increases as the total capacitance increases.

Considering a calendar life of 20 to 40 years, it would be possible to select the capacitor (and related electronics) for the reference WSU, with a combination of several units according to the needed voltage as well as the drift of the capacitance.

If there were commercial available supercapacitors in the market with the parameters values worked-out by previous steps, the selection procedure would be finished. If not, iteration of the lifetime, voltage per supercapacitor and number of supercapacitors in series should be done. Temperature and current demand are considered invariant parameters. If not, an iteration process should be made for the selection.

As a conclusion, by following the design procedure described above, the needed capacitance of the reference WSU would be around hundreds of farads. Leakage currents of the state-of-the-art ultracapacitors of this size are in the order of magnitude of the currents provided by the harvesting system, thus hindering the utilization of the supercapacitors for the application.

Electrochemical pseudocapacitors and hybrid capacitors: Lithium Ion capacitors (LICs) have been recently commercialized with the objective to solve the drawbacks of supercapacitors and batteries previously discussed. They are hybrid capacitors that use a carbon-based material as the negative electrode that can be doped with lithium. The calendar life and life characteristics of these devices are under analysis and information about long lifetime (20-40 years) is not available. Studies as [41] demonstrate that Li-ion supercapacitors calendar aging is highly dependent on temperature and the state of the charge (voltage) along the operational time.

Pseudocapacitors: The pseudocapacitors are an evolution of supercapacitors with the objective of improving the drawbacks with respect to Li-ion batteries [22], 7.1.2. Commercial pseudo capacitors are available [23], 7.1.2, nevertheless their performance with respect to lifetime and self-discharge is not as good as Li-ion capacitors discussed above.

Battery-supercapacitor storage devices: Other interesting approach is the combination of supercapacitors/pseudocapacitors and batteries. Different studies such as [24], [25], [26], 7.1.2 analyse the potential of combining battery and supercapacitors.

3.2.1.6 Overall conclusions

The analyses and pilot systems indicate that the proposed three power sourcing technologies (thermoelectric energy harvesting, wireless energy transfer, nuclear generators) are relevant and feasible for powering repository monitoring wireless sensor units (WSUs). The activities helped to improve the understanding of the effects of the repository environment on the behavior and performance of the power sourcing and scaling the capacity of the power sourcing by adjusting the design parameters.

A rough comparison of the three technical options is given in Table 4.

Table 4. Rough comparison of the investigated energy sourcing options

Power sourcing option / Required/ desired feature	Thermoelectric energy harvesting from the HLW containers	Wireless energy transfer through the repository barriers	RTG nuclear battery
Typical output power capacity	tens of μW to a few mW per unit	tens of μW to several mW	several W
Operation mode	continuous power output	continuous or discontinuous power output	continuous power output
Temporal variations in power output	slowly decreasing power output, depending on decay heat of HLW	constant power output, can be adapted on demand by adjusting the power level of the power transmitter	slowly decreasing power output, depending on selected radionuclide(s)
Placement	one or more units can be placed in a disposal cell; application limited to heat-generating waste	placement preferably close to the sealing plug; application in all waste sections possible	flexible unit placement possible; consideration of heat transport necessary; application in all waste sections possible
Expected impact on disposal concept	low impact, placement in single barrier is possible with minor alteration of the overall heat flow	low, due to placement close to the plug	safety assessment of introduced radionuclides necessary, interactions between heat pipes and the EBS need to be considered
Specific future research needs	energy storage options, long-term reliability	energy storage options, long-term reliability, interactions with electrically conductive and magnetic permeable materials in the EBS, (automatic) antenna tuning	safety and long-term reliability, heat transport in specific placements, energy storage options in applications with high peak power consumption

The powering of the WSUs with limited power sources such as a thermal energy harvester using low temperature gradients or a wireless energy transfer system requires an additional intermediate energy storage that accumulates the sourced energy for the further need of the sensor and communication payload.

Typically, WSUs have a low duty cycle, i.e. the operation scenario allows long (e.g. several hours or even several days) energy accumulation periods between short activity cycles with sensor measurements and wireless communication. In this operation scenario, the sensor and communication payloads are kept in an ultra-low power sleep mode or even totally unpowered, and are activated periodically by an ultra-low power wake-up circuit. With this kind of WSU arrangement, which is also commonly applied in energy harvesting wireless devices in general, power sourcing levels even down to around 10 μW can be exploitable.

The work in Modern2020 Task 3.3 has also improved the understanding for designing the intermediate energy storage subsystem. Depending on the power sourcing capacity, power needs of the sensor and communication payload, and the required lifetime and environmental conditions, the energy storage subsystem can be a critical part for the performance and the reliability of the entire repository monitoring WSU. This concerns especially the lifetime (aging), the self-discharge of the energy storage components, and the maximum output power than can be supplied. Even though several energy storage technologies such as rechargeable batteries, electrostatic double-layer supercapacitors and newer type pseudocapacitors are commercially available, the design of an energy storage subsystem that can fulfil all requirements of typical repository monitoring WSUs can be a challenging task. The design of the energy storage subsystem may also set additional requirements to the capacity of the power sourcing and to the sensor and communication payload design concerning e.g. its operation scenario.

With the basic features of the proposed technologies well understood and its principal working demonstrated in this research, the follow-on steps after project Modern2020 should be targeted to the further development, demonstration and verification of the energy sourcing parts as more complete building blocks. Beyond this, the follow-on steps should also be targeted to integration, demonstration and verification of more complete pilot repository monitoring systems according to comprehensive repository monitoring strategies. In addition to the energy sourcing, these pilot systems should also include interim power storage and the management of the sensor and communication payload, encapsulation that can tolerate the target repository environment, and the external parts that interact with the EBS. The verification of these comprehensive repository monitoring pilot systems should take place in a testing environment that emulates as much as possible the final repository environment, including e.g. the ambient bentonite with moisture saturation, pressure and temperature drift. For thermoelectric energy harvesting, this could be based e.g. on a real-scale heater experiment. For wireless energy transfer, the testing environment should also involve all metallic and magnetic permeable components with potential effects to the magnetic field. Since monitoring behind safety relevant barrier usually does not allow accessing the devices after the installation, the future actions should also involve measures for improving the reliability such as redundancy, design by drift margins and component derating, and qualification and screening procedures.

3.2.1.7 Power sourcing

Three alternative power sourcing technologies were addressed closer in project Modern2020:

1. thermoelectric energy harvesting by exploiting the heat generated by the HLW (high-level waste),
2. wireless energy transfer through the repository walls or plug by LF (low frequency) magnetic fields,
3. RTG (radioisotope thermoelectric generator) type nuclear battery inside ILLL (intermediate level long lived) waste vaults.

Chapter 3.2.1.1 reports a feasibility study and laboratory experiments of a thermoelectric energy harvester pilot based on a TEG of size 40 mm x 40 mm and exploiting the heat generated by the HLW in the Dutch OPERA disposal concept. It concludes that the proposed energy harvester concept is an appropriate power sourcing option for wireless repository monitoring sensors and provides a relatively simple technical implementation. Assuming a long interim storage of 100 years, thermoelectric harvesting still allows providing energy over a period of more than 100 years after disposal. The output power capacity is limited by the temperature gradient across the barrier in which the harvester is placed. However, a higher output power might be achieved for waste with a shorter interim storage history (i.e. < 100 years), or if the harvester device bridges more than a single barrier component, as is conservatively assumed here. To increase the output power, several TEGs can also be applied in a TEH, and several TEHs can also be distributed over a disposal cell. The low output voltage of the TEG (typically in tens of millivolts) results in a rather small efficiency of the voltage step-up converter that is necessary at the TEG output. The decay of the heat production of the HLW will drop the output power capacity in the course of the repository operation. This is not necessarily a problem, assuming that the intervals between the sensor activity cycles will become longer in the course of the repository operation, which is relevant due to the slower changes of the HLW and the EBS after few decades. Still, output power levels of several hundreds of microwatts at the beginning and some tens of microwatts after 100 years operation are possible with the pilot concept. This can power low duty cycle operation of various wireless sensor nodes by use of intermediate energy storage to accumulate the energy for the activity cycles of the sensor payload and the communication parts. Further research is needed when it comes to qualifying the used materials and components with respect to long-term reliability and moderate radiation field as present in the proposed concept.

Chapter 3.2.1.3 reports the feasibility studies and pilot experiments of inductive wireless energy transfer by magnetic field between two loop antennas. It concludes that this is also a relevant power sourcing option for wireless repository monitoring sensors. For example, supplying some tens of microwatts by a 100 W power transmitter to a WSU behind a 10 m repository barrier comprised of low-conductivity host rock is possible with a 2 m x 2 m power transmitter antenna and a 180 mm diameter power receiver antenna in the WSU. Energy transfer through an electric conductive media is shown to be feasible as well, if interactions are understood and covered in the design of the energy transmitter. With an optimized antenna design, link efficiencies of several hundred ppm were achieved, despite of interactions with the conducting medium. For the wireless distance of interest (10 m), interactions with the medium need to be considered in the case of argillaceous host rocks, (saturated) bentonite or cementitious materials. In case of higher conductivities (> 50 mS/m), lower frequencies than 125 kHz should be preferred. For reasonable power levels, resonance tuning of the antennas is necessary. The operation distance and powering capacity can be improved by increasing the antenna diameters that can be adapted to meet the powering needs of the sensor and the size constraints of the repository environment. In general, LF (e.g. 125 kHz) magnetic fields can penetrate through the host rock and the EBS, but larger metallic parts in the repository structures may degrade the powering capacity due to field attenuation, and may also require additional effort for keeping the antennas tuned. On the other hand, materials with high magnetic permeability can also enhance the powering capacity, and careful analysis and testing of each application case is necessary to optimize the power transfer efficiency. As with the thermoelectric energy harvesting, accumulation of the energy into an intermediate energy storage with associated sleep mode arrangements of the sensor payload and communication parts are obviously necessary. A useful option in the wireless energy transfer is the implementation of wireless communication by shared antennas and RF front end, which makes the overall system more compact and eliminates possible co-existence problems and double efforts of the adaptation of two independent inductive systems. An advantage of the wireless energy transfer is also the absence of wearing parts, even though the temperature variations and long-term aging of electronic components may cause performance degradation, especially because of antenna detuning. Another advantage of the wireless energy transfer is its lower impact to the disposal concept in general, since its components can be placed close to sealing plug. A general conclusion from all the previous is that the wireless energy transfer systems have to be adapted carefully to the specific repository environment, which also calls for additional research efforts.

Chapter 3.2.1.4 reports a generic state-of-the-art of nuclear batteries, which is followed by a feasibility analysis, conceptual design and thermal modelling of an RTG type nuclear battery in an ILLL disposable vault. It concludes that further steps for developing an RTG prototype are relevant, for which the results also give guidelines. The RTG is composed of a specific radioisotope heat source with α-particle emission and a TEG. Thus, the physical operation principle of the RTG is much the same as that of the thermoelectric energy harvester that exploits heat generated by the HLW. However, the power output capacity of RTG's is much higher due to the higher temperature gradient across the TEG, which is enabled by the better thermal connection between the TEG and the radioisotope heat source due to the absence of the design constrains caused by the repository concept. In many cases, the high output power can cancel the need of the intermediate energy storage that is prone to limit the lifetime of the WSU. According to the estimations in Chapter 4.2.1.4.1, an RTG with 1 kg Am_2O_3 heat source can produce several watts of electric power, which can be enough for continuous powering of many types of repository monitoring sensor nodes without any intermediate energy storage. Due to the relatively long half-life of ^{241}Am (433 yr) compared to the main isotopes that dominate heat production in HLW, the decay of the output power capacity is slower than with the proposed thermoelectric energy harvesting concept.

3.2.1.8 Energy storages

In WSUs, the peak power consumption during measurements or data transmission can be larger than what is continuously supplied by a power source. Here, a rechargeable intermediate energy storage subsystem is necessary for buffering the sourced energy. To define the requirements of the energy storage subsystem, an energy budged analysis of the WSU is a useful tool.

The energy storage subsystem is a critical component, affecting the performance and reliability of the repository monitoring WSUs. Relevant features are the lifetime (aging) and the self-discharge of the energy storage system. These features depend much on the technology of the energy storage, but also on the environmental conditions such as the temperature, and on the operational conditions such as the terminal voltage, charging state or the rate of charge-discharge cycles. In addition, the energy storage capacity, output current capacity and the voltage range of the energy storage components have to be addressed in the design. The design of the energy storage subsystem should also consider the optimal configuration of the energy storage components in series and in parallel, the voltage conversions between the power source and the WSU payload, and energy storage component derating (selecting oversized capacity). The combination of all these requirements makes the design of the intermediate energy storage subsystem a challenging task.

Currently, the intermediate energy storage subsystem of WSUs in general is typically based on small rechargeable batteries or supercapacitors, which are not optimal for repository monitoring WSUs, especially because of their limited lifetime, which can be characterized as both calendar life and cycle life (maximum number of the charge-discharge cycles). In many repository monitoring application cases, the self-discharge (concerning especially supercapacitors) and the output current capacity (concerning especially batteries) of the energy storage components may also cause problems. Since the aging of the batteries and supercapacitors depends much on the operation temperature, WSUs operating at relatively high temperatures should be avoided.

To overcome the above mentioned problems of the rechargeable batteries and supercapacitors, the component manufacturers have developed novel energy storage technologies such as electrochemical pseudocapacitors and hybrid capacitors, which are potential energy storage technologies for repository monitoring WSUs but currently lack reliable data about the effects of aging. There are also novel long-life non-rechargeable (primary) batteries based on Lithium Thionyl Chloride chemistry that, combined with a capacitor for supplying peak currents, can be a possible energy sourcing solution for repository monitoring WSUs with relatively low energy consumption.

3.2.1.9 System integration

The work behind this document has been focused to the development and evaluation of the energy sourcing technologies as separate building blocks without any actual integration into entire repository monitoring WSUs or systems. Thus, the follow-on activities after Modern2020 should also involve the integration and verification of the energy sourcing parts as a building block of more complete systems that also involve the sensor payload, wireless communication, encapsulation and the necessary repository external parts. Moreover, this work should also be connected to the overall design of the monitoring systems with possibly several wireless sensor nodes, and even to the repository monitoring strategies.

For the repository monitoring WSU integration, a key issue is the matching of the power/energy sourcing capacity and the power/energy consumption demand, which may require scaling either or both of these parts. With limited energy sources such as thermal energy harvesting from the HLW or wireless energy transfer, an intermediate energy storage and WSU energy budged analysis are necessary. The energy budged analysis should address e.g. the energy consumed by each activity cycle of the sensor (joules), the rate of the activity cycles (measurements per hour/day/week), and the peak power consumption during activity cycles (watts). The power/energy consumption may be scaled e.g. via the rate of the activity cycles and the sensor configuration in each activity cycle. The power/energy sourcing may be scaled e.g. via the number of the TEGs or the size of the power transmitter and power receiver antennas, in which the design constraints due to the repository environment have to be taken account of.

3.2.1.10 Reliability improvements

Since monitoring devices that are installed behind safety relevant barriers do not allow access after the installation, among the most important future design drivers of the energy sourcing parts (as well as the repository monitoring WSUs in general) will be maximizing their reliability. For this, following measures are applicable:

- redundancy,
- anticipating drift margins and component derating,
- qualification and screening.

Redundancy, i.e. the duplication of critical components or functions of a system, is conventionally being applied e.g. in spacecrafts. In the case of the energy sourcing parts of repository monitoring WSUs, the redundancy can mean e.g. including several thermoelectric energy harvesters, a combination of thermoelectric energy harvester with a wireless energy transfer system, or including several energy storage subsystems by cold redundancy, i.e. keeping the redundant subsystems unpowered.

Allowing drift margins for changing environmental conditions (e.g. temperature) and component aging, as well as component derating (operating a device below its maximum rating in order to extend its lifetime) are also widely used design methods in critical systems. For example, ensuring the long-term performance of wireless energy transfer systems requires drift margins for the antenna tuning, which may also call for some auto-tuning arrangements. Component derating concerns especially the energy storage devices, the aging of which depends typically much on their operating conditions such as the voltage and the temperature. Nevertheless, the aging of the energy storage devices reduces their capacity, and thus some capacity drift margin is necessary, too. It is also important to minimize the environmental stress of the WSUs in the system level design of the repository monitoring, for example by placing the devices in low and constant temperatures as much as possible.

Qualification means a procedure of actions for providing that a system or its component perform correctly under the requirements. The qualification procedure can be applied to the whole system or to its critical subsystems or components. As examples, the qualification of the energy storage subsystem can involve performance tests by accelerated aging at high temperatures or accelerated charge-discharge cycles, and qualification of the electrical components and subsystems may involve radiation tests if the effects of the radiation are assessed as a risk. The same procedures can also be applied e.g. to screening the energy storage component lot for the final implementation.

3.3 New sensors

3.3.1 Introduction

Task 3.4 of Modern2020 was intended for carrying out several RTD developments in order to devise new in-situ sensors tailored to geological disposal. A nuclear waste repository is a harsh environment. This feature is a major issue for the design of reliable, long-life equipment. Expected environmental conditions in each of the identified potential monitoring areas are mainly defined by seven parameters: temperature, mechanical pressure, hydraulic pressure, water saturation, salinity, radiation and displacement.

As given by previous MoDeRn project there are sensors and techniques to develop solutions for monitoring the most relevant parameters that inform about the proper THMC evolution of the EBS system of the repository. However, for some parameters the existing ones are not good enough or for others simply they do not exist. This is the reason to propose the development of new solutions or **new sensors**. Besides, the traditional monitoring technologies are in general based on wired sensors, these wires could impair the functioning of the EBS designed for the Repository and thus alternatives should be used to avoid that. First option could be to use **distributed fibre optics** solutions that provide multiple measurements using one single and thin cable. This is the second research line proposed for task 3.4.

The summary of the developed sensors and studied techniques is as follows. They are described in more detail in this chapter.

NEW SENSORS:

- Thermocouple psychrometer
  Development of a new sensor based on thermocouple psychrometers operating under the dew point method to measure water content in the bentonite barriers when close to saturation state.
- Displacement sensor (non-contact)
  Research on non-contact techniques for new short-range displacement sensors to be buried into the engineered barriers system to track potential movements of canisters, plugs, etc. This kind of sensors should solve the problems (mechanical damages and preferential paths in the EBS) due to the use of standard extensometers.
- Ion selective electrodes
  Development/adaptation of ion-selective electrodes to repository conditions for measuring e.g. Ca^{2+}, Mg^{2+}, Na^{+}, K^{+}, S^{2-}, and H^{+} ion activities to monitor chemical processes in the long term.
- Combined THMC sensor
  Development of a combined Thermal Humidity Mechanical Chemistry (THMC) sensor intended to reduce the volume and energy need of these sensors that use to be installed in parallel. Thus a small combined cell to measure total pressure, temperature, pore pressure and optionally humidity will be developed. Besides, it will be designed to eliminate the weak points of existing total pressure cells (the tube connecting the measuring cell with the transducer and its big size) while maintaining the same precision and accuracy. The proposed integration of transducers and electronics will improve the reliability by providing digital data.

DISTRIBUTED FIBRE OPTIQUE SOLUTIONS:

- Research on custom-made fibre Bragg gratings (FBGs) in order to obtain an irradiation sensor based on FBGs photo-inscribed in specialty optical fibres by means of a femtosecond pulses laser. Improve a hydrogen sensor based on FBGs surrounded by a catalytic sensitive layer made of tungsten oxide doped with platinum. Develop a pH sensors based on tilted FBGs covered with a micro-porous coating consisting of a pH indicator (bromophenol blue) encapsulated in a silica sol-gel matrix.
- Development of an optoelectronic sensing chain to supply distributed measurements of four parameters: temperature, strain, hydrogen and radiation, separately or at the same time. It will be done taking advantage of the huge influence of optical fibre dopants and primary coatings to enhance the influence of one only parameter while annealing the influence of the three other. To reach this ambitious goal, the system will rely on two or three scattering measurements, namely Brillouin, Rayleigh and Raman scatterings.

- Development of a method, based on fibre-optic distributed sensing of thermal conductivity, to measure density and water content in the EBS by means of heatable fibre-optic cables as well as development of fibre-optic pressure cells for borehole applications.

3.3.2 New sensors

3.3.2.1 Thermocouple psychrometer

In previous MoDeRn project it was identified the need for better water potential monitoring on bentonite-based materials near saturation (100% RH) because the existing ones were not optimal for work in this type of facilities. Thermocouple psychrometers usage has been demonstrated for bentonite suctions below -6200kPa (95%-100%RH).

3.3.2.2 Measuring basis

There are two different methods to obtain the water potential values of a sample, the dew point method and the psychrometric method. In both methods a pulsed current cools the junction below dew point temperature and Water droplets are deposited on junction. In the Psychrometric method the Current injection stops, junction is let to return to thermal equilibrium and water evaporates at dew point temperature producing a slope, see Figure 29 In the dew point method a current modulation compensates the evaporation process and the water neither condensates nor evaporates, achieving equilibrium at dew point temperature.

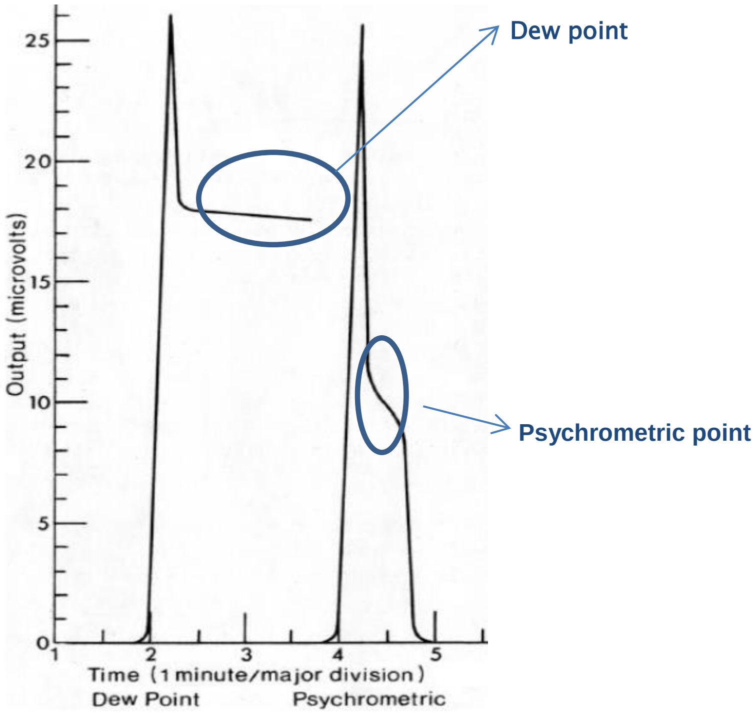

Figure 29. Graph of water potential

3.3.2.3 New sensor

The existing thermocouple psychrometers (manufactured by Wescor USA) were so far read using the psychrometric method, using a datalogger. This method with time conducts to the deposition of salts in the measuring head and then to their fast malfunctioning by corrosion. A new electronics to measure the sensor based on thermocouple psychrometers was developed by Arquimea, operating under the dew point method to measure water content in the bentonite barriers when close to saturation state (100% RH).This method keeps the measuring chamber in equilibrium with the surrounding material and avoids the deposition of salts being more accurate as well. In addition, the sensor was protected by means of a steel body and a more robust filter. The new sensor is designed to be buried, with low power consumption, cost-effective, lightweight and versatile. A photo of the developed senor is shown in Figure 30.

Figure 30. Thermocouple psychrometer view

3.3.2.4 New electronics

The require electronics has been designed on a printed circuit board and some demonstrators have been manufactured, like the one shown in Figure 31.

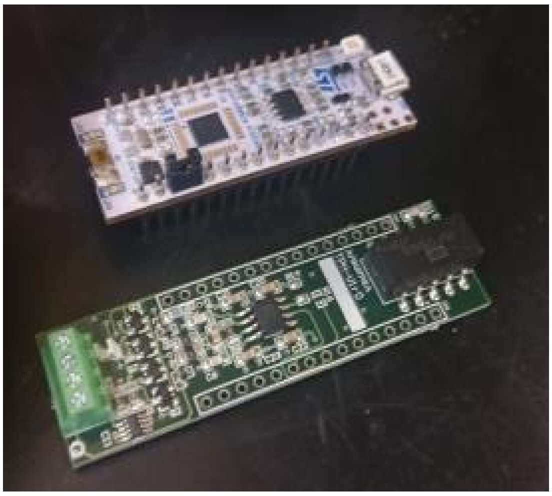

Figure 31. Proposed electronics

Two configurations for the sensor and readout units have been considered;

- Electronics integrated together with the sensor in a same casing. This configuration can be used in other applications different than nuclear waste repositories (for instance in the agricultural sector).
- Sensor and readout unit are separated and connected between them via cable. This configuration is the one that was fabricated for the demonstrator LTRBM.

3.3.2.5 Testing

Two different tests were done to check the sensor sensitivity, one internally in the Arquimea installations and the second one with an independent laboratory.

The internal tests were done inside an adiabatic sample chamber, Figure 32, using calibrated water potential standards (-725 kPa & -2500 kPa).

Figure 32. Chamber used in the internal tests

The obtained results demonstrated sensitivity to water potential changes are shown in Figure 33 and Table 5.

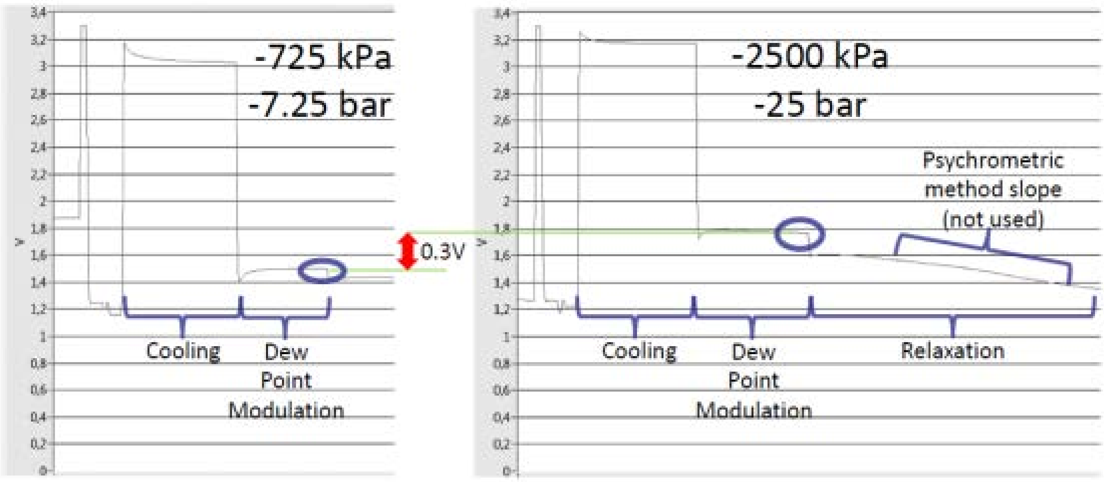

Figure 33. Water sensitivity obtained with the internal tests

Table 5. Results of thermocouple psychrometer internal testing

Specimen	Water Potential of the sample	Date	Hour	Measured dew point	Statistics	Comment
#0	-25 bar	21/05/2018	15:51	18.28 µV	$\bar{X} = 18.36$ µV $\sigma = 0.06$ µV	Good sensitivity: 0.85 µV/bar
#0	-25 bar	21/05/2018	16:02	18.35 µV		
#0	-25 bar	21/05/2018	16:05	18.40 µV		
#0	-25 bar	21/05/2018	16:08	18.40 µV		
#0	-7.25 bar	22/05/2018	17:20	3.15 µV	$\bar{X} = 3.28$ µV $\sigma = 0.12$ µV	
#0	-7.25 bar	22/05/2018	17:29	3.20 µV		
#0	-7.25 bar	22/05/2018	17:39	3.41 µV		
#0	-7.25 bar	22/05/2018	17:51	3.36 µV		

The external tests were done using a calibrated humidity generator, working within the 97.8-98.8% range. Five different sensors were tested, Figure 34, two units were evaluated in relation with sensitivity with 6 points and the other 3 units were evaluated regarding accuracy with 2 points.

Figure 34. Sensor prototypes view

The obtained results are shown in Table 6.

Table 6: Thermocouple psychrometer external testing results

Specimen	#0	#0	#0	#0	#0	#0	#1	#1	#1	#1	#1	#1	#2	#2	#3	#3	#4	#4
RH reference (R, %)	97.80	97.90	98.10	98.61	98.60	98.38	98.06	98.09	97.87	98.65	98.58	98.57	98.40	98.30	98.44	98.36	98.18	98.35
RH measured (M, %)	98.57	98.57	98.60	98.80	98.83	98.85	98.63	98.62	98.62	98.96	99.03	99.05	97.16	97.34	98.75	98.75	98.17	98.33
Error (E, %)	0.77	0.67	0.50	0.19	0.23	0.47	0.57	0.53	0.75	0.31	0.45	0.48	1.24	0.96	0.31	0.39	0.01	0.02
Statistics	$\sqrt{\sum E^2}$=0.52%, M≈0.36·R, r2 = 0.85						$\sqrt{\sum E^2}$=0.53%, M≈0.61·R, r2 = 0.91						$\sqrt{\sum E^2}$=1.11%		$\sqrt{\sum E^2}$=0.35%		$\sqrt{\sum E^2}$=0.02%	
Comment	Good sensitivity						Best sensitivity!						Bad accuracy		Good accuracy		Best accuracy!	

3.3.2.6 Conclusions

The results showed that the new developed sensor, which uses the dew point method to obtain suction measurements, meets the objectives. The sensor sensitivity and accuracy were tested with calibrated samples showing a good behaviour.

3.3.2.7 Demonstration

Four units were installed in the LTRBM demonstrator of WP4.

3.3.3 Techniques for non-contact displacement measurement

3.3.3.1 Introduction and objectives

Under MoDeRn Project, impressive progress has been made in developing and analysing the capabilities of monitoring technologies in the fields of measurement probes and methods, data transmission, and energy supply. Many problems remained to be investigated, for example the possibility of measuring specific physical parameters by using non-contact techniques. This study should be preliminary to the design of new sensors able to overcome all the issues reported in past studies.

The objective of this work was to better understand whether non-contact techniques could be a promising solution for measurements in a harsh environment, in particular for monitoring displacements. The evolution of repository structures along time is one of the critical issues to be continuously monitored. The evolution could give rise to several deformations, e.g. deformation of openings (orientations and apertures, propagation rates) or canister movements due to the buffer maturation. Detecting displacements is the typical measurement method for the monitoring of repository structures and structural stability of openings.

Therefore, the aim of this work was to find alternative measuring methods with respect to the contact type sensors to track the position of the future canisters in the repository (see Figure 35), in order to avoid the lack of reliability and to better follow the movements, or to better ascertain the potential retrievability of the canister by checking the gap between canister and metallic liner or a concrete lining or the rock itself.

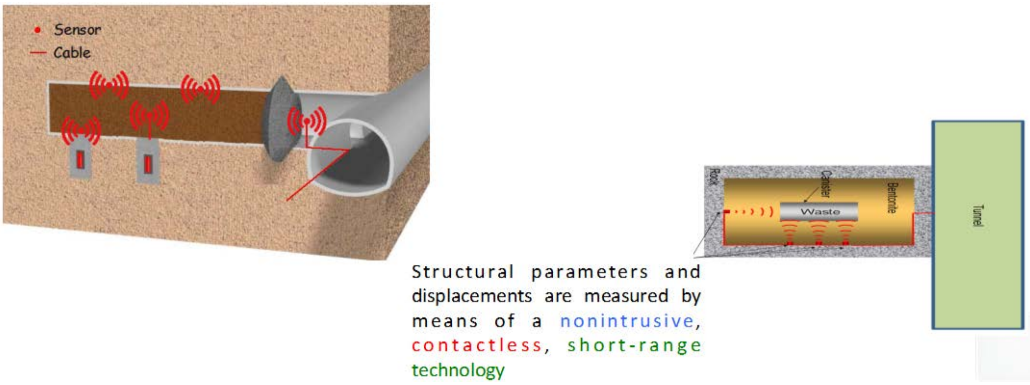

Figure 35. Schema of potential implementation of the sensor. (a) Overall view from the tunnel. (b) View inside the hole

3.3.3.2 Carried out work

Three different non-contact techniques for monitoring displacements have been investigated by ENEA. It should be observed that the presented approaches do not represent all possible solutions. They are only the methods that, to the authors' knowledge and expertise, give some potentialities for the design of realistic sensors for the considered problem. The three possible approaches have been here taken under investigation are the following:

- Ultrasonic techniques,
- Gradiometric techniques,
- Electromagnetic techniques.

3.3.3.3 Main results

3.3.3.3.1 Ultrasonic waves sensor

In this case the control of the metal body of the canister is carried out by means of ultrasound probes inserted in channels created in the bentonite or on the sides of the cavity. The ultrasound probes (20 - 50 KHz) can transmit or receive the waves in a timed manner, for example on 4 positions (Figure 36).

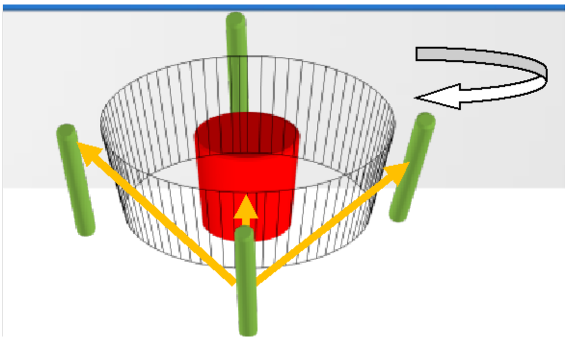

Figure 36. Ultrasound Sensor Scheme

The waves propagating from a transmitting probe in the bentonite/rock will invest the canister, which in turn will take the wave in different directions, that is eventually received by the 3 receiving probes. The process sees a transmitter probe and 3 receivers in alternating way, which rotates their role at each cycle.

Each cycle will have 3 different signals for the 3 receiving probes, i.e. for 12 cycles become 12 different signals.

The channels will have a certain length Y in which the probes run through (for example at every cm), and the probes emit and receive the corresponding 12 signals. After this scan, a mapping along the whole length of the cavity is obtained, and as a result of both the canister and the bentonite. This mapping is represented by a series of slices or morphological profiles that must remain unchanged over time.

3.3.3.3.2 Gradiometric Sensor

This is a completely new approach based on the fact that each object to be monitored produces a small but not completely negligible gravitational field produced by its mass distribution. Given a mass density distribution $\rho(\vec{x})$ describing the mass contained in each element of the object being monitored, a gravitational potential is produced, given by:

$$V(\vec{x}) = \int \frac{\rho(\vec{x})}{|\vec{x}-\vec{x'}|} d^3x'.$$

The integral is extended to the overall mass being monitored. This potential can be used to obtain various derived quantities, notably the gravitational force acting on whatever another object outside the first. An experimental procedure able to measure some of these derived quantities provides information on the potential $V(\vec{x})$ and therefore on the mass distribution generating it. Two types of measurement could be performed:

1. a **gravimetric** one;
2. a **gradiometric** one.

The first implies a measurement of the gravitational field in selected spatial positions outside the body (unit of measurement: Gal); the second a measurement of the field gradient (‘difference’) between couples of closely spaced points (unit of measurement: Eötvös).

An important difference between the two quantities is that (considering for simplicity a spherical mass distribution) the first scales as r^{-2}, while the second scales as r^{-3}, r being the distance between the sensor and the mass. Therefore, proximity to the mass being studied is an important factor to be considered, in order to obtain a sufficiently high signal-to-noise ratio. This should not be a significant concern for the present proposal, but it could require a further assessment in case of a realistic implementation.

The key point is that in principle a given motion of the object being monitored would produce a gravitational signal that could be measured by the gravimeter or gradiometer. It has to be underlined that the inverse problem one wants to solve (determining the mass distribution given the gravitational field it produces) does not admit a unique solution, as it is well known in geodesy and geophysics.

An important advantage of the gradiometric technique with respect to the gravimetric one is that the first – by construction – relies on the difference between two closely spaced measurements. Therefore, any disturbance external to the system (so-called ‘common mode’) would be largely cancelled, thereby greatly suppressing the corresponding systematic contribution in the measurement error budget.

Two different types of sensors can be designed and proposed for the detection of the displacement as in Figure 37. The first sensor is composed by two accelerometers in a differential configuration (sensing mass 1 and sensing mass 2) so to give a measure of the horizontal component. The second differential sensor is used for measuring the vertical component. While the first sensor is used in parallel to the cross-section of the canister, the second sensor will be inserted in the borehole and used as a moving sensor on a carriage inside the borehole. Using two sensors allows studying both displacement directions in a more feasible way, thus improving the reliability of results.

Figure 37. Schematic of potential implementation of the sensor

3.3.3.3.3 The EM waves technique

The EM approach proposed here is based on a combination of Ground Penetrating Radar (GPR) and Nuclear Magnetic Resonance (NMR) methods widely known in the literature. An EM method requires a specific characterization of the dielectric parameters the signal passes through. Several works proposed validated models that have been used in the simulations.

It should be underlined that the diagnostic systems based on the propagation of RF waves are limited from the maximum depth of penetration. This in turn is inversely proportional to the alternating current (AC) conductivity of the medium penetrated by the radiofrequency (RF) wave and therefore inversely proportional to the water concentration of the medium. In the presence of non-negligible water concentrations, it is therefore necessary to reduce the frequency of the RF wave so that it penetrates in the medium and can be detected with sufficient signal-to-noise ratio. In this way, however, the spatial resolution (limited by diffractive phenomena) tends to decrease overall, despite of a reduction in the length of the RF wave in the presence of media with a higher water content. The criterion to be adopted in order to operate in a dissipative medium consists in confining the electromagnetic field as much as possible using shields and/or conductive surfaces, and favoring the occurrence of resonant electromagnetic phenomena possible using shields and/or conductive surfaces, and favouring the occurrence of resonant electromagnetic phenomena.

The graph below (Figure 38) also shows the resonant frequencies where the measurement system has its best performance.

The first point allows limiting the power of the RF source that must guarantee, during the design phase, the exceeding of the minimum threshold of the signal-to-noise ratio allowed by the measurement system.

The second point allows to intrinsically improving the resolution of the measurement method but limits its measurement dynamics in which the system's response is linear.

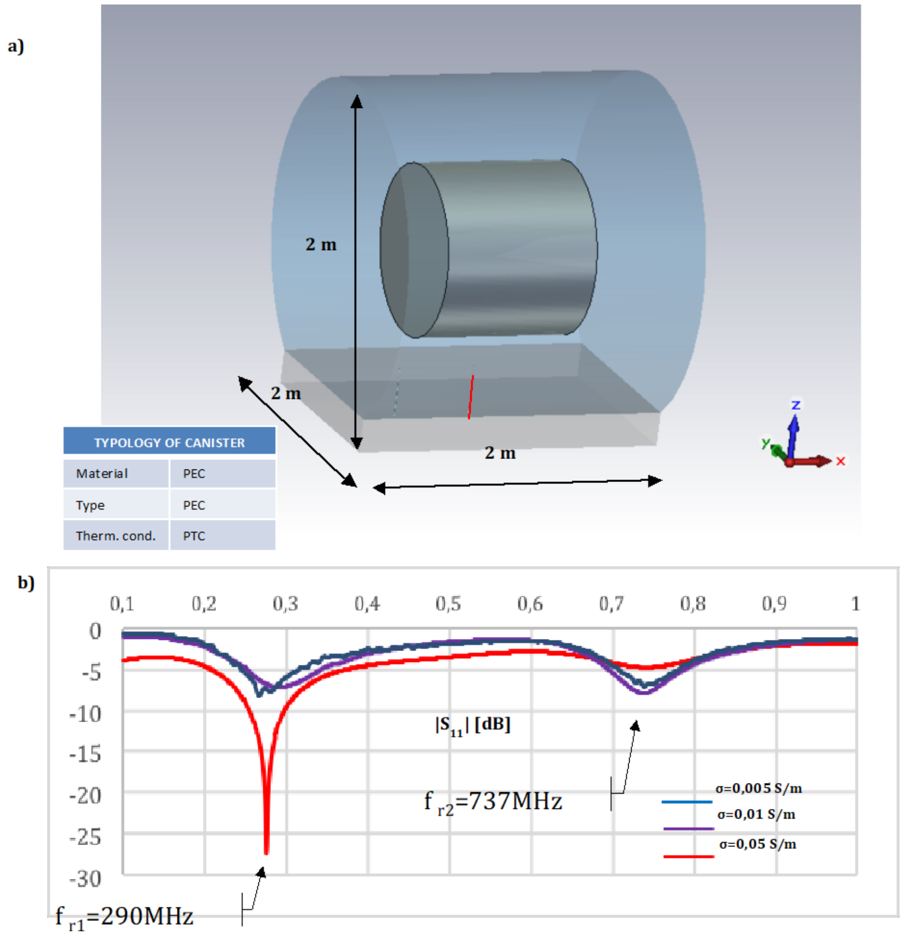

Figure 38. a) Example of a simulated scenario (in red the peakup antenna); b) trend of the scattering parameter S_{11} as a function of the frequency of the RF signal and of the conductivity of the medium σ or of the aqueous concentration

It is therefore clear that the resolution depends here on the quality factor of the analysed resonant mode, which in turn is inversely proportional to the water concentration of the medium. Both points can be guaranteed by selecting the range of wavelengths on which the measurement system will operate and the size and configuration of the measurement scenario (Figure 39.a).

The diagnostic method that will be examined evaluates the frequency response of the scattering parameters in reflection (Figure 39.b, where the trend of the scattering parameter S_{11} is shown at the two resonance frequencies as a function of the conductivity of the medium). The measuring system employs two or more electromagnetic peakups through which the resonance frequencies depend exclusively on the geometric conformation of the conductive surfaces will be preliminarily identified.

These resonance frequencies are the only ones able to propagate in the dissipative medium and be detected with sufficient confidence by the measurement method used. Figure 39 shows, for example, the distribution of the EM field relative to the scenario of Figure 39.a corresponding to two resonance frequencies for which it is possible to detect from the peakup antenna a signal with the best signal-to-noise ratio.

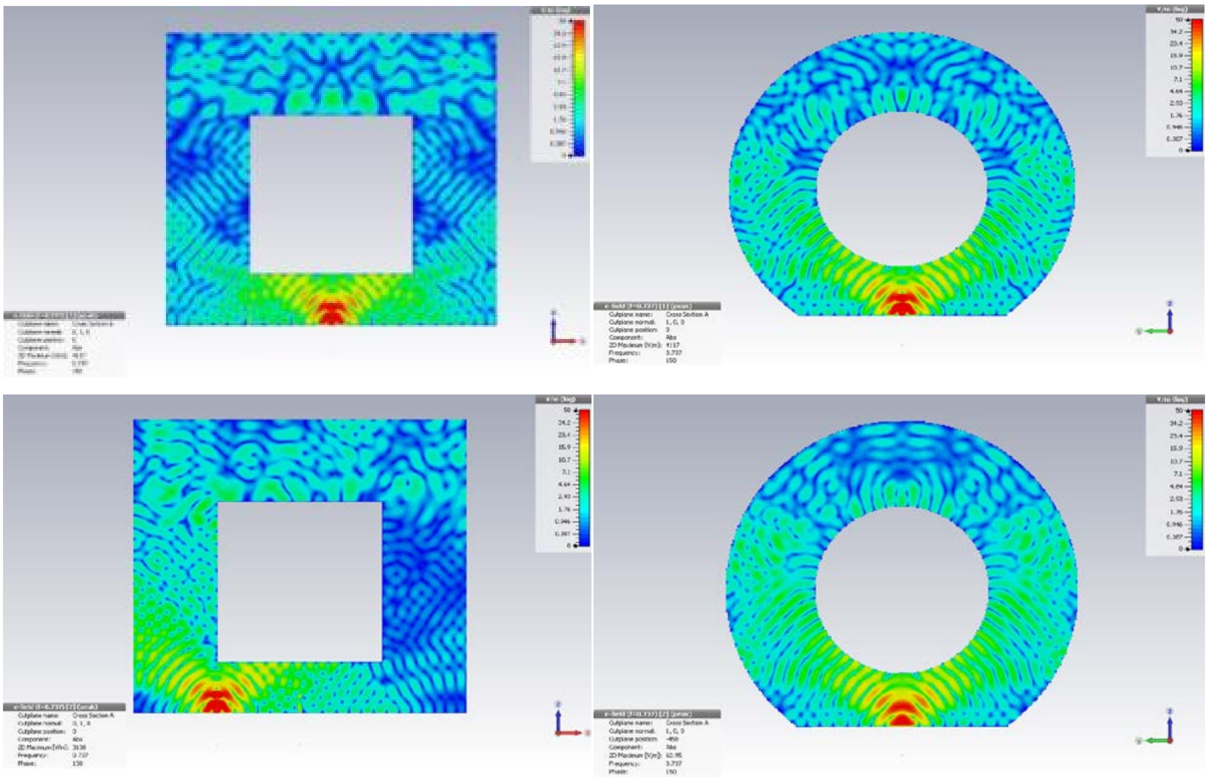

Figure 39. Distribution of the electromagnetic field produced by a patch antenna in correspondence of the frequency f_1 (top) and frequency f_2 (bottom) related to Figure 38.b

An elementary system of detection of the scattering parameters can be implemented by means of a bidirectional coupler that allows evaluating the ratio between the signal obtained in the reflection and the excitation signal.

Thanks to this measuring system it is possible to detect any variation in the geometry of the conductive surfaces: in fact, these correspond to a variation of the phase and the amplitude of the resonance frequencies.

The linearity of the phase and amplitude shift with the displacement of the analysed object and the corresponding sensitivity require a preliminary analytical and numerical study of the scenario.

3.3.3.4 Conclusions

According to the carried out work, all approaches could be suitable to solve the studied problem, yet several technical issues are to be faced before defining the best solution, which will be the result of a trade-off among accuracy, depth of penetration and complexity of the detection system.

A direct comparison among them in terms of pros and cons have not been considered being well beyond the scope and the objectives of this work, as it should involve not only physical considerations but also a direct evaluation of the maturity level of the correspondent technology.

Though, the objective of this activity has been to understand potential approaches to the individuation of alternatives to cable or contact existing technologies.

The *ultrasound waves technique* can be considered a mature technique already used in several applications for similar purposes. But in order to arrive to a real study of feasibility on the realization of a contactless sensor to be used for displacements measurement, more effort is required in order to design and test a prototype in a realistic application.

The so-called *gradiometric technique* is a novel technique, originally proposed by the authors for the first time in the context of the Project Modern2020, but it should be considered at this stage as a pure conceptual proposal, yet a very promising one.

More attention was paid to the third approach, i.e. the *EM waves technique*. This possibility has been widely considered both on the theoretical and the simulation point of view.

It was found that in the presence of non-negligible water concentrations, it is therefore necessary to reduce the frequency of the RF wave. However, the spatial resolution tends to progressively decrease. By effectively confining the electromagnetic field using conductive surfaces and appropriately choosing the wavelength range it is possible to favour the propagation of stationary electromagnetic waves which improve the overall signal-to-noise ratio of the device. However, the quality factor of the aforementioned modes is strongly influenced by the aqueous concentration of the dielectric medium. Vice versa, the frequency and the phase of the main resonant modes will be influenced by the position of the conductive objects and / or surfaces. Therefore, the analysis of the scattering parameters in reflection in correspondence to the resonant modes can be used to evaluate the variation of position of the conductive objects.

The linearity of the frequency/phase shift with the displacement of the analysed object and the corresponding sensitivity require a preliminary analytical and numerical study of the scenario. Preliminary simulation results confirm that as the frequency increases, the depth of penetration tends to dramatically reduce. But decreasing the frequency means that a higher antenna should be used. As a consequence, the design of the sensor should be done by a tradeoff between accuracy and geometrical dimension of the sensor (that should be designed so as to be easily included in the proposed environment). A detailed design could be done only after a thorough experimental campaign. The presented results could be used as a basic reference guide to start with.

3.3.4 Ion selective electrodes

3.3.4.1 Introduction and objectives

Direct measurement of ion activities in pore water of compacted bentonite are exceedingly difficult to perform because of the huge swelling pressure, which most of the sensors cannot withstand, also the low amount of the free water available for the sensors and long measuring times. VTT has developed a methodology for measuring pH and Eh in compacted bentonite. The aim of this study is to broaden the method of in-situ measuring relevant ion activities in the pore water of compacted bentonite. In this study commercial and house-made Ag/AgCl Cl-sensitive electrodes and Na sensitive “Nasicon” electrode with solution filling are tested in batch experiments, as well, H^+ sensitive IrOx electrode in diffusion experiment.

3.3.4.2 Basis

The ion selective electrodes used in this study are based on measurement of electrical potential difference between an ion selective electrode and a reference electrode. In an ideal situation the reference electrode is independent of the solution composition and the membrane of the ion selective electrode will be selective only for one species. The reference electrode will give constant potential and the potential of the ion selective electrode will change with changing chemical activity of the measured ion in a solution according to Nernst equation (1). Where, E is the measured potential, E_0 the constant value measured according to arrangement, R is the gas constant, T is absolute temperature, z is the charge of the ion, F is the Faraday constant and a is the activity of the ion in the solution (Janata, 2009).

$$E = E_0 + \frac{2.303RT}{zF}\log a \qquad (1)$$

Measurement is performed by placing pre-calibrated ion-selective electrodes in the holes bored in the compacted bentonite samples. Bentonite is then slightly compacted in order to obtain a good contact between bentonite and the electrode. The potential difference between the ion-selective electrode and an external reference electrode is measured by a voltmeter. The reference electrode is in contact with bentonite via solution (Figure 40). At the end of the measurement the ion-selective electrode and the reference electrode are calibrated again. The ion activity is calculated according to the calibration curve obtained.

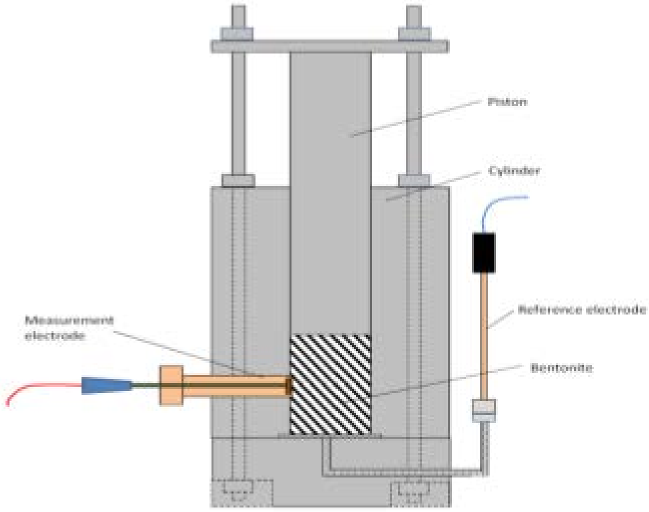

Figure 40: Schematic presentation of the test bench for ion-selective electrode batch testing. (Muurinen and Järvinen, 2013)

3.3.4.3 Preparation and compaction of the samples

Bentonite consists of montmorillonite and accessory minerals and both have an effect on the composition of pore water. Thus, bentonite has to be purified from accessory minerals and dissolved ions, e.g. chloride, if certain ion activities are to be measured. An example of initial chloride concentration effect on Cl activities in compacted bentonite samples can be seen in Figure 41.

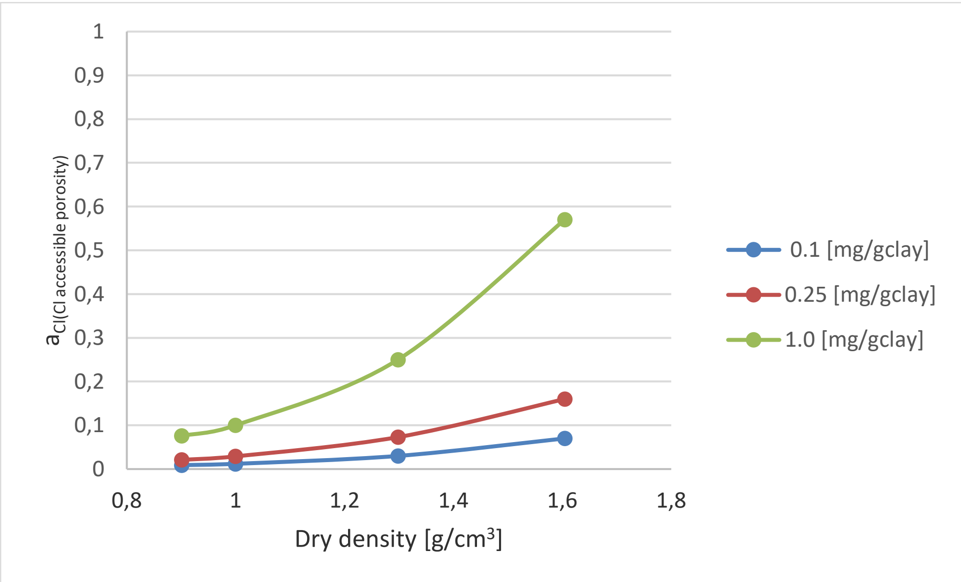

Figure 41. Bentonite initial Cl content effect on Cl activity in compacted samples when Cl accessible porosity is taken into account (Muurinen & Carlsson, 2013). The chloride activities were calculated based on the species in the Thermoddem database when using the *PHREEQC* code

The method described in Tributh and Lagaly (1986) was followed to purify the MX-80 bentonite at VTT. Photos of purified samples are shown in Figure 42. The unpurified MX-80 samples were used for testing chloride sensitive electrodes in batch experiments. Na-montmorillonite purified from commercially available MX-80 bentonite in tests with liquid-filled Na-sensitive electrodes was used. Diffusion experiment to measure pH changes in bentonite was performed using MX-80.

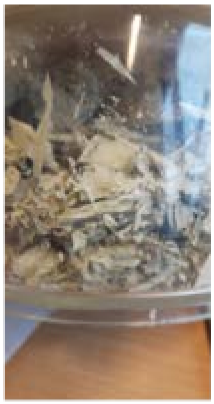

Figure 42. Purified Ca-montmorillonite on the left, MX-80 and grinded Na- and Ca-montmorillonites purified from MX-80 on the right

Two different procedures were tested for preparing samples. In the first case bentonite powder were mixed with salt solution of composition of studied salt concentrations (0.01, 0.1 and 1.0 M NaCl). Then mixtures were compacted at the target dry densities. In the second case bentonite powder was mixed with deionized water. Then mixture were compressed in diffusion or squeezing cells at the target dry density and were left for wetting first with deionized water for a month to guarantee fully saturated state of the sample.

The external saturation solution was changed to studied solution (e.g. 0.5M NaCl) and external water was allowed to equilibrate with studied sample by diffusion. In both cases the amount of liquid was calculated so that the samples reach fully saturated state at the target dry density. The picture of wetting samples can be seen in Figure 43.

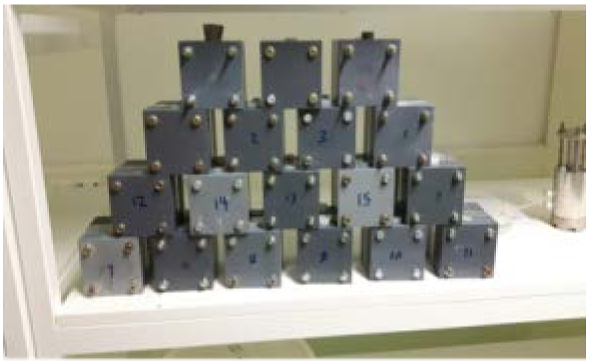

Figure 43. Diffusion cells for wetting compacted bentonite samples. On the right diffusion cell where external water sources are below and above of stainless steel sample holder. Liquid is separated from bentonite sample by sinters

3.3.4.4 Electrodes manufacturing

House-made electrodes (e.g. pH and Na) were prepared according to methods described in Yao et al. (2001), Muurinen & Carlsson (2007), Caneiro et al. (1991). Commercially available reference and chloride electrodes were modified to be suitable for test-bench. Some house-made and modified electrodes are presented in Figure 44.

Figure 44. On the right side house-made liquid filled Na-sensitive Nasicon and pH sensitive IrOx electrodes. On the left electrodes ready for experiments

3.3.4.4.1 Cl selective electrode

The chloride electrodes were made in-house at VTT by dipping a silver wire in molten AgCl and was used in experiments where samples were equilibrated by mixing. The commercial Ag-AgCl coated silver wires prepared from a fine- grain homogeneous mixture of silver and silver chloride (In Vivo Metric, Healdsburg, California, USA) was used in experiment where samples were equilibrated by diffusion. The coated wires are 1 mm in diameter and 2.5 mm in height with 10 mm silver wire. The silver wire was first soldered to a 7 cm long electric wire and placed into a PEEK tube in a PEEK screw. The PEEK tube was then filled with epoxy so that also the bottom of the Ag-AgCl pellet was fixed into the PEEK screw. When the epoxy was hardened, the slot between the sides of the Peek tube and the screw was filled with epoxy. A longer electric wire was soldered to the electrode and the joint was supported with epoxy.

3.3.4.4.2 pH electrode

Solid iridium oxide (IrOx) pH electrodes was prepared by high-temperature oxidation method (Yao et al. 2001) in which an iridium oxide film is formed on iridium metal wire in lithium carbonate melt. The pH electrodes were prepared in the following way: Ir metal wires (0.15 mm diameter, 99.9% purity, from Aldrich Chemical Company) of about 50 mm in length was cleaned first with 6 M HCl and then with deionized water. The wires were placed in a gold crucible filled with Li_2CO_3 powder. The oxidation of the Ir wires were performed at 870 °C for 5 h in a furnace under air atmosphere. After cooling down to room temperature, the solid carbonate in the crucible was dissolved with hydrochloric acid. The oxidized wires were then washed with deionized water to remove any attached soluble components. Finally, the wires were dried at 120°C overnight. As a result, a black oxide layer grew on the surface of the wire. In order to fabricate the pH electrode, a 10 mm long section of the oxidized wire were scraped clean and a connecting wire for the data logger was soldered to this bare end. The whole electrode, except the 7–10 mm long sensor part, was covered with a protective PEEK tube filled with epoxy glue and the soldering supported with a tube filled with epoxy glue.

3.3.4.4.3 Reference electrode

The reference electrode used was a commercially available Ag/AgCl electrode (LF-2) from Innovative Instruments, Inc., USA. The filling electrolyte is 3.4 M KCl. The electrode body is constructed from PEEK. The electric contact of reference electrode with the bentonite could be established through water in contact with the compacted sample through a sinter. Due to shifting of the potential, the electrode has to be checked frequently.

3.3.4.4.4 Na electrode with liquid filling

The aim of this part of the study was to find out if liquid filling as a conductor between membrane and conduction wire will improve stability of electrodes. Soldering was replaced by NaCl solution and Ag/AgCl electrode were used as inner reference electrode (Figure 45).

A Natrium Super Ionic Conductor (Nasicon) pellet was used for the membrane of the sodium electrode (Caneiro et al. (1991). The Nasicon powder was pressed for two hours at 4000 bars at 200 °C and sintered in an oven at 1000 °C. The membrane was fixed with epoxy to the electrode body and the electric contact between the membrane and the electric wire in the electrode was made with NaCl solution. The schematic presentation of liquid filled Na-electrode is presented in Figure 45.

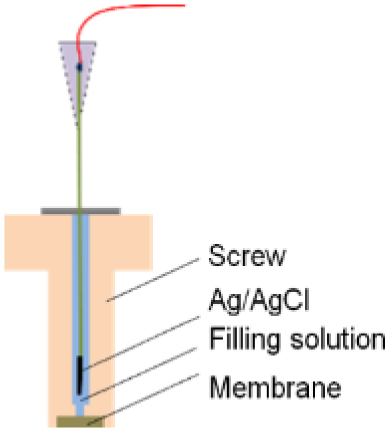

Figure 45. Schematic presentation of the liquid filled ion selective electrode

3.3.4.5 Results

3.3.4.5.1 Experiments with Cl selective electrodes

Chloride activities were studied in compacted MX-80 samples equilibrated with NaCl solution by diffusion or mixing method. House-made and commercial Ag/AgCl electrodes were used to measure Cl activities. Chloride content in samples was analysed by aqueous leaching method, where 0.3 g of dry bentonite were dissolved in 30 mL of deionized water, centrifuged, ultrafiltered and analysed by IC (ion chromatography).

Chloride activity was calculated using the analysed amount of Cl in sample [mg/gclay], water content measurements of sample and modelling. Water content was used to determine total porosity and dry density of samples according to equation:

$$\rho_d = \frac{\rho_s \times \rho_w}{\rho_s \times w + \rho_w}$$

where ρ_d is dry density, ρ_s = rock density, w = water content and ρ_w = water density. The Cl accessible porosity was calculated according to experimental equations determined for compacted MX-80 by Muurinen & Carlsson (2013). The modelling of chloride activity in studied samples was performed by PhreeqC using thermoddem database. The modelled Cl activities were compared with measured activities determined by ion selective electrodes.

Results of the measured Cl activities from samples prepared by mixing as example shown in Table 7.

The initial chloride content in studied samples are about 0.1 mg/g_{clay}, which means chloride activities from 0.01 to 0.06 for compacted bentonite samples in this study when dry density vary between 0.9 - 1.6 g/cm^3 (Table 7). This means that chloride activities in samples meant to be originally close to 0.01 are closer to 0.1, and thus 0.01 and 0.1 series have almost same Cl activities.

The calculated Cl activity according to analysed values and measured Cl activity with Ag/AgCl electrode correspond quite well with in most of the samples. Anyhow, some samples measured Cl activity with electrode is much lower than expected according to theoretical value (samples 1.1 & 1.4 in Table 7). This might be caused by inhomogeneous distribution of chloride due to mixing method used for preparation of the samples.

Table 7: Measured chloride activities by Cl^- selective electrodes for different densities and salt solutions

Sample Code	Target C_{Cl}	Water content	Dry density	Cl content	Experimental $C_{(Cl)tot\_vol}$	Experimental $C_{(Cl)accessible}$	PhreeqC $a_{(Cl)tot\_vol}$	PhreeqC $a_{(Cl)access.}$	ISE $_{Cl1}$ $a_{(Cl)}$	ISE $_{Cl2}$ $a_{(Cl)}$
[-]	[mol/L]	[w-%]	[g/cm^3]	[mg/gclay]	[mol/L]	[mol/L]	[-]	[-]	[-]	[-]
1.1	1	77.4	0.88	13.89	0.51	1.31	0.33	0.80	0.31	0.14
2.1	0.1	77.3	0.88	0.29	0.01	0.03	0.01	0.03	0.25	0.11
3.1	0.01	73.0	0.92	0.18	0.01	0.02	0.01	0.02	0.07	0.06
1.2	1	63.1	1.01	9.42	0.42	1.34	0.28	0.82	0.75	0.61
2.2	0.1	59.4	1.05	1.16	0.06	0.19	0.05	0.14	0.36	0.24
3.2	0.01	53.2	1.12	0.18	0.01	0.04	0.01	0.03	0.078	0.05
1.3	1	43.6	1.26	3.23	0.21	1.06	0.15	0.65	0.96	0.45
2.3	0.1	38.7	1.34	0.13	0.01	0.05	0.01	0.04	0.23	0.07
3.3	0.01	37.4	1.36	0.07	0.01	0.03	0.01	0.03	0.1	0.05
1.4	1	28.0	1.56	1.90	0.19	1.60	0.14	0.98	0.12	0.13
2.4	0.1	26.7	1.59	0.09	0.01	0.08	0.01	0.06	0.17	0.2
3.4	0.01	27.2	1.58	0.07	0.01	0.06	0.01	0.05	0.14	0.25

An example of the alternative preparation method for samples, where studied chloride concentration is equilibrated with sample by diffusion instead of mixing. Measured chloride activity by commercially available Ag(AgCl) Cl^- sensitive electrode seems to correspond very well with calculated activity in Cl^- accessible porewater.

3.3.4.5.2 Na selective electrodes with liquid filling

Na sensitive "Nasicon" electrode with filling solution was tested in Na-montmorillonite obtained by purifying MX-80, compacted at the target dry density 1.5 g/cm^3 and equilibrated with 0.1 M Na_2SO_4 solution by diffusion. The electrode was calibrated twice before experiments and once after experiments, results of the measurements are given in Figure 46.

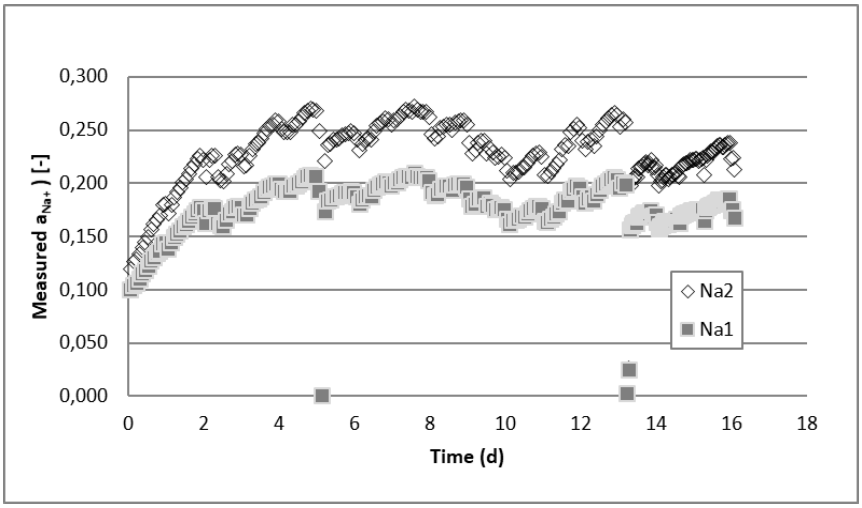

Figure 46. Measured activity of Na^+ in compacted bentonite saturated with 0.1 M Na_2SO_4 solutions.

According to PhreeqC calculations, the activity of Na+ in this kind of solution should be about 0.12. Na1 as calibration 1before experiments and Na_2 as calibration 2 before experiments.

The measured activity was close to 0.2. Anyhow, the simple geochemical modelling of studied solution showed the activity for Na+ about 0.12 in 0.1M Na_2SO_4 solutions. The calibration before experiments gave a straight line with a good corresponding with sodium activity changes in solution. After experiments the calibration curve slope was changed sign and work as the anion sensitive electrode (Equation 1). The reason for this might be the small leakage between membrane and screw which allows solution, used in calibration, to penetrate in inner part of electrode. Thus inner reference electrode (Ag/AgCl), sensitive for chloride, may cause the potential changes obtained by voltammeter.

3.3.4.5.3 Diffusion experiments with IrOx electrodes

The effect of a high pH solution on the pH in bentonite is studied with diffusion test bench in anaerobic conditions. The compacted bentonite sample was prepared using anaerobic MX-80 bentonite and anaerobic deionized water. Bentonite was mixed with water and compacted in a compaction cell nitrogen atmosphere inside a glove-box. The compacted sample was subsequently moved into the titanium tube. The dry density of the bentonite sample was about 1.5 g/cm^3. The three pH electrodes made of iridium oxide wire were placed in the bentonite and anaerobic deionised water was added to the external vessel. After 271 days the external solution was changed from the deionised water in equilibrium with bentonite (pH 8.4) to a saline solution of pH about 11.7 in order to simulate the effect of low-pH cement on bentonite in saline groundwater. Muurinen & Carlsson, (2008) started to experiments at 2006 and experiments have been kept going on since.

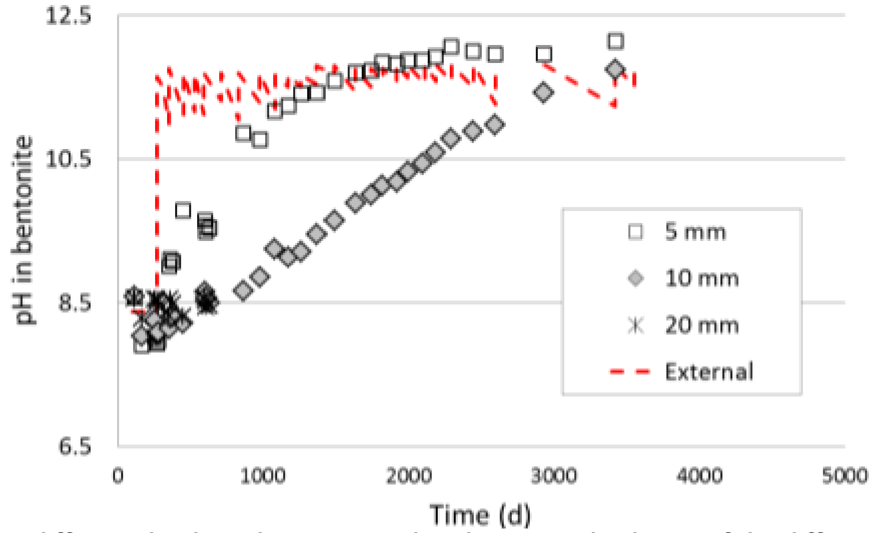

Figure 47. pH at different depths in bentonite and in the external solution of the diffusion cell sample. The solution chemistry was changed at 271 days from low-pH to high-pH

The same IrOx electrodes have been kept measuring during the last ten years, while as, reference electrodes have been calibrated and changed multiple times.

3.3.4.6 Results and demonstration

Obtained results showed that the developed electrodes could be applied to a real test to ascertain their performance. Three electrodes to measure pH, Eh & CL- plus the reference one were manufactured to be installed in the LTRBM demonstrator of WP4.

3.3.5 THMC smart cell

3.3.5.1 Introduction and objectives

There is a quite big range of total pressure cells on the market. They usually have at least 230 mm in diameter with a transducer attached in the steel tube. Typical transducers are vibrating wire (GeoKon), pneumatic (GLOTZL) or lately fibre optics. The CTU has developed and uses such pressure cells for civil engineering applications over 20 year. Although these sensors are reliable, there are some disadvantages of their usage for EBS. In particular, the size, the necessity to use them in combination with other sensors and with a data logger.

The desired new cell is basically a pressure cell, but it integrates also temperature, pore pressure and RH sensors and the reading electronic in the same package. Other requirements for the smart cell design were small size –less than 100 mm diameter-, low power & long-term battery operation, integrated processing plus data logging and digital interface (RS485, SDI-12) pH, Eh & CL-). From the mechanical point of view the design of smart cell is driven by the necessity to combine the pressure exchanger, which transfer total pressure from the surface of the cell into pressure sensor itself and housing for the electronics and other sensors.

The development of the smart cell has been performed joint by CTU and TUL.

3.3.5.2 Cell design

The new integrated cell is cylindrical 80mm in diameter and 25mm in height. It consists of a main stainless steel body, which has a membrane welded on top and steel lid on bottom covering the electronics compartment.

- The main body is major structural element. It holds all the sensors in place and provides shielded space for the electronics.
- The total pressure is measured using piezo resistive sensor submerged in the oil reservoir at the top main body. The reservoir is enclosed by top of main body and welded on membrane. It effectively acts as pressure exchanger transferring total pressure from environment into sensor. The range can be selected.
- The pore pressure is measured using same type of pressure transducer directly connected to the environment via side holes in the body and porous stone acting as filter. The usage of same sensor types allowed simplifying the electronics. The range can be selected.
- The RH sensor is exposed to the environment in similar way as pore pressure sensor. It sits in side chamber and it is protected by porous stone. It also serves for measurement of temperature along thermometers on electronics board.

Several versions of the body were manufactured before to reach the final design, Figure 48.

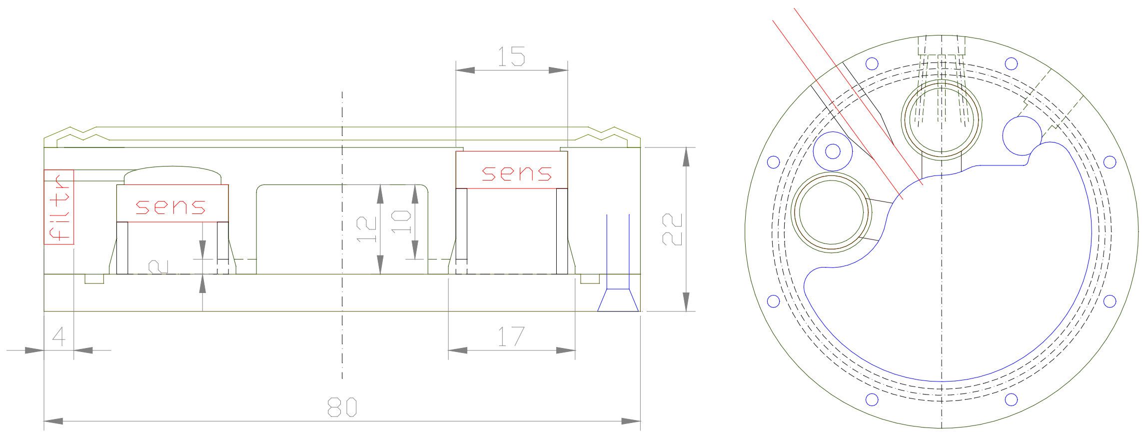

Figure 48. Cross section of the body design (images not to scale)

3.3.5.3 Cell electronics

Core electronics of the smart sensor cell is described below.

Power supply: lithium single cell battery (2.0-3.3 V). Model: CR-2354/GUN (Li-MnO2, 560 mAh)

Pressure Sensor:

- Resistance full bridge having overall resistance about 3 kΩ,

- Voltage to be supplied: 3 V,
- Diagonal output signal is amplified with a gain about 20.

Operational Amplifier: ADA4051

- Rail-to-rail, zero-drift chopping amplifier,
- Voltage to be supplied: 1.8-5.5 V with low consumption (13 μA).
- Low input current 5 pA does not load the bridge output.

Temperature & Relative Humidity (RH) sensor: SHT-25

- Resolution: 0.01 °C | 0.04 %RH,
- Precision: ±0.2 °C | ±1.8 %RH,
- Voltage to be supplied: 2.1 V with consumption 0.3 mA,
- Digital output of the sensor is read by I2C interface,
- Its slave address cannot be selected so only single device can be served.

Temperature sensor: SHT-21

- Same parameters than SHT-25
- Its slave address is different to SHT-25, so both sensors can communicate on the same I2C bus.

Data EEPROM Memory: AT45DB321E

- 32 Mb memory in 8-pad DF,
- N package with fast SPI interface,
- Working range: 2.3-3.6 V.

Microcontroller: STM32L052K8

- 32-bit RAM, Cortex-M0+ core,
- 1.65-3.6 V consumed, 88μA/MHz (core only, approx. per MIPS),
- 64 KB Code Flash,
- 8 KB SRAM,
- 2 KB EEPROM

Supply circuits and communication interfaces of the sensor cell are depicted in .

- **RS-485** is a standard, wide-spread and well-known industrial communication interface. Its driver chip requires 5 V with sufficiently high supply current but it works at high baud rates and long distances,
- **SDI-12** is a special interface for slow data rate sensors (e.g. meteorological) connected to a datalogger. It works half-duplex over single wire at 5-V-logical levels with baudrate 1200 Bd.

Both interfaces require signal for switching output driver on and the 5 V supply which is stabilized from an external voltage. Input supply voltage can vary not only due to external supply selection but also due to voltage drop on a connection cable.

The cell is connected to a remote data converter either stand-alone RS 485/Ethernet or notebook's RS-485/USB or to a datalogger (SDI-12) with standard 4-pair shielded UTP cable. The cell communicates at RS-485 baudrate 115.2 kBd that makes possible using the cable with length up to 300 m.

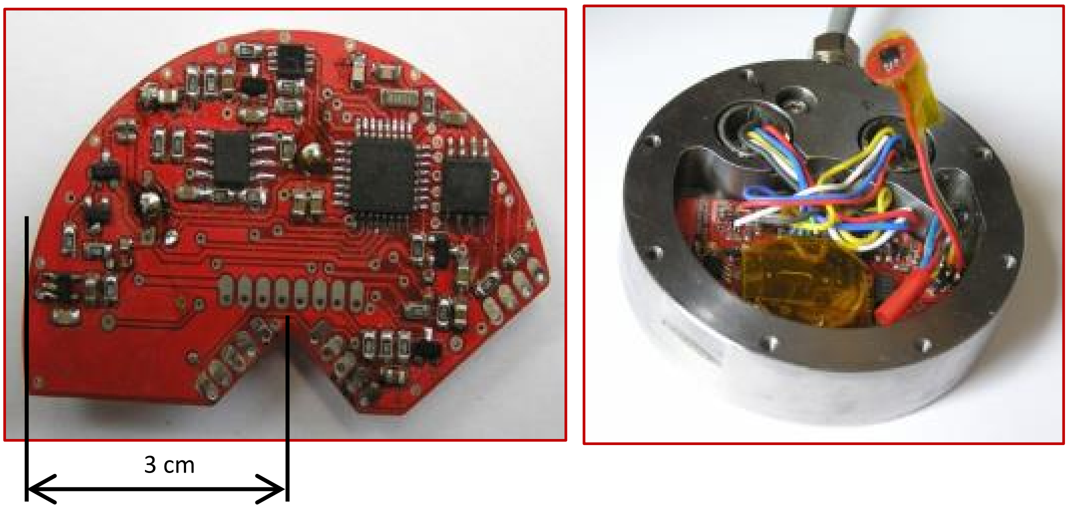

Figure 49. Bottom view of the PCB and cell electronic compartment

Since a record of one measurement sample contains 8 items of 16-bit integer number (compressed date, compressed time, 2×pressure, 2×temperature, humidity, battery voltage) the 32-Mbit data memory can store up to 262144 samples i.e. 3 samples/hour for 10 years.

3.3.5.4 Testing

The prototype (including electronics) was tested at CEG labs, Figure 50. The tests were promising but however too high temperature dependency was discovered. That has been tracked down to the oil expansion in the pressure exchanger.

Figure 50. 1st porotype test in press (heat toleration test in progress)

3.3.5.5 Results

It was tested with a laboratory supply replacing the battery. The pressure sensors were replaced with resistor bridges. Stable 14-bit value on the pressure channels has been achieved due to a huge ADC oversampling. Within the full voltage range 2.0–3.3 V a deviation of the value is only 0.3 %FS. Although the data sheets of some components show narrower supply range the electronics runs down to 2.0 V that makes possible full exploitation of the battery capacity.

Testing in a temperature chamber has verified a functionality of the electronics in the temperature range at least -20…+90 ˚C. A deviation of the pressure value within the temperature range 0…+85 ˚C is 0.6 %FS.

Consumptions at ambient and maximal working temperature are written in the table below. Energy spent during one MCU run period (i.e. sampling of all sensors and storing data inside memory) is recalculated per year at sample period of 3 samples/hour.

Table 8. Power consumptions

Temperature	Sleep current	Consumption	Energy/samp.	Cons. @ 3 S/h
+25 °C	1.04 μA	9.1 mAh/yr	$1.91 \cdot 10^{-4}$ mAh	5.0 mAh/yr

+85 °C	2.09 μA	18.3 mAh/yr	$1.99 \cdot 10^{-4}$ mAh	5.2 mAh/yr

Considering real (due to self-discharge and higher temperature) capacity of the battery as ½ of nominal, battery life at consumption 24 mAh/yr can reach 10 years minimally.

From the point of view of remote and sealed (behind the barriers) placement of the cell, an average demanded communication rate is 0.4 kbit/hour (0.1 bit/s) at above mentioned sample rate 3 S/h. It assumes to send data more efficiently, in binary form, which would require minor changes in firmware.

3.3.5.6 Demonstration

One cell was installed in the LTRBM (Figure 51), the electronic was completely potted for additional water protection. It was connected to the LTRBM PC via RS485 interface. As the LTRBM Data Acquisition System requires MODBUS protocol connection a new software was developed in order to connect the smart cell. The software translates smart cell asci based protocol into MODBUS.

Figure 51. View of two manufactured smart cells (cell on the left designed for LTRBM)

3.3.6 Optical Fibre Techniques

3.3.6.1 Fibre optics basis

Optical fiber technology is more and more studied for its use as transmitting element or as sensors in all industrial fields and particularly for nuclear industry. The reason comes from the optical fiber insensitivity to electromagnetic pulses and interferences as the key material is amorphous silica glass (SiO_2). Moreover, the low weight and small dimensions of the fibers make them also very attractive for space applications and reduce the quantity of waste after nuclear power plant dismantlement. Finally, this technology enables remote sensing; measuring devices can be placed hundreds of meters away from the sensing area, in safe enclosure where maintenance is ensured, which provides longevity for the whole sensing system.

In its simplest form, an optical fibre consists of two coaxial cylinders of different materials (core of refractive index nco and cladding of refractive index ncl) and a protection (jacket generally made in polymer material) as depicted in Figure 52.

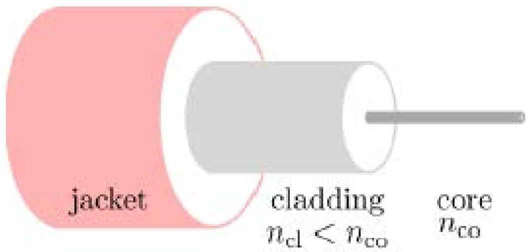

Figure 52. Geometrical structure of a singlemode optical fibre whose typical for silica-based fibres

Optical fibre sensors can be categorized in punctual (OFS) or distributed ones (DFOS) and can be used to measure many of the parameters and several optical technologies are possible. Given that the interest is to minimise the number of cables of the future monitoring system of a repository we concentrated on distributed techniques such as:

- Fibre Bragg grating for multiple **localized** signals of temperature, strain, radiation, hydrogen, pH, etc.,

- Fibre itself measured with three scatterings (Brillouin, Rayleigh and Raman) for **distributed** measure of temperature, strain, hydrogen, pore pressure, bentonite density evolution, radiation, etc.

3.3.6.2 Fibre sensitivity to radiation

Expected environmental conditions for the FO in the repository include the presence of radiation and hydrogen. When fibres are exposed to gamma radiation, the attenuation increases through the interaction of the gamma flux with the color centers or point defects present in SiO_2. This creates the so-called radiation-induced attenuation (RIA) that will limit the performance of the optical system. The RIA is complicated to study because it depends on the fibre chemical composition, the fibre history, and the nature and parameters (gamma, neutrons, continuous, pulsed, dose rate, total dose, etc.) of the radiation. It has been shown that the most impacting factor is the nature of the fibre dopants (Ge, P, Al or N are used to increase the refractive index whereas F or B decrease it) used to realize the refractive index profile. Many data exist in the literature leading to the conclusion that pure silica core fibres with F dopants in the cladding are the most radiation resistant fibres whereas P-doped core fibres are the most sensitive.

3.3.6.3 Rayleigh, Raman and Brillouin scattering

Optical Time Domain Reflectrometry (OTDR) is a technique described in Figure 53 that consists of launching an optical pulse from an optical source (LD) into the fibre under test (FUT) and analyzing the Rayleigh backscattered signal with a photodetector (PD). If the light velocity is known, the time delay between the injected pulse and the backscattered pulse can be converted in a distance along the fibre length, allowing to locally sense the fibre. This is indeed a distributed metrology used for temperature, strain, etc sensing. Total distance range can reach kilometers; standard spatial resolution is 1 m, improved down to the centimeter scale in the most recent developments.

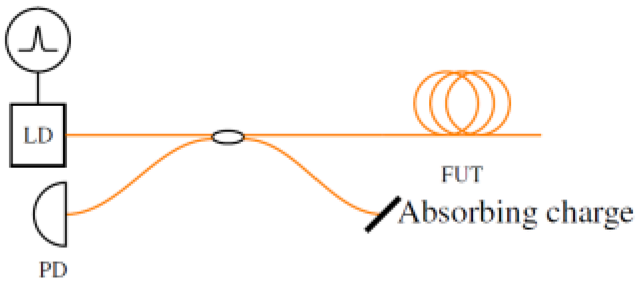

Figure 53. Basic principle of optical reflectometry, LD laser diode, PD photodetector and FUT fibre under test

Rayleigh scattering is quite simple to use, but it is sensitive at least to strain and temperature simultaneously. So, special optical fibre cables design should be used to discriminate strain and temperature.

OTDR works in the time domain with optical pulses as short as some nanoseconds. An alternative way is to work in the frequency domain with a technique referred to as Optical Frequency Domain Reflectometry (OFDR).

Classical OTDRs/OFRDs use the Rayleigh backscattered power to get the attenuation picture of optical links and detect anomalous events along the light path. To get the temperature or strain, two measurements are done: one is a reference trace and the other one is the perturbed trace by temperature change ΔT or strain change $\Delta\varepsilon$. By doing cross-correlation analysis between these two traces, the Rayleigh spectral shift $\Delta\nu_R$ given by:

$$\Delta \nu_R = C_T^R \Delta T + C_\varepsilon^R \Delta \varepsilon$$

is computed from which temperature or strain profiles can be recovered. C_T^R and C_ε^R depend on the fiber composition and typical values are $-1.5\text{GHz}/^\circ\text{C}$ and $-0.15\text{GHz}/\mu\varepsilon$ respectively.

The response of silica material to light becomes nonlinear for intense electromagnetic fields propagating into the core. Among all nonlinear effects, Raman and Brillouin scatterings can be used for distributed sensing purposes.

Raman scattering is an inelastic interaction between the light and the molecular structure of the fibre that can transfer a small fraction of the incoming power into two other fields whose frequencies are downshifted and upshifted by an amount that is linked to the vibrational modes of the fibre. As shown in Figure 54, incident light at wavelength λ_0 acts as a pump to generate a Stokes wave at λ_S and an anti-Stokes wave at λ_A.

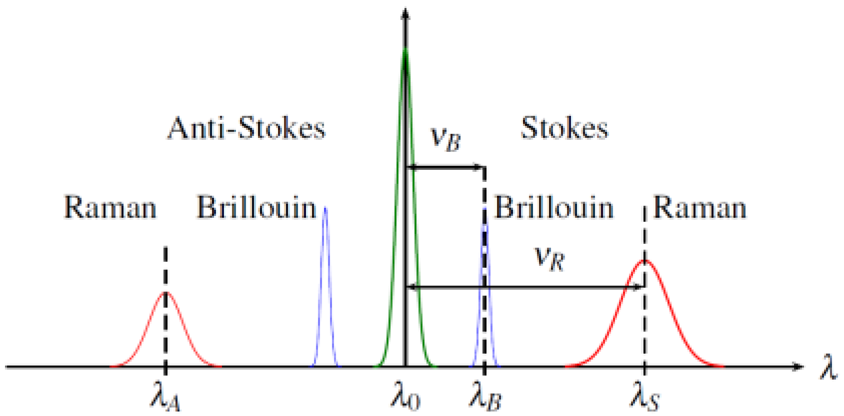

Figure 54. Typical spectra of Raman and Brillouin waves generated by a pump wave at l0 (not to scale)

In Raman scattering, the ratio R of the anti-Stokes to the Stokes wave intensities is function of the temperature T according to:

$$R(T) = \left(\frac{\lambda_S}{\lambda_A}\right)^4 \exp\left(-\frac{h\nu_R}{k_B T}\right)$$

where h is the Planck's constant, c is the velocity of light, ν_R is the Raman frequency shift, k_B is the Boltzmann's constant and T is the absolute temperature. If Raman scattering and OTDR are combined, it is possible to measure this ratio R(T) at every location along the fibre length. This then gives the temperature profile that can be used for monitoring purposes and this technique is called Raman Distributed Temperature Sensor (RDTS). It is worth to note that strain does not affect the temperature measurement.

Brillouin scattering is similar to Raman scattering, except that the nonlinear interaction is taking place through the acoustic modes of the fibre to generate a Stokes wave at λ_B and an anti-Stokes wave. Being linked to the acoustic velocity in the fibre, Brillouin scattering is mainly used for structural health monitoring, because it is possible to retrieve temperature and/or strain. Indeed, sensing information is encoded in the Brillouin frequency shift (BFS) noted ν_B and the variation $\Delta\nu_B$ of this shift is proportional to the temperature variation ΔT and the strain variation $\Delta\varepsilon$:

$$\Delta\nu_B = \nu_B - \nu_{B0} = C_T^B \Delta T + C_\varepsilon^B \Delta\varepsilon$$

where ν_{B0}, C_T^B and C_ε^B depend on the fibre composition and typical values are respectively 1MHz/°C and 0.05MHz/µε [2, 4]. If Brillouin scattering and OTDR are combined, the system is referred to as Brillouin Optical Time Domain Analysis (BOTDA) and can be used to measure the profile of the temperature or the strain.

As summary, Raman distributed measurements is a good technology for temperature profile measurement, whereas Rayleigh and Brillouin distributed measurements are a good candidates to monitor temperature and strain distribution in the underground galleries, provided that the fibre properties are not affected by the environmental conditions inside the tunnels (radiation level, humidity, oxygen and hydrogen concentrations, etc.). Table 9, summarizes main properties of the techniques used for distributed measurements.

Table 9. Main characteristics of distributed optical sensors

	Rayleigh	Brillouin	Raman
Diffusion type	elastic	inelastic	inelastic
Fiber type	singlemode	singlemode	multimode singlemode
Measuring distance	20 km (OTDR) 70 m (OFDR)	30 km	30 km
Spatial resolution	20 cm (OTDR) 10 mm (OFDR)	10 cm	1 m
Temperature sensitivity	$C_T^R = -1.5\,\text{GHz/°C}$	$C_T^B = 1\,\text{MHz/°C}$	0.1 °C
Strain sensitivity	$C_\varepsilon^R = -0.15\,\text{GHz}/\mu\varepsilon$	$C_\varepsilon^B = 0.05\,\text{MHz}/\mu\varepsilon$	insensitive
Measuring time	10 min (OTDR) 10 s (OFDR)	10 min	1 min
Power budget	10 dB (OTDR) 70 dB (OFDR)	10 dB	10 dB

3.3.6.4 Fibre Bragg gratings

A fibre Bragg grating (FBG) is achieved by creating a *z*-periodic modulation of the refractive index of the fibre core, which generates a distributed reflector characterized by its period Λ and modulation depth δ*n* (see Figure 55).

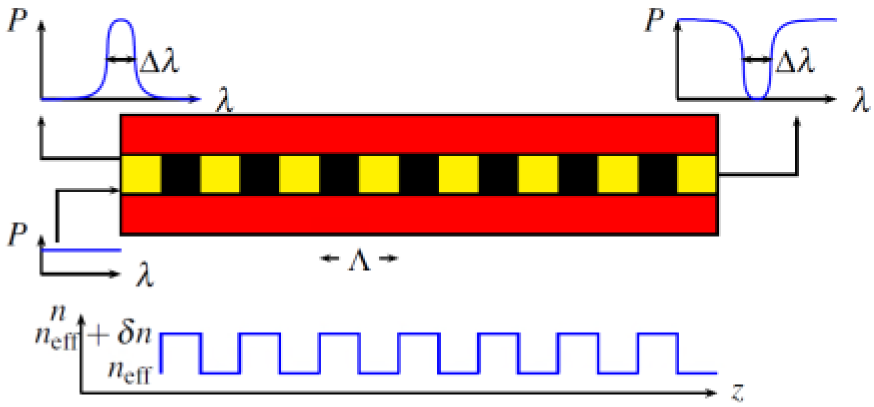

Figure 55: Basic principle of fibre Bragg grating

When a white light is injected into the FBG, the wavelength satisfying the Bragg condition:

$$\lambda_B = 2n_{\mathrm{eff}}\Lambda$$

is reflected whereas the other wavelengths are transmitted. The FBG acts thus as a pass-band filter in reflection and a notch filter in transmission. FBGs are excellent sensors because λ_B changes linearly with strain variations Δε and temperature variations Δ*T* according to:

$$\frac{\Delta\lambda_B}{\lambda_B} = \left\{\frac{1}{n_{\mathrm{eff}}}\frac{\partial n_{\mathrm{eff}}}{\partial \varepsilon} + \frac{1}{\Lambda}\frac{\partial \Lambda}{\partial \varepsilon}\right\}\Delta\varepsilon = (1 - p_e)\Delta\varepsilon$$

$$\frac{\Delta\lambda_B}{\lambda_B} = \left\{\frac{1}{n_{\mathrm{eff}}}\frac{\partial n_{\mathrm{eff}}}{\partial T} + \frac{1}{\Lambda}\frac{\partial \Lambda}{\partial T}\right\}\Delta T = (\xi + \alpha)\Delta T$$

where $p_e \approx 0.22\times10^{-6}$ $\mu\varepsilon^{-1}$, $\xi \approx 8.6\times10^{-6}$ °C^{-1} and a ≈ 0.55×10^{-6} °C^{-1} are respectively the strain-optic coefficient, the thermo-optic coefficient and thermal expansion coefficient and the values are those for silica-based optical fibers. FBG are thus used for point temperature and point strain monitoring [2], 7.1.3. Again, many data exist in the literature leading to the conclusion that FBG can sustain radiation under proper conditions, making them very useful for metrology in nuclear applications.

3.3.7 Obtained results by parameter

Results obtained from the R&D performed in the project are synthesized hereafter by measured parameter.

3.3.7.1 Distributed temperature measurements

3.3.7.1.1 Reference solution (Raman scattering)

Reference solution makes use of Raman scattering for temperature measurements. Indeed, Raman scattering provides better uncertainties (0.1 °C) than Brillouin scattering (1 °C) and does not require specific mechanical isolation since it is only sensitive to temperature.

A Silixa device was tested ona bench designed for optical fiber distributed temperature measurement evaluation (collaboration with EDF and LNE (*Laboratoire National de Métrologie et d'Essais, France*)). It makes use of a standard commercial multimode fiber, OM-2 type, with 50 µm core and acrylate primary coating. Both the interrogator and the sensing optical fibre are placed in their own thermal enclosures. Two initiating/ending sections of the optical fiber are immersed into the thermal enclosure dedicated to the interrogator, in order to decouple them from the main part of the sensing optical fibre.

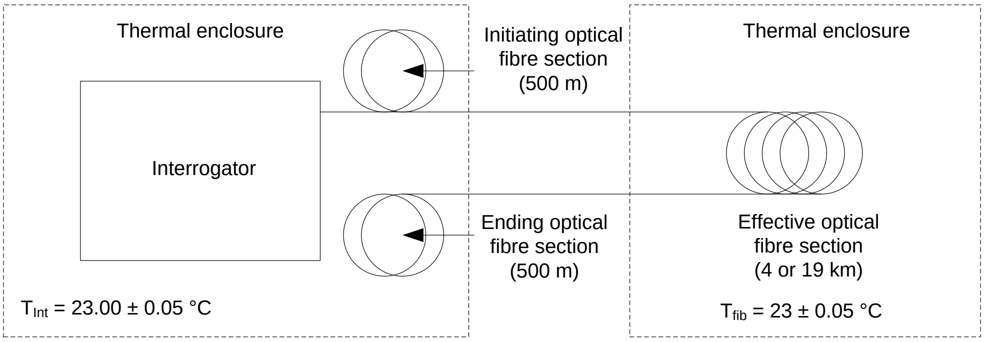

Figure 56. Schematic experimental arrangement for evaluating performances of DTS Raman interrogator

The temperatures of the two enclosures are controlled by the mean of 100 Ω platinum probes. The sensing/effective optical fiber has a length of 4 km and the two initiating/ending optical fibre sections have a length of 500 m each. Then, the whole optical fibre length is 5 km, the maximal distance range of the device. Each optical fibre section is wounded without any spool support, and just arranged on the floor of the thermal enclosure, in order to limit the mechanical constraints.

As expected, temperature measurement uncertainty is very good, tenth of degree, and increases with the distance along the fiber. Surprisingly, the dependence is not linear.

More precisely, a mean temperature value is computed over an interval of 10 successive samples centred on a considered point along the optical fiber. The mean trueness error (MTE) is the difference between the mean temperature and the true temperature measured at the same time by a 100 ohms standard platinum resistance thermometer, positioned at the centre of the wound optical fibre coil. It was calculated every 500 m along the fiber; the experiment was repeated 4 times for four target temperatures, 3 °C, 23 °C, 40 °C and 60 °C.

3.3.7.1.2 Influence parameters

The performance of the Silixa Raman sensing device was determined (i) in single-ended versus double-ended schemes (ii) paired with a MM-Fibers (MultiMode), designed to endure high-level radioactive waste repository environment. Besides, a special fiber developed by iXBlue to convey resistance to radiation and hydrogen-rich environment was tested too.

Measurements done in a single-ended scheme are strongly affected by radiations: F-doped optical fiber is mandatory but not efficient enough to reduce temperature measuring errors based on Raman scattering. A solution is to implement other Raman scattering measuring configurations, namely double-ended measurements, which provide good evaluation of the temperature even for measurements done with irradiated MM fibers. However, temperature measurement quality is significantly degraded: measured temperature error reaches 5 °C.

There are new devices recently commercialized, based on other sensing architecture, a DTS with two pumping wavelength, one standard and the second placed at the corresponding Stokes wavelength. This solution might cancel the differential solution problem. However, the coupled hydrogen and radiation influence is still pending.

3.3.7.1.3 Back-up solution (Brillouin or Rayleigh scattering with a loose tube)

The possibility to pair Brillouin or Rayleigh scattering with a loose tube was evaluated, to get rid of strain influence and be able to provide temperature measurement only. At the end, it was proved that loose tube is efficient to isolate the sensing fiber from mechanical stress. It showed to be an interesting back-up solution for temperature sensing, since temperature uncertainty actually remains similar for the three scatterings after radiation impact.

3.3.7.2 Distributed strain measurements

3.3.7.2.1 Reference solution (Brillouin scattering)

Brillouin scattering is the reference solution selected to obtain distributed strain measurements. Maximal distance range is larger than 30km; best spatial resolution is 1cm. Since the interrogator can be placed in safe rooms, far from repository cells, where maintenance is possible, the interrogation technique was not a development topic during this project. Andra work was dedicated first to select the primary coating and then to the design and realization of the external sheath. Once realized, question was the possible strain sensing performance differences between “naked” optical fibers and jacked optical fiber (cable).

Andra work could thus be summarized as follows:

(i) design a radiation-hard optical fiber compatible with insertion into strain sensing cable

(ii) select a primary coating suitable for harsh environment (both radiation and hydrogen)

(iii) realize such optical fiber

(iv) select or design a strain sensing cable

(v) insert the specific optical fiber (in its primary coating) inside the cable

(vi) evaluate Brillouin and Rayleigh strain sensitivity *(vii) and the possible evolution during aging of this global product. This last topic means checking whether the radiation influence on Brillouin and Rayleigh scatterings obtained post-mortem at room temperature remain similar on-line and at the working temperature. It also includes verifying the durability of the hydrogen hermeticity of the product.

Andra was assisted by two subcontractors to cover the entire sensing chain realization, namely to supply and develop special optical fiber sensing cables. iXBlue (France) has developed and supplied the optical fibers for strain sensing (singlemode fibre) and temperature sensing (multimode fiber). They used F-dopant exclusively, for high-tolerance to radiation. They selected a special primary coating (carbon) to prevent hydrogen migration into silica (the fiber material). BRUGG company (Switzerland) has inserted the iXblue fibers into a sensing cable, made the cable external sheath to obtain a product suitable for civil engineering outdoor test. Andra selected the sensing cable called V9. The inner metallic tube should provide durability, on top of hermetic sealing (against hydraulic stress and hydrogen migration). The corrugated external profile should enhance the grip once embedded into concrete. The external diameter, 3.2 mm, remains small which limits invasiveness.

Strain sensing cable are usually made of a tight sheath around the optical fiber, to ensure optimized transfer of mechanical field from the host material (where the strain measurement is requested) to the core of the optical fiber (where the measurement is actually performed). A drawback of such design is that the external sheath might induce (micro-) curvatures on the optical fiber, hence optical losses if the guiding properties are not carefully selected. Several performances of the final strain sensing cable are highly dependent on the optical fiber performances. For instance there are (i) the minimum bending radius, supposed to be 15 times the diameter, (ii) the crush resistance, claimed at 250 N/cm for standard

V9 product (iii) the optical attenuation at 1550 nm, smaller than 0.5 dB/km, the central Brillouin frequency, 10.6 GHz, the Brillouin strain sensitivity, 450 MHz/%. Since the iXBlue fiber had to be inserted into a Brugg sensing cable, time has been taken to agree on required specifications: Product release in iXBlue and entry control in Brugg. We discussed on the maximal tolerated optical losses and the tensile strength the fiber should handle (in the present case, 200 kPsi, which was not a standard evaluation at iXBlue). We also agreed on the methodology to quantify these parameters. For instance, the measured optical losses depend on the size of the wheel where the fiber is wounded. Regarding temperature tolerance, we initially planned to replace acrylate constitutive material by polyimide. This was too different from Brugg standard production lines. This is why we decided to stick with acrylate material, yet high-temperature acrylate. The carbon-coated fiber also had to be covered by acrylate to enter the production line.

Once this product is realized, we would evaluate the performances of sensing cable performances, comparing them with naked fiber ones.

We initially planned to perform:

- Optical losses evaluation to quantify whether the encabling process has degraded the optical fiber performances
- Rayleigh and Brillouin strain sensitivities measurements will be measured and compared, on the fiber alone and the sensing cable (the fiber in the external sheath)
- Irradiation tests to evaluate possible influence of the external sheath (degradation of material constituting the sensing cable?) on radiation tolerance. This includes the possible influence of radiation on hydrogen hermeticity of the optical fiber and its coatings.

3.3.7.2.2 Ageing under irradiation

Ageing tests were designed in collaboration with several partners, IRSN (France) and SCK-CEN (Belgium) who could provide access to irradiation chambers, and University of Mons who was also willing to irradiate optical fiber sensors.

Total dose and dose rate are two influencing parameters. Regarding Cigéo application case, at the external surface of the HLW repository cell metallic liner, where OFS would be implemented, gamma dose rate reaches 1 Gy/h. For 100 years measurement, total dose reaches 1 MGy (air). This is why the IRMA ^{60}Co facility of IRSN (France, Modern2020 partner) was selected. In November 2017, optical fibers were measured on line while being exposed to dose rate of about 3.2-3.4 kGy/h, exact value depending on the sample position, up to a total dose of about 1 MGy (in air, which is similar for SiO_2).

To ensure temperature regulated during irradiation, samples were packaged inside thermally-controlled silicones able to withstand radiation environments up to 1 MGy and to regulate temperatures up to 150 °C. Samples have been irradiated at different temperatures, representative of the targeted application: room temperature (RT), 80 °C, 100 °C and 120 °C.

The fiber samples were taken from a reference Ge-doped fiber and the custom F-doped fiber. Indeed, on top of the developed samples (F-doped fiber), as a reference, we made use of a standard commercial Ge-doped fiber: Ge-doped fibers from Fibertronix (now Fibercore), with 5.2% Ge-SiO_2 core and pure silica cladding, with a carbon-polyimide primary coating.

For the online measurements, every sample was connected to the Neubrescope measuring device, located in a radiation-free zone. More precisely, the heated fibers were put in series after 60 m length of a connection cable fiber, while the sample at room temperature was connected after a 20 m long patch-cord. Each sample was measured on a specific optical line, thanks to the Neubrescope switch. Samples at ambient temperature were not inserted inside silicones. Both Brillouin and Rayleigh scatterings were measured during this ageing campain. Regarding the large number of measurements to be performed, a trade-off between the measurement duration, the frequency scan range and the signal level was needed. For this reason, the following acquisition parameters were selected for the fibers tested at high temperature: distance range of 200 m, 100 cm of spatial resolution, 20 cm sampling interval, averaging count of 217, +1 dBm and +30 dBm respectively for the probe and the pump output powers, frequency range of [10.70 – 11.40] GHz with span of 2 MHz. For the sample tested at room temperature similar settings were used, except for different distance range limited to 100 m and another frequency range of [10.60-11.30] GHz.

Another sample, only with the specific F-doped fiber, was prepared and placed for on-line optical spectrum measurement, to determine the RIA.

Finally, on top of primary-coated optical fiber samples, the developed sensing was included into the accelerated ageing tests to evaluate whether the strain transfer function of optical fiber strain sensing cables (in other words, the function that links the concrete host material to the optical fiber core through the coatings and sheaths of the cable) might change after gamma exposure. 200 m of strain sensing cables were exposed to gamma rays. However, only Brillouin and Rayleigh scatterings were measured on-line on the sensing cable. Later in 2018, the irradiated cable samples were placed on mechanical loading machines to evaluate possible evolution of the strain transfer function of the cable.

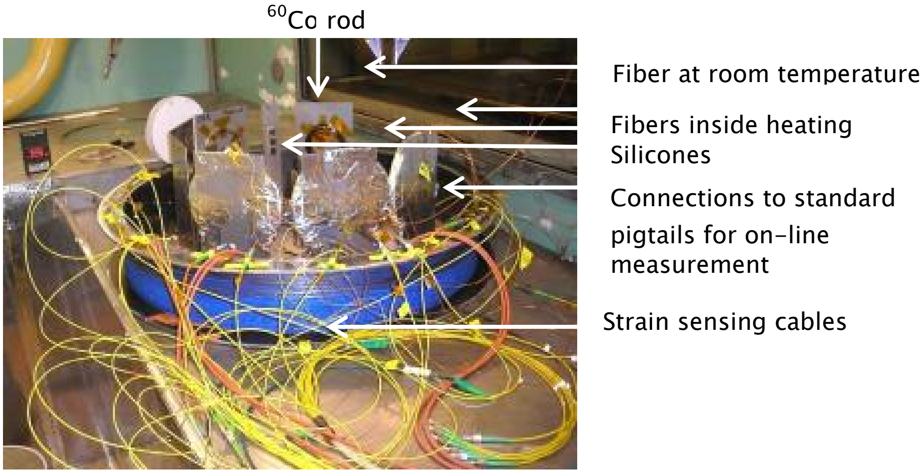

Figure 57. Pictures of the silicone with the optical sample and thermocouple (left) and the irradiation test (right) prior to the radioactive rod emplacement with optical fibers heated at three controlled temperatures

3.3.7.2.3 Conclusions

Coupled effects of temperature and radiation improve the sensing performances of strain distributed sensors exploiting the Stimulated Brillouin Scattering in Ge-doped and F-doped single-mode fibers. At 80 °C, 100 °C and 120 °C, compared to room temperature, the radiation induced attenuation is significantly reduced. However, the Brillouin frequency shift is not modified by coupled temperature influence, as it remains in the order of 4 MHz at 1 MGy (air) for the Ge-doped fiber and only 2 MHz with the developed F-doped fiber, which approximately corresponds to 40 µm/m maximal error in strain measurement.

Rayleigh scattering has proved to be a very promising solution for strain sensing. It is even less affected by radiation than Brillouin scattering. With the custom fiber based on F-dopants instead of Ge-dopants, the influence of radiation on Rayleigh frequency shifts is as small as -4 GHz, or 2.5 µm/m error, whatever the working temperature (80, 100 or 120 °C). The influence of temperature is fully novel and should probably be published rapidly.

Further work is required to finalize data analysis, for all measurements acquired during the experimental campaign organized at IRMA facility (IRSN partner). From the Radiation Inducted Attenuation, maximal distance range of distributed measurements will be determined.

The main difficulty is the degradation of carbon-coating hydrogen-hermeticity after 10 MGy dose. We must reproduce the test with the optical fiber we have developed within the project (the preliminary test was performed on a commercial fiber) and after several gamma doses.

3.3.7.3 Distributed hydrogen sensing

3.3.7.3.1 Introduction

Hydrogen leakage in the gallery is a potential high-risk problem that should be detected as earlier as possible. Three fibre-based techniques have been tested: a specialty fibre incorporating hydrogen sensitive material, the use of Brillouin shift versus hydrogen concentration, and a fibre Bragg grating (FBG) surrounded by a hydrogen sensitive layer that modifies FBG Bragg wavelength.

3.3.7.3.2 Reference solution (Pd dopped FO and Brillouing scattering)

Hydrogen naturally diffuses into silica optical fiber and induces absorption bands. This phenomenon is reversible: hydrogen is spread out when fibers are no longer exposed to H_2. Efficient hydrogen sensing was achieved by using standard G652 optical fibers with:

i) Pd films deposited on the fiber cross-section,

ii) laid around the fiber,

iii) around the core or

iiii) around tapered fiber.

In contact with H_2 gas, Pd forms an hydride PdH_x (with x is a functions of the gas rate) leading to a variation of both the material refractive index and lattice cell volume. However, these sensors suffer from untimely deterioration in harsh environments and poor robustness.

To develop distributed measurements, pairing the capacity of silica to absorb hydrogen with localization processes such as OTDR, provides truly distributed hydrogen sensing. However, aging of optical fibers, radiations, unexpected mechanical solicitations also increase propagation losses. To obtain durable and long-term measurement, a wavelength-encoded principle, such as Brillouin scattering seems more attractive. At 25 °C, with an acrylate-coated fiber, the Brillouin frequency shift is almost linear with hydrogen concentrations in the silica core. In the contrary, to avoid hydrogen influence fully hermetic coating has to be found like the carbon coating.

3.3.7.3.3 Increase of sensitivty and response time

In order to improve the sensitivity of standard single mode silica fiber to hydrogen, Andra and Xlim proposed to introduce Metallic particles (Pd) into the silica cladding of optical fibers. This design should protect the sensing metal from harsh environments, solving the well-known palladium deterioration. Embedding Pd into fibers should also improve the sensitivity and the response time of the distributed fiber gas sensor, by exploiting the mechanical strain induced by the crystal lattice expansion of Pd particles in contact with H_2 gas.

The fabrication feasibility of this kind of optical fiber had been demonstrated using an original powder technology: many palladed fibers had been realized by Xlim before the beginning of the project.

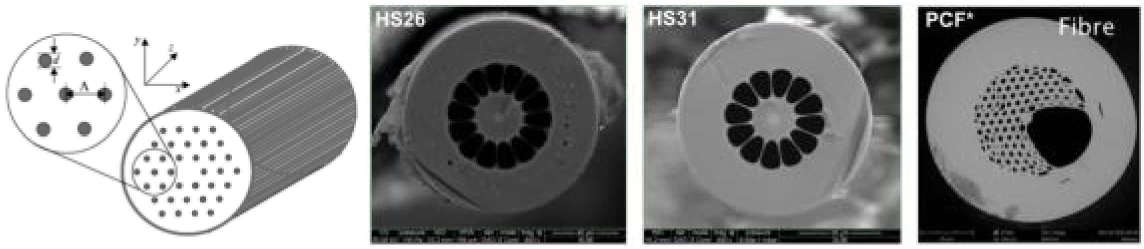

Figure 58. Sketch of the special fiber with Pd in the cladding and SEM pictures of the three drawn fibers

The work was dedicated to:

- Repeat and improve Pd-particules fibres and characterize performance during on_line measurement under hydrogen
- Secondly, understand the diffusion mechanisms of hydrogen inside silica optical fiber in function of temperature, pressure, and optical fiber size.

3.3.7.3.4 Conclusions for Pd dopped FO and Brillouing scattering

Sensing performance of Pd particules fibers was not fully demonstrate. Rayleigh and Brillouin measurements in palladed fibers remains a challenge because of very high propagation losses. To improve attenuation losses, an important modification of the synthesis process, based on a powder method, is required.

3.3.7.3.5 Implemented back-up solution: birefringence approach

High losses of Pd-particules fiber attributed to small amounts of metallic particles diffusing from the cladding to the optical core. To prevent such spreading, it was decided to localize palladium inside capillary; more precisely, Stress Applying Parts (SAPs) of birefringent fibers were used.

Measuring birefringence offers larger working amplitude and it is more promising that Brillouin scattering in situation of high propagation losses. It remains an interferometric process (not based on intensity variation). As such one can expect durable and long-term measurement.

Carried out tests with several fibers helped to distinguish the effects of temperature and pressure from the direct effect of hydrogen on the palladed optical fibers. These results demonstrate Palladium increases the sensitivity and decreases the response time of the sensor. Andra and Xlim applied for a patent in November 2017.

3.3.7.3.6 FBG Hydrogen sensor made by UMONS

Uniform FBGs were inscribed into standard singlemode fiber by means of a frequency-doubled Argon-ion laser emitting at 244 nm. Prior to the UV exposure, to increase its photosensitivity, the optical fiber was hydrogen-loaded at 70 °C and 200 atm during 48 h. After the inscription, the gratings were annealed at 100 °C during 24 h in order to stabilize their properties. Long period Bragg gratings were used for their radiative properties since they are transmissive gratings that couple light from the fiber core to the cladding.

To obtain the sensitive layer, nano-sized tungsten oxide powder was prepared using the sol-gel method. Aqueous sol-gel of tungstic acid (H2WO4) was obtained from Na_2WO_4 with protonated cation-exchange resin. In a first stage, a gel consisting of WO_3 H_2O was formed. The gel was washed, centrifuged several times with demineralized water and dried in air at 60 °C for 6 h. Appropriate amounts of hexachloroplatinic acid (H_2PtCl_6) solution were added to the obtained powder. The mixture was finally annealed at 500 °C for 1 h in order to obtain WO_3 doped with Pt on its surface. At the end of the process, the active layer consists of WO_3 nano-lamellae (cubes of about 1 µm by 1 µm by 50 nm) with Pt dispersed on their surface.

Every grating was written in the middle of a 5 cm long stripped region of the optical fiber. The sensitive layer was finally dispersed in a solvent in order to deposit a uniform layer of the sensitive material (several microns) on the stripped optical fiber using the dip-coating technique, ensuring in any case the same experimental conditions. The molar ratio Pt/W was about 1/14.

Let us also add that the used layer does not react with other pollutants such as methane or carbon monoxide.

In the presence of hydrogen in air, the following chemical reactions occur in the sensitive layer:

$$\mathrm{WO_3 + H_2 \longleftrightarrow WO_2 + H_2O} \qquad \{1\}$$

$$\mathrm{WO_2 + \frac{1}{2}O_2 \longleftrightarrow WO_3} \qquad \{2\}$$

The oxidation of H_2 molecules by O_2 molecules is an exothermic reaction that elevates the temperature around the FBG. H2 sensing is therefore based on the monitoring of the Bragg wavelength shift induced by a temperature change.

In order to decrease the threshold sensitivity, the active layer needs to be heated and this has been realized by adding a long period fiber grating (LPBG) superposed to the FBG covered by the sensitive layer as depicted in Figure 59. In that way, light energy is coupled by the LPBG into the cladding and heats the sensitive layer.

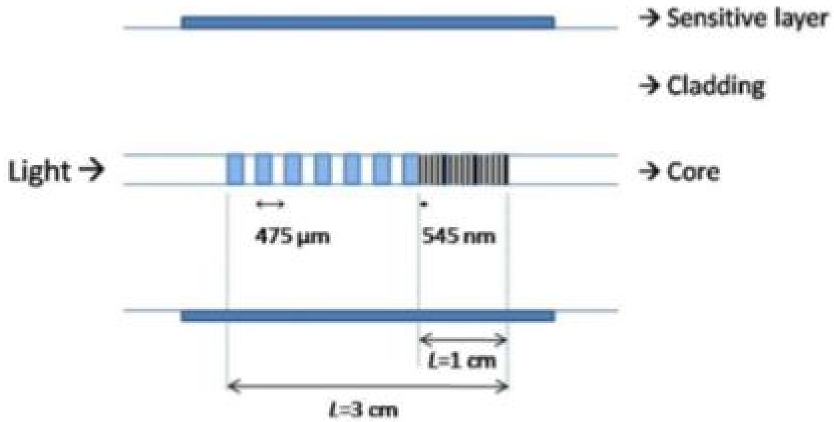

Figure 59. Uniform FBG superimposed in a LPBG for H_2 detection

3.3.7.3.7 Results of the FBG Hydrogen sensor

Due to the need of activation energy (0.15 eV) to initiate the exothermic reaction, there exists a minimum of H_2 concentration below which the reaction will not start. In other words, there exists a threshold value in terms of H_2 concentration below which the sensor does not react. In practice, this threshold value can be decreased thanks to an external energy contribution. This could be done for instance by a local heating of the sensitive layer. A LPBG provided a light energy coupling to the sensitive layer to decrease the H2 detection threshold while the FBG was used to track the temperature increase. Very good sensing performances have been reported: fast response, high sensitivity, reversibility, frequency multiplexing capability and H2 concentrations detection well below the explosion limit of 4 %, whatever the relative humidity level and for temperatures down to -50 °C.

3.3.7.3.8 Radiation effects

For the FBGs, it was not possible to expose the sensors to hydrogen while under radiation. Analysis after the campaign has revealed that the sensitive layers were physically degraded and in some cases appeared destroyed to the naked eye. It is suspected that the problem mainly comes from a lack of adhesion of the layer and transport dislodging the layer in part or in totality. When transported but un-irradiated samples were tested for hydrogen sensitivity and all were found inoperative.

3.3.7.3.9 Conclusions

If palladium is added in the fibre core, the core properties are sensitive to hydrogen and measuring the Brillouin frequency shift or the induced birefringence allow to estimate hydrogen concentration. Proof of concept has been demonstrated but still many tests should be done to fully qualify this sensor.

Point hydrogen concentration can be detected with coated fibre Bragg gratings. Uniform FBGs were inscribed into standard singlemode fibre and recovered by a hydrogen sensitive layer made of WO_3 nano-lamellae. In the presence of hydrogen in air, the oxidation of H_2 molecules by O_2 molecules is an exothermic reaction that elevates the temperature around the FBG. H_2 sensing is therefore based on the monitoring of the Bragg wavelength shift induced by a temperature change. By optimizing the fabrication, H_2 concentration detection well below the explosion limit of 4% was obtained, whatever the relative humidity level and for temperatures down to -50 °C. nevertheless, tests under radiation reveal poor adherence of the sensitive active layer and more progress should be done.

3.3.7.4 Distributed gamma sensing

Al or P doped fibers are known to be highly radiation sensitive. Andra make use of RIA (radiation induced attenuation) measured inside fibers with several dopant types and concentrations.

The attenuation measurements have been performed either using an OTDR from VIAVI operated at 1550 nm with one meter resolution or with a setup consisting in a white light source and a spectrophotometer, both from Ocean Optics. The irradiation experiments were carried out at the IRMA facility of the IRSN at Saclay.

The characteristics of the irradiation were:

- Continuous regime irradiation;
- Photons energy ~1.2 MeV (60Co source);
- Radiation doses up to ~1 MGy;
- Radiation dose rates of about ~2.6 kGy/h

The investigated samples were all acrylate-coated with the following characteristics:

- Ge-sample: CMS fiber from iXBlue this singlemode optical fiber contains only Ge in its core, but in high concentration. As a consequence, it possesses a medium sensitivity to radiation and can act as the reference for this experiment.
- GeP sample: from Alcatel, this prototype singlemode fiber contains Ge in its core and a small amount of P in its cladding. It corresponds to a fiber with enhanced radiation sensitivity.
- Al sample: provided by SCK-CEN. It is a singlemode optical fiber contains Al in its core, this dopant is known to strongly increase the fiber radiation sensitivity.

3.3.7.4.1 Testing results

As expected, the Al-doped sample was clearly the most radiation sensitive. This fiber was the first one lost. Then it was lost the GeP-doped fiber, whereas the Ge-doped could be measured till the end of the irradiation test. It is impressive to notice how a small amount of P in the fiber core is sufficient to increase its radiation sensitivity by a factor of more than 10.

In parallel spectral measurements with the OTDR measurements were performed on the GeP optical fiber that presents the intermediate radiation response in terms of sensitivity.

By comparing the RIA recorded via the OTDR and the spectrometer is possible to highlight if the differences between the used power levels (mW for OTDR, µW for white light source) lead to some differences in the GeP radiation response due to photobleaching.

3.3.7.4.2 Conclusions

Al-doped sample is clearly the most radiation-sensitive: 1m of fiber measured at 1.55 µm could provide distributed measurement until a dose of 470 Gy, with a sensitivity of about 5dB/Gy. Then the GeP-doped fiber should be favoured. It worked until 4 kGy. The Ge-doped could be measured until the end of the irradiation, despite lower sensitivity.

So, combination of fibres should be used to measure the full range up to Mgray. Moreover, optical fibre lengths and working wavelength are nevertheless two other parameters to adjust to the application. Further work is still necessary as a strong dependence of curing effect and coupled temperature and radiation influences was demonstrated.

3.3.7.5 pH sensor

3.3.7.5.1 pH sensor developed by UMONS

The sensor is based on TFBGs (tilted fiber Bragg grating, Figure 60) classically manufactured into hydrogen loaded single mode optical fiber by means of a 1 095 nm uniform phase mask and a frequency-doubled Argon-ion laser emitting at 244 nm. The phase mask was tilted in the plane perpendicular to the incident beam. An external tilt angle of 6° was chosen. The protection coating was mechanically removed before inscription. After that, and before coating, gratings were annealed at 80°C during 12 hours in air to remove the hydrogen and stabilize their physical properties. TFBGs with maximum peak-to-peak amplitude of 25 dB around 1 562 nm are obtained in air. The Bragg peak amplitude is about 4 dB.

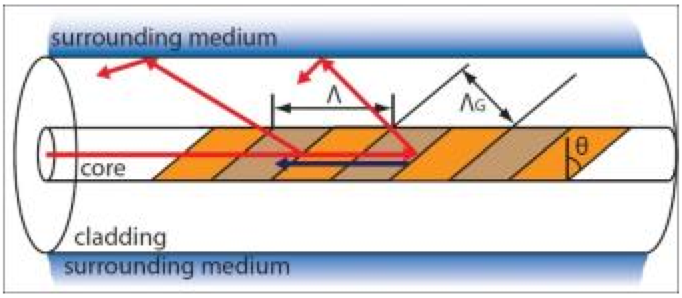

Figure 60. Scheme of a tilted fiber Bragg grating and its mode couplings

The deposition of the coating induces a reduction of the peak amplitudes of the cladding modes.

The sensitive sol-gel coating was obtained by incorporation of the pH indicator, here bromophenol blue, in a pure alcoholic solution (15 ml) containing TEOS (TetraEthoxyOrthoSilicate) as precursor (15 ml), distilled water (3 ml), PEG 6000 (PolyEthyleneGlycol) (1 mg) and HCl as catalyst (2 m, 0.25 ml).

The solution was heated at 60 °C (reflux) for 1 hour and aged for 1 week before use. The sensitive layer was then deposited on the fiber by dip coating in one step and annealed at 80 °C for 1 hour, yielding a 5 µm thick transparent yellowish layer.

3.3.7.5.2 Results

Figure 61 displays the TFBG amplitude spectra for various pH values. It can be observed that the resonance modes are drastically affected by the pH variations. The peak-to-peak amplitude decreases as pH increases while the wavelengths of the resonance peaks shift to longer wavelengths. As expected the Bragg peak remains unchanged and can be used as an internal reference for temperature variations. From analysis of these peaks, the pH can be computed.

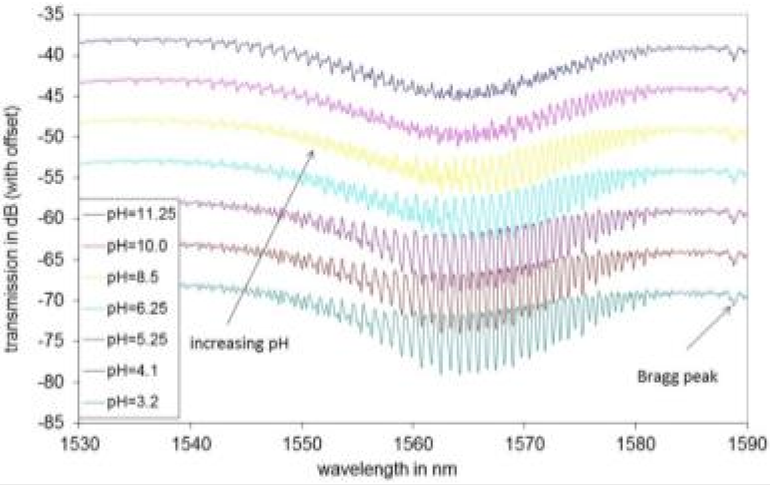

Figure 61. Transmission spectrum of the TFBG at different pH values

As could be expected, the response of the sensor presents a reversible sigmoidal shape although a small hysteresis (0.3 pH unit near 7) is observed. The hysteresis could be reduced by increasing the porosity of the film. The response is almost linear in the range 4.5 to 9.5 centered around pH = 7. The slope of the variation of the transmission as a function of pH is −1.36 dB/pH unit.

The wavelength shift of the peaks could also be exploited but for high pH values the amplitude of the peaks decreases and it is more difficult to accurately determine the position of the peaks. This sensor works correctly around a pH of 7.

3.3.7.5.3 Conclusions

pH sensors still require a lot of effort to be tested in radiation field. They should first be tailored for the pH range of 11-13, which is very challenging.

3.3.7.6 Bentonite density measurement

3.3.7.6.1 Introduction

Detailed monitoring of the GBM dry density distribution under in-situ conditions is challenging because of a lack of measurement techniques. In the unsaturated porous media, thermal conductivity depends on density, porosity and water content. For an engineered barrier system (EBS) consisting of granulated bentonite mixture (GBM), emplacement density and water content are key monitoring parameters. These parameters determine the thermal conductivity of the EBS which controls the heat transfer from the waste. The water content of the GBM is a known parameter at the time of emplacement.

DTS is a well-established technology for measuring temperature along a fiber optic cable, distributed Raman scattering has been adapted to determine the distribution of the thermal conditions (density and water content) around an optical sensing cable placed inside an engineered barrier made of bentonite (swelling clay). It provides with a continuous temperature profile along the cable for up to several kilometers. The obtained temperature information is defined by the spatial resolution (decimeter to meter scale) and the temporal resolution (seconds to hours) of the measuring device.

3.3.7.6.2 DTS installed in FE experiment

A heated fibre-optic cable was placed inside bentonite granular material (GBM) in the FE experiment of Mont Terri URL. The heatable fiber-optic (FO) cable used in this study was the multi-component cable (BRUsens LLK-BSTH 85 °C) manufactured by Brugg Kabel, AG in Switzerland. Its outer diameter is 4 mm and smallest bending radius is 60 mm. Four optical fibers (two single-mode, two multi-mode) are embedded loosely in the center stainless tube that are surrounded by stainless and copper wires. The total length of the FO cable used in this study was 150 m.

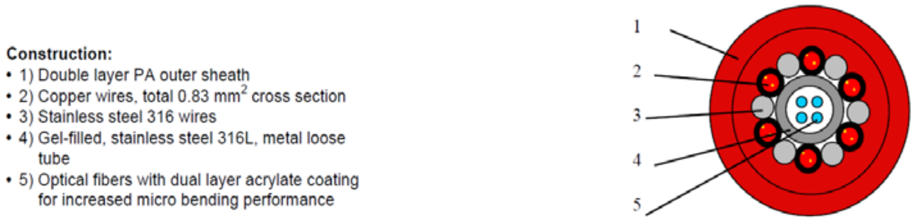

Figure 62. Schematic cross-section of the heatable FO cable (taken from Brugg Cables, 2015)

Note: Fibers in metal tube are for temperature sensing, copper wires are for heating. Both ends of the 150 m-long FO cable were equipped with E2000 end connectors. The copper wires on both ends were extended by attaching a copper cable with a larger cross-section. This was done to avoid unnecessary temperature rise along the extended part.

The DTS unit used in this study was a Raman DTS in Fig. 2-13 (Silixa Ultima S). The cable length can be up to 5 km. Sampling resolution can be set to 0.127, 0.254, 0.508 and 1.017 m (spatial resolution is twice as much).

3.3.7.6.3 Calibration and measurement

The response of the DTS was calibrated first versus varied dry densities of GBM mixture and varied water contents.

By heating the bentonite with the heating part of the cable and recording the distributed temperature profiles by the Raman effect in the fibre part of the cable, distributed thermal conductivity can be estimated. Analyses of heating and cooling behavior along the cable enabled to recover the distributed thermal conductivity, from which the dry density and the water content of the bentonite are recovered using the calibration performed.

In Figure 63, the temperature profiles before the heating of the FO cable started (0_min) at 60 min heating are shown.

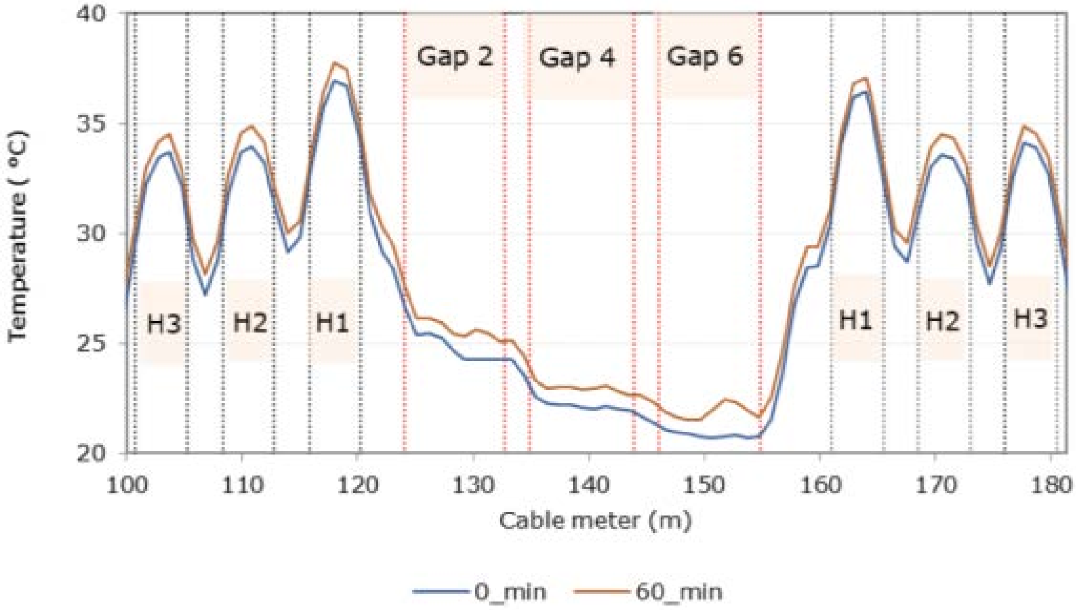

Figure 63. Temperature profiles before and after the FO cable heating test on April 30, 2015

Thermal conductivities along the FO cable were calculated and plotted in Figure 64.

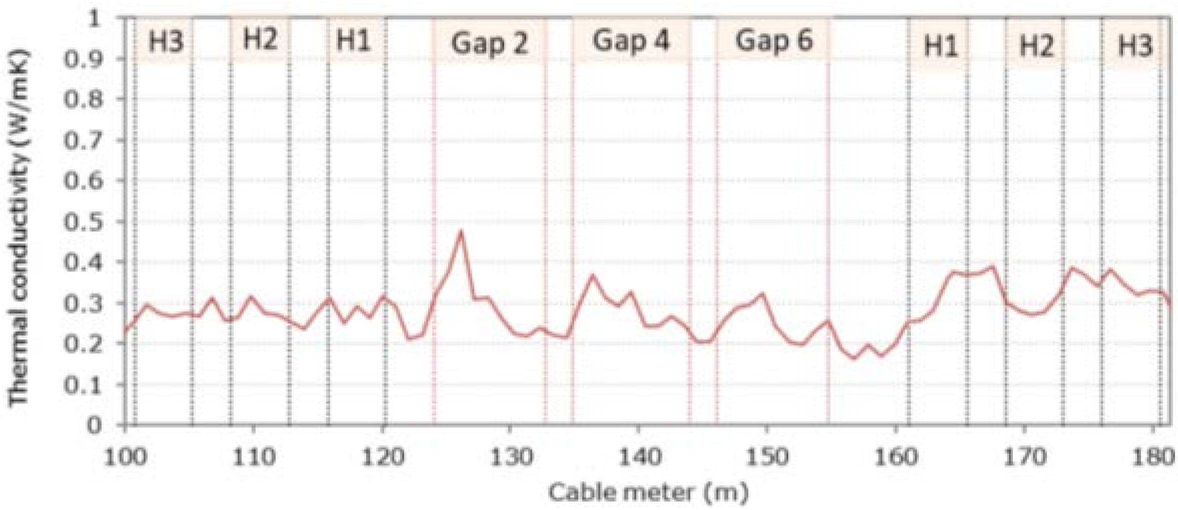

Figure 64. Thermal conductivity profile along the FO cable

Note: The profile is calculated by using equation 1 around the FO cable at the crown of the FE tunnel.

3.3.7.6.4 Conclusions

The initial dry density in the FE tunnel determined using the thermal conductivity method was approximately 1300 kg/m3 around the FO cable along the top section of the tunnel. This value was lower than the average value calculated by the mass balance method (~1450 kg/m^3) at the time of emplacement [1], 7.1.3. However, it should be considered that the latter method calculates the dry density averaged over the entire tunnel volume. Near the crown of the tunnel, the dry density tends to be lower compared to other sections of the tunnel. When compared to earlier studies [2 and 3], the estimated dry densities along the top section around the FO cable generally showed a reasonable agreement.

3.3.7.7 Conclusions from FO measurement

Many experimental data obtained during the project have shown the viability of these optical technologies in radioactive waste geological disposal sites. The project enabled to qualify not only the optical fibre but the whole sensing cables; ageing tests were performed under gamma and temperature constraints to quantify the durability of these technologies.

The main conclusions drawn during the project are:

1. Temperature is retrieved from Raman scattering in a multimode fibre. To fulfill the nuclear waste disposal conditions, carbon-primary coating is mandatory to prevent hydrogen diffusion and F-doped fibre is mandatory to reduce the RIA but is not sufficient to suppress dramatic radiation impact on temperature sensing. Double-ended configuration proved to be efficient, at the expense of temperature uncertainty, which reach 5 °C at 1MGy.

2. Strain is retrieved from Brillouin scattering in a singlemode fibre. Again, carbon-primary coating is mandatory to prevent hydrogen diffusion and F-doped fibre is mandatory to reduce the RIA and Brillouin frequency shift. Coupled effects of temperature and radiation have been quantified. Temperature reduces the negative impact of radiation on distributed sensors exploiting the Stimulated Brillouin. At 80 °C, 100 °C and 120 °C, compared to room temperature, the radiation induced attenuation is significantly reduced and maximal distance range will thus be improved. The Brillouin frequency shift is in the order of 4 MHz at 1MGy for the Ge-doped fibre and only 2 MHz with the F-doped fibre, which approximately corresponds to 80 µm/m and 40 µm/m maximal errors in strain measurement.

3. Rayleigh scattering has proved to be a very promising solution for strain sensing. It is even less affected by radiation than Brillouin scattering. With fibres based on F-dopants instead of Ge-dopants, the influence of radiation on Rayleigh frequency shifts is as small as −3.75GHz, or 25 µm/m error, whatever the working temperature (80 to 120 °C).

4. Regarding distributed radiation sensing, Al-doped sample is clearly the most radiation-sensitive and Ge-doped sample the less sensitive. A combination of different fibres should be deployed to measure the radiation spatial distribution on the MGy range.

5. Hydrogen sensing has been obtained by palladed silica optical fibres paired with Brillouin scattering and by functionalized fibre Bragg gratings. Proof of concept has been obtained but there is still a lot of research to do to assess the lifetime of the sensitive element.

6. pH sensing is feasible but should be tuned to the range 11-13.

7. Special cable to measure bentonite properties through distributed Raman temperature has been designed and proved to be a viable solution.

3.4 Geophysical methods

3.4.1 Introduction

Geophysical techniques offer powerful means for the implementation of non-invasive monitoring of radioactive waste repositories. The indirect nature of geophysical measurements (i.e., material properties are not measured directly, but through the geophysical data that are affected by the material properties relevant to repository system) allows obtaining information on the repository and it engineered barrier system (EBS) without placing sensors within the regions of interest. This is a particularly welcome feature for monitoring radioactive waste repositories, since geophysical experiments do not create leakages and thus preferential flow paths within the engineered barriers. However, this can result in considerable uncertainties and ambiguities and more research is required for obtaining meaningful diagnostic information. Extensive reviews of previous work indicated that seismic full waveform inversion (FWI) currently offers the most promising opportunities, but also geoelectrical methods, Electrical Resistivity Tomography (ERT) and Induced Polarization Tomography (IPT), can provide very useful information.

Four partners, namely ETH Zurich, Switzerland (ETH), Technical University of Liberec, Czech Republic (TUL), University of Strathclyde, U.K. (STRATHCLYDE) and the VTT Technological Research Center, Finland (VTT) teamed up to tackle some of the most burning problems. The main task of ETH was to further improve seismic FWI technologies, such that they become applicable to repository monitoring. Furthermore, novel differential tomography techniques should be explored that will allow the identification of subtle temporal changes. Since the tomographic imaging methods to be developed by ETH represent a considerable computational chore, TUL's mandate was to establish quick and inexpensive means to just identify (not necessarily image) anomalies. VTT and STRATHCLYDE joined forces to explore possibilities and limitations of electrical methods. For that purpose, the task of VTT was to establish suitable tomographic algorithms, with which not only geoelectrical data, but also induced polarization (IP) measurements can be inverted. STRATHCLYDE's focus lied on the calibration of the electrical data, such that the corresponding electrical parameters can be related to other physical parameters of interest (temperature, pressure, moisture content, etc.).

The results from several studies are synthetized hereafter, in which a variety of geophysical techniques, suitable for high-level radioactive waste repository monitoring, have been employed. In particular, novel FWI (4.4.2) and differential tomography techniques (4.4.3), suitable for waveform data, are presented, an anomaly detection algorithm is discussed (4.4.4), and geoelectrical and induced polarization techniques are proposed (4.4.5). Finally, an innovative calibration technique is presented (4.4.6) that allows conversions from geophysical quantities to engineering parameters, such as moisture content and temperature.

Further detail about the activities carried out and the results gathered can be found in Deliverable 3.5 « Geophysical Methods for Repository Monitoring » of Modern 2020.

3.4.2 Improvement of seismic full waveform inversion technologies

3.4.2.1 Introduction, background and objectives

In the seismic method elastic wave is generated at a safe distance from the repository. The generated elastic waves propagate through the repository and are recorded by an appropriate seismic acquisition system. Due to interaction between seismic waves and the repository the recorded seismograms are influenced by the elastic properties of the repository. For example, water saturation of a bentonite layer will lead to swelling of the bentonite. As a result of closure of pores in the bentonite seismic velocities are expected increase. Similarly, appearances of cracks in the engineered barriers or the host rock will lead to decrease of seismic velocities. These changes of material properties are expected to produce detectable changes in the recorded seismic data. With anomaly detection algorithms, one can quickly detect these changes in the recorded data and have a rough estimation of the physical property changes. This can be followed with FWI, which can produce high resolution images of elastic properties of the repository. The unknown physical parameters, influencing the seismic waves, include the elasticity tensor, and density.

The work carried out in previous MoDeRn and ESDRED projects regarding the seismic monitoring has highlighted that seismic data contain valuable information about the state of the repository (Manukyan et al., 2012b) and still major progress in FWI needs to be made before this technique can be used in radioactive waste repositories. In particular, it was found out that for an anisotropic host rock, such as most clay formations, inversion for elements of the elasticity tensor does not produce satisfactory tomographic images, even for noise-free synthetic data sets (Manukyan, 2011). Application to field data would be even more challenging due to the ambient noise, three-dimensional effects, variable source and receiver coupling terms, etc. More recent work has shown (e.g. Alkhalifah and Plessix, 2014; Gholami et al., 2013; Guitton and Alkhalifah, 2017) that an appropriate model parameterization is essential for the success of anisotropic FWI.

The methodological development was therefore as follows:

- identification and implementation of suitable parameterizations of anisotropy,
- applying structural constraints for improving the reliability of FWI inversions, and
- application to field data.

3.4.2.2 Suitable parameterizations of anisotropy

As a first subtask, the model parameterisation of the anisotropic FWI algorithm was improved by replacing the elasticity tensor and the density as independent inversion parameters with P- and S- wave velocities parallel and perpendicular to the symmetry axis, the density and a combined parameter $\sqrt{C_{13}/\rho}$, which describes the curvature of the velocity dependence on the propagation direction. With this new model parameterisation, the FWI results of the same 2D synthetic data set were significantly improved.

3.4.2.3 Structurally constrained FWI

In the case of 2D elastic transversely isotropic FWI, there are five independent elastic inversion parameters. For elastic isotropic FWI, which has only three independent inversion parameters, (Manukyan et al., 2012a) have shown that the resolution characteristics of different model parameters strongly depend on the parameter type. Moreover, depending on the experimental configuration there might be strong cross talks between different model parameters during the inversion. Since FWI is an iterative process, both the poorer convergence of some model parameter types and the parameter trade-offs can adversely affect the overall convergence of the inversion. To improve the convergence behavior of the inversion for elastic isotropic FWI (Manukyan et al., 2018) a structurally constrained FWI approach was developed, which additionally penalizes structural differences between different model parameters.

The structurally constrained FWI was extended to the anisotropic case, and the inversion of the same data set shows that structurally constrained FWI is able to produce much sharper tomographic images.

3.4.2.4 Testing of improved FWI

Seismic tomography experiments were conducted at the Mont Terri URL in the Opalinus Clay in north-west Switzerland. The experiments were focused on the imaging of the 1-m-diameter HG-A tunnel and its excavation damage zone (EDZ) (Figure 65) by using seismic waveforms. Seismic signals were generated with a high frequency P wave sparker source at every 0.25 m in the lower borehole and recorded with 48 three-component geophones. The geophones were cemented in the upper borehole with 0.5 m spacing between the sensors.

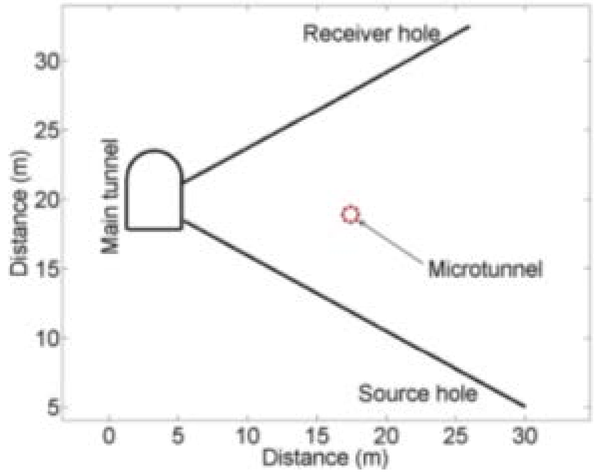

Figure 65. Schematic drawing of the layout of the non-intrusive seismic tomography experiment in the HG-A micro-tunnel at Mont Terri URL

Since FWI for 3D anisotropic media is computationally very expensive, and the design of the experiment allows for the 2D approximation, similar to the synthetic study, 2D FWI for transversely isotropic media was performed.

Figure 66 shows VTI FWI results of the Mont Terri data. Images of V_P^{90}, V_S^0 and V_{13} show a clear, 1-2 m wide layer with lower velocities. This layer is the high frequency fracture zone detected by borehole logging (Lanyon, 2008). Additionally, reconstruction of V_P^0 shows a rather blurred image of the microtunnel and its EDZ. A hint of the microtunnel and the EDZ can be seen also on V_P^{90} and V_{13} images. Despite the application of the structural constraints, there are large differences between different model parameter types close to borehole ends. This could be due to attenuation of the host rock that is not taken into account in the inversion. A comparison of recorded and predicted data is shown in Figure 67. It can be seen that the model is able to match both receiver components very well.

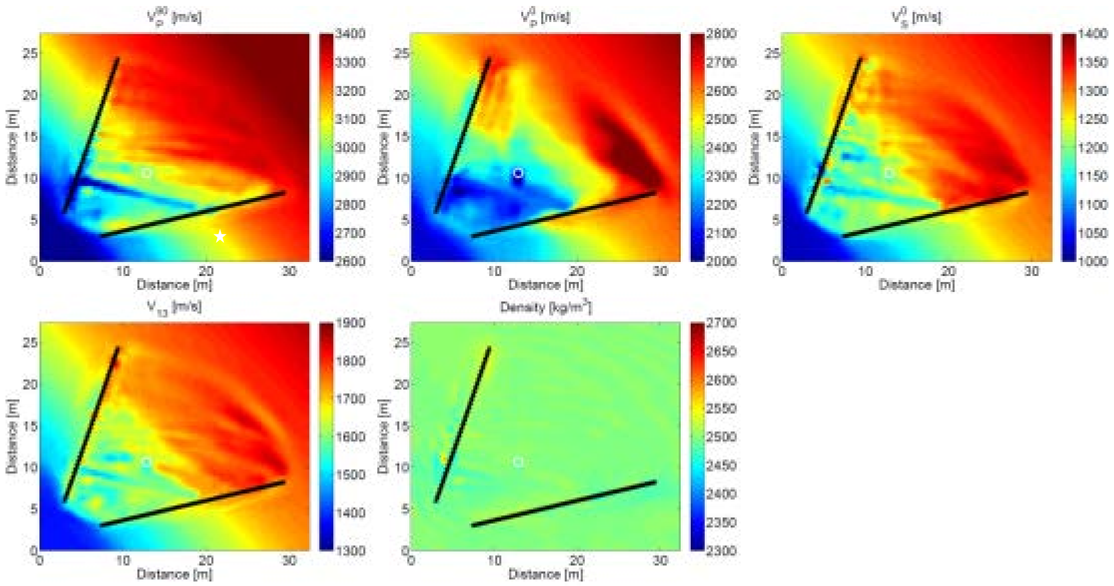

Figure 66. FWI results of data recorded in Mont Terri

The coordinate system is rotated in order to make the direction of symmetry axis vertical. Black crosses indicate locations of sources and receivers. White circles indicate location of the microtunnel. White star indicates the source location for shot gathers of Figure 67.

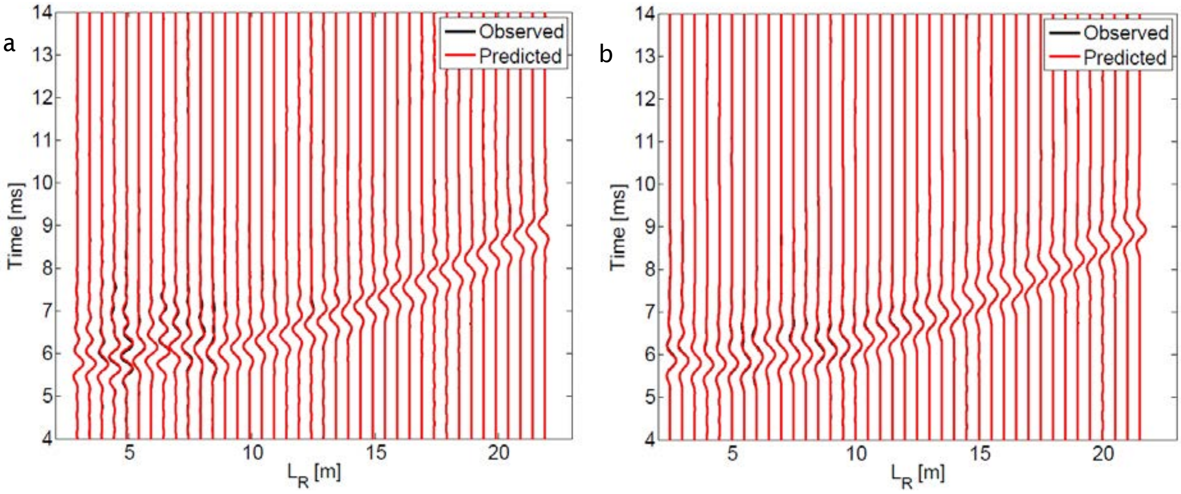

Figure 67. Comparison of observed and predicted seismograms for geophone direction parallel (a) and perpendicular (b) to the receiver borehole for a source indicated by a white star in Figure 66.

3.4.2.5 Discussion of results and conclusions

With the carried out work on the non-intrusive seismic monitoring of radioactive waste repositories, a model parameterisation was discovered, which allows successful FWI for 2D TI media. Furthermore, the numerical experiments performed show that incorporation of structural constraints into the anisotropic FWI allows further improvement of tomographic images. The new algorithm was applied on the data recorded around HGA tunnel in the Mont Terri URL. First inversion results show that with FWI it was able to detect the microtunnel and its EDZ as well as prominent repository structures, such as the predicted fracture zone.

In the calculations, the effect of inelastic attenuation was mainly absorbed by source and receiver terms since the effect of inelastic attenuation was not taken into account. Hence, the tomographic images can be further improved by developing a robust algorithm for calculation of inelastic attenuation. Further improvements can be made by replacing the pressure sources by directional sources or by using both of them.

3.4.3 Differential tomography with borehole radar data

3.4.3.1 Introduction, background and objectives

Monitoring temporal changes within a volume of interest is one of the primary missions of geophysical surveying, and it finds many applications related with near surface targets, such as groundwater fluctuations (e.g., [6], 7.1.3), freezing and thawing of permafrost (e.g.,[7], 7.1.3), and radioactive waste repository monitoring (e.g., [8], 7.1.3).

The simplest monitoring option is to perform repeated surveys in a consistent manner and to analyze the data sets individually. Temporal changes can then be inferred by qualitative or quantitative comparisons of the results (parallel difference strategy, e.g. [9], 7.1.3). If a tomographic inversion algorithm is involved in the data analysis, the results obtained from a first data set can be used as the initial model for the inversion of the follow-up data set (sequential difference strategy). It is also possible to invert directly for the differences of two data sets. This is referred as the double-difference strategy [9]. This approach is particularly useful (i) in the presence of systematic data errors, and (ii), when the data differences can be determined more accurately and/or more consistently than the actual data.

Differential inversions of monitoring data are expected to provide more accurate results, because they consider only differential changes between experiments, and are thus less susceptible to systematic errors compared with traditional inversions. Here, it is investigated if such methods can be applied to ground-penetrating-radar (GPR) data acquired in the framework of a full-scale emplacement (FE) experiment conducted in the Mont Terri Rock laboratory.

It should be noted that GPR travel times instead of seismic waveforms were considered in the FE experiment. Furthermore, this is an intrusive experiment. Nevertheless, the methodological developments and the lessons learned from the field experiment can be transferred in a relatively straightforward manner to non-intrusive FWI experiments.

3.4.3.2 Experimental setup, the FE experiment

Double-difference traveltime tomography was applied to a borehole radar data set acquired in the framework of the FE full scale experiment at Mont Terri [10], 7.1.3. Its main objective is to demonstrate that high-level radioactive waste can be stored safely in a deep geological repository. For that purpose, a 3 m diameter tunnel was drilled that should mimic a full-scale repository. High-level radioactive waste canisters are simulated by placing three heaters within the tunnel. After their installation, the tunnel was backfilled with a granulated bentonite mixture (GBM) and finally sealed with a shotcrete plug. The heaters were then switched on, and temperatures reached approx. 130 °Celsius on the heater surfaces, and, depending on the position, 45 to 60° at the tunnel walls.

For monitoring temporal changes of the GBM, two fiberglass pipes were inserted prior to the installation of the shotcrete plug. As shown in Figure 66, these pipes extended beyond the first heater in the tunnel. They were employed for a variety of borehole logging surveys and cross-hole measurements.

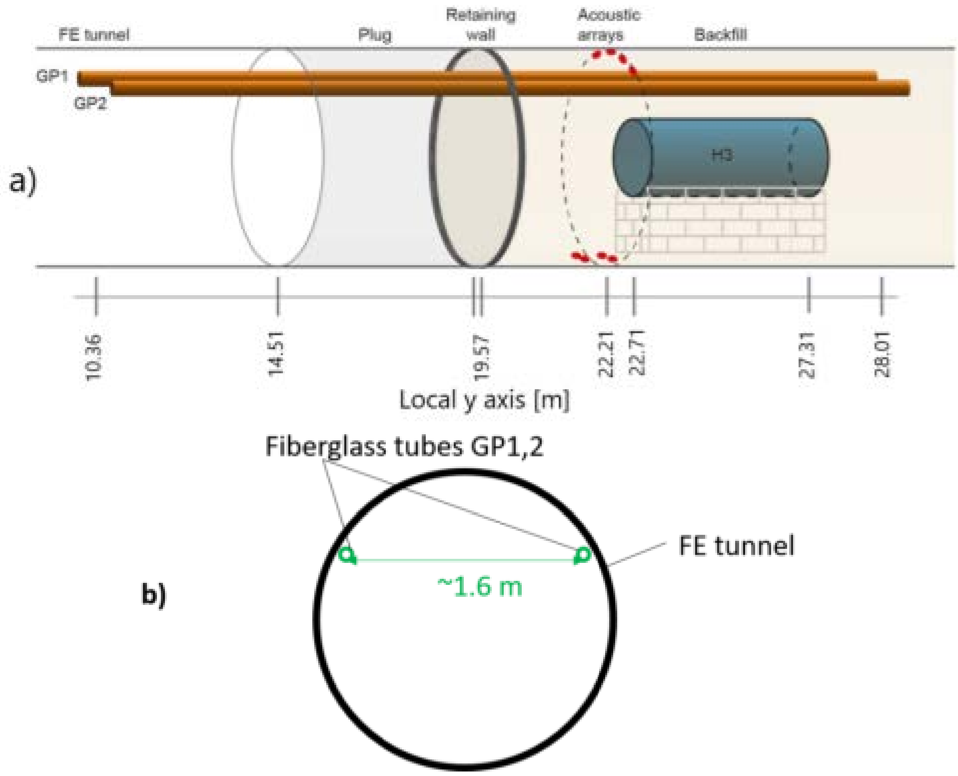

Figure 68. Setup of the FE experiment. a) Side view – GP1 and GP2 are the fiberglass tubes within which the crosshole experiments were performed. H3 represents the heating unit. b) View along the tunnel axis

3.4.3.3 Methodological Developments

Determining high-precision differential travel time data: Initially, the first break arrival times were picked manually. Then, the accuracy and consistency of the picks was improved using a procedure that automatically eliminates traces with a poor signal-to-noise ratio. Furthermore, it reduces the influence of random errors and problematic data points that can be eliminated prior to the tomographic inversions.

Double difference tomography: Similar to the procedure employed for optimizing the travel time data, this approach does not only provide more consistent results, but it can also identify problematic velocity parameters, where the discrepancies between the original and refined velocity differences are particularly large. Furthermore, the methodology can be transferred in a straightforward manner to differential amplitude inversions.

3.4.3.4 Validation with experimental data

Subsequently, the double difference tomography and the refinement procedures, as described above, were applied to the cross-hole radar measurements performed between GP1 and GP2. Travel-time tomography results are shown in Figure 69.

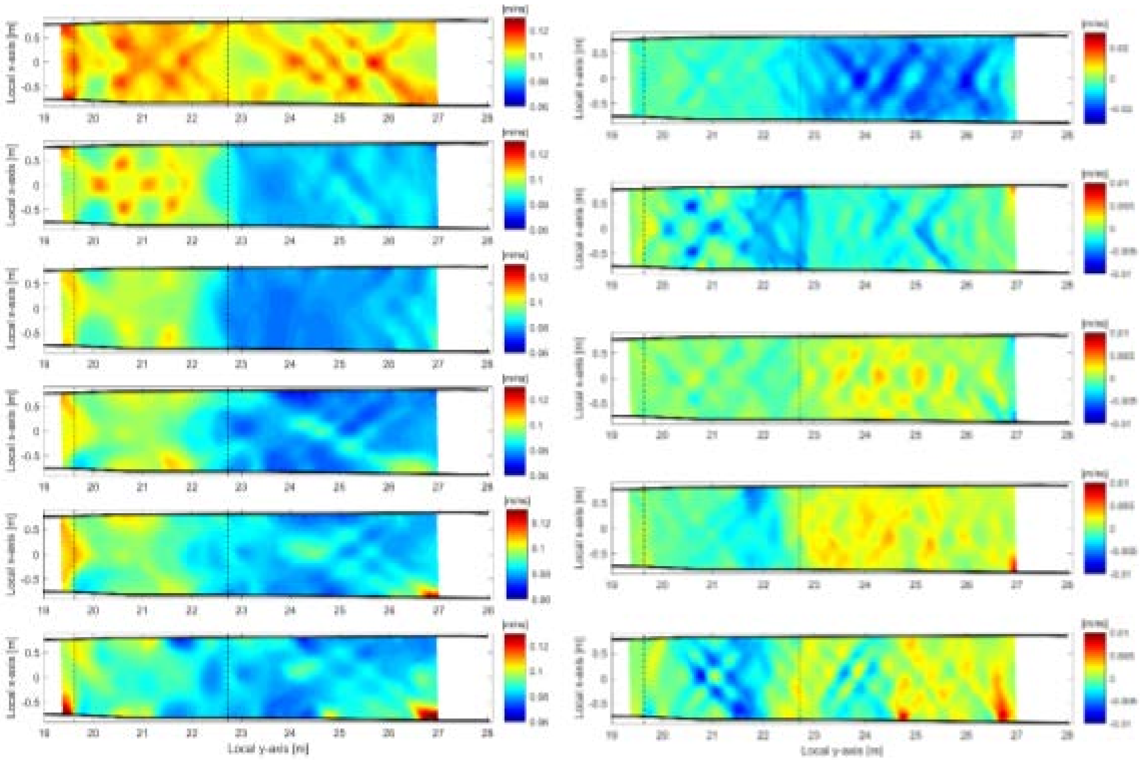

Figure 69. Results from cross-hole radar tomography. Left panels show absolute tomograms, and right panels show double-difference tomography results (differences of consecutive experiments)

The left panels show absolute tomograms of the six experiments carried out so far. The first experiment was performed prior to switching on the heater. After switching on the heater, there is a considerable drop of radar propagation velocity in the region of the heater. This is due to the temperature dependency of the dielectric permittivity that governs the radar velocities. At later experiments, we observe the appearance of low- and high-velocity heterogeneities. They can be attributed to the penetration of moisture into the GBM and the formation of air-filled voids. The right panels in Figure show the results obtained from double-difference tomography. These images are particularly useful for studying the evolution of the small-scale heterogeneities that appeared in the course of the experiments.

3.4.3.5 Discussion of results and conclusions

A novel procedure was developed for determining high-precision and highly consistent GPR travel time data, with which the potential of double-difference tomography can be fully exploited. Furthermore, a refinement technique was proposed that allows redundant differential tomograms to be made more consistent. Both procedures do not only lead to improvements of the accuracy of the results, but they also offer powerful means for identifying data glitches and problematic areas in the differential tomograms. The data refinement procedure is restricted to waveform data (i.e. GPR and seismics), but the differential refinement procedure can be applied to any inversion type during a post-processing step. The technology proposed can readily be applied for monitoring radioactive waste repositories. It is not only suitable for GPR data, as described in this report, but it can be extended in a straightforward manner to other data types (e.g., seismic or geoelectrical data).

3.4.4 Anomaly detection algorithm

3.4.4.1 Introduction, background and objectives

Geophysical tomography often requires extensive data analyses and substantial computer resources. Therefore, it would be valuable to detect temporal changes in a repository using quick and inexpensive imaged tools, such as the so called anomaly detection algorithms. The methodology is based on the idea of using the computer vision techniques to describe the structures in the geophysical data and detect the anomaly using the feature vectors and direct inversion (Kosková and Novák, 2012). The original algorithm was implemented for the gravity field data, and it was tested on predefined set of simple anomaly bodies with density contrasts.

During the past ten years, machine learning and supervised classification was often applied in the domain of geophysical data processing. With focus to seismology data, we can see the application of artificial neural networks (ANN) as well as the support vector machines (SVM) and other types of the classification methods. A detailed overview of ANN application is given in (Diersen et al. (Diersen et al., 2011). The ANN were used to detect the arrival time of the first break, as event classifiers, or to differentiate the natural earthquakes from human caused explosions (Orlic and Loncaric, 2010). The artificial intelligence was also tested to control or monitor the civil infrastructure (Fisher et al., 2017). Ruano et al. (Ruano et al., 2014) gives an example of the implementation of the real-time seismic monitoring system based on the multi-layer perceptors and support vector machines.

3.4.4.2 Algorithm development

The application to the Modern2020 data sets required to redefine the algorithm to be usable with the seismic data for repository monitoring. As the underlying physical model in seismics is more complex compared to gravity, it was decided not to use the direct inverse calculations and to focus on the supervised learning based on the DT and SVM.

The heart of the modified algorithm is a pre-trained classifier with ability to distinguish predefined normal and abnormal repository configurations. The algorithm itself was updated using synthetic seismic data. The model was simulating an experimental analogue of the repository tunnel with different levels of water saturation. The configuration with low water saturation was selected as an abnormal situation and corresponding data sets were labelled as abnormal, the rest of the data were labelled as normal.

The first step was to decide what type of structures should be detected in the data and what is the correct labelling of the data for the supervised training. Several initial synthetic data sets for different configuration of the repository were generated and it was decided to concentrate on the standard circular shape of the tunnel and detect different water saturation (from 0 to 100 %).

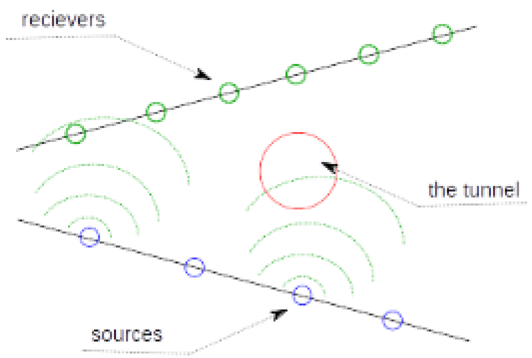

Figure 70. The configuration for the synthetic data set

The input data model included 113 sources and 108 receivers. All the waveforms were separated and converted to a set of matrices resulting in 113 images of the tunnel for each water saturation. This matrices were normalized from real values to the value range from the interval <0,1>. Normalized data were thresholded at 9 levels from 0.1 to 0.9. The thresholded images were binary black and white data. With different water saturation of the tunnel, we can see different number of objects in the thresholded images. Also, the total area of the object is different. Therefore it was decided to create a characteristic vector each concrete situation. The data preprocessing (normalization, thresholding, object detection and labelling) was implemented in Matlab. The data were stored in a Matlab Table structure. The general chain of the data pre-processing is depicted in Figure 71.

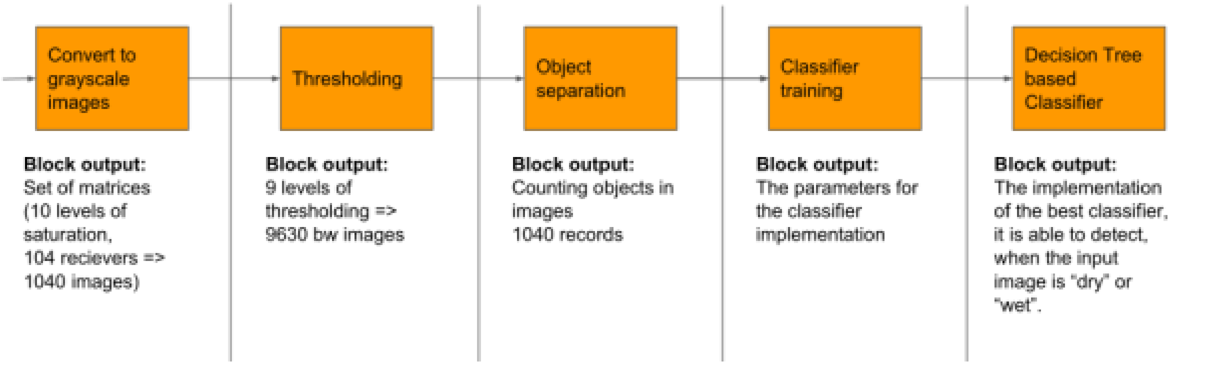

Figure 71. The data preprocessing for the classifier training. Original data are normalized, thresholded, the objects are detected and counted, and characteristic vector is created to get the training data

3.4.4.3 Algorithm testing

The prepared data sets were used to train and verify the classification decision trees and the support vector machines. Two different tools were used to supervise machine learning: the Classification Learner application from Matlab and our own implementation in Python with support of TensorFlow.

The seismic velocity and elasticity parameters in the saturated tunnel are so close to those of the host rock, such that the tunnel is nearly invisible. The dry tunnel exhibits more contrast - the reflection of the waves in the tunnel are visible in the thresholded images. The images were converted into feature vectors of the form [N_{01}, …, N_{09}, S_{01}, S_{02}, …,S_{09}] (N_{0n} is the number of objects detected at the threshold level n and S_{0n} is the total area of the objects detected at the corresponding threshold level).

To select the most suitable architecture of the classifier, the Matlab Classification Learner was used to identify the best fitting classifier structure. The best results were obtained with the fine decision tree using the Gini diversity index and maximum number of splits was set to 100. Table 10 summarizes the accuracy of the classification for different classifier types.

Table 10. The different classifier structures and accuracy of the classification

Classifier type	Fine tree	Medium tree	Coarse tree	SVN linear	SVN quadratic	SVN cubic	SVN Gaussian
Detailed Description	Max 100 splits	Max 20 splits	Max 5 splits	Linear kernel	Quadratic kernel	Cubic kernel	Gaussian kernel, scale 0.75
General accuracy of classification	87.3 %	85.5 %	82.9 %	77.8 %	81.1 %	86.9 %	87.7 %

3.4.4.4 Validation with experimental data

Field data were acquired in the Bedrichov tunnel locality the Czech Republic. It was not possible to acquire seismic data, but the anomaly detection algorithm can also be applied to other data types. Therefore, it was decided to acquire geoelectrical data in the tunnel. The data were acquired in February 2019, and the data analysis is currently underway.

3.4.4.5 Discussion of results and conclusions

The best results were obtained with the fine decision tree and the SVN based on a fine Gaussian kernel. The abnormal situation in the repository ("dry tunnel") was correctly detected in 91 % of all the simulations using the fine decision tree and in 92 % of all the cases using the SVN structure. In a next step, the algorithms were implemented with the support of Tensor Flow and its libraries. The decision tree classifier was trained with the same training data as in the Matlab environment. The average classifier accuracy was of 88 %. The full algorithm is now available in Python.

3.4.5 Development of a method based on combined Electrical Resistivity Tomography and Induced Polarisation Tomography

3.4.5.1 ERT and IPT fundamentals

ERT and IPT are electrical geophysical techniques used to measure the earth's electrical properties, resistivity and chargeability. Resistivity is known to be sensitive to changes in water content (Michot et al., 2003, Binley et al., 2002, Zhou et al., 2001, Fukue et al., 1999, McCarter, 1984, Archie, 1942, amongst others) and temperature (Aaltonen, 2001, Campbell et al., 1948, Schlumberg, 1989, Bottraud et al., 1984). Similarly, induced polarization also has been used to measure changes in water content and temperature (Ghorbani et al, 2009). The tomographic time-lapse electrical resistivity and induced polarization monitoring can be carried out simultaneously and non-destructively in 3D in the buffer-backfill-canister bedrock systems using the full waveform low frequency resistance information in time-domain between numerous current injection dipoles and potential difference dipoles. The 3D electrode chains can be embedded into boreholes, bentonite-bedrock interfaces (pellet layers), tunnel floors, backfill materials etc.

The base principle of the ERT is very simple: a continuous electric current of intensity I (in mA) is generated between two current electrodes A and B – where A is the injection electrode (positive), and B is the reception electrode (negative) – placed at the surface of a ground. The more the two electrodes are spaced the more the spatial extent of electrical field is. If we add at this two current electrodes two potential's electrodes, M and N, allowing the measurement of the difference of potential ΔV (in mV) due to the joint action of A and B, the resulting quadripole allows measuring the ground apparent resistivity ρ_a (in Ωm). A geometric factor is involved in the calculation that depends on the geometry of the electrode array and the topography.

In electrochemistry, polarization is defined as the change in the equilibrium potential of an electrochemical reaction. There are two types of induced polarization (IP) known to geophysicists, the membrane polarization known as the background or normal IP, where there are variations in the mobility of ions in fluids throughout the material, and the electrode polarization where there are variations between ionic and electronic conductivity where metallic bodies are present. Both are indistinguishable by IP measurements.

IP measurements can be done in two ways, known as - time-domain and frequency-domain induced polarization. In the time-domain IP the current is cut off and voltage decay is recorded. The Residual Voltage *V(t)* existing at a time *t* after the current is cut off is compared with the steady voltage *V* during the current-flow interval (Figure 72, left). Chargeability, *m*, is the parameter used to measure the IP in time-domain. In the frequency-domain (Figure 70, right) the apparent resistivity is measured at two or more frequencies usually in the range between 0.1 and 10 Hz.

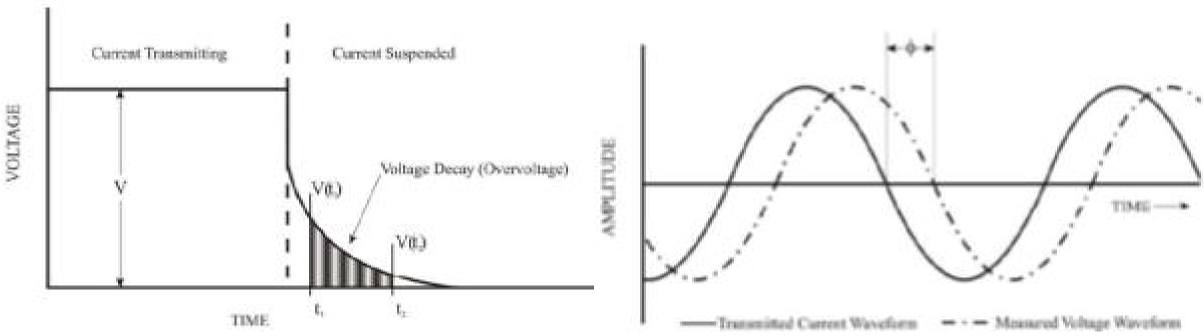

Figure 72. Voltage decay in time-domain induced polarization (left) and Frequency variations in frequency-domain induced polarization (right) (Source: Glaser, 2007)

3.4.5.2 Objectives

The overall goal was to develop the IPT algorithms for the whole time-domain, on-time portions of the time-domain "spectral" full waveform potential recordings. These inversions can be carried out simultaneously with the ERT data. The IP information is picked as resistances against frequency from the current ON measured full waveform time-domain potential signals. In this way the same geologically-structurally constrained 3D/4D inversion process can be applied to IP responses as is used to invert the resistivity changes. On-time signals have a little better signal-to-noise ratio than off-time information (Olsson et al., 2015).

Specific objectives of this activity include

- development optimal numerical conceptualization, monitoring protocol and inversion processes for the combined ERT/IPT in the canister-buffer-bedrock system, and
- development of 3D/4D ERT/IPT inversion process with the possibility to thermo-hydro-chemical (THC) constraints (information from point-sensor time-series, from petrophysical dependences as well as from dynamic THC behaviour/knowhow.

3.4.5.3 3D ERT/IPT inversions

The idea of the time-lapse (repeated) measurements is to use the same fixed network of electrodes and use exactly the same measurement protocol for all monitoring cycles. Either the initial data set or the previous data set can be used to constrain the inversion of the later time data sets so as to minimize changes in the model resistivity that are unlikely to be due to actual changes.

Three alternative procedures for time-lapse inversions were developed. Prior information can be incorporated via regularization with respect to a reference model according to three basic protocols: 1. independent regularization involving a single reference model, 2. background regularization involving a reference model obtained via inversion of pre-injection data, and 3. time-lapse regularization involving an evolving reference model obtained via inversion of data from previous experimental stages.

3.4.5.4 Time lapse inversions

Considering different types of error sources and the correlation between errors of the different time-lapse data sets can help to improve significantly time-lapse inversion results (Doetsch, 2011).

A data set recorded at time step contains static, numerical and random errors. One common means of removing static and numerical errors is the difference inversion approach of LaBrecque and Yang (LaBrecque and Yang, 2001), which was successfully applied by Kemna et al. (Kemna et al., 2002). This inversion option has been also applied in this study.

3.4.5.5 Validation with experimental data

In the monitoring-inversion experiment a transparent laboratory column (a plexiglass tube of 20 cm inner diameter and 80 cm height) was filled up to 55 cm level with bentonite pellets (Figure 73). These roller compacted pellets have an initial water content of about 16% and were made from MX-80 bentonite. The saline water was injected at intervals from the same injection point into the pellet filling. The salinity of the injected water was 10 g/kg.

The electrode layout consists of four sets of vertical electrode chains (Figure 73). Each vertical line included 16 electrodes and each vertical level includes a symmetrically arranged four-electrode quadrupole. Vertical electrode spacing was 4 cm and the electrode lines were named as T1, T2, T3 and T4. The water injection point was in the middle of the electrode lines T1 and T2 on the height of 21 cm. The ERT monitoring that covered the whole test period and was carried out using all 64 electrodes. The near electrode surroundings were dry in the beginning of the test.

Repeated Electrical Resistivity Tomography (ERT) measurements in the interval of 12 hours were then used to map non-destructively in 3D the progress of infiltration fronts and water content changes. The test was carried out between 26.4.2017 and 18.6.2017. The salt solution was injected six times (27.4, 28.4, 30.4, 2.5, 3.5 and 19.5) in 75-100 minute intervals into the column and each time 1000 g of water was injected.

In this experiment, the multi-gradient protocol (Dahlin and Zhou, 2006) was applied in programming the 1304 measured dipole-dipole pairs with 64 electrodes. After acquisition, the data are pre-processed to remove bad measurements.

The primary results of the ERT test are the 3D resistivity distributions that are calculated for each single monitoring. These results are typically studied as 2D vertical and horizontal slices that are cut from the 3D models or in 3D as selected colour contours. The other alternative is to present results as 2D rectangular surfaces as a function of distance from the centre of the cylinder structure. Some examples are shown in Figure 74.

The results of the resistivity distributions seem to be rather stable between the measurements and the progress of the wetting front can be traced during the injection periods (27.4-3.5). During the longer non-injection period (3.5-19.5) the changes in the resistivity distribution are small as expected.

From the 2D rectangular outer surface presentations (Figure 74) the progress of the water content changes around the column cylinder can clearly be followed (only results from the main injection period are selected and presented).

After the test, the experiment structure was dismantled and the water samples were taken to analyse in some points the water contents. The water content information correlated well with the final 3D resistivity distribution.

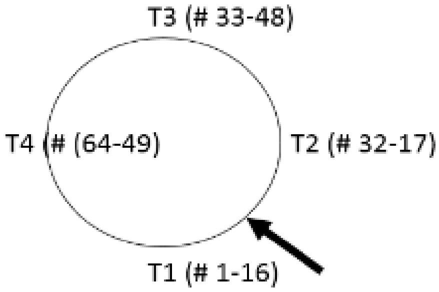

Figure 73. The test column with the locations of vertical electrode chains T1, T2, T3 and T4 as well as numbering of 64 electrodes and the location of the injection point between T1 and T2

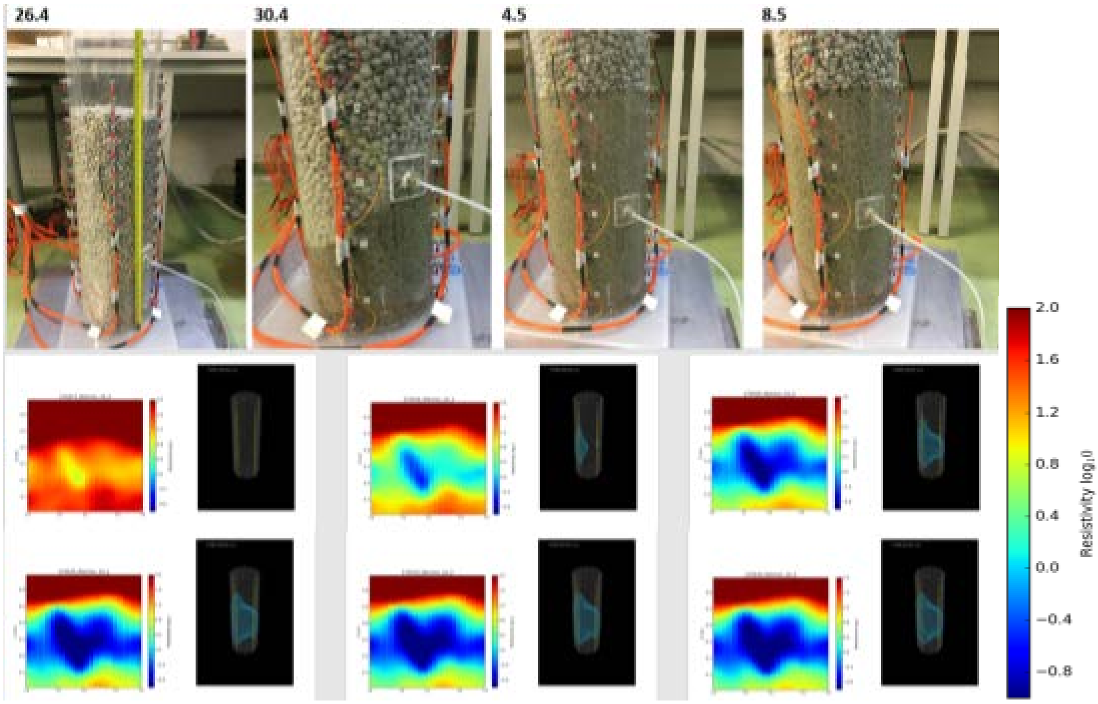

Figure 74. The 3D resistivity results for the beginning of water injection period presented as daily snapshots. These daily snapshots are presented as 2D rectangular surfaces representing the outer volume the cylinder structure

3.4.5.6 Discussion and conclusions

A time-lapse (4D) inversion was developed. Furthermore, measuring and signal processing protocols for simultaneous ERT and IPT imaging of the canister-buffer-bedrock systems were established. Besides, data processing algorithms were developed for identifying and removing noise, signal spikes and the self-potential drift from the full-waveform recordings of measured potentials in order to increase the signal-to-noise ratio and thus widen the spectral time-lapse information (Olsson et al., 2016).

According to the results obtained, the induced polarization tomography offers a valuable, cost-effective addition to ERT monitoring. It can be carried out simultaneously inside the common ERT monitoring process. In the time-domain, the simplest IP process will only double the duration of each monitoring cycle.

In the near future the 3D ERT and induced polarization measurements will be used more and more together with the 3D reactive transport simulations. The overall, time-lapse resistivity and chargeability distributions offer an effective calibration and updating platform for hydro-geochemically modelled temperature-salinity-water content responses.

3.4.6 Calibration and validation of constitutive relationships between electrical parameters and temperature and volumetric water content

3.4.6.1 Background and objectives

In the bentonite environment ERT imaging is especially sensitive to spatial and temporal changes in water content. Induced polarization imaging is in turn especially sensitive to changes related to cation exchange capacity. Both techniques are in principle sensitive to changes of same electrical properties in bentonite and bedrock environment but differently (and thus to water content, salinity, temperature and clay content (electrical changes in electrical double layers of minerals). By combining these methods, the interpretation of the data can be more precise and it helps to individually identify the actual cause for changes in time and space. A priori knowledge of parameters from the sensor (point) measurements, such as temperature, pressure, moisture content and salinity can be used as additional (model) constraints that can be embedded into ERT/IP data inversion.

Previous researches conducted in repository like conditions have been successful in using Electrical Resistivity Tomography (ERT) for monitoring the EBS (Furche and Scuster, 2014; Rothfuchs et al., 2004). However, to the best of the authors knowledge there has been no attempt in investigations to date to implement and develop the approach to monitor the EBS beyond the research phase, as a non-intrusive technique, as in these studies cited, the ERT electrodes are buried inside the EBS.

Thus, In addition to developing the tomographic inversions codes, it was also planned to establish relations between the electric material properties and geotechnical properties, such as water content, temperature, etc. This was achieved using the following steps:

- Bentonite and compaction methods for the samples to be used for the calibration programme were selected.
- A system for DC electrical resistivity and induced polarisation measurement consisting of four electrode probes (coupled with the same electronic system to be used for ERT and IPT testing) was calibrated against salt solutions of known electrical conductivity and chargeability at different temperatures.
- Homogenous samples prepared at different water content (ranging from compaction water content to full saturation) were tested at different temperatures (ranging from 20°C to 80°C). Steady-state and transient voltage measurements were performed.
- Single-variable inversion of the steady-state electrical field allows inferring the real part of the electrical conductivity and single-variable inversion of the transient electrical field allows inferring the imaginary part of the electrical conductivity. Complex electrical conductivity can therefore allow the calculation of the DC Electrical Conductivity and Chargeability.
- A cuboidal sample was heated on side and wetted on the opposite side. The advancing water and thermal fronts propagated within the sample and ERT/IPT were performed. Reconstruction of thermal and hydraulic field via uncoupled and coupled inversion was compared with local measurements of water content/suction and temperature.
- Validation in a full field-scale demonstration, where the temperature and water content fields were compared against local measurements via wireless sensors.

For the operational monitoring phase of buffer materials in deep geological repository, saturation and temperature are two key parameters. If a constitutive relationship between the geoelectrical/induced polarisation data and saturation and temperature can be established, this will offer powerful means for non-invasive monitoring of engineered barriers.

3.4.6.2 Calibration test: Measurements of resistivity and Induced Polarization on Bentonite samples using the four-point method

For establishing a relationship between geoelectrical/induced polarisation data and saturation and temperature, comprehensive laboratory measurements on bentonite samples were carried out. They were prepared by mechanically mixing bentonite clay with synthetic water up to the target gravimetric water content at 1000 rpm for 5 minutes. All samples were left in a sealed bag for 24 h for homogenization before any test was performed.

The volumetric water content and temperature of the samples was varied systematically, while measuring the electrical resistance and induced polarisation effects. The data were acquired by injecting the current into copper electrodes located at both extremes of the sampler in contact with the cross section of the sample and the difference in potential generated are read by two electrodes located on the top of the sample.

Figure 75 shows the electrical resistivity as a function of volumetric water content and temperature. Resistivity values of the bentonite samples are relatively low, even in samples with low volumetric water content. This was expected, given the good conductivity property of the bentonite material. As expected, resistivity values decrease with increase of volumetric water content, and there is a decrease of resistivity values with increase of temperature of exposure. Those differences are becoming less pronounced with increasing volumetric water content.

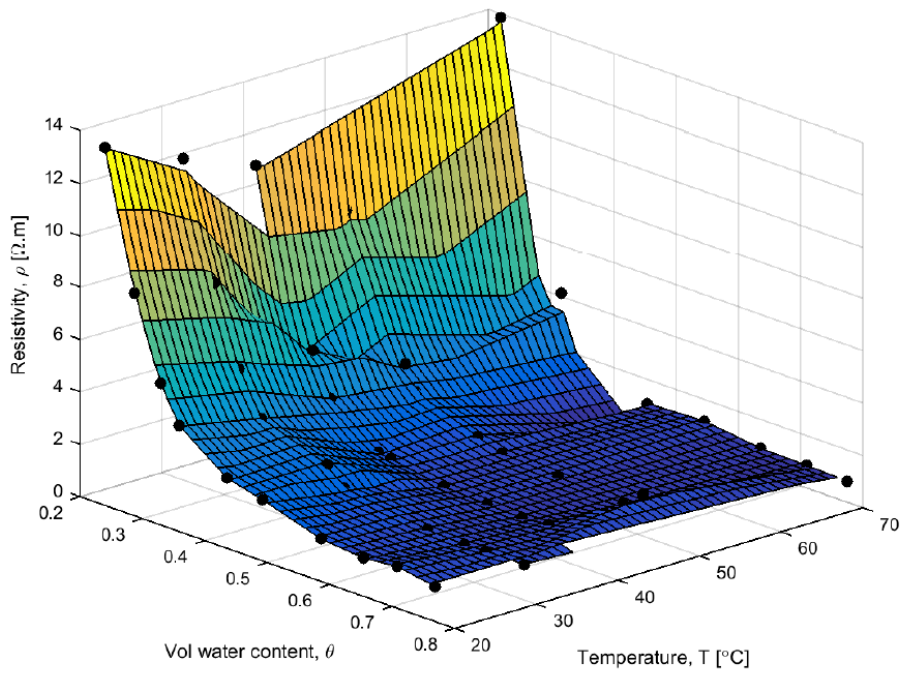

Figure 75. Resistivity results of bentonite samples. Black dots indicate measurements.

The relationship between volumetric water content, temperature and chargeability is harder to assess (Figure 76). It can be observed that for all temperature series the peak chargeability values are reached between 30 and 50% of volumetric water content. This behaviour may be explained by the presence of fixed sites on the clay surface that are responsible for active IP. When only a few of these sites are occupied by water, there are only a few mobile ions, as they are closely attached to the clay surface, as a result the IP response is small. However, as the volumetric water content increases, the sites become available for ion exchange, which gives a marked increase in the IP response.

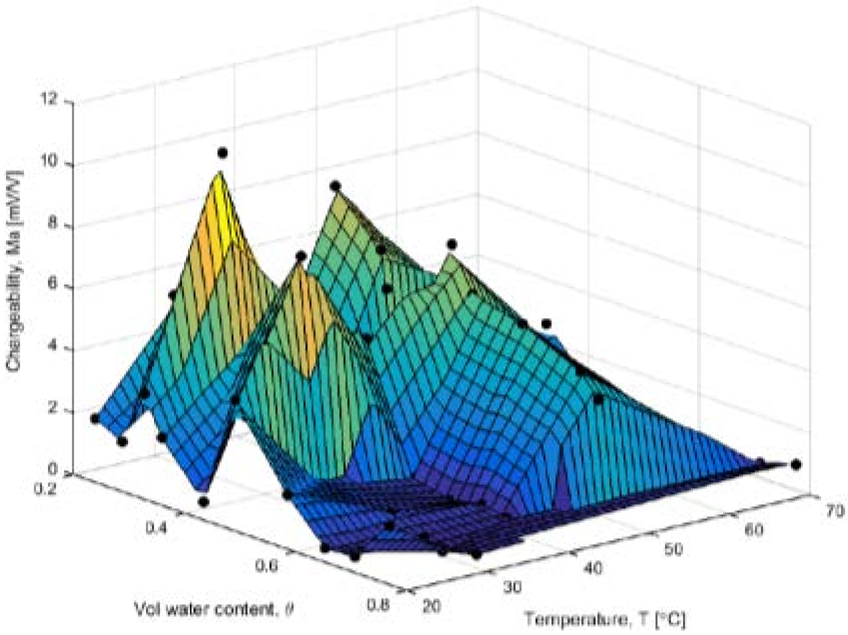

Figure 76. Chargeability results of bentonite samples. Black dots indicate measurements.

3.4.6.3 Discussion of results and conclusions

The calibration studies performed on bentonite samples revealed an expected relationship between resistivity and moisture content as well as resistivity and temperature. The relationships between chargeability and moisture content and chargeability and temperature, although harder to assess, were consistent with what have been reported elsewhere.

Quantitative analysis is harder to report, even for the resistivity parameter, due to the nature of the relationship. There is a sharp reduction in resistivity in a narrow saturation range, followed by almost constant values of resistivity for values of volumetric water contents higher than 40%. The same is observed for the relationship between resistivity and temperature.

To improve further the approach, IP surveys could potentially be incorporated to give additional information to the ERT surveys. However, the interpretation of the chargeability results needs have to be carefully considered, since they are not straightforward.

3.4.7 Overall conclusions and achieved TRL improvement

As written in this report, most research objectives were achieved, and it is judged that these new findings will provide significant information for designing and monitoring future high-level radioactive waste repositories. Here, we briefly summarize the achievements and provide, where appropriate, suggestions for further research.

Seismic waveform inversions (FWI)

Seismic anisotropy of the host rock is a long-standing problem that has precluded application of the powerful FWI techniques for monitoring radioactive waste repositories. With the new developments in the framework of this project, this problem could be addressed. In particular,

- a suitable parameterizations of anisotropy was found and implemented,
- structural constraints for improving the reliability of FWI inversions were established,
- suitable pre-processing workflows were developed, and
- the methodology was tested with field data.

FWI technologies are continuously further developed, and novel developments need to be critically assessed, if they could be beneficial for radioactive waste monitoring purposes. Besides methodological improvements of the FWI technology, it will be required to establish constitutive relationships between elastic parameters and quantities, such as temperature and moisture content (similar as discussed in Section 4.4.6 for ERT/IPT data).

Differential tomography

A novel technique was established that allows consistent and high-precision differential changes of physical parameters to be delineated. The methodology was tested successfully in the framework of the Mont Terri Full-scale Emplacement (FE) experiment. As input data, travel times and amplitudes were employed, and it should be a relatively straightforward task to apply the technology to FWI problems.

Anomaly detection algorithms

A detection algorithm was established and tested with synthetic data. Further tests with field data will be required to validate the capabilities of the algorithm.

Geoelectrical techniques

The potential of geoelectrical techniques for monitoring radioactive waste repositories was tested in the framework of this project. For that purpose, ERT and IPT algorithms were implemented and tested. In particular, the performance of the ERT algorithm was validated with laboratory experiments.

Besides the algorithmic developments, extensive calibration tests with bentonite samples were performed. Furthermore, relationships between the electrical parameters, such as resistivity and chargeability, and other physical parameters, such as temperature and moisture content could be established. The methodology is currently further tested with a demonstrator experiment in Tournemire.

TRL improvement

The improvement achieved for the different techniques during the project is estimated in the following table.

Table 11. TRL improvements made thanks to Modern2020 project

Technique	Initial TRL	Final TRL
Seismic waveform inversions (FWI)	6	7
Differential tomography	5	6
Anomaly detection algorithms	2	3
Geoelectrical techniques	6	6-7

Results, obtained so far with these techniques, show that there is a great margin for further improvements.

3.5 Reliability and qualification of monitoring components

3.5.1 Introduction

Technical or operational requirements imposed on monitoring equipment may be attributed to different reason as for instance:

- Individual national monitoring concepts and scopes;
- Essential safety functions, that should not be impaired, e.g. barrier performance;
- Specific nature of the parameters that need to be measured;
- Necessary sensitivity of a method or the range of values that need to be measured;
- Necessary specificity of a method and the cross-sensitivity to other environmental variables;
- Etc.

Many of the performance measurement issues that WMOs will face could be extremely challenging. At the cell scale, the monitoring devices and installed equipment must further resist to the severe environmental conditions existing in a repository, which may include high temperatures, high pressures, humidity and/or submersion, chemically aggressive environments, and levels of radiation that may degrade electrical and optical cables performances.

Typical requirements also include the longevity (several decades) of expected monitoring (without real possibility of accessibility to maintain equipment, except by robotized devices), the high level of needed confidence in signal reliability, and the absence of interference with barrier performances, in particular as pertaining to long term safety. This is a key requirement of the monitoring system not to degrade the favourable conditions and expected performances for long-term safety of the repository.

The harsh environmental conditions present in a facility deep below the surface are a major issue for the design of reliable, long-living equipment. In view of the challenging conditions expected for the components of the future monitoring system intended for DGR the development of a robust procedure for their proper qualification is a must.

This chapter synthesises the progress made by eight expert organisations AMBERG (Spain), ANDRA, IRSN, EDF & UMONS (France), EURIDICE (Belgium), SKB (Sweden) and VTT (Finland) under the lead of IRSN, on a common multi-stage methodology for qualifying monitoring components (MC) of the measurement chain (sensor, connecting cable and/or wireless system/controller) for a Deep Geological Repository (DGR).

The carried out research addresses the following objectives of the task 3.6 of Modern2020 project:

1. To gather and analyze the transferable experience from other industries on the performance of relevant sensors and other monitoring equipment that could be used in a repository context.
2. To search and analyze case studies of long lived electronic components and fibre-optics components that have been in operation for as many years as possible in applications worldwide and in conditions similar to those expected in repositories.
3. To develop a methodology for selecting monitoring components to be tested on testing benches.
4. To test the selected components and equipment using different techniques with the aim of producing robustness tests and accelerated ageing under the conditions to be found in a repository: temperature, humidity and pressure, chemical attack/corrosion and radiation.
5. To analyse the results and proposal of most adequate techniques and equipment through the proposal of a general methodology assumed convenient to all WMOs.

The complete results were reported as document D3.6 “Reliability and Qualification of components” [1] in the Modern2020 project.

3.5.2 State of the art and gathering of transferable experiences from other fields

3.5.2.1 Followed approach

The ability to ensure reliable and durable monitoring system with repeatable quality through the time life is critical for DGR implementation. However, as there is still no implemented DGR existing analogies can also be a way for qualifying the monitoring components (MCs) and obtain reliable equipment over the long term. The analysis of transferable experience from other fields aims at summarizing the different protocols used by other industries with respect to the monitoring components to deliberately accelerate their ageing and qualify their use. This was done by taking into account the feedback from industries working in harsh environments through a bibliographic research made around two major companies EDF and ESA, involved in the energy and the space field, respectively and by comparing it to the approach proposed by Andra, the French agency for radioactive waste management, for the Cigeo project.

3.5.2.2 Experience from the energy industry field

Innovations (eg. new design of the hydraulics at Marèges, France), accidentology (eg. Malpasset, Rance) and pathologies of works at dams (alkali-reaction concrete at Chambon, France) promoted a need for remote long-term quality monitoring. This especially concerned reliability of data transmission as dams are not easily accessible in winter. Nuclear power plant monitoring was inspired by these practices by using similar sensors as dam monitoring, for instance telemetry systems. However, in order to take into account different characteristics between these structures, as well as the large number of sensors involved in hydraulic and nuclear power plants (around 20,000 sensors in 600 civil engineering works), EDF has defined and implemented an industrial policy for the choice, the qualification and the maintenance in operational conditions of auscultation equipment. It is based on the following three main principles:

- Use of a limited number of types of equipment,
- Development of a selection and qualification process for materials,
- Sustainability of qualified materials.

This has conducted EDF to develop an original approach for selecting and qualifying the components for the monitoring of Dams and of Nuclear power plants implemented through five main tasks summarized in Figure 77 after [2] and including:

Figure 77: Selection and qualification process implemented at EDF for monitoring components

The selection of material and suppliers further to a permanent watch on technologies is based on the following features: accuracy (absence of drift over time), insensitivity to environmental conditions (temperature, humidity, surges), reliability (inaccessible device, continuity of measurements), robustness (hostile environment: humidity, cold, lightning...), and maintainability.

The materials are selected according to their manufacturer characteristics. EDF is preferably looking for "close" (European) suppliers who are well represented in the area to benefit from a better after sales service and easier dialogue as part of a partnership. The cost aspect of the material is obviously considered. However, this criterion is weighted against the others (in particular the reliability and the robustness) because the recurrent failures of a hardware installed on an isolated site become very quickly expensive.

The laboratory qualification includes the verification of metrological characteristics, tests for sensitivity to influence quantities, verification of functional and ergonomic features, and verification of compliance with the standards in force, robustness and ageing tests.

At last, on-site qualification is performed either on large scale mock-up or on real structures. The former is generally operated in parallel with devices already in place and qualification pronounced after a satisfactory exploitation time lasting at least one year. The use of large-scale mock-up aims at verifying the behaviour of components at a larger time scale and at conditions similar to real ones or even better controlled. One example is that of the Vercors (Monitoring System for Reduced Scale Containment Model) experiment developed for verifying the behaviour of components associated to a reactor structure [3].

3.5.2.3 Experience from the space field

Concerning the space field, Europe via The European Space Agency (ESA) has created its own European “organism” for space qualification, namely the European Space Components Coordination (ESCC). It is shown that despite different influencing parameters, due to the rocket take-off (vibrations) or the space conditions (vacuum, temperature, radiations), the qualification process is rather similar to that developed in the energy field. The selection of components is a complex process that alone accredited companies (SAFT, TRAD, IAS) are able to perform. It includes the analysis of performances, design, operational, simulation of harsh environment, manufacturing and testing. The testing of components requires qualification campaigns in space simulators, controlled clean environments, thermal vacuum space cycling, vibration pot and irradiation facilities and is considered as achieved when the Part Approval Document (PAD) is fully filled up and signed (Appendix 6.1)[4].

3.5.2.4 Andra’s approach for the repository field

An overview of typical environmental conditions, expected operating performances such as durability and precision, and other specific constraints imposed by the repository safety requirements were presented in the MoDeRn Technical Requirements Report [5]. It is recommended that available state-of-the-art monitoring technology is adapted and qualified to meet these requirements, and where necessary innovative technology is developed and qualified as well. To illustrate this recommended approach, a succinct description of the qualification process that Andra has set up is provided. It entails testing and qualifying the complete measurement chain, by progressive steps, knowing, to be able to anticipate them, the failure rates and mastering the possible long term drifts. The overall process is inspired from the qualification guide for non-destructive methods. Global test sequence includes four stages such as in Figure 78:

- Stage one consists in acquiring in-depth knowledge of the sensing technology, engineering solutions, practical implementation constraints. It aims at selecting the technologies best suited to the specific requirements of monitoring the geological repositories for long-lived nuclear wastes. When commercially-available sensing chain performances do not fulfil requirements, research programs will be initiated.
- Stage two consists in carrying out laboratory tests, under fully supervised and/or controlled environmental conditions, to qualify the sensitive component and assess the complete measurement chain performances. Sensors are tested in air, and embedded in host material of interest.

- Stage three consists in outdoor tests, to evaluated field implementation influence. At this stage, the sensing chain is preserved from hazardous conditions, extreme temperature or gamma rays. Unexpected influence parameters might thus be revealed.
- Fourth stage involves hardening in view of the application environmental conditions. In the envisioned French geological repository, temperature (25°C to 90°C), gamma radiation (dose rate of 10 Gy/h at HLW contact), and hydrogen (up to 100%) are amongst the main stresses to be analysed.

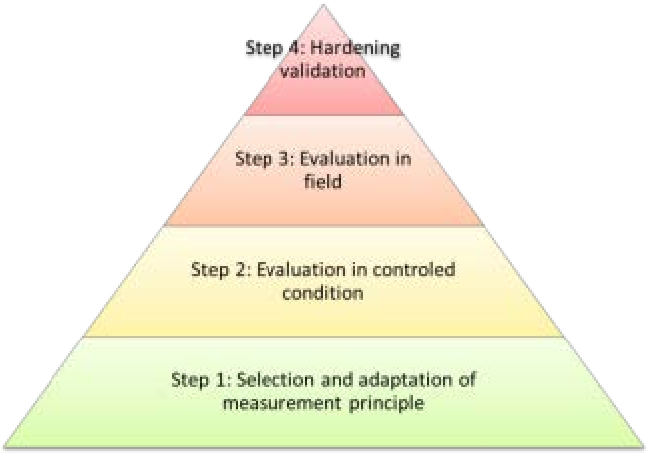

Figure 78. Qualification process for technology implementation in the Cigéo project

3.5.2.5 Results

Results indicate that there is a strong synergy between DGR and other fields (Energy, Space,) concerning the needs, such as robustness, long-life power supply, and optimization of communications. All fields consider at least three common stages: i) Selection of components, ii) Laboratory qualification and iii) On-site qualification.

3.5.3 Lessons learned from existing long-term experiments

3.5.3.1 Selected experiments

The second part of this study concerned the analysis of case studies of monitoring components operating in conditions close to those expected in repositories. The main idea was to obtain information about ageing, accuracy, possible drift over time and robustness of sensors installed. This was done through a selection of large in situ experiments performed at URLs or in large mock-ups (GCR, FEBEX, SEALEX, POPLU, PROTOTYPE). The selected experiments can be split into two categories: demonstrator and long-term as listed in Table 12 with a schematic description of experiments illustrated in Figure 79.

Table 12. Overview of Long-term experiments in URLs selected for their monitoring components with indication of duration.

Partner URL/LAB (country)	**ANDRA** LMHM(F)	**NAGRA AMBERG** GTS(CH)	**EURIDICE** Hades(B)	**IRSN** (F) Tournemire	**SKB** Äspö (S)	**VTT** Onkalo (FIN)	**SKB** Äspö (S)
Dismantled long-term and demonstrator experiments	GCR	FEBEX In situ					
Long-term experiments			CLIPEX	SEALEX	MPT	POPLU	Prototype
Duration (years)	6	18	18	6	5	5	8

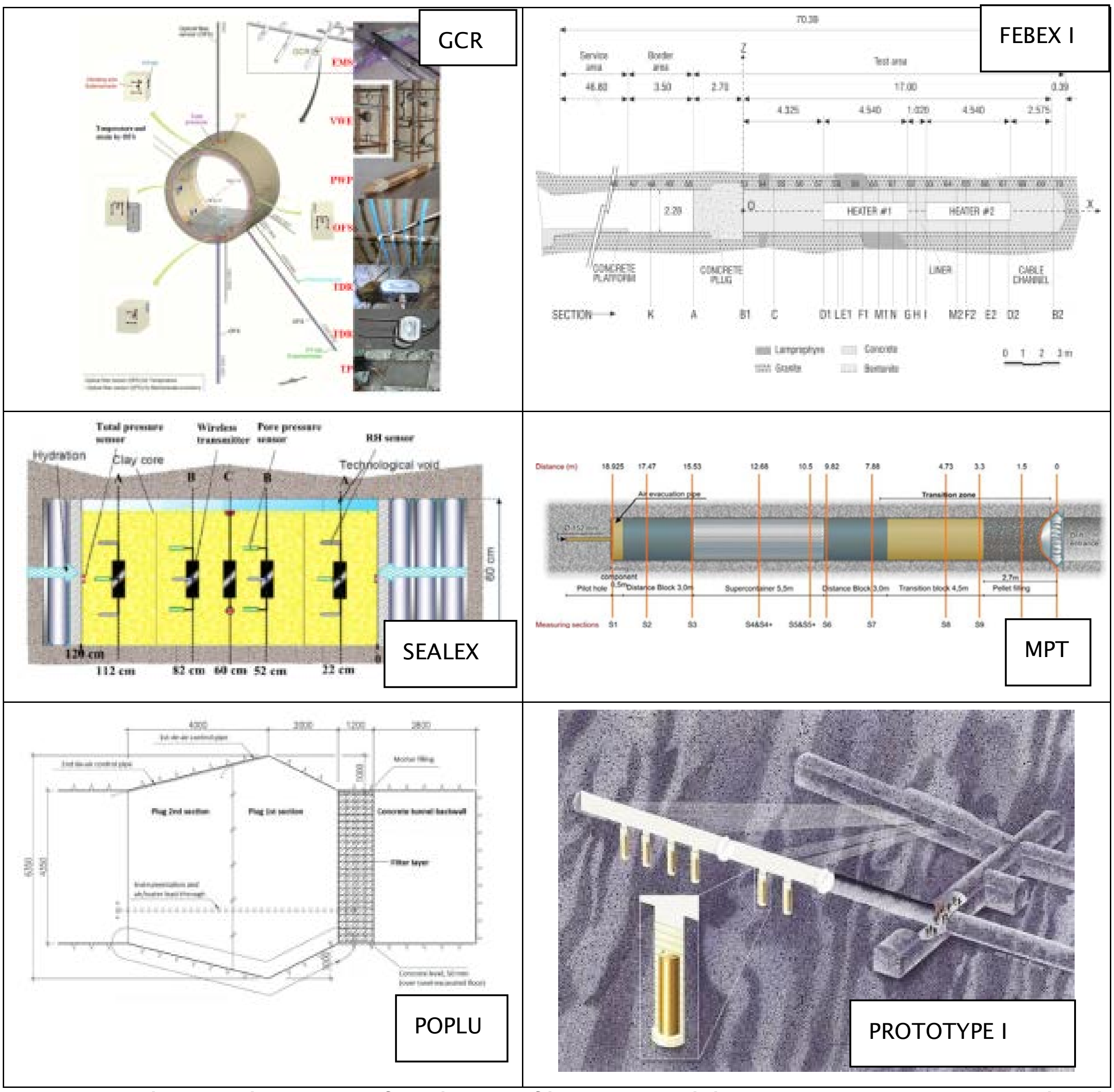

Figure 79. Schematic description of a selection of long-term and demonstration experiments analyzed for the behavior of their monitoring components Sensors performance

In demonstrators the general rule was to use high Technology Readiness Level (TRL) monitoring components essentially wired connected sensors such as in GCR and FEBEX. However, for the sake of redundancy and also for qualifying new or low TRL instruments, more innovative components including wireless sensors were applied in long-term experiments such as in POPLU, MPT or in SEALEX.

Each selected experiment was summarized through an experiment form detailing the type (long-term or demonstrator), present status (dismantled or on-going), goals, means and main results with respect to survival rate of sensors, the failure origin, if any, and the possible improvements [1]. Table 13 summarizes main conclusions with respect to the survival rate of wired/wireless sensors for the given experiment duration.

Table 13. Long-term experiments performed in URL and selected for their monitoring components with indications of duration, number of sensors wired and wireless and of their survival rate

Sensors/Experiment	GCR	FEBEX	SEALEX	MPT	POPLU	Prototype
Strain & Displacement						
SG				32/23	32/12	
D-LVDT					12/0	
D-VW	21/0	11/9				
FO Brillouin	4/3					
Temperature						
T	42/1	54/14			58/4	80/15
T-VW	22/0					
Multimode OFS	7/2					
Moisture & Humidity						
WC		34/34	54/54	34/19	7/4	67/?
WP		24/19		32/2		67/59
Volumetric Water Content						
WT	14/0	10/7				
WF				13/13		
Pore Pressure						
PP-P	6/0		54/40	50/20		18/15
PP-VW		28/23			11/0	26/7
Total Pressure						
TP-P	3/1		41/19	43/13		31/22
TP-VW		6/3			11/0	39/7
Gas Pressure						
GP				3/0		
Convergence						
EMS	15/0					
Inclination						
IB				6/2		
Flow & leakage						
FM				1/0	1/0	
Wired/Wireless		176/0	149/105	194/33	132/0	328/0
Total/damaged % survival rate	134/9 93%	176/108 39%	149/113 24%	227/99 56%	132/20 85%	328/125? 61%?

3.5.3.2 Results

The first lesson is that experiments only lasted a few years which is far below the 100 year operational phase expected for DGRs. The second finding is that despite a strict selection of the best technical solution of the moment, the analysis of the different long-term and demonstrator experiments suggest improvements on monitoring components: 1) For wired sensors, preference was given to passive measuring methods such as the vibrating wire technique and the optical fibre distributed sensing for which an extension of recording time is required to demonstrate the absence of water short circuits along the cables. In case of potential leakage, wireless technologies should be used and the size and number of cables should be limited; cables should also be more armoured and resistant to corrosion to prolong their service life. 2) For wireless sensors many problems occurred during swelling of the bentonite-based seal under water flow. Improvements mostly concern a better isolation between transmitters and sensors to avoid electrical short circuit with free water and the extension of batteries' lifetime.

3.5.4 Development of a qualification process

This task aimed at developing a protocol for selecting components potentially used in the repository monitoring system.

3.5.4.1 Selection of monitoring compounds

The selection must first consider the list of influence parameters which are DGR context and site specific. As for referenced monitoring fields, the selection must include the following requirements:

- Verification of metrological characteristics and performances (compliance with environment requirements including lifetime, radiations levels, mechanical stress, thermal stress, humidity exposure, and storage duration…).
- Sensitivity to influence parameters (Temperature, Humidity, Stress, Strain, Corrosion under in situ conditions, Hydrogen,…).
- Verification of functional and ergonomic characteristics and design.
- Verification of compliance with current standards (safety, CE marking, **PAD**, approved at accredited labs…).
- Operation: input/output power, operating temperatures, wavelength, modulation, consumption, end of life, etc.
- Testing: evaluation and qualification plan, test methods, screening definition.
- Quality and Product Assurance: focus on reliability and traceability, define the customers' reviews as early as possible, the list of documents to be delivered, how the hardware is accepted for delivery, and criteria for batch rejection.
- Verification of the Technology Readiness Level (**TRL**).

The highest **TRL** value is preferred for each component. Only **TRL**'s above 7 could be parameter and **DGR** specific as discussed in the WP 3.1 of Modern2020.

3.5.4.2 Methodology for testing and evaluating monitoring compound

The second step of the qualification process consists in testing of components under laboratory or real conditions of use. It is recommended that laboratory tests be conducted prior to field testing. A test form was sent to partners with the goal of having their feedback from laboratory testing methodologies. Two categories of laboratory tests were identified: Tests of robustness and ageing tests [1]. In both cases tests seek to estimate the degree to which a system or component can function correctly in the presence or stressful environmental conditions but ageing tests alone look at the normal degradation with actual time of use by accelerating artificially the process through a time-dependent stress.

Ageing is a testing process to accelerate artificially the normal degradation of a monitoring component (MC) with time of use. The process may be artificially accelerated with Temperature, Radiation, Chemistry, Humidity, Strain… It is meant to be representative for DGR service conditions, but with higher intensity of stresses, in order to reduce the duration of experiments. Irradiation test is a good example of <u>ageing test</u> such as those performed on new sensors developed in the framework of Modern2020. Tests were performed at the IRSN (IRMA) and CEN-SCK (RITA) facilities as in Figure 80 with Total Ionizing Dose (TID) of less than 0.1MGy and of 1 MGy, respectively. Most of the tests concerned Optical fibers and provided very promising results in view of their integration in a DGR. However, a lot of work remains to do to quantify precisely the Radiation Induced Attenuation on the fiber itself with the necessity to use a dopant or to evaluate the coupled impact of influence parameters (temperature, radiation, hydrogen…) on the sensing cable.

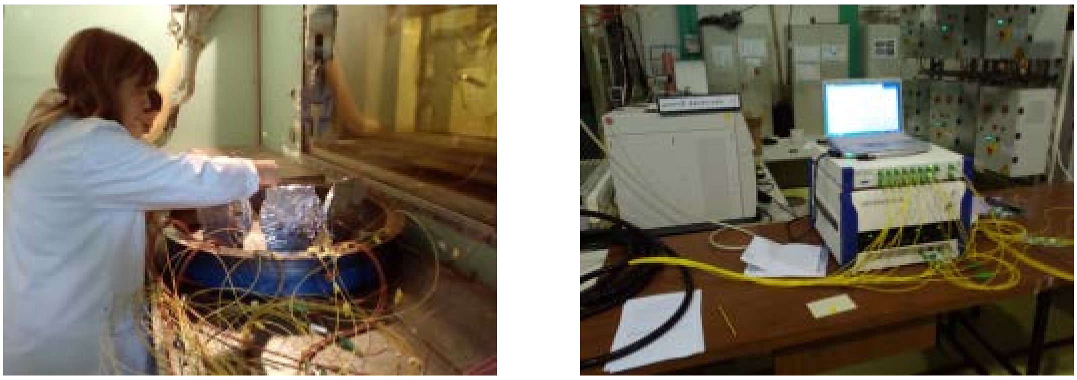

Figure 80: γ-irradiation at IRMA

Robustness is the degree to which a system or component can function correctly in the presence or stressful environmental conditions. Contrary to ageing tests, it is not intended to accelerate the normal degradation over the full time of use. They are a first stage of qualification to be done prior in situ testing. An example of robustness test is proposed by VTT for the Nordic repository case with the aim of developing a procedure to simulate long-term conditions in EBS environment as illustrated in Figure 81. Robustness tests are planned to be done in cycles so that it will give provisional results already during the test program. Test plan will consist of selected sensors and dummy sensors made to mimic the shape and having the same piping and tightness as the real ones and manufactured from different materials. The idea is to test sensor enclosure and sensor cable armouring/sheltering pipe with the dummy sensors. A test would consist of 20 iterative steps as shown in Figure 82.

Figure 81. Non irradiated robustness tests for a cable embedded in concrete at (left) 20, 40 or 60°C oven controlled temperature, (centre) alkaline solution tank at room temperature, (right) compressive creep bench and associated instrumentation.

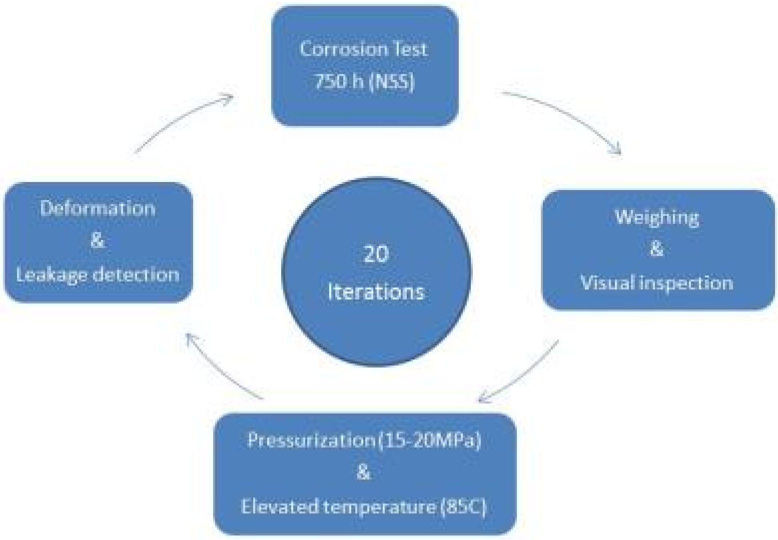

Figure 82. Example of cyclic robustness test applied to monitoring compounds to simulate their long-term conditions in the EBS environment

Contrary to laboratory tests, on-field tests may allow testing the complete measurement chain metrologically and functionally under real conditions of use. But for the moment, only demonstrators in underground, long-term experiments at on-site/off-site laboratories or at large mock-up can serve as dummy on-site tests. Monitoring strategies like that proposed by Andra also suggests using some “sacrificial”, “surveillance” or “witness” structure exhaustively equipped to fulfil the monitoring goals at the future repository.

3.5.5 Discussion and conclusions

The study resulted from a multi-stage analysis including: i) the study of transferable experience gained from other industry fields, ii) the analysis of case studies operating in conditions close to those expected in repositories, iii) the initiatives for the development of a qualification process for selecting and testing the monitoring components and at last iv) the proposal for a global protocol appropriate to all monitoring contexts. The carried out work led to the following conclusions:

- Each country is asked to develop its own project that will necessarily require the development of a different monitoring system and equipment. For this reason, the proposal of a generalized qualification process must overwhelm differences between projects and focus on the essential.
- There is a strong synergy with respect to the monitoring components between energy and space fields with needs for a DGR facility such as robustness, long-life power supply, and optimization of communications. The qualification process of those different fields always consider at least three stages including i) Selection of components, ii) The laboratory qualification and iii) On-site qualification.
- Despite a strict selection of the best technical solution of the moment, in situ and long-term experiments performed at URLs or at large mock-ups suggest improvements that can only be checked in situ where conditions will be as close as possible of the real one at DGRs.
- The Initiatives for the development of a generalized qualification procedure must combine robustness, ageing and on-field tests.

This enables to propose the following guideline that can be summarized by the global sketch given in Figure 83. This global sketch denotes an increasing complexity that may require a retrofit process in case of dissatisfaction of one of the three/four major steps.

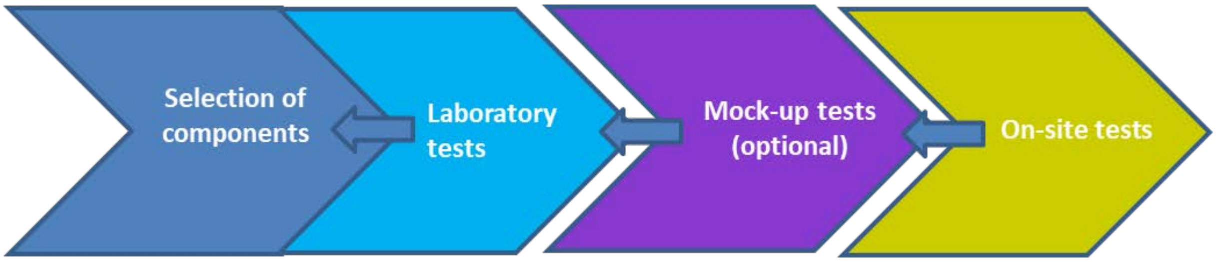

Figure 83: Global sketch for the qualification of monitoring components in DGRs

The first step concerns the selection of components (sensors, cables, housing, DAS etc.). It can be described as a desk exercise with lots of input from the manufacturers and from earlier tests for measuring influence parameters (Physical quantities and functionalities to be tested) very often performed at accredited laboratories. This selection first require preliminary steps such as: i) to set up the list of metrological and functional requirements in relation to the process to be measured, ii) to list influence factors and environmental constraints, iii) to perform a technological watch about devices and influence factors. The different steps linked to the selection of components are:

- ✓ Selection of components with the highest TRL (such as recommended in D31 of Modern2020 task 3 and rejection of components that do not fit the expected TRL value) and, if available, reliability features (MTTF of critical components).
- ✓ Verification of metrological characteristics (compliance with requirements).
- ✓ Sensitivity to influence parameters (Temperature, Humidity, Radiation, Stress, Strain, …).
- ✓ Verification of functional and ergonomic characteristics.
- ✓ Verification of compliance with current standards (safety, CE marking…).

The second step is that of Laboratory Tests of the selected monitoring components. It concerns testing of components/combined components under adverse conditions. This second step implies first to identify the devices (manufacturing date, software version, etc.) after verification of main functional and ergonomic characteristics and verification of compliance with current standards (safety, CE marking …). Those tests are preferentially carried out in accredited/certified laboratories (need to develop new testing benches, independent control). Each test must be achieved by a report detailing the protocols and main results with estimates of parameters uncertainty, and main conclusions about strength and weaknesses of the component. They include the succession of three kinds of steps:

- ✓ 1) Tests of robustness (Temperature, Hygrometry, Elongation, Crash….). They first include a calibration and verification of compliance with the target of use (nominal / degraded measurement range, maximal errors in the nominal measurement range, sensitivity, linearity, hysteresis) in controlled environment (no influence factor, no extra operational constraint). Next they must provide a detailed analysis of the influence of prominent parameters like temperature, humidity, radiation, stress, strain… and checking of the insignificancy of second order parameters like vibration for instance. They must provide the overall uncertainty based on testing reports.
- ✓ 2) Ageing tests under single then coupled influence parameters (γ Radiation, Temperature, Humidity, Salinity, O_2, H_2, H_2S, high pH, strain, deformation…). Those tests aim at accelerating artificially the normal degradation of a monitoring component (MC) with time of use. It is meant to be representative for DGR service conditions, but with higher intensity of stresses, in order to reduce the duration of experiments.
- ✓ 3) Communication tests for a multitude of monitoring components in cybersafe conditions as close as possible of that of the future DGR.

The third step concerns testing on-site meaning testing of the whole system under realistic conditions. It is done targeted to assess the whole system under realistic conditions. It can also be part of the safety demonstrations. Tests have to be performed under real conditions of use, and to qualify the complete measurement chain (sensor, connecting cable and/or wireless system/controller) including all the improvements identified earlier. To reach this goal several additional steps are required:

- ✓ Choice of real reference structures to be instrumented with the sensing solution: the structure should be enough representative of the final structure or similar to it. Is should not have any specifics which could disturb the qualification procedure (example: seasonal opening of cracks, alkali aggregate reaction in the concrete). As far as known, the best reference structures can be found in current long-term experiments at URLs and in dismantled long-term experiments. Direct experiments at the future Repository could also be considered (when possible)
- ✓ List of setup and commissioning requirements on site.
- ✓ Choice of an already qualified sensor system which allows to demonstrate that the new measurement chain meet its requirements on the field (inter-comparison metrology).
- ✓ Comparison of responses coherence based on main metrological features (inter-comparison exercises).
- ✓ Follow-up of ageing clues of the sensing chain.
- ✓ Validation of the communication devices.
- ✓ Periodic synthesis about metrological discrepancies, unidentified influence factors, operational constraints and clues about ageing (back to step 2 or 1 depending on the complexity).

At last, previous to on-site tests, **an optional step based on mock-up tests** may be considered if there is a need such as in the Vercors mock-up realized for a more realistic use of components.

By following the described methodology for all components, a much improved result in the selection process would be expected. The best way to articulate this methodology could be filling up a template similar to that utilized in the space industry (Appendix 6.1) and presented in Appendix 6.2. The objective of the ADOC document is to provide information about a monitoring component and its acceptability with respect to its selection, laboratory test and on-site test. The entity in charge of the surveillance of the repository shall document the ADOC sheet for approval of each component type intended for use in the repository.

3.5.6 Selection of monitoring technologies taking into account the required parameters to measure and the TRL of the available techniques

A screening methodology was developed In WP2. The Modern2020 Screening Methodology provides guidance on the steps that a WMO may take in identifying and managing a list of repository monitoring parameters, linked to processes, and repository monitoring strategies and technologies.

This screening methodology was tested through different test cases. Table 14 to Table 19 provide the outcome of several test cases: Cigéo, ANSICHT, Opalinus clay, OPERA, Turva 2012 and SR-Site. The tables describe the parameters of interest, the location of the measures, the selected technology in function of the state of art (highest TRL) and a justification of the relevance of this parameter.

Note that, with the exception of the ANSICHT test case, the results from the test cases relate to this exercise only, and do not represent fully underpinned decisions on parameters that would or would not be monitored in monitoring programmes implemented by WMOs in the future. The ANISICHT test case represents a preliminary iteration of the monitoring programme that could be implemented in a geological repository programme in Germany

Table 14. Parameters identified in the Cigéo test case

Parameter	Element	Strategy and Technology	Justification
Temperature	Disposal cell and surrounding near-field rock	Monitored directly in some disposal cells using **platinum probe** and/or **optical fibre sensors**.	Relevant to post-closure safety and retrievability (in that it provides information about possible rock deformation). Monitoring could provide confidence that the repository is behaving as expected and/or feed into repository design improvements and/or feed into periodic safety case updates.
Porewater pressure	Near-field rock	Monitored directly in some disposal cells using **vibrating wire or optical fibre piezometers**.	With temperature, provides information about interstitial overpressure in the near-field host rock, which is relevant to post-closure safety. Monitoring could provide confidence that the repository is behaving as expected and/or feed into repository design improvements and/or feed into periodic safety case updates.
Confining pressure	Total pressure on cell sleeve	Monitored directly in some disposal cells, using **optical fibre sensors**.	Provides information about the mechanical load acting on the cell sleeve, which is relevant to demonstrating retrievability of the disposal package. Monitoring could provide confidence that the repository is behaving as expected and/or feed into repository design improvements and/or feed into periodic safety case updates.
Diameter	Cell sleeve	Monitored directly in some cells using optical fibre sensors. Evolution of the sleeve will also be measured directly by **3D scanning.**	Provides information about the deformation of the sleeve, which is relevant to demonstrating retrievability of the disposal packages. Monitoring could provide confidence that the repository is behaving as expected and/or feed into repository design improvements and/or feed into periodic safety case updates.
Strain	Cell sleeve	Monitored directly in some cells, using **optical fibre sensors.**	Provides information about the deformation of the sleeve, which is relevant to demonstrating retrievability of the disposal packages. Monitoring could provide confidence that the repository is behaving as expected and/or feed into repository design improvements and/or feed into periodic safety case updates.
Hydrogen concentration	Cell atmosphere	Monitored directly in some cells using **LiDAR** and/or **thermal gas conductivity** and/or gas density and viscosity measurements.	Relevant to demonstrating retrievability of the disposal packages. Monitoring could provide confidence that the repository is behaving as expected and/or feed into repository design improvements and/or feed into periodic safety case updates.
Oxygen concentration	Cell atmosphere	Monitored with **luminescence sensors**	Relevant to demonstrating retrievability of the disposal packages. Monitoring could provide confidence that the repository is behaving as expected and/or feed into repository design improvements and/or feed into periodic safety case updates.
Relative humidity	Cell atmosphere	Monitored in some disposal cells using **capacitive sensors** (based on an electrical capacitor).	Provides information about the explosivity of the cell atmosphere, which is relevant to demonstrating retrievability of the disposal packages. Monitoring could provide confidence that the repository is behaving as expected and/or feed into repository design improvements and/or feed into periodic safety case updates.

Table 15. Parameters identified in the ANSICHT test case

Parameter	Element	Strategy and Technology	Justification
Temperature	Deposition hole seal (bentonite plug and concrete abutment)	Monitored directly in monitoring deposition boreholes at a number of "monitoring levels", e.g. using **resistance temperature detector** (RTD) or **fibre optic-based systems**.	Provides information about heat flow and temperature evolution in the seal, which is relevant to the performance target that the bentonite element shall be free from tensile stresses. Monitoring could provide confidence that the repository is behaving as expected.
Porewater pressure	Deposition hole seal (bentonite plug and concrete abutment)	Monitored directly in monitoring deposition boreholes at a number of "monitoring levels", e.g. using **vibrating wire** and/or **fibre optic sensors**.	Provides information about fluid pressure from below (due to thermal expansion and gas generation), which is relevant to the overall safety function of the seal and to the related performance target that the bentonite element shall be free of tensile stresses. Monitoring could reduce uncertainty and/or increase knowledge beyond that gained from the wider RD&D programme and/or provide confidence that the repository is behaving as expected and/or support repository design improvements and/or feed into periodic safety case updates.
Permeability/ groundwater flow velocity	Deposition hole seal (bentonite plug and concrete abutment)	Monitored by an indirect method using **pressure sensors** at different monitoring levels in dummy boreholes as well as in monitoring boreholes.	Provides information about fluid flow through the deposition hole seal, both into and out of the borehole. These are processes that are directly relevant to the overall safety function of the seal and to the related performance targets on permeability and swelling pressure of the bentonite element, and have an impact on modelled system performance. Monitoring could reduce uncertainty, increase knowledge beyond that gained from the wider RD&D programme, provide confidence that the repository is behaving as expected, support design improvements, and/or feed into periodic safety case updates.
Confining pressure	Deposition hole seal (concrete abutment)	Monitored directly in monitoring deposition boreholes at a number of "monitoring levels", e.g. using **vibrating wire** and/or **fibre optic sensors**.	Provides information about the mechanical load on the abutment from above (including backfill mass and, later, rock pressure), which is relevant to the performance target on the expansion of the bentonite element (increase in plug length). Monitoring could support design improvements.
Swelling pressure	Deposition hole seal (bentonite plug and concrete abutment)	Monitored directly in monitoring deposition boreholes at a number of "monitoring levels", e.g. using **vibrating wire** and/or **fibre optic sensors**.	Provides information about the swelling pressure evolution of the bentonite plug, which is relevant to the performance target on the swelling pressure of the bentonite element, and has an impact on modelled system performance. Monitoring could reduce uncertainty beyond the knowledge that gained from the wider RD&D programme, provide confidence that the repository is behaving as expected, and/or support repository design improvements.
Displacement	Deposition hole seal (vertical displacement of concrete abutment)	Monitored directly in monitoring deposition boreholes at a number of "monitoring levels", e.g. using **specific displacement sensors**.	Provides information about the displacement of the concrete abutment in the direction of the drift above, which is relevant to the performance target on the expansion of the bentonite element (increase in plug length). Monitoring could reduce uncertainty beyond the knowledge that gained from the wider RD&D programme, provide confidence that the repository is behaving as expected, and/or support repository design improvements.

Parameter	Element	Strategy and Technology	Justification
Water content/ saturation	Deposition hole seal (bentonite plug)	Monitored directly in monitoring deposition boreholes at a number of "monitoring levels", e.g. **using azimuthal deep resistivity (ADR) or ThetaProbes**.	Provides information about the saturation evolution of the bentonite plug, which is relevant to the overall safety function of the seal and to the related performance targets on permeability and swelling pressure of the bentonite element, and has an impact on modelled system performance. Monitoring could reduce uncertainty beyond the knowledge that gained from the wider RD&D programme, provide confidence that the repository is behaving as expected, and/or support repository design improvements.

Table 16. Parameters identified in the Opalinus Clay test case

Parameter	Element	Strategy and Technology	Justification
Temperature	Near-field host rock	Monitored in pilot facility (before and after sealing) using wired **fibre-optic distributed temperature sensors** and/or **wired or wireless thermocouples.**	A criterion has been set for host rock temperature that it should remain below the maximum palaeotemperature experienced by the host rock (if met, thermally-induced mineralogical changes can be excluded). Based on modelling, there is some uncertainty as to the extent to which the criterion will be satisfied within the monitoring timeframe, so it is deemed useful to monitor.
Porewater pressure	Near-field host rock	Monitored in on-site URCF.	A criterion has been set for host rock porewater pressure that it should remain below lithostatic pressure at repository depth (if met, the possibility that preferential release pathways will be generated by hydraulic fracturing can be excluded). Based on modelling, there is reasonable confidence that this criterion will be met within the monitoring timeframe but less confidence thereafter; therefore, monitoring may be useful to check the ability of the models to accurately predict later evolution.
Fluid (gas) pressure	At the bentonite/host rock interface	Monitored in on-site test facility (URCF), pilot facility (before and after sealing) and potentially in emplacement rooms, using distributed fibre optics and/or pressure sensors.	Gas pressure should remain below 80% of lithostatic pressure. This criterion is met if pathway dilation can be excluded and the analysis of the system can be simplified. Based on modelling, there is uncertainty as to whether this criterion would be met at least after the monitoring timeframe and possibly within it as well (depending on whether conservative gas generation rates are used), so it is deemed to be useful to monitor.

Table 17. Parameters identified in the OPERA test case

Parameter	Element	Strategy and Technology	Justification
Confining pressure	Supercontainer – carbon steel overpack	Not defined.	Provides information about mechanical disturbance to the overpack due to corrosion, cold cracking or welding, which is directly relevant to the supercontainer safety function of preventing contaminant release in the facility abandonment and poor sealing alternative evolution scenarios.
	Supercontainer – concrete buffer	Not defined.	Provides information about mechanical load (from external forces) on the buffer, which is indirectly relevant to the supercontainer safety function of preventing contaminant release and in the abandonment of facility and poor sealing alternative evolution scenarios.
	Supercontainer – steel envelope	Not defined.	Provides information about mechanical load (from external forces) on the envelope, which is indirectly relevant to the supercontainer safety function of preventing contaminant release in the abandonment of facility and poor sealing alternative evolution scenarios.
Displacement	Supercontainer – carbon steel overpack	Not defined.	Provides information about mechanical disturbance to the overpack due to corrosion, cold cracking or welding, which is directly relevant to the supercontainer safety function of preventing contaminant release in the abandonment of facility and poor sealing alternative evolution scenarios.
	Supercontainer – concrete buffer	Not defined.	Provides information about mechanical load (from external forces) on the buffer, which is indirectly relevant to the supercontainer safety function of preventing contaminant release in the abandonment of facility and poor sealing alternative evolution scenarios.
	Supercontainer – steel envelope	Not defined.	Provides information about mechanical load (from external forces) on the envelope, which is indirectly relevant to the supercontainer safety function of preventing contaminant release in the abandonment of facility and poor sealing alternative evolution scenarios.
Hydrogen concentration	Supercontainer – carbon steel overpack	Not defined.	Provides information about steel corrosion of the overpack following water ingress, which is directly relevant to the supercontainer safety function of preventing contaminant release in the abandonment of facility and poor sealing alternative evolution scenarios.
	Supercontainer – steel envelope	Not defined.	Provides information about steel corrosion of the envelope due to interaction with Boom Clay porewater, which is indirectly relevant to the supercontainer safety function of preventing contaminant release in the abandonment of facility and poor sealing alternative evolution scenarios.

Parameter	Element	Strategy and Technology	Justification
Porewater pH	Supercontainer – concrete buffer	Not defined.	Provides information about geochemical evolution due to porewater/concrete interaction, which is directly relevant to the supercontainer safety function of preventing contaminant release in the abandonment of facility and poor sealing alternative evolution scenarios.
Porewater / groundwater chemistry	Supercontainer – concrete buffer	Not defined.	Provides information about geochemical evolution due to porewater/concrete interaction, which is directly relevant to the supercontainer safety function of preventing contaminant release in the abandonment of facility and poor sealing alternative evolution scenarios.
Redox potential	Supercontainer – carbon steel overpack	Not defined.	Provides information about steel corrosion of the overpack following water ingress, which is directly relevant to the supercontainer safety function of preventing contaminant release in the abandonment of facility and poor sealing alternative evolution scenarios.
	Supercontainer – concrete buffer	Not defined.	Provides information about geochemical evolution due to porewater/concrete interaction, which is directly relevant to the supercontainer safety function of preventing contaminant release in the abandonment of facility and poor sealing alternative evolution scenarios.
	Supercontainer – steel envelope	Not defined.	Provides information about steel corrosion of the envelope due to interaction with Boom Clay porewater, which is indirectly relevant to the supercontainer safety function of preventing contaminant release in the abandonment of facility and poor sealing alternative evolution scenarios.

Table 18. Parameters identified in the TURVA 2012 test case

Parameter	Element	Strategy and Technology	Justification
Temperature	Canister, but measured in tunnels	Monitored indirectly from tunnels (not directly related to a specific requirement on the canister).	Related to the performance target that the canister should not impair the safety functions of other barriers, hence relevant to post-closure safety, although primarily verified through design, dimensioning and QC (limited value in monitoring).
Permeability/ groundwater flow velocity	Tunnels and host rock around repository	Monitored directly from tunnels (away from deposition holes). Deposition tunnel plugs monitored visually while accessible.	Indirectly related to canister, buffer and backfill as these elements are designed to perform within specific boundary conditions. If these conditions are maintained in the geosphere then there is confidence that the canister, buffer and backfill will perform as designed, so they are considered useful to monitor. May include “light” monitoring of flow through deposition tunnel plugs.
	Deposition tunnel plug	Monitored directly during operations until tunnels backfilled, using a weir.	Provides information about piping/erosion in the buffer, since flow through the plug is related to flow through unsaturated deposition holes and could therefore indicate piping. This process is directly related to the safety function for the buffer to limit advective mass transfer. There is value in monitoring during the early development of the repository.
Swelling pressure	Buffer	Monitored in full-scale and/or *in situ* test, using sensors.	Directly relevant to several buffer performance targets, e.g. isostatic load from the buffer swelling pressure should be <10 MPa in the lower part of the buffer; swelling pressure should be less than the yield strength of copper canister and Olkiluoto host rock.
	Backfill	Monitored in full-scale and/or *in situ* test, using sensors.	Directly relevant to several backfill performance targets, e.g. swelling pressure at all points in the deposition tunnel >0.1 MPa in fully saturated state; backfill shall contribute to the mechanical stability of the deposition tunnels.
Geometry	Canister	Monitored in full-scale and/or *in situ* test (at installation and dismantling).	Directly relevant to several canister performance targets: canister must remain intact, copper shell must remain >0mm, should withstand asymmetric buffer swelling pressure loads of 3-10 MPa, which are relevant to overall safety function of preventing radionuclide release.
	Buffer	Monitored in full-scale and/or *in situ* test (at installation and dismantling).	Provides information about buffer water uptake, related to performance targets that buffer displacement should be limited, diffusion should be the dominant transport mechanism, and limits on isostatic load from buffer swelling. The process takes a long time, however, *in situ* tests could provide performance model validation.
	Backfill	Monitored in full-scale and/or *in situ* test (at installation and dismantling).	Provides information about backfill water uptake, related to performance targets on backfill hydraulic conductivity, swelling pressure, limited deformation and requirement to contribute to mechanical stability of tunnels. The process takes a long time, however, *in situ* tests could provide performance model validation.
Displacement	Tunnels and host rock around the repository	Indirect, regional monitoring. Also addressed through the RSC methodology.	Seismicity, including potential rock displacements, are indirectly related to the canister, buffer and backfill (e.g. related to performance targets for canister to remain intact and for copper shell to remain >0mm thick), with an emphasis on suitable deposition hole locations. If such locations are seismically suitable then there is confidence that the barrier elements will perform as designed.

Parameter	Element	Strategy and Technology	Justification
Relative humidity	Backfill	Monitored in full-scale and/or *in situ* test (using sensors).	Provides information about water uptake and swelling, which are relevant to several backfill performance targets.
Water content/ saturation	Buffer	Monitored in full-scale and/or *in situ* test (at installation and dismantling).	Related to characteristics and processes affecting performance of buffer, e.g. water uptake and swelling.
	Backfill	Monitored in full-scale and/or *in situ* test (at installation and dismantling).	Related to characteristics and processes affecting performance of backfill, e.g. water uptake and swelling.
Porewater / groundwater chemistry	Host rock around repository	Monitored directly from tunnels (away from deposition holes).	Indirectly related to canister, buffer and backfill as these elements are designed to perform within specific boundary conditions. If these conditions are maintained then there is confidence that they will perform as designed, so they are considered useful to monitor.
Mineralogy and chemistry	Buffer	Monitored in full-scale and/or *in situ* test (at installation and dismantling).	Related to performance of buffer as expressed in several performance targets (e.g. maintain favourable chemical conditions, should deform sufficiently to maintain canister integrity).
	Backfill	Monitored in full-scale and/or *in situ* test (at installation and dismantling).	Related to performance of backfill (e.g. performance target that backfill should have limited potential to be a source of sulphide).
Density (dry and bulk)	Buffer	Monitored in full-scale and/or *in situ* test (at installation and dismantling).	Related to various characteristics and processes affecting performance of buffer (e.g. water uptake) as expressed in performance targets (e.g. buffer displacement should be limited, diffusion should be the dominant transport mechanism, limits on isostatic load from buffer swelling, should deform sufficiently to maintain canister integrity).
	Backfill	Monitored in full-scale and/or *in situ* test (at installation and dismantling).	Related to various characteristics and processes affecting performance of buffer (e.g. water uptake) as expressed in performance targets (e.g. backfill hydraulic conductivity, swelling pressure, limited deformation and requirement to contribute to mechanical stability of tunnels).
Pore structure	Buffer	Monitored in full-scale and/or *in situ* test (at installation and dismantling).	Directly related to the performance target that the buffer should have sufficiently fine pore structure to filter radiocolloids, which is directly relevant to post-closure safety.
Piping and erosion	Backfill	Monitored in full-scale and/or *in situ* test (at installation and dismantling).	Directly relevant to hydraulic conductivity of the backfill, which is the subjected to a performance target, as well as to homogenisation of density.

Table 19. Parameters identified in the SR-Site test case

Parameter	Element	Strategy and Technology	Justification
Permeability/ groundwater flow velocity	Deposition tunnel plug	Monitored directly during operations until tunnels backfilled, using a weir.	Provides information about piping/erosion in the buffer, since flow through the plug is related to flow through unsaturated deposition holes and could therefore indicate piping. This process is directly related to the safety function for the buffer to limit advective mass transfer. There is value in monitoring during the early development of the repository.
Porewater / groundwater chemistry	Host rock around repository	Monitored via borehole **sampling.**	Relevant to safety functions for backfill and buffer to retain sufficient mass over their lifecycle. To do this, they must be stable in contact with groundwater with a certain total charge equivalent of cations. Therefore, the relevant parameter is the electrical conductivity of the host rock groundwater. There is limited value in monitoring in order to build further confidence in the post-closure safety case as the relevant process is very slow; however, groundwater chemistry is already monitored through sampling at repository level as part of the host rock monitoring programme.
Corrosion rate	Canister	Monitored indirectly using **corrosion coupons (*in situ* batch tests).**	Directly related to safety function for canister to withstand corrosion (indicator criteria: copper thickness must remain >0mm). There is value in monitoring as understanding the early stages of corrosion may provide additional detailed and/or site-specific understanding not gained through previous RD&D.

4 Technology Readiness Levels

4.1 Introduction

Technology development is a process that starts when the basic principles are observed and reported. A practical way of assessing the status/maturity of a technology or its readiness to be effectively implemented is to assign a TRL (Technology Readiness Level) based upon documented evidences.

In Modern2020 we have used the proven NASA and DoD technology assessment model [100] that ranges from 1 (basis principles) to 9 (successfully proved under operational conditions).

The following table provides a succinct description of the meaning/description of each level.

Table 20. TRL levels as described by DoD

Relative Level of Technology Development	Technology Readiness Level	TRL Definition	Description
System Operations	**TRL 9**	Actual system operated over the full range of expected mission conditions.	The technology is in its final form and operated under the full range of operating mission conditions. Examples include using the actual system with the full range of wastes in hot operations.
System Commissioning	**TRL 8**	Actual system completed and qualified through test and demonstration.	The technology has been proven to work in its final form and under expected conditions. In almost all cases, this TRL represents the end of true system development. Examples include developmental testing and evaluation of the system with actual waste in hot commissioning. Supporting information includes operational procedures that are virtually complete. An Operational Readiness Review (ORR) has been successfully completed prior to the start of hot testing.
	TRL 7	Full-scale, similar (prototypical) system demonstrated in relevant environment	This represents a major step up from TRL 6, requiring demonstration of an actual system prototype in a relevant environment. Examples include testing full-scale prototype in the field with a range of simulants in cold commissioning[1]. Supporting information includes results from the full-scale testing and analysis of the differences between the test environment, and analysis of what the experimental results mean for the eventual operating system/environment. Final design is virtually complete.
Technology Demonstration	**TRL 6**	Engineering/pilot-scale, similar (prototypical) system validation in relevant environment	Engineering-scale models or prototypes are tested in a relevant environment. This represents a major step up in a technology's demonstrated readiness. Examples include testing an engineering scale prototypical system with a range of simulants.[1] Supporting information includes results from the engineering scale testing and analysis of the differences between the engineering scale, prototypical system/environment, and analysis of what the experimental results mean for the eventual operating system/environment. TRL 6 begins true engineering development of the technology as an operational system. The major difference between TRL 5 and 6 is the step up from laboratory scale to engineering scale and the determination of scaling factors that will enable design of the operating system. The prototype should be capable of performing all the functions that will be required of the operational system. The operating environment for the testing should closely represent the actual operating environment.
Technology Development	**TRL 5**	Laboratory scale, similar system validation in relevant environment	The basic technological components are integrated so that the system configuration is similar to (matches) the final application in almost all respects. Examples include testing a high-fidelity, laboratory scale system in a simulated environment with a range of simulants[1] and actual waste[2]. Supporting information includes results from the laboratory scale testing, analysis of the differences between the laboratory and eventual operating system/environment, and analysis of what the experimental results mean for the eventual operating system/environment. The major difference between TRL 4 and 5 is the increase in the fidelity of the system and environment to the actual application. The system tested is almost prototypical.

<table>
<tr><th>Relative Level of Technology Development</th><th>Technology Readiness Level</th><th>TRL Definition</th><th>Description</th></tr>
<tr><td>Technology Development</td><td>TRL 4</td><td>Component and/or system validation in laboratory environment</td><td>The basic technological components are integrated to establish that the pieces will work together. This is relatively "low fidelity" compared with the eventual system. Examples include integration of ad hoc hardware in a laboratory and testing with a range of simulants and small scale tests on actual waste[2]. Supporting information includes the results of the integrated experiments and estimates of how the experimental components and experimental test results differ from the expected system performance goals. TRL 4-6 represent the bridge from scientific research to engineering. TRL 4 is the first step in determining whether the individual components will work together as a system. The laboratory system will probably be a mix of on hand equipment and a few special purpose components that may require special handling, calibration, or alignment to get them to function.</td></tr>
<tr><td rowspan="2">Research to Prove Feasibility</td><td>TRL 3</td><td>Analytical and experimental critical function and/or characteristic proof of concept</td><td>Active research and development (R&D) is initiated. This includes analytical studies and laboratory-scale studies to physically validate the analytical predictions of separate elements of the technology. Examples include components that are not yet integrated or representative tested with simulants.[1] Supporting information includes results of laboratory tests performed to measure parameters of interest and comparison to analytical predictions for critical subsystems. At TRL 3 the work has moved beyond the paper phase to experimental work that verifies that the concept works as expected on simulants. Components of the technology are validated, but there is no attempt to integrate the components into a complete system. Modeling and simulation may be used to complement physical experiments.</td></tr>
<tr><td rowspan="2">TRL 2</td><td rowspan="2">Technology concept and/or application formulated</td><td>Once basic principles are observed, practical applications can be invented. Applications are speculative, and there may be no proof or detailed analysis to support the assumptions. Examples are still limited to analytic studies.</td></tr>
<tr><td rowspan="2">Basic Technology Research</td><td>Supporting information includes publications or other references that outline the application being considered and that provide analysis to support the concept. The step up from TRL 1 to TRL 2 moves the ideas from pure to applied research. Most of the work is analytical or paper studies with the emphasis on understanding the science better. Experimental work is designed to corroborate the basic scientific observations made during TRL 1 work.</td></tr>
<tr><td>TRL 1</td><td>Basic principles observed and reported</td><td>This is the lowest level of technology readiness. Scientific research begins to be translated into applied R&D. Examples might include paper studies of a technology's basic properties or experimental work that consists mainly of observations of the physical world. Supporting Information includes published research or other references that identify the principles that underlie the technology.</td></tr>
</table>

[1] Simulants should match relevant chemical and physical properties.

[2] Testing with as wide a range of actual waste as practicable and consistent with waste availability, safety, ALARA, cost and project risk is highly desirable.

4.2 Application and setting of TRL levels

It should be recognized that the notion of technology maturity, or technology development progress, is a multi-dimensional problem, and it must be treated as such

The setting of the TRL levels is quite straightforward until TRL 5, however, above this level the scoring could be different depending on whom is doing the evaluation because the “relevant environment” depends on the concept and the host rock. An internal exercise was developed to request the TRL levels from the involved Modern2020 partners for well know sensors and monitoring technologies. The gathered results were diverse for many of them by the indicated reasons.

In this respect, is expected that the qualification methodology developed in task 3.6 (see section 4.5) could provide more objective results in the future.

In Table 15 the best estimation of the initial and final TRL for each of the technologies considered in the project is provided in agreement with the evaluation made by the experts involved in each of the R&D tasks.

Table 21. TRLs for Modern2020 technologies

Technology	**Initial TRL**	**Final TRL**	**Comments**
Short range wireless data transmission	3 or 4	**5**	System has been demonstrated in a relevant (**typical; not stressing**,) environment
Long range wireless data transmission	3 or 4	**5**	System has been demonstrated in a relevant (**typical; not stressing**,) environment
Combined Short-Long range wireless data transmission	3	**5**	System has been demonstrated in a relevant (**typical; not stressing**,) environment
Nuclear Batteries*	2	**3**	An analytical and experimental proof-of-concept has been demonstrated
Thermal Harvesting	3	**4**	Demonstration in a laboratory (controlled) environment has done Depends on the relevance of the “scaling”
Wireless energy transmission	2	**4**	Demonstration in a laboratory (controlled) environment has been done
Energy storage*	1	**2**	A concept has been formulated during the project
Dew-point Psychrometer	2 or 3	**5**	System has been demonstrated in a relevant (typical; not stressing,) environment Radiation effects not considered yet
Non-contact displacement measurement	2	**3**	An analytical and experimental proof-of-concept has been demonstrated
Chemical electrodes	2 or 3	**4**	Demonstration in a laboratory (controlled) environment has been done. Radiation effects not considered yet
THMC smart cell	2 or 3	**5**	System has been demonstrated in a relevant (typical; not stressing,) environment. Radiation effects not considered yet
Distributed FO temperature measurement	4	**6**	a prototype system has been demonstrated in a relevant environment, (included gamma radiation)
Distributed FO strain measurement	4	**5**	System has been demonstrated in a relevant (**typical; not stressing**,) environment
Distributed FO hydrogen measurement	2	**3**	An analytical and experimental proof-of-concept has been demonstrated
Distributed FO radiation measurement	2	**4**	Demonstration in a laboratory (controlled) environment has been done
FO pH measurement	2	**3**	An analytical and experimental proof-of-concept has been demonstrated

			pH sensors still require a lot of effort to be tested in radiation field. They should first be tailored for the pH range of 11-13, which is very challenging
Distributed FO density measurement in GBM	2-3	5	System has been demonstrated in a relevant (typical; not stressing,) environment
Seismic waveform inversions (FWI)	5	6	system has been demonstrated in a relevant environment (FE experiment)
Differential tomography	5	6	system has been demonstrated in a relevant environment (ERT experiment)
Anomaly detection algorithms	2	2-3	Concept has been formulated and analytical proof-of concept has been started

* As mentioned in previous section, for few technologies the given final TRL raises some debate between partners.

As can be observed, none of the new technologies have been validated as part of a demonstrator, and therefore the assigned TRL is below TRL 7.

A way of improving the TRL assignment is to provide a “statement” that gives some indication on how much efforts are necessary to develop a certain technology into application - and probably even more important - to give some guidance on the associated project risks when selecting a monitoring technology to enable decisions as elaborated in the Modern2020 workflow in WP2. This approach is less subjective and more suitable measure for our purpose.

4.3 Conclusions

The most relevant message when evaluating the work done in WP3, with independence of the exact value of the final TRL, is that all the technologies considered progressed significantly since the start of the project but none of them was so far successfully applied as part of a demonstrator under a relevant environment, so they are below TRL 7. Only those technologies included in LTRBM demonstrator could reach TRL7 if they show a convincing long-term performance. This simply means that the development of a certain technology into application starting from a relatively low TRL requires considerable work and time, as it could be expected from the beginning. Thus, additional work is really required to make them ready enough to be part of a reliable monitoring system intended for the future repository.

5 Stakeholders Participation

Comprehensible overview of the technologies has been developed during the project through Innovative Technical data sheet (see appendix 9.3) for the participating stakeholders to get acquainted with these technologies and their potential for repository monitoring.

The work on the innovative technical sheet has been discussed during the WP3 Paris workshop (29/11-01/12 2016) with delegates from the WP5.

The Innovative Technical data sheet serves has a background for the elaboration of the Stakeholders guide (Modern2020 D5.2)

6 Overall results and conclusions

6.1 Main results

The R&D working groups created in Modern2020 have achieved much better that initially expected, in particular due to the great job made by the task leaders (see Figure 1), and although the objectives were challenging, the results can be considered excellent. Several specific papers and abstracts were produced to syntethize the gathered results as those presented in the Modern2020 Final Conference [Deliverable n°6.3. Modern2020 Final Conference Proceedings] but few of the main outcomes are listed hereafter.

- Concerning wireless data transmission systems for repository monitoring, a major step has been reached in understanding, designing and demonstrating specific solutions that allow transmitting data through components of the EBS or the host rock. The performance of the developed technologies depends on a number of factors but different technological solutions operating at frequencies between 4 kHz and 2.8 MHz and covering transmission distances between 0.5 m and more than 275 m have been developed and tested.
- The research work on alternative power sourcing technologies was focused on wireless sensor units (WSUs) for nuclear repository monitoring. The general goal of the research has been to investigate the applicability and technical bottlenecks of more promising technologies: thermoelectric energy harvesting based on thermal gradients around the high-level waste (HLW) containers, wireless energy transfer through repository, and radioisotope thermoelectric generator (RTG) type nuclear batteries. With limited power sources, the WSU has typically to operate in a low duty cycle mode comprising alternating long energy accumulation periods with no activity and short activity cycles with sensor measurements and wireless communication. This entails a need of internal energy storage with appropriate energy and output power capacity, long lifetime and low self-discharge rate. Thus the research has also included potential technologies for the internal energy storage as part of the powering subsystem.
- The R&D developments in order to devise new in-situ sensors tailored to geological disposal included several initiatives listed hereafter. Research on custom-made fiber Bragg gratings (FBGs) in order to adapt an irradiation sensor, improve a hydrogen sensor and develop new pH sensors. Development of an optoelectronic sensing chain, using two or three scattering methods (Brillouin, Rayleigh and Raman) to provide distributed measurements of four parameters: temperature, strain, hydrogen and radiation. Obtain a fiber-optic distributed sensing solution of thermal conductivity, density and water content in the EBS by means of heatable fiber-optic cables. Advancing on having fiber optic pressure cells for boreholes. Production of new sensors to measure suction based on thermocouple psychrometers operating with the dew point method. Study of more promising non-contact techniques for short-range displacement sensors. Adaptation of ion-selective electrodes to measure Cl, Na and pH. Development of a smart cell by combining Thermal Humidity Mechanical Chemistry (THMC) sensors.
- Options for non-invasive monitoring based on geophysical techniques were improved by the development of a novel model parameterization and the incorporation of structural constraints to further improve the quality and reliability of seismic full waveform inversion (FWI) algorithms. Besides, a novel differential tomography methodology has been developed for better characterizing small differential changes between two consecutive experiments, which could be transferred to FWI problems in order to reduce the required data analyses and computer resources. In addition, tomographic algorithms for geoelectrical and induced polarization data have been established; they can provide valuable information for repository monitoring of temperature and moisture content evolution.
- Finally, a common multi-stage methodology for qualifying monitoring components of the measurement chain (sensor, connecting cable and/or wireless system/controller) at a Deep Geological Repository (DGR) has been proposed. It is the result of a multi-stage analysis, which comprises the study of transferable experience from other industry fields, the analysis of similar case studies operating in conditions close to those expected in repositories and different initiatives for the development of a qualification process for selecting and testing the monitoring components.

- WP3 members produces Innovative Technical data sheet for the interaction with the public stakeholders

6.2 Conclusions

The research carried out provided an improved readiness for all the technologies considered. However, the work cannot be considered concluded as there is room for improvement and still challenges to face. For instance, few of the more relevant are:

- A generic key topic is the energy efficiency, particularly for long range data transmission systems, where it can present a limiting factor of the amount of data that can be transmitted. Furthermore, short range wireless solutions are also in competition with other data transmission systems (i.e. Fiber Optics), and a general understanding of the energy needs may support strategic choices on the overall monitoring strategy.
- Other topics of interest with respect to future work on long range wireless solutions are the study of long-term power supply sources, the potential interactions of transmitter antennae with magnetic permeable materials in a repository (e.g. steel used for gallery support) and the effect of heterogeneities on field propagation through the overburden. Besides, the demonstration of data transmission over a distance beyond 275 m, since the typical repository depth is 500 m or deeper, and the development of more sophisticated data processing methods to improve significantly the overall performance due to the variability of noise and interferences on day-to-day level.
- Relevant topics related with short wireless solutions comprise to develop them at a more mature state, for 125 KHz the development of an automatic tuning of the antennas is necessary, because surrounding materials and metal parts of an antenna buried in a disposal will change the delicate tuning of the antenna coil. Further topics include improved packaging and increased automation.
- The follow-on activities after Modern2020 should involve the integration and verification of the energy sourcing parts as a building block of more complete systems that also involve the sensor payload, wireless communication, encapsulation and the necessary repository external parts. Moreover, this work should also be connected to the overall design of the monitoring systems with possibly several wireless sensor nodes, and even to the repository monitoring strategies.
- Further elaboration of the wireless energy transfer towards final repository monitoring implementations is needed for maintaining the antenna resonance with nearby moisture and other materials with electrical conductivity, permittivity and magnetic permeability. For the integration of the bi-directional data transfer, the most important development needs are improving the immunity of the data uplink to the external noise e.g. with more advanced modulation technologies or increased RF power level, and the design of the TDM based protocol for powering, data uplink and data downlink.
- An efficient interim energy storage with appropriate energy and output power capacity for the sensor operations, long lifetime and low self-discharge rate is needed.
- Raman scattering in a multimode fiber is suitable for FO temperature measurement but using carbon-primary coating to prevent hydrogen diffusion and F-doped fiber to reduce the RIA, although not enough to suppress dramatic radiation impact. Double-ended configuration proved to be efficient, at the expense of temperature uncertainty, which reach 5 °C at 1MGy.
- Strain is FO measured using Brillouin scattering in a singlemode fiber with carbon-primary coating to prevent hydrogen diffusion and F-doped fiber to reduce the RIA and Brillouin frequency shift. Coupled effects of temperature and radiation have been quantified. Rayleigh scattering has proved to be a very promising solution for strain sensing with fibers based on F-dopants. It is even less affected by radiation than Brillouin scattering.
- Regarding FO distributed radiation sensing, Al-doped sample is clearly the most radiation-sensitive and Ge-doped sample the less sensitive but a combination of different fibers should be deployed to measure the radiation spatial distribution on the MGy range.
- Special FO cable to measure bentonite properties through distributed Raman temperature has been designed and proved to be a viable solution.
- FO Hydrogen sensing has been obtained by palladed silica optical fibers paired with Brillouin scattering and by functionalized fiber Bragg gratings. Proof of concept has been obtained but there is still a lot of research to assess the lifetime of the sensitive element.
- FO pH sensing is feasible but should be tuned to the range 11-13.
- The newly developed dew point method psychrometer has been tested using calibrated samples at laboratory but it needs to be validated under conditions similar to those expected in the repository.
- The same challenge is identified in relation with the new developped ion-selective electrodes to measure Cl, Na and pH.
- The identified non-contact techniques for short-range displacement sensors should be implemented in practice in order to improve the readiness level.

- The so-called smart cell intended for simultaneous measurement of total pressure, pore pressure and/or relative humidity has been tested in the laboratory but as in the previous case needs to be validated under realistic conditions.
- Another generic key topic is the long-term reliability of monitoring solutions. Although some work on reliability and radiation hardness has been done, in particular for FO sensors, more extended testing of at least the wireless solutions is recommended. Several measures are applicable as redundancy, anticipating drift margins and component derating, or qualification and screening.
- Cost evaluation is an important parameter too to make the right choice among the different monitoring solutions at hand.
- Despite the various successes got in relation with the techniques for geophysical monitoring, further research is required for making these technologies applicable for actual repository monitoring. Important tasks that are already scheduled include the application of the newly developed differential tomography algorithm to FWI problems, the validation of the anomaly detection algorithm with field data, and larger-scale geoelectrical investigations at the Tournemire test site.
- The developed guidelines for multi-stage qualification methodology applicable to each component of the monitoring system needs to be applied systematically in order to ascertain its validity and improve it if required.

Other topic that should be pointed out is that, in parallel with the development of the measuring techniques, the same is required concerning the system intended for gathering, filtering, managing and displaying the information. The new monitoring techniques provide much more information (huge amounts of digital or analog data) that the standard data acquisition systems can not properly handle. Furthermore, the fast spreading of the BIM (Building Information Modelling) technologies to all kind of civil works is demanding to integrate the monitoring data as part of the digital model of the future repository.

Although the list of potential improvements is large, it does not mean that the work done was unsatisfactory, quite the contrary. The R&D created teams thanks to the support of Modern2020 are currently capable of developing the required activities, but they need additional funds and time, being a shame not taking advantage of these resources.

7 References

[1] MoDeRn, “Monitoring Reference Framework Report,” MoDeRn Deliverable D-1.2.1, 2013.

[2] Aitemin, “Wireless sensor network demonstrator report,” MoDeRn Deliverable D3.3.1, 2013.

[3] T. J. Schröder and E. Rosca-Bocancea, “Wireless Data Transmission Demonstrator: from the HADES to the surface,” MoDeRn Deliverable D.3.4.2, 2013.

[4] P. C. Clemmow, An Introduction to Electromagnetic Theory, Cambridge, U.K: Cambridge University Press, 1973.

[5] G. Lehner, Elektromagnetische Feldtheorie für Ingenieure und Physiker. 6th ed., Heidelberg: Springer Verlag, 2008.

[6] Aitemin, NDA, Andra, NRG, NAGRA, ENRESA, EURIDICE, ETH-Zurich, RWMC, D. TEC, POSIVA, SKB, RAWRA and GSL, “State of Art Report on Monitoring Technology,” MoDeRn Deliverable D2.2.2, 2013.

[7] Suzuki, K., Eto, J., Tanabe, H., Takamura, H., Suyama, Y., Bertrand, J., Hermand, G., “Development of Miniaturized Wireless Transmitter and Borehole type Receiver with Low Frequency Magnetic Waves,” in *Proceedings of an International Conference and Workshop of MoDeRn Project, Appendix C, Full Conference Papers*, Luxembourg, 19 – 21 March 2013.

[8] T. Spillmann, “Application of wired, wireless and non-intrusive standard monitoiring techniques. The TEM Project at the Grimsel Test Site - ANNUAL REPORT,” Nagra Arbeitsbericht NAB 08-52, Wettlingen, Switzerland, 2008.

[9] Tsubono, K., Kobayashi, M., Yamakawa, H., Hasui, A., Masumoto, K., Matsushita, T., Sugahara, N., Tanaka, T., Nagai, C., “Development of Wireless Monitoring Systems for Geological Disposal,” in *Proc. of the 6th East Asia Forum on Radwaste Management*, Osaka, Japan, November, 2017.

[10] Modern2020, “Long-term power supply sources for repository monitoring,” Modern2020 Deliverable D3.3, submitted.

[11] Suyama, Y., Takamura, H., Aoki, K., Wada, R., Shimbo, H. and Okutsu, K. , “Wireless transmission monitoring in a geological disposal repository (I) Concepts and Advantages,” in *Mater. Res. Soc. Symp. Proc., Vol. 1193, pp. 135-141*, 2009.

[12] Takamura, H., Shimbo, H., Okutsu, K., Suyama, Y., Aoki, K. and Wada, R. , “Wireless transmission monitoring in a geological disposal repository (II) Research and Development,” in *Mater. Res. Soc. Symp. Proc., Vol. 1193, pp. 143-150*, 2009.

[13] Eto, J., Suzuki, K., Tanabe, H., Takamura, H., Suyama, Y., Bertrand, J., Hermand, G., “Development of Wireless Monitoring System for Stepwise Backfill/Sealing of Geological Repository,” in *Proceedings of an International Conference and Workshop of MoDeRn Project, Apendix C, Full Conference Papers*, Luxembourg, 19 – 21 March 2013.

[14] RWMC, “Development of Advanced Technology for Engineering Components of HLW Disposal, Development of Monitoring Technology,” 2015.

[15] K. Nishimura, “Data coding technique and basis of error correction: revised edition,” CQ Publisher, pp. 133-134, 2010.

[16] RWMC, “Development of Advanced Technology for Engineering Components of HLW Disposal, Development of Monitoring Technology,” 2017.

[17] RWMC, “Development of Advanced Technology for Engineering Components of HLW Disposal, Development of Monitoring Technology,” 2018.

[18] N. Lammens, G. Luyckx, E. Voet, W. Van Paepegem and J. Degrieck, “SMARTFIBER: miniaturized optical-fiber sensor based health monitoring system,” in *6th International Conference on Emerging Technologies in Non Destructive Testing*, 2015.

[19] J. R. Wait, “Criteria for Locating an Oscillating Magnetic Dipole Buried in the Earth,” pp. 1033-1035, 1971.

[20] E. Verhoef, E. Neeft, J. Grupa and A. Poley, Outline of a disposal concept in clay, OPERA-PG-COV008, COVRA N.V., 2014.

[21] ANDRA, “CGNTAMTD150056, Spécification technique de besoin. Alimentation autonome pour la transmission sans fil en condition de stockage géologique. Modern2020 WP3.3, (2015), 15 pages.”.

[22] *Product Guide – Maxwell Technologies BOOSTCAP Ultracapacitors,* Maxwell Technologies Doc. No. 1014627.1, 2009.

[23] D. S. Tucker and S. Paley, "Flexible Hybrid Battery/Pseudocapacitor," NASA, 2015.

[24] *2.3V 50F Pseudocapacitor Cell,* Maxwell Technologies doc. no. 3001969-EN.2, 2018.

[25] X. Jiang, J. Polastre and D. Culler, "Perpetual environmentally powered sensor networks," in *Fourth International Symposium on Information Processing in Sensor Networks (IPSN 2005)*, Boise, ID, USA, 2005.

[26] F. S. Garcia, A. A. Ferreira and J. A. Pomilio, "Control Strategy for Battery-Ultracapacitor Hybrid Energy Storage System," in *Applied Power Electronics Conference and Exposition (APEC 2009)*, Washington, DC, USA, 2009.

[27] F. Ongaro, S. Saggini and P. Mattavelli, "Li-Ion Battery-Supercapacitor Hybrid Storage System for a Long Lifetime, Photovoltaic-Based Wireless Sensor Network," *IEEE Transactions on Power Electronics,* vol. 27, no. 9, pp. 3944-3952, 2012.

[28] C. McCaffrey, J. Häkli, M. Hirvonen, I. Huhtinen, K. Nummila, T. Lehikoinen, "Magnetically coupled wireless communication for buried environmental sensor," in *12th International Conference on Environment and Electrical Engineering*, Wroclaw, Poland, 5-8 May 2013.

[29] N. J. Cassidy, Electrical and magnetic properties of rock, soils and fluids. In: Jol, H.M. (ed.). Ground Penetrating Radar Theory and Applications, Amsterdam: Elsevier Science, 2009, pp. 41-72.

[30] AITEMIN, "Technical requirements report," MoDeRn Deliverable D.2.1.1, 2011.

[31] AITEMIN, NDA, Andra, NRG, NAGRA, ENRESA, EURIDICE, ETH-Zurich, RWMC, D. TEC, POSIVA, SKB, RAWRA and GSL, "State of Art Report on Monitoring Technology," MoDeRn Deliverable D2.2.2, 2013.

[32] J. R. Wait and K. P. Spies, "Electromagnetic Fields of a Small Loop in a Stratified Earth," IEEE Trans. Antennas and Propagation, AP-19 (5), 1971.

[33] T. J. Schröder and E. Rosca-Bocancea, Wireless Data Transmission Demonstrator: from the HADES to the surface, MoDeRn Deliverable D.3.4.2, 2013.

[34] Modern2020, Long-term power supply sources for repository monitoring, Modern2020 Deliverable D3.3, submitted.

[35] Aitemin, Wireless sensor network demonstrator report, MoDeRn Deliverable D3.3.1, 2013.

[36] RWMC, Development of Advanced Technology for Engineering Components of HLW Disposal, Development of Monitoring Technology, 2017.

[37] K. Nishimura, Data coding technique and basis of error correction: revised edition, CQ Publisher, pp. 133-134, 2010.

[38] RWMC, Development of Advanced Technology for Engineering Components of HLW Disposal, Development of Monitoring Technology, 2018.

[39] Suyama, Y., Tanabe, H. and Eto, J., "Monitoring strategy to support decision making for geological repository closure," in *Proceedings of the 3rd East Asia Forum on Radwaste Management, p.172-179*, Gyeongju, Korea, November 2010.

[40] Suyama, Y., Eto, J., Tanabe, H. and Takamura, H., "Wireless Transmission Monitoring for Geological Disposal," in *Poster Presentation on the MoDeRn Workshop on Monitoring Technologies*, Troyes, France, June 2010.

[41] Suyama, Y., Takamura, H., Aoki, K., Wada, R., Shimbo, H. and Okutsu, K., "Wireless transmission monitoring in a geological disposal repository (I). Concepts and Advantages," in *Proceedings of MRS'09 Symposium: The 33rd International Symposium "Scientific Basis for Nuclear Waste Management"*, Saint Petersburg, Russia, May 2009.

[42] MoDeRn, "Development Report of Monitoring Technology, MoDeRn project Deliverable D-2.3.1," 2013.

[43] MoDeRn, "Hades monitoring demonstrator results and analysis report, MoDeRn project Deliverable D-2.4.2," 2013.

[44] Spillmann, T., Blechschmidt, I., Rösli, U., Parsons, S., Marelli, S., Maurer, H.R., Manukyan E., Breen, B., Martinez V. & Bárcena, I., "Comparison of wireless signal transmission and seismic tomography for monitoring radioactive waste repositories," in *8th International Symposium on Field Measurements in GeoMechanics*, Berlin, Germany, 2011.

[45] MoDeRn, “Monitoring Reference Framework Report, MoDeRn project Deliverable D-1.2.1,” 2013.

[46] (MISL), Magneto-Inductive System Limited, “MI Signal Measurements HADES Underground Research Facility,” MISL Document No.: ED-102190, Nova Scotia, Canada, 2006.

[47] J. R. Wait, Criteria for Locating an Oscillating Magnetic Dipole Buried in the Earth, Proc. IEEE, 59 (6), 1971, pp. 1033-1035.

[48] J. a. K. S. Wait, Electromagnetic Fields of a Small Loop in a Stratified Earth, IEEE Trans. Antennas and Propagation, AP-19 (5), 1971, pp. 717-718.

[49] AITEMIN, Technical requirements report, MoDeRn Deliverable D.2.1.1, 2011.

[50] AITEMIN, NDA, Andra, NRG, NAGRA, ENRESA, EURIDICE, ETH-Zurich, RWMC, D. TEC, POSIVA, SKB, RAWRA and GSL, State of Art Report on Monitoring Technology, MoDeRn Deliverable D2.2.2, 2013.

[51] F. Pavailler and A. Piron, “Monitoring of civil engineering structures – Quality control of measurement ,” 2012.

[52] N. Rosin-Corre, C. Noret and J.-L. Bordes, “L'auscultation par capteurs à corde vibrante, 80 ans de retour d'expérience.,” in *Colloque CFBR. Auscultation des barrages et des digues - Thème 2: Auscultation et suivi des ouvrages*, Chambery, 2012.

[53] CIBG 2000, Bulletin 118, “Système d’auscultation automatique des barrages.,” 2000.

[54] IECS 2010 J.Sausse, “Automated dam monitoring - 25 years of experience at EDF.”.

[55] E. Oukhemanou, D. Solenne, E. Buchoud, S. Michel-Ponnelle and A. Courtois, “VeRCoRs Mock-Up: Comprehensive Monitoring System for Reduced Scale Containment,” in *TINCE*, 2016.

[56] C. Bringer, 2015. [Online]. Available: https://escies.org/download/webDocumentFile?id=63892.

[57] J.-M. Henault, *Methodological approach for performance and durability assessment of distributed fiber optic sensors: Application to a specific fiber optic cable,* 2013.

[58] “MoDeRn. Monitoring Reference Framework Report. MoDeRn project Deliverable D-1.2.1,” 2013.

[59] K. Finkenzeller, RFID Handbook, Chichester, England: John Wiley & Sons Ltd, 2003.

[60] E. Strömmer, M. Jurvansuu, T. Tuikka, A. Ylisaukko-oja, H. Rapakko and J. Vesterinen, “NFC-Enabled Wireless Charging,” in *4th International Research Workshop on Near Field Communication, NFC 2012*, Helsinki, Finland, 2012.

[61] Y. Lee, “Antenna Circuit Design,” Microchip AN710, 2003.

[62] J. L. Bierschenk, Optimized Thermoelectrics For Energy Harvesting Applications, In: Priya, S., Inman, D.J. (ed): Energy Harvesting Technology, SpringerScience+Business Media, 2009, p.337-351.

[63] A. Bitschi, Modelling of thermoelectric devices for electric power generation, PhD. thesis ETH, 2009.

[64] C. Auvigne, Electrical and Magnetical Modeling of Inductive Coupled Power Transfer Systems, Thesis, Ecole Polytechnique Federale de Lausanne, 2015.

[65] J. H. Scott, Electrical and magnetic properties of rock and soil. Technical Letter Special Projects-16, Colorado: United States Department of the Interior, Geological Survey, Denver, 1966.

[66] S. F. Pichorim and P. J. Abatti, Design of Coils for Millimeter- and Submillimeter-Sized Biotelemetry, IEEE Transcations on biomedical Engineering, 51 (8), 2004, pp. 1487-1489.

[67] M. B. Kraichman, Impedance of a Circular Loop in an Infinite Conducting Medium, Journal of Research of the National Bureau of Standards - D. Radio Propagation, 66D (4), 1962, pp. 499-503.

[68] R. R. Harrison, Designing Efficient Inductive Power Links for Implantable Devices, IEEE International Symposium on Circuits and Systems, 2007, pp. 2080-2083.

[69] K. Schuylenberg and R. Puers, Inductive Powering: Basic Theory and Application to Biomedical Systems, Springer Science + Business Media B.V., 2009.

[70] [Online]. Available: www.oceanologyinternational.com/files/AUV_Marketplace_John_Westwood.pdf.

[71] [Online]. Available: http://www.futura-sciences.com/fr/news/t/terre-3/d/lobservateur-sous-marin-qui-ne-remontera-jamais_10643/.

[72] “Modern2020 project Milestone number MS11 – final report on “Using Nuclear Batteries for Geological Disposal Monitoring: State of the Art”, 47 pages.,” 2016.

[73] A. Harmon, “NASA’s Radioisotope Power System Program. Science Mission Directorate. OPAG.,” 2007.

[74] R. L. Cataldo and G. L. Bennett, "U.S. Space Radioisotope Power Systems and Applications: Past, Present and Future," NASA Glenn Research Center and Metaspace Enterprises, USA, 2011.

[75] M. A. Prelas, C. J. Weaver, M. Watterman, E. Lukosi, R. Schott and D. A. Wisniewski, "A review of nuclear batteries," *Progress in Nuclear Energy,* vol. 75, pp. 117-148, 2014.

[76] S. T. Revankar and T. E. Adams, "Advances in Betavoltaic Power Sources," *Journal of Energy and Power Sources,* vol. 1, no. 6, pp. 321-329, 2014.

[77] W. R. Corliss and R. L. Mead, "Power from Radioisotopes, Understanding the atom series," United States Atomic Energy Commission, Division of Technical Information, 1971.

[78] D. Leone, "Plutonium Still Scarce, Production Restart Still Slow for Needy NASA," 2015. [Online]. Available: http://spacenews.com/doe-to-crank-out-new-plutonium-238-in-2019/.

[79] McNutt, "RL Physics and Chemistry of Space-certified RPS : what do you need to know," The John Hopkins University applied physics laboratory. Committee on Astrobiology and Planetary Science Space Study Board, 2014.

[80] R. D. Abelson, "Big Things Come in Small Packages: Mission Concepts Potentially Enabled by Small Radioisotopes Power Systems. Systems & Mission Architecture Section," in *CalTech*, 2005.

[81] "DLC 037 0017 Rév. 2, Document logiciel Calcul - ANSYS - Dossier de validation théorique," AREVA, 2015.

[82] "DLC 037 0019 Rév. 2, Document logiciel Calcul - ANSYS – Manuel utilisateur," AREVA, 2015.

[83] J. R. Wait, "Complex Resistivity of the Earth," *Progress In Electromagnetics Research,* vol. 1, pp. 1-173, 1989.

[84] J. R. Wait and K. P. Spies, Electromagnetic Fields of a Small Loop in a Stratified Earth, IEEE Trans. Antennas and Propagation, AP-19 (5), 1971, pp. 717-718.

[85] T. Christen and M. W. Carlen, "Theory of Ragone plots," *Journal of Power Sources,* vol. 91, no. 2, pp. 210-216, 2000.

[86] W. Zuo, R. Li, C. Zhou, Y. Li, J. Xia and J. Liu, "Battery-Supercapacitor Hybrid Devices: Recent Progress and Future Prospects," *Advanced Science,* vol. 7, no. 4, 2017.

[87] A. Sato, "TAIYO YUDEN Lithium Ion Capacitors: An Effective EDLC Replacement," TAIYO YUDEN.

[88] Murata, *Small Energy Device Laminate type (UMAL). C2M1CXS-313(E),* 2016.

[89] "Battery and Energy Technologies," Electropaedia, [Online]. Available: https://www.mpoweruk.com/index.htm.

[90] S. Sudevalayam and P. Kulkarni, "Energy Harvesting Sensor Nodes: Survey and Implications," *IEEE Communications Surveys & Tutorials,* vol. 13, no. 3, pp. 443-461, 2011.

[91] *Lithium-ion battery life,* Saft, 2014.

[92] Tecate Group, "Ultracapacitor & Supercapacitor Frequently Asked Questions," [Online]. Available: https://www.tecategroup.com/ultracapacitors-supercapacitors/ultracapacitor-FAQ.php.

[93] P. Mars, "Coupling a supercapacitor with a small energy-harvesting source," *EDN-Electronic Design News,* pp. 39-42, 7 June 2012.

[94] A. Schneuwly and R. Gallay, "Properties and Applications of Supercapacitors From the State-of-the-art to Future Trends," in *Proceeding PCIM2000*, Rossens, Switzerland, 2000.

[95] Tecate Group, *Tecate PowerBurst Ultracapacitors Technical Guide Document,* Tecate Group document no. 9100760000 Rev M .

[96] G. Alcicek, H. Gualous, P. Venet, R. Gallay and A. Miraoui, "Experimental study of temperature effect on ultracapacitor ageing," in *European Conference on Power Electronics and Applications*, Aalborg, Denmark, 2007.

[97] D. Linzen, S. Buller, E. Karden and R. W. De Doncker, "Analysis and evaluation of charge-balancing circuits on performance, reliability, and lifetime of supercapacitor systems," *IEEE transactions on industry applications,* vol. 41, no. 5, pp. 1135-1141, 2005.

[98] Y. Diab, P. Venet, H. Gualous and G. Rojat, "Self-Discharge Characterization and Modeling of Electrochemical Capacitor Used for Power Electronics Applications," *IEEE Transactions on Power Electronics,* vol. 24, no. 2, pp. 510-517, 2009.

[99] MoDeRn, "Monitoring Reference Framework Report," MoDeRn Deliverable D-1.2.1, 2013.

[100] GAO-16-410G GAO Technology Readiness Assessment Guide, Best Practices for Evaluating the Readiness of Technology for Use in Acquisition Programs and Projects, August 2016.

T.J. Schröder (ed.), E. Rosca-Bocancea, J.L. García Siñeriz, G. Hermand, H.L. Abós Gracia, J.C. Mayor Zurdo, J. Verstricht, P. Dick, J. Eto, M. Sipilä, J.M. Saari, Wireless data transmission systems for repository monitoring, Modern2020 Deliverable D3.2.

T 3.3 Electric Power Sourcing of Wireless Repository Monitoring Sensors (Esko Strömmer)

T 3.4 Overview of Optical Fiber Technologies for Radioactive Waste Disposal Site Monitoring (Patrice Mégret)*

T 3.5 Geophysical Monitoring of High-Level Radioactive Waste Repositories (Hansruedi Maurer)

T 3.6 Methodology for Qualifying the Monitoring Components (Jean-Michel Matray)

J. Eto, M. Kawakubo, Y. Suyama, N. Sugahara, Development of a wireless relay system for monitoring of geological disposal using low- frequency electromagnetic waves. Poster of 2nd International Conference on Monitoring in Geological Disposal of Radioactive Waste. Cité Universitaire Paris, April 2019.

T. J. Schröder, E. Rosca-Bocancea, C.N.J. Stam, G. Hermand, P. Dick, Demonstration of a two-staged wireless transmission chain out of the LTRBM borehole to the surface of the Tournemire plateau. Poster of 2nd International Conference on Monitoring in Geological Disposal of Radioactive Waste. Cité Universitaire Paris, April 2019.

T. J. Schröder, E. Rosca-Bocancea, C.N.J. Stam, Long Distance Data Transmission Through The Underground: Lessons Learned From Two Demonstrators. Poster of 2nd International Conference on Monitoring in Geological Disposal of Radioactive Waste. Cité Universitaire Paris, April 2019.

7.1.1 References Wireless data transmission systems

[1] T. J. Schröder and E. Rosca-Bocancea, "Wireless Data Transmission Demonstrator: from the HADES to the surface," MoDeRn Deliverable D.3.4.2, 2013.

[2] P. C. Clemmow, An Introduction to Electromagnetic Theory, Cambridge, U.K: Cambridge University Press, 1973.

[3] G. Lehner, Elektromagnetische Feldtheorie für Ingenieure und Physiker. 6th ed., Heidelberg: Springer Verlag, 2008.

[4] N. J. Cassidy, Electrical and magnetic properties of rock, soils and fluids. In: Jol, H.M. (ed.). Ground Penetrating Radar Theory and Applications, Amsterdam: Elsevier Science, 2009, pp. 41-72.

[5] Aitemin, "Wireless sensor network demonstrator report," MoDeRn Deliverable D3.3.1, 2013.

[6] Aitemin, NDA, Andra, NRG, NAGRA, ENRESA, EURIDICE, ETH-Zurich, RWMC, D. TEC, POSIVA, SKB, RAWRA and GSL, "State of Art Report on Monitoring Technology," MoDeRn Deliverable D2.2.2, 2013.

[7] Suzuki, K., Eto, J., Tanabe, H., Takamura, H., Suyama, Y., Bertrand, J., Hermand, G., "Development of Miniaturized Wireless Transmitter and Borehole type Receiver with Low Frequency Magnetic Waves," in *Proceedings of an International Conference and Workshop of MoDeRn Project, Appendix C, Full Conference Papers*, Luxembourg, 19 – 21 March 2013.

[8] T. Spillmann, "Application of wired, wireless and non-intrusive standard monitoiring techniques. The TEM Project at the Grimsel Test Site - ANNUAL REPORT," Nagra Arbeitsbericht NAB 08-52, Wettlingen, Switzerland, 2008.

[9] Tsubono, K., Kobayashi, M., Yamakawa, H., Hasui, A., Masumoto, K., Matsushita, T., Sugahara, N., Tanaka, T., Nagai, C., "Development of Wireless Monitoring Systems for Geological Disposal," in *Proc. of the 6th East Asia Forum on Radwaste Management*, Osaka, Japan, November, 2017.

[10] Modern2020, "Long-term power supply sources for repository monitoring," Modern2020 Deliverable D3.3, submitted.

[11] J. R. Wait, "Criteria for Locating an Oscillating Magnetic Dipole Buried in the Earth," pp. 1033-1035, 1971.

[12] Suyama, Y., Takamura, H., Aoki, K., Wada, R., Shimbo, H. and Okutsu, K. , "Wireless transmission monitoring in a geological disposal repository (I) Concepts and Advantages," in *Mater. Res. Soc. Symp. Proc., Vol. 1193, pp. 135-141*, 2009.

[13] Takamura, H., Shimbo, H., Okutsu, K., Suyama, Y., Aoki, K. and Wada, R. , "Wireless transmission monitoring in a geological disposal repository (II) Research and Development," in *Mater. Res. Soc. Symp. Proc., Vol. 1193, pp. 143-150*, 2009.

[14] Eto, J., Suzuki, K., Tanabe, H., Takamura, H., Suyama, Y., Bertrand, J., Hermand, G., "Development of Wireless Monitoring System for Stepwise Backfill/Sealing of Geological Repository," in *Proceedings of an International Conference and Workshop of MoDeRn Project, Apendix C, Full Conference Papers*, Luxembourg, 19 – 21 March 2013.

[15] RWMC, "Development of Advanced Technology for Engineering Components of HLW Disposal, Development of Monitoring Technology," 2015.

[16] K. Nishimura, "Data coding technique and basis of error correction: revised edition," CQ Publisher, pp. 133-134, 2010.

[17] RWMC, "Development of Advanced Technology for Engineering Components of HLW Disposal, Development of Monitoring Technology," 2018.

[18] RWMC, "Development of Advanced Technology for Engineering Components of HLW Disposal, Development of Monitoring Technology," 2017.

[19] N. Lammens, G. Luyckx, E. Voet, W. Van Paepegem and J. Degrieck, "SMARTFIBER: miniaturized optical-fiber sensor based health monitoring system," in *6th International Conference on Emerging Technologies in Non Destructive Testing*, 2015.

[20] C. McCaffrey, J. Häkli, M. Hirvonen, I. Huhtinen, K. Nummila, T. Lehikoinen, "Magnetically coupled wireless communication for buried environmental sensor," in *12th International Conference on Environment and Electrical Engineering*, Wroclaw, Poland, 5-8 May 2013.

[21] AITEMIN, "Technical requirements report," MoDeRn Deliverable D.2.1.1, 2011.

[22] AITEMIN, NDA, Andra, NRG, NAGRA, ENRESA, EURIDICE, ETH-Zurich, RWMC, D. TEC, POSIVA, SKB, RAWRA and GSL, "State of Art Report on Monitoring Technology," MoDeRn Deliverable D2.2.2, 2013.

[23] MoDeRn, "Monitoring Reference Framework Report," MoDeRn Deliverable D-1.2.1, 2013.

[24] J. R. Wait and K. P. Spies, "Electromagnetic Fields of a Small Loop in a Stratified Earth," IEEE Trans. Antennas and Propagation, AP-19 (5), 1971.

[25] T. J. Schröder and E. Rosca-Bocancea, Wireless Data Transmission Demonstrator: from the HADES to the surface, MoDeRn Deliverable D.3.4.2, 2013.

[26] Modern2020, Long-term power supply sources for repository monitoring, Modern2020 Deliverable D3.3, submitted.

[27] Aitemin, Wireless sensor network demonstrator report, MoDeRn Deliverable D3.3.1, 2013.

[28] RWMC, Development of Advanced Technology for Engineering Components of HLW Disposal, Development of Monitoring Technology, 2017.

[29] K. Nishimura, Data coding technique and basis of error correction: revised edition, CQ Publisher, pp. 133-134, 2010.

[30] RWMC, Development of Advanced Technology for Engineering Components of HLW Disposal, Development of Monitoring Technology, 2018.

[31] Suyama, Y., Tanabe, H. and Eto, J., "Monitoring strategy to support decision making for geological repository closure," in *Proceedings of the 3rd East Asia Forum on Radwaste Management, p.172-179*, Gyeongju, Korea, November 2010.

[32] Suyama, Y., Eto, J., Tanabe, H. and Takamura, H., "Wireless Transmission Monitoring for Geological Disposal," in *Poster Presentation on the MoDeRn Workshop on Monitoring Technologies*, Troyes, France, June 2010.

[33] Suyama, Y., Takamura, H., Aoki, K., Wada, R., Shimbo, H. and Okutsu, K., "Wireless transmission monitoring in a geological disposal repository (I). Concepts and Advantages," in *Proceedings of MRS'09 Symposium: The 33rd International Symposium "Scientific Basis for Nuclear Waste Management"*, Saint Petersburg, Russia, May 2009.

[34] MoDeRn, "Development Report of Monitoring Technology, MoDeRn project Deliverable D-2.3.1," 2013.

[35] MoDeRn, "Hades monitoring demonstrator results and analysis report, MoDeRn project Deliverable D-2.4.2," 2013.

[36] Spillmann, T., Blechschmidt, I., Rösli, U., Parsons, S., Marelli, S., Maurer, H.R., Manukyan E., Breen, B., Martinez V. & Bárcena, I., "Comparison of wireless signal transmission and seismic tomography for monitoring radioactive waste repositories," in *8th International Symposium on Field Measurements in GeoMechanics*, Berlin, Germany, 2011.

[37] MoDeRn, "Monitoring Reference Framework Report, MoDeRn project Deliverable D-1.2.1," 2013.

[38] (MISL), Magneto-Inductive System Limited, "MI Signal Measurements HADES Underground Research Facility," MISL Document No.: ED-102190, Nova Scotia, Canada, 2006.

[39] J. R. Wait, Criteria for Locating an Oscillating Magnetic Dipole Buried in the Earth, Proc. IEEE, 59 (6), 1971, pp. 1033-1035.

[40] J. a. K. S. Wait, Electromagnetic Fields of a Small Loop in a Stratified Earth, IEEE Trans. Antennas and Propagation, AP-19 (5), 1971, pp. 717-718.

[41] AITEMIN, Technical requirements report, MoDeRn Deliverable D.2.1.1, 2011.

[42] AITEMIN, NDA, Andra, NRG, NAGRA, ENRESA, EURIDICE, ETH-Zurich, RWMC, D. TEC, POSIVA, SKB, RAWRA and GSL, State of Art Report on Monitoring Technology, MoDeRn Deliverable D2.2.2, 2013.

[43] F. Pavailler and A. Piron, "Monitoring of civil engineering structures – Quality control of measurement ," 2012.

[44] N. Rosin-Corre, C. Noret and J.-L. Bordes, "L'auscultation par capteurs à corde vibrante, 80 ans de retour d'expérience.," in *Colloque CFBR. Auscultation des barrages et des digues - Thème 2: Auscultation et suivi des ouvrages*, Chambery, 2012.

[45] CIBG 2000, Bulletin 118, "Système d'auscultation automatique des barrages.," 2000.

[46] IECS 2010 J.Sausse, "Automated dam monitoring - 25 years of experience at EDF.".

[47] E. Oukhemanou, D. Solenne, E. Buchoud, S. Michel-Ponnelle and A. Courtois, "VeRCoRs Mock-Up: Comprehensive Monitoring System for Reduced Scale Containment," in *TINCE*, 2016.

[48] C. Bringer, 2015. [Online]. Available: https://escies.org/download/webDocumentFile?id=63892.

[49] J.-M. Henault, *Methodological approach for performance and durability assessment of distributed fiber optic sensors: Application to a specific fiber optic cable,* 2013.

7.1.2 References Alternative Power Supply Sources

[1] MoDeRn, "Monitoring Reference Framework Report," MoDeRn Deliverable D-1.2.1, 2013.

[2] Aitemin, "Wireless sensor network demonstrator report," MoDeRn Deliverable D3.3.1, 2013.

[3] T. J. Schröder and E. Rosca-Bocancea, "Wireless Data Transmission Demonstrator: from the HADES to the surface," MoDeRn Deliverable D.3.4.2, 2013.

[4] P. C. Clemmow, An Introduction to Electromagnetic Theory, Cambridge, U.K: Cambridge University Press, 1973.

[5] G. Lehner, Elektromagnetische Feldtheorie für Ingenieure und Physiker. 6th ed., Heidelberg: Springer Verlag, 2008.

[6] Aitemin, NDA, Andra, NRG, NAGRA, ENRESA, EURIDICE, ETH-Zurich, RWMC, D. TEC, POSIVA, SKB, RAWRA and GSL, "State of Art Report on Monitoring Technology," MoDeRn Deliverable D2.2.2, 2013.

[7] Suzuki, K., Eto, J., Tanabe, H., Takamura, H., Suyama, Y., Bertrand, J., Hermand, G., "Development of Miniaturized Wireless Transmitter and Borehole type Receiver with Low Frequency Magnetic Waves," in *Proceedings of an International Conference and Workshop of MoDeRn Project, Appendix C, Full Conference Papers*, Luxembourg, 19 – 21 March 2013.

[8] T. Spillmann, "Application of wired, wireless and non-intrusive standard monitoiring techniques. The TEM Project at the Grimsel Test Site - ANNUAL REPORT," Nagra Arbeitsbericht NAB 08-52, Wettlingen, Switzerland, 2008.

[9] Tsubono, K., Kobayashi, M., Yamakawa, H., Hasui, A., Masumoto, K., Matsushita, T., Sugahara, N., Tanaka, T., Nagai, C., "Development of Wireless Monitoring Systems for Geological Disposal," in *Proc. of the 6th East Asia Forum on Radwaste Management*, Osaka, Japan, November, 2017.

[10] Modern2020, "Long-term power supply sources for repository monitoring," Modern2020 Deliverable D3.3, submitted.

[11] Suyama, Y., Takamura, H., Aoki, K., Wada, R., Shimbo, H. and Okutsu, K. , "Wireless transmission monitoring in a geological disposal repository (I) Concepts and Advantages," in *Mater. Res. Soc. Symp. Proc., Vol. 1193, pp. 135-141*, 2009.

[12] Takamura, H., Shimbo, H., Okutsu, K., Suyama, Y., Aoki, K. and Wada, R. , "Wireless transmission monitoring in a geological disposal repository (II) Research and Development," in *Mater. Res. Soc. Symp. Proc., Vol. 1193, pp. 143-150*, 2009.

[13] Eto, J., Suzuki, K., Tanabe, H., Takamura, H., Suyama, Y., Bertrand, J., Hermand, G., "Development of Wireless Monitoring System for Stepwise Backfill/Sealing of Geological Repository," in *Proceedings of an International Conference and Workshop of MoDeRn Project, Apendix C, Full Conference Papers*, Luxembourg, 19 – 21 March 2013.

[14] RWMC, "Development of Advanced Technology for Engineering Components of HLW Disposal, Development of Monitoring Technology," 2015.

[15] K. Nishimura, "Data coding technique and basis of error correction: revised edition," CQ Publisher, pp. 133-134, 2010.

[16] RWMC, "Development of Advanced Technology for Engineering Components of HLW Disposal, Development of Monitoring Technology," 2017.

[17] RWMC, "Development of Advanced Technology for Engineering Components of HLW Disposal, Development of Monitoring Technology," 2018.

[18] N. Lammens, G. Luyckx, E. Voet, W. Van Paepegem and J. Degrieck, "SMARTFIBER: miniaturized optical-fiber sensor based health monitoring system," in *6th International Conference on Emerging Technologies in Non Destructive Testing*, 2015.

[19] J. R. Wait, "Criteria for Locating an Oscillating Magnetic Dipole Buried in the Earth," pp. 1033-1035, 1971.

[20] E. Verhoef, E. Neeft, J. Grupa and A. Poley, Outline of a disposal concept in clay, OPERA-PG-COV008, COVRA N.V., 2014.

[21] ANDRA, "CGNTAMTD150056, Spécification technique de besoin. Alimentation autonome pour la transmission sans fil en condition de stockage géologique. Modern2020 WP3.3, (2015), 15 pages.".

[22] *Product Guide – Maxwell Technologies BOOSTCAP Ultracapacitors,* Maxwell Technologies Doc. No. 1014627.1, 2009.

[23] D. S. Tucker and S. Paley, "Flexible Hybrid Battery/Pseudocapacitor," NASA, 2015.

[24] *2.3V 50F Pseudocapacitor Cell,* Maxwell Technologies doc. no. 3001969-EN.2, 2018.

[25] X. Jiang, J. Polastre and D. Culler, "Perpetual environmentally powered sensor networks," in *Fourth International Symposium on Information Processing in Sensor Networks (IPSN 2005)*, Boise, ID, USA, 2005.

[26] F. S. Garcia, A. A. Ferreira and J. A. Pomilio, "Control Strategy for Battery-Ultracapacitor Hybrid Energy Storage System," in *Applied Power Electronics Conference and Exposition (APEC 2009)*, Washington, DC, USA, 2009.

[27] F. Ongaro, S. Saggini and P. Mattavelli, "Li-Ion Battery-Supercapacitor Hybrid Storage System for a Long Lifetime, Photovoltaic-Based Wireless Sensor Network," *IEEE Transactions on Power Electronics,* vol. 27, no. 9, pp. 3944-3952, 2012.

[28] C. McCaffrey, J. Häkli, M. Hirvonen, I. Huhtinen, K. Nummila, T. Lehikoinen, "Magnetically coupled wireless communication for buried environmental sensor," in *12th International Conference on Environment and Electrical Engineering*, Wroclaw, Poland, 5-8 May 2013.

[29] N. J. Cassidy, Electrical and magnetic properties of rock, soils and fluids. In: Jol, H.M. (ed.). Ground Penetrating Radar Theory and Applications, Amsterdam: Elsevier Science, 2009, pp. 41-72.

[30] AITEMIN, "Technical requirements report," MoDeRn Deliverable D.2.1.1, 2011.

[31] AITEMIN, NDA, Andra, NRG, NAGRA, ENRESA, EURIDICE, ETH-Zurich, RWMC, D. TEC, POSIVA, SKB, RAWRA and GSL, "State of Art Report on Monitoring Technology," MoDeRn Deliverable D2.2.2, 2013.

[32] J. R. Wait and K. P. Spies, "Electromagnetic Fields of a Small Loop in a Stratified Earth," IEEE Trans. Antennas and Propagation, AP-19 (5), 1971.

[33] T. J. Schröder and E. Rosca-Bocancea, Wireless Data Transmission Demonstrator: from the HADES to the surface, MoDeRn Deliverable D.3.4.2, 2013.

[34] Modern2020, Long-term power supply sources for repository monitoring, Modern2020 Deliverable D3.3, submitted.

[35] Aitemin, Wireless sensor network demonstrator report, MoDeRn Deliverable D3.3.1, 2013.

[36] RWMC, Development of Advanced Technology for Engineering Components of HLW Disposal, Development of Monitoring Technology, 2017.

[37] K. Nishimura, Data coding technique and basis of error correction: revised edition, CQ Publisher, pp. 133-134, 2010.

[38] RWMC, Development of Advanced Technology for Engineering Components of HLW Disposal, Development of Monitoring Technology, 2018.

[39] Suyama, Y., Tanabe, H. and Eto, J., "Monitoring strategy to support decision making for geological repository closure," in *Proceedings of the 3rd East Asia Forum on Radwaste Management, p.172-179*, Gyeongju, Korea, November 2010.

[40] Suyama, Y., Eto, J., Tanabe, H. and Takamura, H., "Wireless Transmission Monitoring for Geological Disposal," in *Poster Presentation on the MoDeRn Workshop on Monitoring Technologies*, Troyes, France, June 2010.

[41] Suyama, Y., Takamura, H., Aoki, K., Wada, R., Shimbo, H. and Okutsu, K., "Wireless transmission monitoring in a geological disposal repository (I). Concepts and Advantages," in *Proceedings of MRS'09 Symposium: The 33rd International Symposium "Scientific Basis for Nuclear Waste Management"*, Saint Petersburg, Russia, May 2009.

[42] MoDeRn, "Development Report of Monitoring Technology, MoDeRn project Deliverable D-2.3.1," 2013.

[43] MoDeRn, "Hades monitoring demonstrator results and analysis report, MoDeRn project Deliverable D-2.4.2," 2013.

[44] Spillmann, T., Blechschmidt, I., Rösli, U., Parsons, S., Marelli, S., Maurer, H.R., Manukyan E., Breen, B., Martinez V. & Bárcena, I., "Comparison of wireless signal transmission and seismic tomography for monitoring radioactive waste repositories," in *8th International Symposium on Field Measurements in GeoMechanics*, Berlin, Germany, 2011.

[45] MoDeRn, "Monitoring Reference Framework Report, MoDeRn project Deliverable D-1.2.1," 2013.

[46] (MISL), Magneto-Inductive System Limited, "MI Signal Measurements HADES Underground Research Facility," MISL Document No.: ED-102190, Nova Scotia, Canada, 2006.

[47] J. R. Wait, Criteria for Locating an Oscillating Magnetic Dipole Buried in the Earth, Proc. IEEE, 59 (6), 1971, pp. 1033-1035.

[48] J. a. K. S. Wait, Electromagnetic Fields of a Small Loop in a Stratified Earth, IEEE Trans. Antennas and Propagation, AP-19 (5), 1971, pp. 717-718.

[49] AITEMIN, Technical requirements report, MoDeRn Deliverable D.2.1.1, 2011.

[50] AITEMIN, NDA, Andra, NRG, NAGRA, ENRESA, EURIDICE, ETH-Zurich, RWMC, D. TEC, POSIVA, SKB, RAWRA and GSL, State of Art Report on Monitoring Technology, MoDeRn Deliverable D2.2.2, 2013.

[51] F. Pavailler and A. Piron, "Monitoring of civil engineering structures – Quality control of measurement ," 2012.

[52] N. Rosin-Corre, C. Noret and J.-L. Bordes, "L'auscultation par capteurs à corde vibrante, 80 ans de retour d'expérience.," in *Colloque CFBR. Auscultation des barrages et des digues - Thème 2: Auscultation et suivi des ouvrages*, Chambery, 2012.

[53] CIBG 2000, Bulletin 118, "Système d'auscultation automatique des barrages.," 2000.

[54] IECS 2010 J.Sausse, "Automated dam monitoring - 25 years of experience at EDF.".

[55] E. Oukhemanou, D. Solenne, E. Buchoud, S. Michel-Ponnelle and A. Courtois, "VeRCoRs Mock-Up: Comprehensive Monitoring System for Reduced Scale Containment," in *TINCE*, 2016.

[56] C. Bringer, 2015. [Online]. Available: https://escies.org/download/webDocumentFile?id=63892.

[57] J.-M. Henault, *Methodological approach for performance and durability assessment of distributed fiber optic sensors: Application to a specific fiber optic cable,* 2013.

[58] "MoDeRn. Monitoring Reference Framework Report. MoDeRn project Deliverable D-1.2.1," 2013.

[59] K. Finkenzeller, RFID Handbook, Chichester, England: John Wiley & Sons Ltd, 2003.

[60] E. Strömmer, M. Jurvansuu, T. Tuikka, A. Ylisaukko-oja, H. Rapakko and J. Vesterinen, "NFC-Enabled Wireless Charging," in *4th International Research Workshop on Near Field Communication, NFC 2012*, Helsinki, Finland, 2012.

[61] Y. Lee, "Antenna Circuit Design," Microchip AN710, 2003.

[62] J. L. Bierschenk, Optimized Thermoelectrics For Energy Harvesting Applications, In: Priya, S., Inman, D.J. (ed): Energy Harvesting Technology, SpringerScience+Business Media, 2009, p.337-351.

[63] A. Bitschi, Modelling of thermoelectric devices for electric power generation, PhD. thesis ETH, 2009.

[64] C. Auvigne, Electrical and Magnetical Modeling of Inductive Coupled Power Transfer Systems, Thesis, Ecole Polytechnique Federale de Lausanne, 2015.

[65] J. H. Scott, Electrical and magnetic properties of rock and soil. Technical Letter Special Projects-16, Colorado: United States Department of the Interior, Geological Survey, Denver, 1966.

[66] S. F. Pichorim and P. J. Abatti, Design of Coils for Millimeter- and Submillimeter-Sized Biotelemetry, IEEE Transcations on biomedical Engineering, 51 (8), 2004, pp. 1487-1489.

[67] M. B. Kraichman, Impedance of a Circular Loop in an Infinite Conducting Medium, Journal of Research of the National Bureau of Standards - D. Radio Propagation, 66D (4), 1962, pp. 499-503.

[68] R. R. Harrison, Designing Efficient Inductive Power Links for Implantable Devices, IEEE International Symposium on Circuits and Systems, 2007, pp. 2080-2083.

[69] K. Schuylenberg and R. Puers, Inductive Powering: Basic Theory and Application to Biomedical Systems, Springer Science + Business Media B.V., 2009.

[70] [Online]. Available: www.oceanologyinternational.com/files/AUV_Marketplace_John_Westwood.pdf.

[71] [Online]. Available: http://www.futura-sciences.com/fr/news/t/terre-3/d/lobservateur-sous-marin-qui-ne-remontera-jamais_10643/.

[72] "Modern2020 project Milestone number MS11 – final report on "Using Nuclear Batteries for Geological Disposal Monitoring: State of the Art", 47 pages.," 2016.

[73] A. Harmon, "NASA's Radioisotope Power System Program. Science Mission Directorate. OPAG.," 2007.

[74] R. L. Cataldo and G. L. Bennett, "U.S. Space Radioisotope Power Systems and Applications: Past, Present and Future," NASA Glenn Research Center and Metaspace Enterprises, USA, 2011.

[75] M. A. Prelas, C. J. Weaver, M. Watterman, E. Lukosi, R. Schott and D. A. Wisniewski, "A review of nuclear batteries," *Progress in Nuclear Energy,* vol. 75, pp. 117-148, 2014.

[76] S. T. Revankar and T. E. Adams, "Advances in Betavoltaic Power Sources," *Journal of Energy and Power Sources,* vol. 1, no. 6, pp. 321-329, 2014.

[77] W. R. Corliss and R. L. Mead, "Power from Radioisotopes, Understanding the atom series," United States Atomic Energy Commission, Division of Technical Information, 1971.

[78] D. Leone, "Plutonium Still Scarce, Production Restart Still Slow for Needy NASA," 2015. [Online]. Available: http://spacenews.com/doe-to-crank-out-new-plutonium-238-in-2019/.

[79] McNutt, "RL Physics and Chemistry of Space-certified RPS : what do you need to know," The John Hopkins University applied physics laboratory. Committee on Astrobiology and Planetary Science Space Study Board, 2014.

[80] R. D. Abelson, "Big Things Come in Small Packages: Mission Concepts Potentially Enabled by Small Radioisotopes Power Systems. Systems & Mission Architecture Section," in *CalTech*, 2005.

[81] "DLC 037 0017 Rév. 2, Document logiciel Calcul - ANSYS - Dossier de validation théorique," AREVA, 2015.

[82] "DLC 037 0019 Rév. 2, Document logiciel Calcul - ANSYS – Manuel utilisateur," AREVA, 2015.

[83] J. R. Wait, "Complex Resistivity of the Earth," *Progress In Electromagnetics Research,* vol. 1, pp. 1-173, 1989.

[84] J. R. Wait and K. P. Spies, Electromagnetic Fields of a Small Loop in a Stratified Earth, IEEE Trans. Antennas and Propagation, AP-19 (5), 1971, pp. 717-718.

[85] T. Christen and M. W. Carlen, "Theory of Ragone plots," *Journal of Power Sources,* vol. 91, no. 2, pp. 210-216, 2000.

[86] W. Zuo, R. Li, C. Zhou, Y. Li, J. Xia and J. Liu, "Battery-Supercapacitor Hybrid Devices: Recent Progress and Future Prospects," *Advanced Science,* vol. 7, no. 4, 2017.

[87] A. Sato, "TAIYO YUDEN Lithium Ion Capacitors: An Effective EDLC Replacement," TAIYO YUDEN.

[88] Murata, *Small Energy Device Laminate type (UMAL). C2M1CXS-313(E),* 2016.

[89] "Battery and Energy Technologies," Electropaedia, [Online]. Available: https://www.mpoweruk.com/index.htm.

[90] S. Sudevalayam and P. Kulkarni, "Energy Harvesting Sensor Nodes: Survey and Implications," *IEEE Communications Surveys & Tutorials,* vol. 13, no. 3, pp. 443-461, 2011.

[91] *Lithium-ion battery life,* Saft, 2014.

[92] Tecate Group, "Ultracapacitor & Supercapacitor Frequently Asked Questions," [Online]. Available: https://www.tecategroup.com/ultracapacitors-supercapacitors/ultracapacitor-FAQ.php.

[93] P. Mars, "Coupling a supercapacitor with a small energy-harvesting source," *EDN-Electronic Design News,* pp. 39-42, 7 June 2012.

[94] A. Schneuwly and R. Gallay, "Properties and Applications of Supercapacitors From the State-of-the-art to Future Trends," in *Proceeding PCIM2000*, Rossens, Switzerland, 2000.

[95] Tecate Group, *Tecate PowerBurst Ultracapacitors Technical Guide Document,* Tecate Group document no. 9100760000 Rev M .

[96] G. Alcicek, H. Gualous, P. Venet, R. Gallay and A. Miraoui, "Experimental study of temperature effect on ultracapacitor ageing," in *European Conference on Power Electronics and Applications*, Aalborg, Denmark, 2007.

[97] D. Linzen, S. Buller, E. Karden and R. W. De Doncker, "Analysis and evaluation of charge-balancing circuits on performance, reliability, and lifetime of supercapacitor systems," *IEEE transactions on industry applications,* vol. 41, no. 5, pp. 1135-1141, 2005.

[98] Y. Diab, P. Venet, H. Gualous and G. Rojat, "Self-Discharge Characterization and Modeling of Electrochemical Capacitor Used for Power Electronics Applications," *IEEE Transactions on Power Electronics,* vol. 24, no. 2, pp. 510-517, 2009.

[99] MoDeRn, "Monitoring Reference Framework Report," MoDeRn Deliverable D-1.2.1, 2013.

7.1.3 References New sensors

[1] A. Sihvola. Electromagnetic Mixing Formulae and Applications. Number 47 in IEE Electromagnetic Waves Series. INSPEC, Inc, 2000.

[2] Ana T. Lima, J. P. Gustav Loch, Pieter J. Kleingeld "Bentonite electrical conductivity: a model based on series–parallel transport" J Appl Electrochem 2010 , Pages 1061–1068

[3] Appelo, C.A.J and Postma, D., 1993. Geochemistry, Groundwater and Pollution. Rotterdam, A.A. Balkema, 536 p.

[4] Bradbury, M.H., Baeyens, B., 2002. Pore water chemistry in compacted re-saturated MX-80 bentonite: Physico-chemical characterisation and geochemical modelling. Paul Scherrer Institut Berich Nr. 02-10, Villigen, 2002, p. 42.

[5] Bruno, J., Arcos, D., Duro, L. 1999. Processes and features affecting the near field

[6] C. M. Regalado. A geometrical model of bound water permittivity based on weighted averages: the allophane analogue. Journal of Hydrology, 316:98–107, January 2006.

[7] Caneiro, A., Fabry, P., Khireddine, H., Siebert, E. 1991. Performance characteristics of sodium super ionic conductor prepared by the sol-gel route for sodium ion sensors. Anal. Chem., vol. 63, 2550 - 2557.

[8] Curti, E. 1993. Modelling Bentonite Pore Waters for the Swiss High-level Radioactive Waste Repository. Helsinki: Wettingen, Switzerland, NAGRA, 74 p. + app. 11 p. (NTB 93-45).

[9] David Daniels, Ground-penetrating radar, 2nd ed., The Institution of Electrical Engineers, 2004

[10] Fernández, A.M., Baeyens, B., Bradbury, M., Rivas, P., 2004. Analysis of the pore water chemical composition of a Spanish compacted bentonite used in an engineered barrier. Physics and Chemistry of the Earth, 29, 105-118.

[11] Frazier CH1, Cadalli N, Munson DC Jr, O'Brien WD Jr Acoustic imaging of objects buried in soil. J Acoustic Society American 2000 Jul;108(1):147-56.

[12] Hong C. Rhim, Oral Buyukozturk, "Electromagnetic properties of concrete at microwave frequency range" Aci materials journal, n° 95-M25, May-June 1998, Pages 263-271

[13] Holmboe, M., Wold, S., Jonsson, M., 2012. Porosity investigation of compacted bentonite using XRD profile modelling. J. Contam. Hydrol., 2012 Feb, 1;128(1-4): 19-32.

[14] Hydrochemistry. Groundwater-bentonite interaction. SKB Technical Report TR-99-29.

[15] Janata, J. 2009. Principles of chemical sensors, 2nd ed. Springer Science+Business Media, New York.

[16] Kai and Taining "Experimental study on ultrasonic propagation in water-based bentonite slurry", 2009.

[17] LAN Kai and YAN Taining, Experimental study on ultrasonic propagation in water-based bentonite slurry, Global Geology, 12 (3) :1742178 (2009)

[18] Michael L. Oelze, William D. O'Brien, Jr., and Robert G. Darmod, Measurement of Attenuation and Speed of Sound in Soils, The Journal of the Acoustical Society of America 109, 2287 (2001)

[19] MoDeRn Project, Proceedings of an International Conference and Workshop, Luxembourg, 19 - 21 March 2013

[20] MoDeRn Project, Technical requirements report DELIVERABLE (D-N°:2.1.1), 2011.

[21] Matusewicz, M., Liljeström, V., Pirkkalainen, P., Suurinen, J.P., Root, A., Muurinen, A., Serimaa, R., Olin, M., 2013. Microstructural investigation of calcium montmorillonite. Clay Minerals 48, 267-276

[22] Muurinen, A., Lehikoinen, J. 1999. Porewater Chemistry in compacted bentonite. Report Posiva 99-20.

[23] Muurinen, A, Karnland, O., Lehikoinen, J., 2007. Effect of homogenization on the microstructure and exclusion of chloride in compacted bentonite. Physics and Chemistry of the Earth, Parts A/B/C, 32(1-7), 485-490.

[24] Muurinen, A., Carlsson, T., 2013. Bentonite Pore Structure based on SAXS, Chloride Exclusion and NMR Studies. Posiva Oy, Olkiluoto, Finland. Working Report 2013-53.

[25] Muurinen, A., Järvinen, J., 2013. Ion-selective electrodes in pore water chemistry measurement of compacted bentonite. Posiva Oy, Olkiluoto, Finland. Working Report 2013-24.

[26] N. Wagner, Th. Bore, J.-C. Robinet, D. Coelho, F. Taillade, and S. Delepine-Lesoille, Dielectric relaxation Behavior Of Callovo-Oxfordian Clay Rock: A Hydraulic-Mechanical-Electromagnetic Coupling Approach, Journal Of Geophysical Research: Solid Earth, Vol. 118, 1-16, doi:10.1002/jgrb.50343, 2013.

[27] Norman Wagner, Eberhard Trinks, Klaus Kupfer, Determination of the spatial TDR-sensor characteristics in strong dispersive subsoil using 3D-FEM frequency domain simulations in combination with microwave dielectric spectroscopy, Meas. Sci. Technol. 18 (2007) 1137-1146

[28] Ohe, T., Tsukamoto, M. 1997. Geochemical properties of bentonite pore water in highlevel-waste repository condition. Nuclear Technology. Vol. 118, pp. 49-57.

[29] Ph. Cosenza and A. Tabbagh. Electromagnetic determination of clay water content: role of the microporosity. Applied Clay Science, 26(1-4):21-36, 2004.

[30] Podio et al., Ultrasonic velocity and attenuation measurement in water-based drilling mud, 1990.

[31] Pusch, R., Muurinen, A., Lehikoinen, J., Bors, J., Eriksen, T., 1999. Microstructural and chemical parameters of bentonite as determinants of waste isolation efficiency. European Commission. Nuclear Science and Technology. Project Report EUR 18950 EN.

[32] S. R. Evett and G. W. Parkin. Advances in Soil Water Content Sensing: The Continuing Maturation of Technology and Theory. Vadose Zone J, 4(4):986-991, 2005.

[33] Timo Saarenketo. Electrical properties of water in clay and silty soils. Journal of Applied Geophysics, 40(1-3):73-88, 1998.

[34] Tournassat, C. and Appelo, C.A.J., 2011. Modelling approaches for anion-exclusion in compacted Na-bentonite. Geochimica et Cosmochimica Acta 75, 3698-3710.

[35] Tributh, H., Lagaly, G.A. 1986. Aufbereitung und Identifizierung von Boden- und Lagerstättentonen. I. Aufbereitung der Proben im Labor. GIT-Fachzeitschrift für das Laboratorium 30, 524 - 529.

[36] V. Saltas, F. Vallianatos, D. Triantis, "Dielectric properties of non-swelling bentonite: The effect of temperature and water saturation" Journal of Non-Crystalline Solids Vol. 354, Issues 52-54, 15 December 2008, Pages 5533-5541

[37] Van Loon, L.R., Glaus, M.A. and Muller, W., 2007. Anion exclusion effects in compacted bentonites: Towards a better understanding of anion diffusion. Applied Geochemistry 22, 2536-2552.

[38] Wersin, P., 2003. Geochemical modelling of bentonite pore water in high-level water repositories. J. Contam. Hydrol. 2003 Mar. 61(1-4): 405-22.

[39] Yao, S., Wang, M. and Madou, M. 2001. A pH electrode based on melt-oxidized iridium oxide. Journal of The Electrochemical Society 148 (4), H29-H36.

8 Appendices

8.1 Part Approval Document required qualifying components in the Space field

PROJECT:................ Doc n°:.................... Prepared by: ....
Issue:...................... Date:....................

Approval requested by:...............................
Family:.................... Fcode [ ] Group:.................. Gcode [ ]
Component Number:..
Commercial Equivalent Designation:.....................
Manufacturer/ Country:.................................
Technology/Characteristics (value or range of values with tolerance, voltage, package etc): ....
Pure tin free (Y/N) [ ]
Generic specification:....................
Detail specification:........................ Issue:..... Rev.:..... variant:.......
Specification amendment: .... Issue:..... Rev.:..... variant:.......
Quality level:......................... Procurement by:.............................

APPROVAL STATUS

EPPL Part 1/2 listed (1/2/N) [ ]
ESCC QPL or EQML listed (Y/N) [ ]
MIL QPL or QML listed (Y/N) [ ] If yes: QPL/QML Reference:...............................
Other approvals/former usage ....
Evaluation programme required (Y/N) [ ]
If yes reference of the Evaluation Programme:..............................

PROCUREMENT INSPECTIONS and TESTS

Precap (Y/N) [ ]
Lot acceptance:
ESCC LAT/LVT level or subgroup [ ]
MIL QCI/TCI group [ ]
Buy-off (Y/N) [ ]
DPA (Y/N) [ ] if yes: sample size ....

Complementary tests ....

RADIATION HARDNESS DATA

Radiation Hardness Assurance Plan applicable (Y/N)[ ]
Doc. Ref.: ....

Total Dose Effects:
Evaluation Test Data (report) reference: ....

Single Event Effects: SEL/SEU/SET/SEFI/SEB/SEGR/others: *(cross out when non applicable)*
Evaluation Test Data (report) reference: ....

RVT required (Y/N)[ ]

REMARKS

Approval customer .... Date ....

8.2 Example for ADOC sheet for a monitoring component qualification

Receive: ___/___/______

ADOC - Approval DOCument for a monitoring component qualification

Project:	**Doc n°:**
Prepared by:	**Date:**
Approval requested by:	
Family:	**Component:**
Technology Detail specification:	

Approval status:

Evaluation programme required:	☐ Yes	☐ Not

Component selection

TRL:	Procurement by:	
Influence parameters with measurement range and sensitivity:		
Sensitivity to influence parameters	☐ Ok	☐ Not Ok
Verification of functional and ergonomic characteristics	☒ Ok	☐ Not Ok
Verification of metrological characteristics	☐ Ok	☐ Not Ok
Verification of compliance with current standards	☐ Ok	☐ Not Ok
Requirement for additional tests (in case not ok)	☐ Yes	☐ No
If yes, test required Lab - Robustness	☐ Yes	☐ No
Lab - Ageing tests	☐ Yes	☐ No
In situ – Long-term	☐ Yes	☐ No
In situ – demonstration	☐ Yes	☐ No

Laboratory test (testing of components/combined components under adverse conditions)

1. Test of robustness:	☐ Yes	☐ No
Laboratory name:	Certification/accreditation number:	
Detailed Specifications: (type of test, steps, iterations…):		
Reporting:	Number	Date
Results:	☐ Ok	☐ Not Ok
2. Ageing tests	☐ Yes	☐ No
Laboratory name:	Certification/accreditation number:	
Detailed Specifications: (type of test, steps, iterations…):		
Reporting:	Number	Date
Results:	☐ Ok	☐ Not Ok

On-site test (testing of the whole components under realistic conditions)

1. Tests at URLS:	☐ Yes	☐ No
URL:	Certification/accreditation number:	
Detailed Specifications: (type of test, steps, iterations…):		
Reporting:	Number	Date
Results:	☐ Ok	☐ Not Ok
2. Testing at witness structure/cells at DGR	☐ Yes	☐ No
DGR:	Certification/accreditation number:	
Detailed Specifications: (type of test, steps, iterations…):		
Reporting:	Number	Date
Results:	☐ Ok	☐ Not Ok

8.3 Innovative Technical data sheet for Stakeholders.

Low-frequency data transmission

Partners involved: NRG

Rationale:

Wireless data transmission technology allows monitoring behind safety-relevant barriers, without impairing the safety function of a barrier by the use of wires. High-frequency data transmission techniques are used in a large number of industrial and consumer applications, but propagation through solid materials like the host rock or barrier materials (e.g. concrete, (saturated) bentonite) is limited to few meters. Low-frequency magnetic fields allow transmitting data over longer distances through solid materials in the underground (hundreds of meters), but are rarely used.

Because of the requirement of retrievability of the waste in the Netherlands, NRGs specific interest in *MoDeRn* was to investigate the feasibility of transmitting monitoring data after closure from deep underground waste disposals to the surface. In *Modern2020*, NRG studies this technology further and participates in a common evaluation of a combination of different range wireless systems in order to provide a complete data transmission solution.

Description of the technology:

Low-frequency data transmission technologies make use of magnetic fields that easily penetrates through the underground.

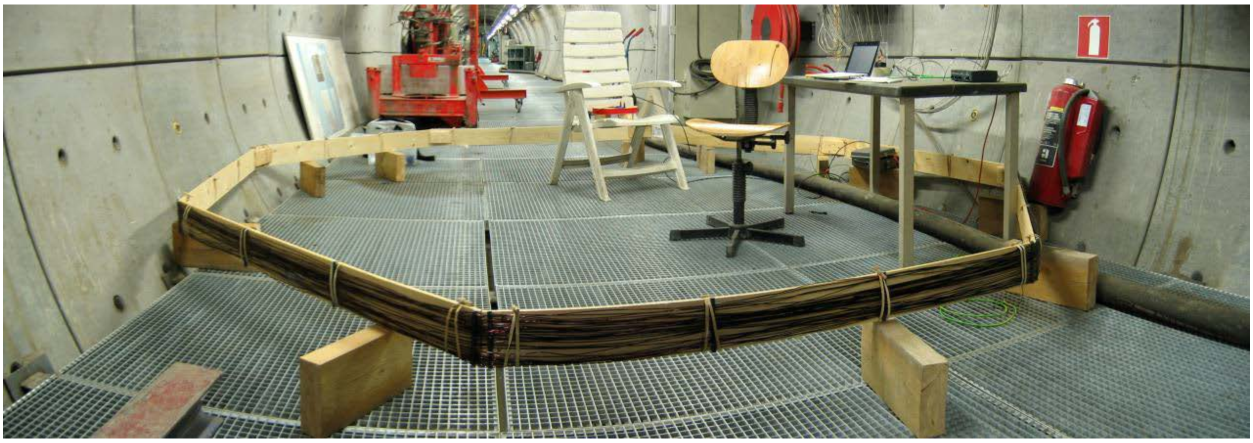

Figure 84 : NRG transmitter in the HADES URL (225 m b.s.l.)

Figure 85 : NRG receiver on top of the HADES URL

Objectives/Specifications:

The most important specification for a data transmission technology in the context of waste disposal is the energy efficiency (expressed as Ws per transmitted bit), because the supply of power is considered as a limiting factor. The energy needed to transmit data depends on several factors, e.g. transmission distance, properties of the materials in the transmission path, antenna size, or local background noise. Table 22 gives example specifications: *demonstrated* specifications are related to long-distance experiments performed in the *HADES URL* in Mol, Belgium (suboptimal antenna size, high surface noise), *expected* specifications are extrapolated to Dutch disposal concepts in Boom Clay (depth 500 m) or rock salt (depth 800 m).

Table 22. Example specifications

Transmission range	demonstrated: up to 225 m expected: ≥800 m
Data rate	demonstrated: 100 sym/s expected: ≥ 30 sym/s
Energy need	demonstrated: 1Ws/bit expected: <1 mWs/s

Indicate the progress expected in TRL

Table 23. Progress expected in TRL

Technology Readiness Level (TRL)	Current	Planned
Basic and applied research (TRL : 1-4)		
Development (TRL : 5-7)	●	●
Manufacturing (TRL : 8-9)		

Development steps:

The work performed in *Modern2020* is divided into three steps:

- Characterization of environmental conditions at the Tournemire URL, France
- Adaption of existing set-up for optimal performance under the local conditions present at Tournemire
- Demonstration of combination of technologies & quantification of energy efficiency at Tournemire

Table 24. Steps Moderne2020 Project

Step	Start time	Completion time
Characterization of Tournemire environmental conditions	2016	2017
Adaption of existing set-up to Tournemire local conditions	2017	2018
Demonstration at Tournemire	2018	

On field test or advanced test example:

In the experiments at the *HADES URL*, the receiver antenna (Figure 2) was situated 225 m on top of the underground transmitter (Figure 1 & Figure 3). In Tournemire, a comparable set-up will be used, resulting in a transmission distance of about 240 m. Transmission distances of up to 500 m can be achieved by shifting the receiver antenna on the surface off-axis (Figure 4).

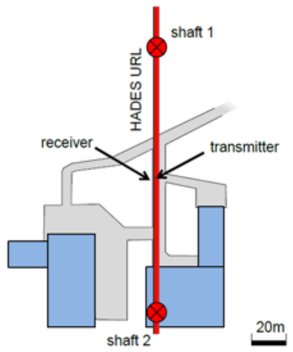

Figure 86: Set-up of experiment at the HADES URL in Mol, Belgium

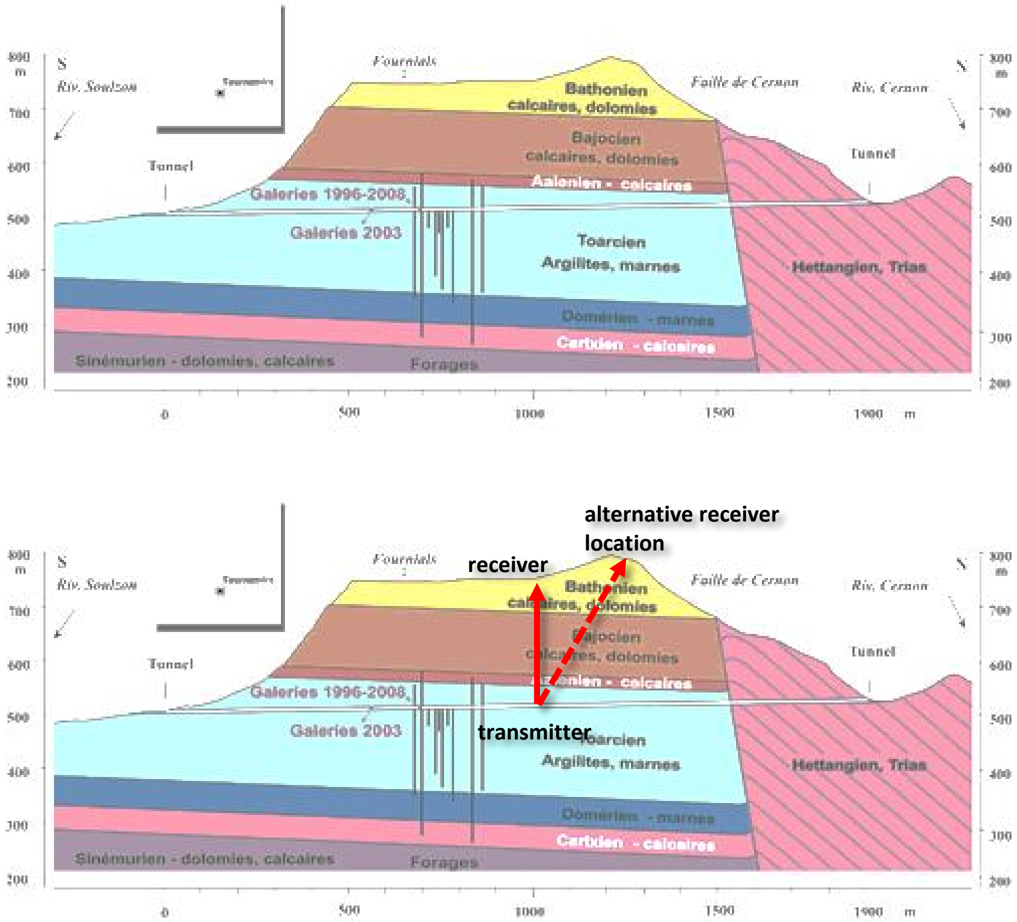

Figure 87: Set-up of experiment at the Tournemire URL, France

Existing alternatives to this technique:

- High-frequency data transmission is an alternative on small to medium distance (<20 m)
- RWMC and Andra develops comparable low -frequency techniques

Advantages

This technology allows transmitting data over larger distances (tens to hundreds of meters) of electrical conducting materials (e.g. aquifers, clay, (saturated) bentonite or cementitious materials) than high-frequency-based technologies. On medium distances (tens of meters), low-frequency transmission might be more energy efficient than high-frequency transmission.

Radioisotope Thermoelectric Generator (RTG)

Partners involved: ANDRA, AREVA

Rationale

The project goal is to develop a long term energy supply for measurement systems which include both sensors & transmission devices. Minituarized Nuclear Power devices, best known as Radioisotopes Thermoelectric Generators (RTG) have attracted the interest of many since the early days of nuclear energy developments and continue to do so. The main reason is the potential for a long battery lifetime (i) autonomy and (ii) security of energy supply.

No current battery technology meets the needs of geological deep disposal of nuclear waste, namely that it should operate continuously and without maintenance for at least 100 years.

Description of the technology

A Radioisotope Thermoelectric Generator is an electricity generator that uses multiple thermocouples to convert heat generated by the decay of a radioisotope material into electricity using the Seebeck effect. Its design is very simple compared to other nuclear devices (Figure 88). An RTG is a system composed of multiple sub-assemblies [Figure 88] :

1. A Radioisotopic source. This subset is usually formed by the radio-isotope itself in the form of a compound and the Nuclear material encapsulation required by nuclear safety regulations
2. One or more thermoelectric converters (Seebeck effect) located between the radio isotopic source and the heat sink
3. The heat sink to remove the thermal power that it is not transformed into electricity (~95%)
4. An insulating layer in order to minimize the thermal loss located between the radioisotope source and the heat sink (in everyplace where there is no thermoelectric converter)

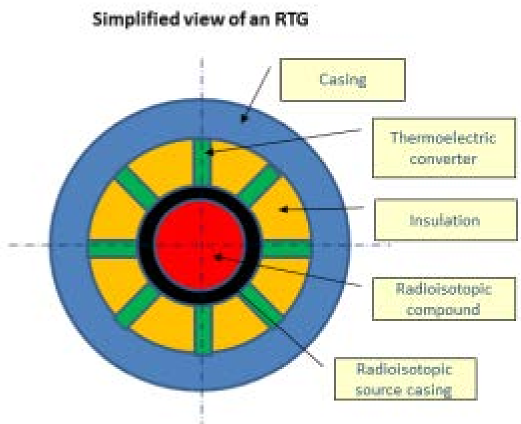

Figure 88: Simplified view of a RTG

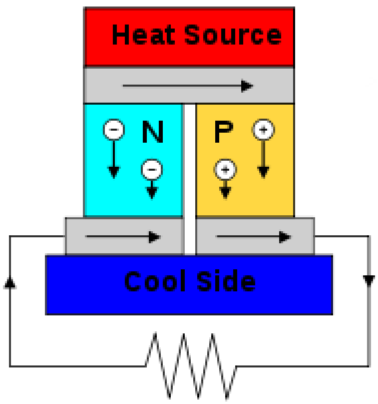

Figure 89: Seebeck effect

Physics behind the technology

The technology is based on the Seebeck effect or thermoelectrical power conversion. A thermoelectric device creates electric tension between two terminals (+ / -) when a difference of temperature is applied on each side of thermoelectric materials. At the atomic side, an applied temperature gradient causes charge carriers in the material to diffuse from the hot side to the cold side (N-P). When properly assembled metals with different properties will deliver electricity on the cold face of the system [Figure 89]

Application of the technology

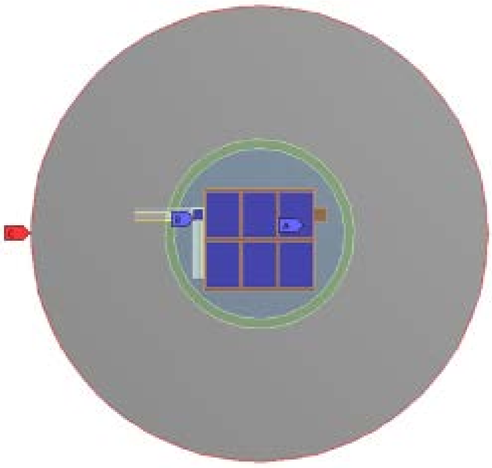

Figure 90: Schematic view of a RTG located inside a cavity with 6 MAVL

Such a technology is expected to provide a permanent electrical energy source to monitor long term geological disposal of nuclear waste. Power generators based on such technology should be placed in disposal vaults within deep storage tunnels as an energy source source for data acquisition (sensors) local storage and transmission to the surface [Figure 90]. It is perceived as a unique technology to provide energy within MAVL vaults, Cigeo project, and without using wires which would be required to bring in energy from distant sources, thereby breaching containment (long term safety requirements).

Specifications

Specifications depend on the temperatures of the hot and cold faces, on the conversion efficiency, on the expected electrical power to be generated....Considering the application expected herein, specifications may be as follow:

Mass range	30 – 56 kg
Power supply range	5We – 10We
Efficiency	5% – 6 %
Conversion	Seebeck Effect
Operation temperature	Depending on the delta T
Thermal power	~100 – 200Wth
Life time	>100 years, up to radioisotope decay

Indicate the progress expected in TRL

Technology Readiness Level (TRL)	Current	Planned
Basic and applied research (TRL : 1-4)		
Development (TRL : 5-7)	●	●
Manufacturing (TRL : 8-9)		

The TRL of RTG for space applications is deemed to be 8 to 9 in the US, and only around 4 in Europe as of today. The planned TRL will depend on the projected date of delivery. A proof of concept, as well as a prototype development, thus needs to be achieved for the target application inside a cavity in geological deep storage facility.

Development steps

N/A in Modern 2020 as the aim of this study is a state-of-art of the RTG.

125 kHz Wireless Sensors Partners involved: VTT, POSIVA.	MODERN 2020 Development and Demonstration of monitoring strategies and technologies for geological disposal

Rationale:

Wireless data transfer is a preferred option for obtaining measurement data from inside the nuclear waste repository to avoid creating potential conduits along the wires for leaks. The different repositories represent widely different environments for the wireless data transfer and thus different needs and requirements e.g. for the transmission range necessary for the various types of materials and structures. Also the required data transfer rate and transmission intervals vary depending on what kind of sensor data is to be transmitted. Thus it is highly challenging to meet all these requirements and probably no single technical solution that suits all the needs exist. Currently there are no ready solutions to meet these needs in all applications and new solutions are needed.

Description of the technology:

The wireless transfer of sensor data is based on using magnetic field at low frequencies. Low frequency magnetic field is mostly unaffected by the transmission medium which allows the signal to propagate through rock, concrete with rebars and other materials that attenuate electromagnetic waves strongly. The selected frequency of operation is 125 kHz, which represents a good compromise between low attenuation at low frequencies and larger bandwidth for faster data transfer at higher frequencies.

The sensor data is digitally coded and modulated to the 125 kHz carrier. A large loop antenna is connected to the receiver that demodulates the signal and decodes the data. The arrangement is illustrated in Figure 91and the sensors and the receiver are shown in Figure 92

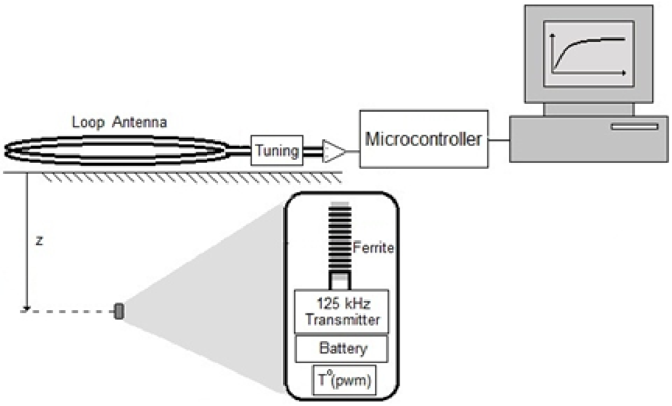

Figure 91: Wireless sensor system.

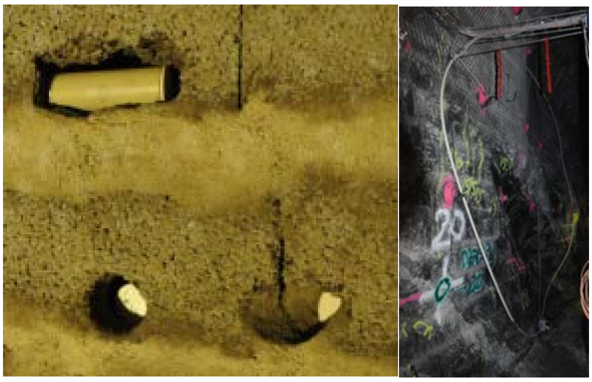

Figure 92: Sensors and the receiver

Objectives/Specifications:

The main objective is to increase the transmission range through rock and other engineered barriers, and to improve the robustness and reliability of the system.

The specific objectives are

- Transmission range of 10-25+ m
- Lifetime 10-20+ years

The progress expected in TRL :

Technology Readiness Level (TRL)	Current	Planned
Basic and applied research (TRL : 1-4)	●	●
Development (TRL : 5-7)	●	●
Manufacturing (TRL : 8-9)	●	●

Development goal is to increase the Technology Readiness Level from TRL 5 to TRL 7.

Development steps:

The development steps are as follows

1) Investigation of new implementation possibilities (updated review of the state-of-the art)
2) Analysis of the current prototype system for potential improvements
3) Tests and analyses of the potential new technologies and potential system improvements
4) Design of the new system prototype with necessary new parts and components (sensors, transmitter, antennas, reader, software etc.)
5) Testing of system components (done as an integral part of the design process)
6) Implementation of the new prototype system
7) Testing of the system

The planned steps to reach the desired objectives.

Step	Start time	Completion time
New Implementation possibilities	June 2015	April 2016
Analysis of the current prototype system	June 2015	June 2016
Testing of the new solutions	March 2016	September 2016
Design of the new system	June 2016	March 2017
Testing of the components	April 2017	June 2017
System implementation	July 2017	December 2017
System Testing	January 2018	May 2018

Existing alternatives to this technique:

- Wired measurement systems
- Similar technologies at different frequencies

Advantages

Wireless data transfer does not need wires going through the barriers that may introduce conduits for leaks. The selected frequency of 125 kHz is a good compromise for propagation through the media and for available bandwidth to send data. Each nuclear waste repository has unique features and needs for which a single technology solution for all applications is not feasible and different solutions are needed.

Autonomous power supply

Partners involved: NRG

Rationale:

Wireless monitoring equipment placed behind barriers needs autonomous power supply solutions. Batteries are widely used as power supply, but the life-time of commercial batteries is limited (<30 years). Because many safety-relevant processes of interest evolve rather slowly, wireless monitoring of these processes depends on the availability of alternative supply options that allows to provide electrical power over several decades (>30 years).

Description of the technology:

The term ‘energy harvesting’ describes the process of conversion, storage and management of electrical energy. NRG is interested to investigate two options for energy harvesting:

- the conversion of heat released by high-level-waste (HLW) canisters by the use of thermo-electric generators (TEGs) due to the so-called “Seebeck” effect.
- the application of wireless energy transmission by low-frequency magnetic fields

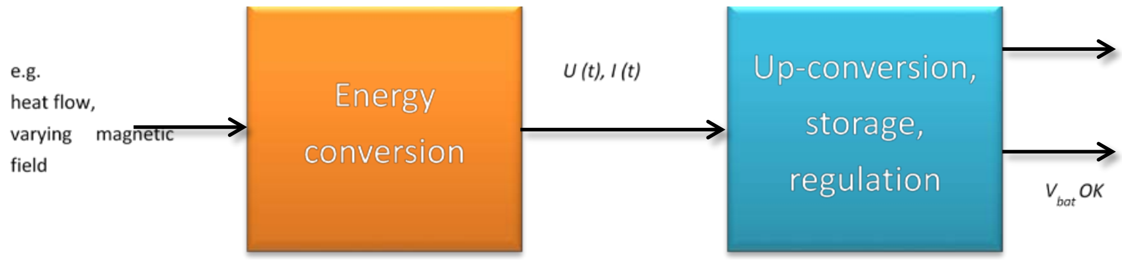

Figure 93: Principal elements of an energy harvesting solution

Objectives/Specifications:

TEG’s are used in several applications where a large temperature gradient is present. The research interest of NRG is directed to the usability of very small thermal gradients (<2°C) present in a radioactive waste facility after relevant time of interim storage (several decades), in order to investigate and quantify under which conditions usable amounts of energy can be collected and stored.

Wireless energy transmission is used in a large number of logistic and consumer applications, but these applications are limited to small distances (mm to cm). Main research interest here is the application of energy transmission by low frequency magnetic fields over medium distances (>10 m), through solid materials as used in engineered barriers (concrete, (saturated) bentonite) or host rock material (granite, clay, etc.).

The following table indicates the progress expected in TRL

Technology Readiness Level (TRL)	Current	Planned
Basic and applied research (TRL : 1-4)		
Development (TRL : 5-7)		
Manufacturing (TRL : 8-9)		

Development steps:

The work performed in *Modern2020* is divided into three steps:

- TEGs will be tested under laboratory conditions and their performance will be characterized
- Wireless energy transmission technology will be developed, tested and optimized in a laboratory and by coplanar surface-surface experiments
- Wireless energy transmission technology will be demonstrated at Tournemire

Step	Start time	Completion time
Test & characterization of TEG performance	2018	2019
Development, test and optimization of wireless energy transmission technology	2016	2018
Demonstration of wireless energy transmission technology at Tournemire	2018	2019

Existing alternatives to this technique:

- Radioisotope thermoelectric generator (RTG, Areva)
- Long-living batteries (>30 years)
- VTT works on a comparable wireless energy transmission technology
- Several other potential options exists, under which the use of mechanical energy (displacement, pressure), chemical reactions, or beta-voltaic batteries.

Advantages

TEGs makes use of available decay heat generated by radioactive waste, and are small autonomous units that are expected to be easily integrated in existing disposal concepts. Wireless energy transmission technology is of interest because it can be used to transmit data wirelessly as well.

Wireless energy transfer Partners involved: VTT	MODERN 2020 Development and Demonstration of monitoring strategies and technologies for geological disposal

Rationale:

Long-term (over 20 years) operation of wireless sensors requires batteryless powering, the technology options for which are energy harvesting and wireless power transfer. Subtask 3.3.3 concentrates on the latter of these.

Description of the technology:

An underground inductive radio frequency system combining wireless energy and data transmission according to Figure 1.

- TDM based multiplexing of powering, data downlink and data uplink.
- Active inductive transmitter scheme for data uplink (load modulation scheme applied e.g. in ISO14443 RFID systems would not provide a range long enough)
    - long powering periods, short data transmission periods
    - an intermediate energy storage at the sensor end is necessary

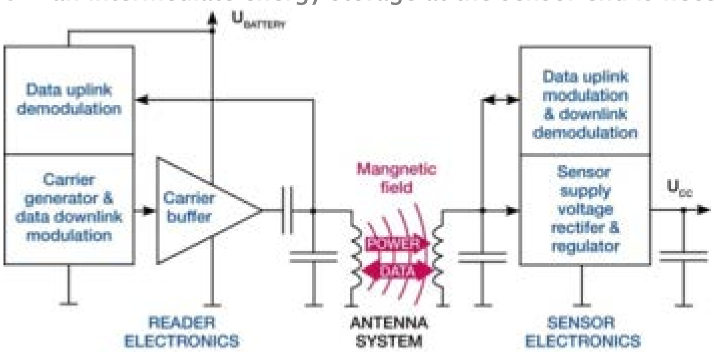

Figure 94: Principal system illustration

Objectives/Specifications:

The target specifications and the technology readiness of the system are as follows:

Operating range	>10 m
Received power	>1 µW
Uplink data rate	TBD
Downlink data rate	TBD
Operation temperature	40 - +85˚C
Life time	>50 year

The following table indicates the progress expected in TRL

Table 25. Progress expected in TRL

Technology Readiness Level (TRL)	Current	Planned
Basic and applied research (TRL : 1-4)	●	●
Development (TRL : 5-7)	●	●

Manufacturing (TRL : 8-9)		

Development steps:

Step	Start time	Completion time
SoTA of the modeling methods	September 2015	February 2016
Prototype specification	January 2016	June 2016
Prototype development & laboratory verification	April 2016	June 2017
Field tests	April 2017	June 2018
Reporting	April 2018	August 2018

On field test or advanced test example:

Field tests are made in some experimental repository station in Olkiluoto (Finland) or in Tournemire (France) if possible.

Results:

Performance evaluation results are not yet available.

Existing alternatives to this technique:

For long-term power supply of underground wireless monitoring sensors, there are following alternative technologies:
Energy harvesting based on thermal gradients (to be investigated in task 3.3.1)
Nuclear generators (to be investigated in task 3.3.4)

Advantages

Integrating the wireless power supply of the sensor to the same implementation with the sensor data uplink and downlink facilitates more compact implementation of the sensors and eliminates co-existence problems of separate RF systems.

Distributed optical fiber sensors Partners involved: ANDRA	MODERN 2020 Development and Demonstration of monitoring strategies and technologies for geological disposal

Rationale:

Security and safety of roads, bridges and tunnels are traditionally based on a routine biennial visual inspections. Continuous sensor-based structural health monitoring should supplement inspection data by measuring quantities that cannot be otherwise observed and by gauging a structure's performance over time and between inspections. New sensing techniques suitable for structures are developing rapidly. Optical fiber sensors are a promising technique because it (i) enables to place the instrument far from measuring points, in a bungalow where electricity is available (ii) reduce high cost of wires (a single fiber car address several measuring points, there are large multiplexing capacity) (iii) it is long-lasting compared with electronics.
Among different kind of optical fiber sensors, one type is especially attractive: distributed sensing. In such devices, measurements is provided along the whole optical fiber, not only in few sensing points (see Figure 92). Such measurement scheme is based on pulse-echo techniques. Temperature and strain distributed sensing with OFS is now a standard in structural health monitoring area. There are different suppliers. Measurement have been qualified, compared with traditional sensors with success. However, possible influence of the harsh environment of underground repositories compromise the quality of measurements (systematic errors, loss of measurements etc.), and durability (drift).
What is more, distributed gamma measurements are a new topic in sensing area. There were old results with performances far from requirements. Recent PhD works, based on new possibilities gatherd from optoelectronic fields, has started developing this topic. Distributed hydrogen sensing is fully new (some publications appeared since 2012).
Finally, cross-linked between these several sensing parameters have not been addressed yet.
The planned work comprises the development (design, realization and tests) of an optoelectronic sensing chain to make distributed measurements of four parameters: Temperature, strain, hydrogen and radiation, separately or at the same time.

Description of the technology:

The study will take advantage of the huge influence of optical fiber dopants and primary coatings to enhance the influence of one only parameter while annealing the influence of the three other. The research will be focused on the sensing cable, with specific optical fiber realizations.
Commercial instruments are available for distributed strain sensing. It pairs an instrument with a standard singlemode fiber whose Brillouin scattering spectrum is localized (position of Brillouin peak is proportional to strain and temperature, as sketched in Figure 97). Commercial instruments are available for distributed temperature sensing: it pairs an instrument with a standard multimode fiber whose Raman scattering intensity is quantified. With these two instruments and two fibers, one should retrieve temperature and strain. More generally, Rayleigh, Raman and Brillouin sensitivity are illustrated in Figure 96.
For hydrogen sensing, Andra and Xlim hold two patents on the Brillouin hydrogen sensing (sensitivity is illustrated in figure 4), associated with special fiber that incorporate palladium particles (highly sensitive to Hydrogen).

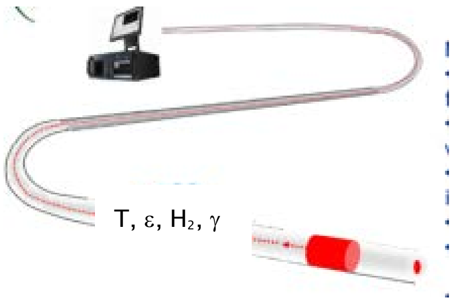

Figure 95: Principle of distributed sensing with an optical fiber

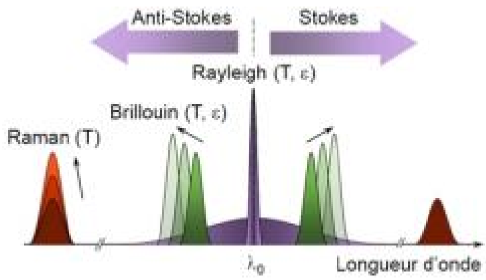

Figure 96 : Schematic representation of the scattering phenomenon in optical fibers and their sensitivity

Radiation topic is a new development. Al and P doped fibers are known to be very sensitive to radiations. They will be tested to perform sensing.
TO summarize, to reach four parameter measurements, the measuring system will rely on two or three scattering measurements, namely Brillouin, Rayleigh and Raman; commercial equipment will be used. The sensitivity is expected to be degraded compared to optical fiber sensors based on Bragg gratings but distributed measurements will solve the problem of locating several measuring points within the structures.

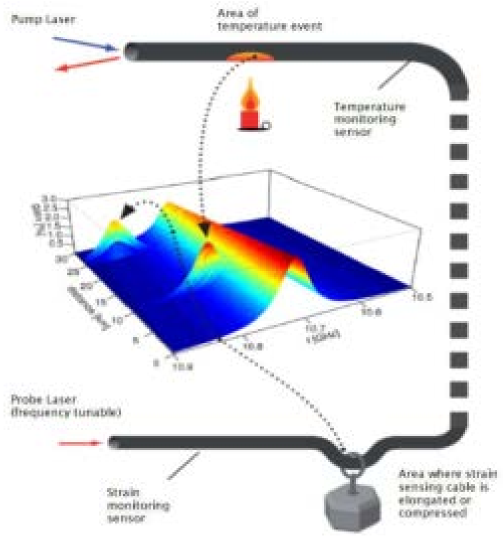

Figure 97 : Schematic representation of the time and frequency domain acquisition for the detection and localization of 2 spots. Copyright Omnisens

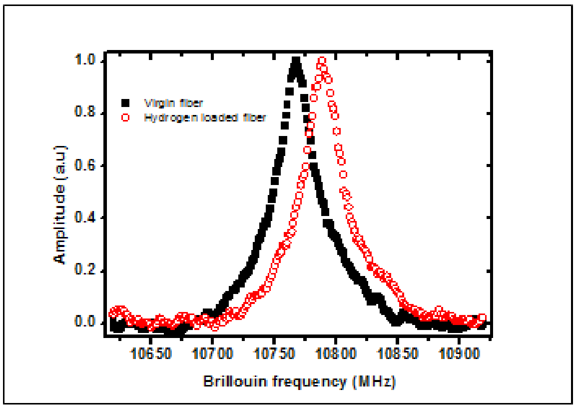

Figure 98 : Measurement of Brillouin scattering in an optical fiber before and after exposition to hydrogen

Objectives/Specifications:

Measuring range	
Accuracy	500 ppm
Response time	< 1s
Repeatability	
Power supply	0, 6.0 – 16.0V
Operation temperature	40 - +85˚C
¿?	no
Life time	4-5 year

Indicate the progress expected in TRL

Technology Readiness Level (TRL)	Current	Planned
Basic and applied research (TRL : 1-4)		
Development (TRL : 5-7)		
Manufacturing (TRL : 8-9)		

Optical fiber for hydrogen gas detection Partners involved: ANDRA, Universite of Mons.	MODERN 2020 Development and Demonstration of monitoring strategies and technologies for geological disposal

Rationale:

Hydrogen concentration is an important parameter to control and monitor into the envisioned French deep geological repository for long-lived high level and intermediate level wastes.

Hydrogen forms explosive mixtures when combined with air for a large concentration range (from 4 to 75 % vol in air). Hydrogen gas can be originated from nuclear waste release and anoxic corrosion of metallic materials. Its monitoring aims at preserving retrievability of wastes (a specificity of the French concept): detecting unexpected release rates would be an indication of potential deterioration of waste packages. It also ensures exploitation security since hydrogen monitoring is a key factor in explosive risk management.

In the harsh conditions of radioactive waste disposal (temperature, humidity, gamma radiation), electronic point-contact hydrogen sensors would probably be rapidly degraded, and large area monitoring involves a large number of detection points or the use of distributed gas sensors. As optical methods such as Raman, Rayleigh or Brillouin scatterings are available for distributed measurements, without dead zone, long length optical fibers are a promising candidate for hydrogen sensors development. Optical fibers are flexible and thin components compatible with severe humidity, pressure, temperature, gas and/or gamma radiation concentrations. Besides, fiber interrogation systems can be placed far from the measuring area. Thus, explosive environments can be monitored without the ignition risk due to electronic switches [S. Leparmentier et al, Proc. of SPIE, 9128, 2014].

Frequency shift of the Brillouin backscattered peak resulting from H2 diffusion into a standard G652 fiber tested at 1.55 µm has been demonstrated [S. Delepine-Lesoille et al., Phot. Tech. Letters, 24 (17), 2012], allowing distributed monitoring of H2 concentration. It is noteworthy that the diffusion kinetics of H2 gas in silica restricts the use of this sensor to monitor slow H2 leakage, in the order or hours, not millisecond. The use of catalysts may thus improve the component reactivity, as for Palladium (Pd). In contact with H2 gas, Pd forms an hydride PdHx (with x is a function of the gas rate) leading to a variation of both the material refractive index and lattice cell volume [L. Goddard et al., IEEE Lasers and Electro-Optics Society, 2008]. Efficient hydrogen sensing was achieved by using standard optical fibers (like G652 fibers used for telecommunications) with local Pd layers. However, these sensors suffer from untimely deterioration in harsh environments and poor robustness. They are mainly dedicated to local gas detection only. We propose to introduce Pd particles into the silica cladding of optical fibers in order to protect the sensing metal from harsh environments and for enabling distributed sensing of H2 gas along long lengths. Embedding Pd into fibers might therefore improve the sensitivity and the response time of the distributed fiber gas sensor, by exploiting the mechanical strain induced by the crystal lattice expansion of Pd particles in contact with H2 gas.

Description of the technology:

We use the Modified Powder-in-Tube (MPIT) technique to fabricate these original optical fibers [J.L. Auguste et al, Materials 7, 2014]. The MPIT is a non-conventional technique based on the use of powdered materials for fabricating fiber preforms. It is well adapted for managing fabrication constraints induced by different materials (due to different thermo-mechanical properties), for controlling and modifying the oxidation state of powder materials inside the preform, and for fabricating fibers with complex topologies by associating it with other fabrication processes such as the stack-and-draw technique.

The preform is realized by filling a silica tube with a powder mixture of silica (SiO2) and palladium oxide (PdO), around a cane positioned in the center (Figure 1). The cane composed of a core and an optical cladding ensures light guiding conditions.

Powdered preforms were then drawn down to optical fibers (Figure 2) with lengths of several hundred meters and a PdO ranging from 0.01% to 5% mol (in addition to SiO2), [S. Leparmentier et al, Optical Materials Express 5 (11), 2015].

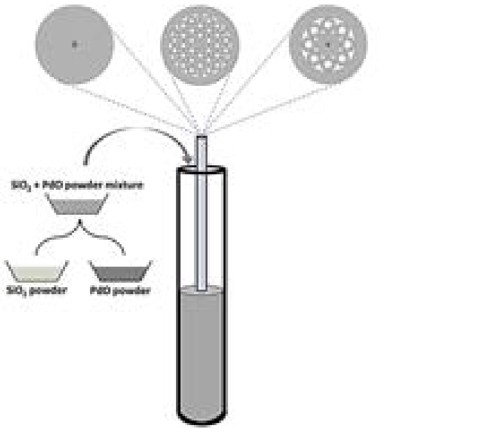

Figure 99: Illustration of the MPIT based process developed for fabricating preforms with Pd particles embedded into the cladding

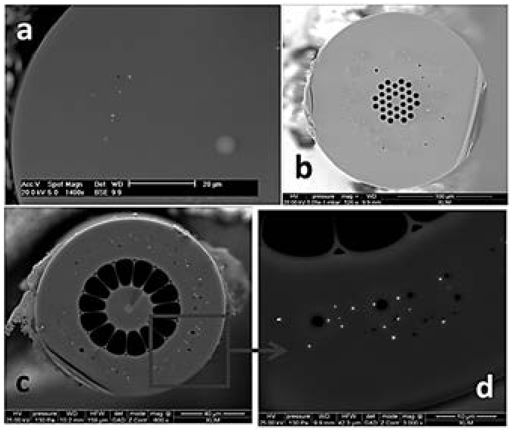

Figure 100: SEM (in the backscattered configuration) photographs of cross-sections of three optical fibers with Pd particles embedded into the silica cladding fabricated by the MPIT process. (a) a SiO2-GeO2 core step index fiber, (b) a pure silica core microstruct

Optical fibers with palladium particles dispersed into the cladding material would then be spliced to standard connectors, and tested under hydrogen gas by Rayleigh and/or Brillouin backscatterings in order to monitor the gas-induced frequencies shifts.

Specific calculations are also carried out to improve the fiber topology that would allow enhanced fast and measurable response even at low gas concentration.

Objectives/Specifications:

Fiber diameter	< 125 µm
Guidance	Single-mode at 1.55µm and compatible with standard connectors
Attenuation of sensor	< 10 dB
Measuring range	0-100 % of H_2
Operating temperature	-25/+125°C (coating)
Life time	> 100 years

Technology Readiness Level (TRL)	Current	Planned
Basic and applied research (TRL : 1-4)		
Development (TRL : 5-7)		
Manufacturing (TRL : 8-9)		

Development steps:

Description of the planned steps to reach the desired objectives

Step	Start time	Completion time

Study of hydrogen effect on the Palladium	January 2016	December 2016
Study of the different design of optical fiber	January 2017	December 2017
Optimization of the optical fiber design	January 2018	December 2018

Distributed Fiber-Optic Monitoring Systems for Determination of Thermal Conductivity, Density, Water Content, Temperature, and Water Pressure

Partners involved: Nagra

Rationale:

In the engineered barrier system (EBS), temperature, thermal conductivity, density, and water content are important parameters to monitor for the understanding of thermal-hydraulic-mechanic processes and as input for numerical models. In addition, water pressure and temperature are the most important monitoring parameters in deep boreholes, which are drilled from the surface in the vicinity of a future geological repository.

Typical sensors measure a certain parameter at one point using an electrical signal. For our monitoring applications we are looking for different sensor technologies as alternative and back-up to standard sensors. Distributed fiber-optic monitoring systems offer a promising technology, because a fiber-optic cable serves as linear sensor, having no electronics at the measurement location and providing a continuous profile with a spatial resolution of dm – m along a several km long cable.

Distributed fiber-optic monitoring systems are an emerging technology and are commercially available to measure temperature and strain distributions along a fiber-optic cable. We want to use a commercial distributed temperature sensing system (DTS) with heatable fiber-optic cables, which are installed in bentonite of the EBS. The objective is to derive distributions of thermal conductivity, density, and water content from the heating and cooling behaviour along the cable. Combination of DTS and heatable cables (called “active DTS”) were used already in dam monitoring and groundwater applications. However, for EBS materials and our applications the active DTS methods need to be improved to get accurate and reliable results. For distributed pressure sensing no commercial system exists at the moment. Therefore, we plan to develop a new method combining distributed pressure and distributed temperature sensing (DPTS) in boreholes.

Description of the technology:

The principle of distributed fiber-optic sensing is based on sensing a laser-pulse into a fiber-optic cable and analysing the backscattered light, which contains information about local temperature and strain. As light instead of electric signal is used, the fiber-optic cable is a very robust sensor, which is immune against corrosion and electro-magnetic disturbance.

Figure 101: Schematic set-up of fiber-optic distributed sensing.

Active DTS

In active DTS the temperature distribution is measured along a fiber-optic cable that is heatable. A heat pulse is sent along the cable that causes a heating and cooling of the cable. The heating and cooling along the cable depends in unsaturated media on the thermal conductivity of the cable-surrounding material. In turn thermal conductivity of unsaturated porous media depends on density and water content. Therefore, we will analyse the heating and cooling curves along the cable to determine the distribution of thermal conductivity, density, and water content along the cable. In passive mode (without heating the cable) the system is used for normal DTS.

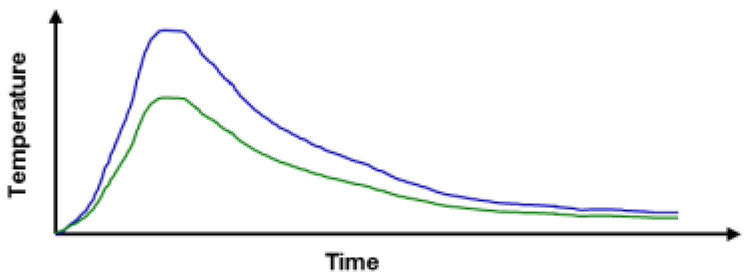

Figure 102: Examples for heating and cooling behaviour resulting from the same heat input, but for different thermal conductivities (Green = high thermal conductivity, blue = low thermal conductivity).

<u>DPTS</u>

Besides temperature, strain also has an effect on some scatter-signals in distributed fiber-optic sensing systems. Water pressure acting on an optic fiber causes strain in the fiber. Therefore, we want to develop a system that measures water pressure and temperature distribution along a fiber-optic cable in a borehole. The scatter signals caused by strain resulting from water pressure on the fiber will be calibrated to derive water pressure values.

Specifications:

<u>Active DTS</u>

Measuring range	Several km long cable
Accuracy	0.15°C, 0.02 W/(m · K), 0.05 t/m³, 5% water content
Spatial resolution	1m
Operation temperature	0 - 85°C
Life time	Decades for sensor

<u>Active DTS</u>

Technology Readiness Level (TRL)	Current	Planned
Basic and applied research (TRL : 1-4)	●	●
Development (TRL : 5-7)	●	●
Manufacturing (TRL : 8-9)	●	●

<u>DPTS</u>

Measuring range	800 bar, 150°C, 2 km depth
Accuracy	< 0.1bar; 0.5°C
Spatial resolution	0.1m
Operation temperature	0 – 150°C
Life time	Decades for sensor

<u>DPTS</u>

Technology Readiness Level (TRL)	Current	Planned
Basic and applied research (TRL : 1-4)	●	●
Development (TRL : 5-7)	●	●
Manufacturing (TRL : 8-9)	●	●

Development steps:

<u>Active DTS</u>

Step	Start time	Completion time
Feasibility study	July 2015	November 2015
Literature study and planning	November 2015	March 2016
Laboratory testing for calibration	April 2016	November 2017

Numerical modelling	November 2016	June 2017
Testing under realistic conditions (FE Experiment)	January 2017	October 2018

DPTS

Step	Start time	Completion time
Design phase for instrument improvement and cable design	July 2015	June 2016
Laboratory testing	July 2016	November 2017
Testing in boreholes	December 2017	October 2018

On field test or advanced test example:

Set up

The figures below show the exemplary set-up for field and laboratory installations.

Figure 103: Heatable fiber-optic cable installed in bentonite during feasibility study.

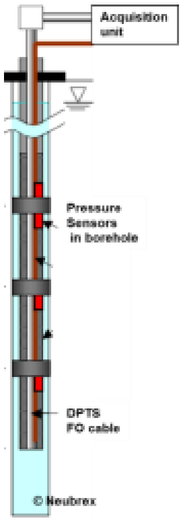

Figure 104: Schematic sketch of borehole instrumentation with fiber-optic cable and pressure sensors.

Existing alternatives to this technique:

<u>Active DTS</u>

- Electronic heat-pulse probes (point measurements) for thermal conductivity
- TDR sensors for water content

<u>DPTS</u>

- Piezoresisitive pressure transducers with analogue or digital output signal.
- Standard thermistors (e.g. PT100) for point temperature measurements.

Advantages

Both methods have the big advantage that no electronics are located at the sensors (fiber-optic cable) and are therefore very durable for long-term monitoring. In addition, the result is a continuous profile over hundreds of meters to kilometres instead of a point measurement.

Integrated Smart Cell Partners involved: CTU, TUL,....	MODERN 2020 Development and Demonstration of monitoring strategies and technologies for geological disposal

Rationale:

There is a quite big range of total pressure cells on the market. They usually come in 230mm diameter cylinder form with transducer attached via steel tube. Typical transducers used are vibrating wire (GeoKon), pneumatic (GLOTZL) or lately fibre optics. The CTU has developed and uses such pressure cells for civil engineering applications over 20 years now.

These cells have some disadvantages:

- They are usually bulky
- They measure only total pressure (and temperature)
- They have weak spot in connections between the cell and transducer (capillary tube)
- No in cell signal processing

The aim of is to develop cell integrated smart cell which will tackle those problems.

Description of the technology:

The proposed new cell is targeted especially (but not exclusively) for measurements in the EBS system.

The cell will have small compact design for localised measurements with electronics integrated into package. The target is to fit everything into package with diameter less than 100mm while maintaining the same precision and accuracy as big cells. The integration of transducer and electronics into cell package will eliminate one of the weak points of typical cells - the tube connecting the cell with transducer.

Although name implies total pressure cell it will integrate temperature and pore pressure sensor in the same package (RH humidity measurement is also an option to be easily added). This way the complete picture of EBS state can obtained at once with much lower demands on space, cabling and power.

From the electrical point of view the cell will be designed for low power operation.

Instead of vibrating wire transducers the piezoresistive sensors will be used (for both total pressure and pore pressure). Their big advantage is no drift, electrically simple interface, instant measurement and very low energy demands.

The aim is to completely process the signal from sensors inside the cell electronics and give the user digital output with no further processing required. This way the noise and other issues (e.g. parasitic capacitance) from analogue cabling will be eliminated and techniques such as oversampling can be employed to further increase precision. Moreover having smart sensors also enables to completely multiply possibilities of measurements and communication. The cell can take measurements as necessary (triggered by various events) and send the data as one package at later stage or raise immediate alarms.

An optional battery only operation will be also investigated. The aim is to be able take measurements, store them into local non-volatile memory as long as possible until the cell is retrieved or communication restored.

Objectives/Specifications:

Measuring range	0 - 20 MPa (customizable)
	-10 – 125°C
	0 – 100% RH (at max 80°C)
Response time	< 1s
Diameter	< 100 mm
Power supply	0, 7.0 – 16.0V
Operation temperature	0 - +85°C (125°C)
Life time	2-10 year (battery operation) >10 year (wired)

Indicate the progress expected in TRL

Technology Readiness Level (TRL)	Current	Planned
Basic and applied research (TRL : 1-4)		
Development (TRL : 5-7)		
Manufacturing (TRL : 8-9)		

Development steps:

Describe the planned steps to reach the desired objectives.

Step	Start time	Completion time
Design of cell body and manufacturing of prototype	June 2015	March 2016 (body) June 2016 (electronics)
Prototype testing	March 2016	February 2017
Revision of cell body	October 2016	June 2017
Test of revised design	May 2017	July 2018
Final design	January 2018	July 2018

Existing alternatives to this technique (if any):

- Traditional cells with:
  - Pneumatic measurement system
  - Vibrating wire sensor
  - Fiber optic sensor…

In combination with other sensors.

Advantages

Smaller size, integration of several sensors in one package, in sensor processing, digital interface, low power design, independent operation possible.

- Measurement of
  - Total pressure
  - Pore pressure
  - Relative Humidity (optional)
- Small size
- Integrated body
- Low power design
- Digital interface (RS485, SDI-12)
- Independent operation (optional battery operation)

Techniques for non-contact displacement measurement (ENEA)

Partners involved: ENEA

Rationale:

The sensor here proposed will provide accurate measurement of the canister displacement during its disposal using contactless techniques. There are several possible approaches that can in principle be suitable for the proposed problem. Yet, when dealing with the real implementation, some issues can arise. As a consequence, prior to proposing the final choice a study of feasibility should be done, aiming at investigating pros and cons of the proposed approach.

From the physical viewpoint, two kinds of carriers may be used: electromagnetic waves and acoustic waves. Even if some promising results already found in the literature about acoustic and ultrasonic techniques could be theoretically extended to the current problem, our first attempt will be devoted to the implementation of techniques using EM fields, in particular using the Ground Penetrating Radar technique

This approach may have many advantages when compared with other techniques based on contact sensors. Every element of our measurement chain can be located outside the disposal tunnel, instead of being buried inside the bentonite layer surrounding the canister. This setup provides the following advantages: (1) sensor long-term performance and reliability issues are less critical, (2) sensor maintenance relatively easier than other methods

Moreover, since our research will focus on low power GPR, we are going to investigate different sensor setup solutions (distance from target, antennas, etc.) in order to identify the minimum power requirements. Preliminary results suggest that, among all contactless displacement sensors, given a chosen target distance, resolution, system complexity, GPR could represent the best choice for a lowpower, low-distance monitoring.

Description of the technology:

Ground Penetrating Radar is a well-established technology, with applications such as geological investigation, landmine detection, cable and pipe location, etc. A monostatic GPR system is composed of a control unit, a power supply and an only antenna, which acts as a transmitter and receiver at the same time. In a bistatic GPR transmitting and receiving antennas are different and are located in different positions as viewed from the target. In both setups, an EM signal modulated in amplitude, frequency or phase, is injected into the bentonite layer (see Fig. 1 for an indicative, yet not exhaustive setup) where the target is buried. The backscattered signal from the target is then detected and processed.

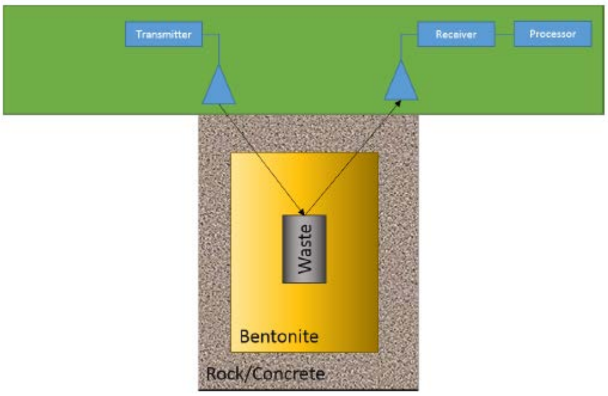

Figure 105: Indicative setup for the installation of the non-contact displacement measurement sensor

The signal undergoes various losses while propagating from the transmitter to the receiver. Path loss contributions include: antenna mismatch, mismatch loss at the interfaces between different materials (rock, concrete, bentonite, etc.), spreading losses, attenuation loss of the various materials and target scattering. Depending on the receiver noise figure and the minimum signal-to-noise ratio required by the chosen processing algorithm, different design

constraints and trade-offs need to be considered, including maximum target distance, minimum transmission power and type of antenna

Objectives/Specifications:

In the following table we report expected results based on preliminary evaluations.

Depth range	1-5 m
Carrier frequency	250-500 MHz
Depth resolution	0.04-0.15 m
Power supply	TBD
Life time	TBD

Indicate the progress expected in TRL

Technology Readiness Level (TRL)	Current	Planned
Basic and applied research (TRL : 1-4)		
Development (TRL : 5-7)	●	
Manufacturing (TRL : 8-9)		●

Development steps:

Describe the planned steps to reach the desired objectives.

Step	Start time	Completion time
Definition of a model using GPR technique for noncontact displacement measurement	1/7/2015	30/6/2016
Investigation of EM waves propagation in bentonite through computer simulations and comparison of simulation results with literature results	1/7/2016	31/12/2016
Development of an accurate wave propagation model taking into account possible source of interference expected in the repository (e.g., interferring materials, ionized medium, etc.)	1/1/2017	31/12/2017
Final results and conclusions	1/1/2018	End of the Project

On field test or advanced test

Set up

N.B: In the following possible complementary experimental activities not included in Modern2020 Project

- Design and setup of a basic sensor prototype to be tested in ENEA laboratory.
- Experimental investigation of wave propagation through bentonite and validation of the theoretical models.
- Development of customized data processing algorithms.
- Case study: application of the proposed sensor in a real deposit.
- Experimental activities addressing device long-term performance and reliability

Results

Based on our preliminary results using a simple, yet well-established model of EM waves propagation through a layered medium, where each layer is characterized by different electrical properties, the overall propagation loss has been computed as:

$$LT = Le + Lm + Lt1 + Lt2 + Ls + La + Lsc$$

where other effects, such as target scattering and spreading losses, were also taken into account. The following symbols have been used:

- □Le = Antenna efficiency loss in dB
- □Lm = Antenna mismatch losses in dB
- □$Lt1$ = Transmission loss from air to bentonite in dB
- □$Lt2$ = Transmission loss from bentonite to air in dB
- □Ls = Antenna spreading losses in dB
- □La = Attenuation loss of bentonite in dB
- Lsc = Canister scattering loss in dB

The electrical characterization of the materials of interest (e.g. bentonite and concrete) has been based on literature data. Preliminary theoretical results are consistent with various experimental investigations (Cook, 1975)

Existing alternatives to this technique

- Buried displacement sensor
- Acoustic imaging of buried objects
- Ultrasonic contactless techniques

Advantages

- No need for moving parts
- The entire sensor chain can be accessed from outside
- No buried elements
- Greater depth of penetration and resolution when compared with acoustic and ultrasonic techniques

Chemical sensors Partners involved: VTT	MODERN 2020 Development and Demonstration of monitoring strategies and technologies for geological disposal

Rationale:

Many safety relevant functions required for the compacted bentonite buffer in the final disposal of spent fuel rely on processes influenced by chemical composition of the pore water in bentonite. Important safety relevant processes are, inter alia, swelling, alteration, precipitation and dissolution reactions, transport of water colloids and ions, as well as corrosion of canister.

The bentonite consists mainly of montmorillonite, smaller amounts of accessory minerals and pore water. The pore water can be divided into interlamellar water (IL-water) and non-IL water (Pusch, 1999; Muurinen et al. 2007; Homboe et al., 2012; Fernandez et al., 2004; Wersin, 2003; Bradbury and Baeyens, 2002). The compositions of the two types of pore water vary due to the negatively charged surfaces in montmorillonite. IL-water layers of less than a few nano meters consist of cations only, whereas in larger non-IL water volumes cations and anions are present in varying amounts, depending on the distance from the negatively charged clay surfaces (Van Loon et al., 2007; Muurinen and Carlsson, 2013; Tournassat and Appelo, 2011). (Figure 1.)

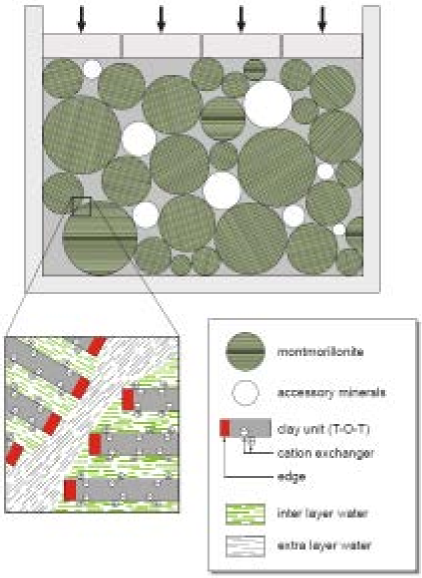

Figure 106. Generalized microstructure of (MX-80) bentonite (wersin, 2003). Extra layer water as non-IL water.

Activity, the effective concentration of a species in solution, should be used in non-ideal solution due the interactions of ions between each other. Ion activity depends on the surrounding conditions, such as temperature, pressure, ionic strength, ion composition, etc… When these variables change also the ion activity of different species will change in solution. (Appelo and Postma, 1994)

The majority of experimental data on the composition of compacted bentonite is based on batch experiments by leaching or using squeezing methods to collect pore water. In these methods pore water is removed from its initial surrounding and analyzed. Because, dissolution of accessory minerals, cation exchange reactions, mixing of different pore water types and interaction of charged surfaces, will cause changes in the ion activities, some uncertainties lay over these methods. Geochemical modelling has also been used to study composition of the pore water, but the uncertainties related in the data obtained experimentally will follow in modelling as well. However, much has been learnt during years and the pore water composition of bentonite can be evaluated, if not strictly quantitatively, at least semi-quantitatively by combining results of different studies (Curti 1993, Ohe & Tsukomoto 1997, Muurinen & Lehikoinen 1999, Bruno et al. 1999, Bradbury & Baeyens 2003, Fernandez et al. 2004).

Direct measurement of ion activities in pore water of compacted bentonite are exceedingly difficult to perform because of the huge swelling pressure, which most of the sensors cannot withstand, also the low amount of the free water available for the sensors is a hindrance. VTT has succeeded earlier to develop a methodology for measuring pH and Eh in compacted bentonite. The aim of this study is to broaden the method in measuring safety relevant ion activities in the pore water of compacted bentonite.

Description of the technology:

The ion selective electrodes used in this study are based on measurement of potential difference between an ion selective electrode and a reference electrode. In an ideal situation the reference electrode is independent of the solution composition and the membrane of the ion selective electrode will be selective only for one species. The reference electrode will give constant potential and the potential of the ion selective electrode will change with changing ion activity according to Nernst equation (1). Where, E is the measured potential, E0 the constant value measured according to arrangement, R is the gas constant, T is absolute temperature, z is the charge of the ion, F is the Faraday constant and a is the activity of the ion in the solution (Janata, 2009).

$$E = E_0 + \frac{RT}{zF} \log a \qquad (1)$$

Measurement is performed by placing pre-calibrated ion-selective electrodes in the holes bored in the compacted bentonite samples. Bentonite is then slightly compacted in order to obtain a good contact between bentonite and the electrode. The potential difference between the ion-selective electrode and an external reference electrode is measured by a voltmeter. The reference electrode is in contact via the solution with bentonite (Figure 2.). At the end of the measurement the ion-selective electrode and the reference electrode are calibrated again. The ion activity is calculated according to the calibration curve obtained.

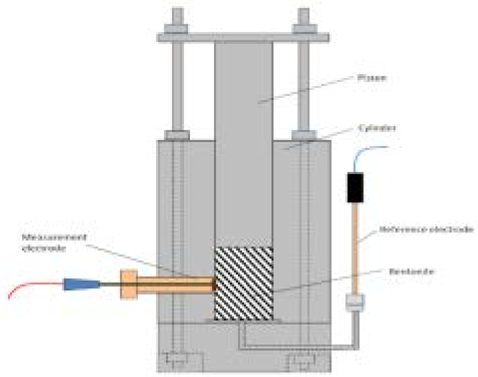

Figure 107. Schematic presentation of the test bench for ion-selective electrode batch testing. (Muurinen and Järvinen, 2013)

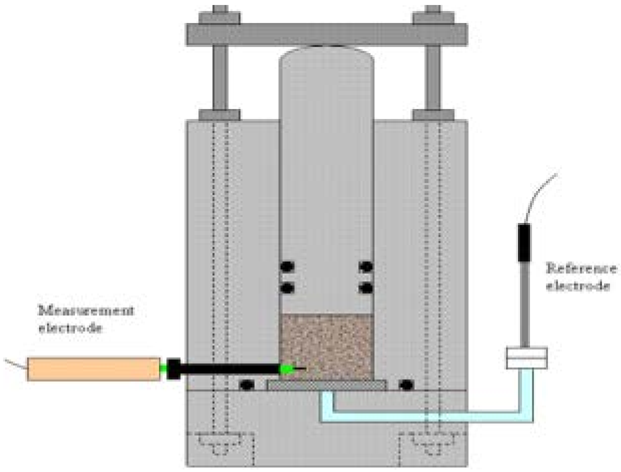

At the beginning of this research commercial mini ion-selective electrodes from Nico2000 and reference electrodes from Innovative Instruments will be tested in a test bench.

Objectives/Specifications:

In the first test series determination of Cl^-, Na^+ and Ca^{2+} ions activities in Na- and Ca-montmorillonites and MX-80 bentonite will be tested.

1. Selectivities: Cl^-, Na^+ and Ca^{2+}
2. Stability of the electrodes: at least 2 weeks
3. Measuring range: 0.01-1M
4. Accuracy: 0.01

ndicate the progress expected in TRL

The aim of this research is to develop a measuring system for determining the activities of the main species in compacted bentonite. The technology readiness level 8-9 (manufacturing) stands for research readiness to study the ion activities in compacted bentonite.

Technology Readiness Level (TRL)	Current	Planned
Basic and applied research (TRL : 1-4)	●	●
Development (TRL : 5-7)	●	●
Manufacturing (TRL : 8-9)	●	●

Development steps:

Modification of electrodes: Structure of the electrodes will be modified to better stand mechanical stress, and able to testing devices.

Batch experiments: Working of ion-selective electrodes will be tested by measuring ion-activities in simplified samples. The ISE's will be assembled in compacted clay samples which are saturated with solution with known concentration of measured ions and potential will be measured against reference electrode during a few weeks. Na- and Ca-montmorillonite and MX-80 bentonite will be used in tests.

Long-term diffusion experiments: The ISE's observed to working correctly in batch experiments will be used in diffusion experiments. ISE's will be assembled in different type fully saturated compacted clay samples. Saturation water composition will be changed and the changes in activities will be followed by ion-selective electrodes.

Describe the planned steps to reach the desired objectives.

Step	Start time	Completion time
Modification of electrodes	September 2015	March 2016
Batch experiments	March 2016	January 2017
Long-term diffusion experiments	December 2016	December 2018

Results

The following steps have been done so far:

1. The structure of the ion-selective electrodes has been modified (Figure 108)
2. Purified materials (Na- and Ca-montmorillonite) are prepared and saturation of compacted samples has been started to make batch experiments possible.
3. First round of calibrations has been performed (Figure 109)

 **Figure 108. Modified Na^+-selective electrode**	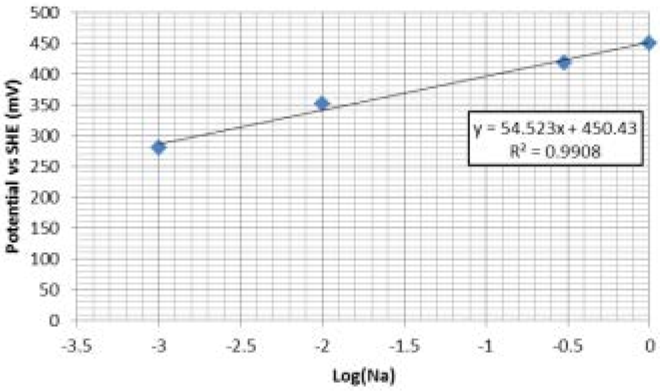 **Figure 109. Calibration curve from the first series of calibrations.**

Existing alternatives to this technique

- Squeezing technique
- Leaching technique
- Geochemical modelling

Advantages

Ion activities can be measured directly from the compacted bentonite under predominant conditions.

Improvement of seismic full waveform inversion technologies

Partners involved: ETH

Rationale:

Seismic measurements have a potential to non-intrusively monitor changes occurring within radioactive waste repositories. The work carried out in MoDeRn regarding the seismic full waveform inversion (FWI) has highlighted that there is still a great margin of improvement for this technique. Particularly an optimal set of parameters for anisotropic FWI needs to be identified. Additionally development of differential inversion will allow identification and imaging of subtle temporal changes of the elastic properties. Finally, this methodology needs to be applied to the real data set for which development of suitable pre-processing strategies will be needed.

Description of the technology:

To non-intrusively characterise elastic properties of the subsurface seismic signal is generated at a safe distance from the repository. The generated elastic waves propagate through the repository and are recorded by seismic acquisition system. Due to interaction between seismic waves and the repository the recorded seismograms are influenced by the physical state of the repository. In seismic FWI a starting subsurface model is chosen and used to generate synthetic seismograms for the same experimental configuration. As a next step the misfit between experimentally recorded and numerically calculated seismograms are calculated. Finally, by taking into account sensitivities of the calculated data to each model parameters, the subsurface model is updated in the direction to minimize the data misfit. Due to the nonlinearity of the inverse problem several iterations of model updates are performed until the misfit between the recorded and calculated data is sufficiently small.

Objectives/Specifications:

Measuring range	10’s of meters
Accuracy	< 1%
Response time	< 1s
Repeatability	Site dependent (see Marelli et al., 2010)
Power supply	12 V and 220 V
Operation temperature	-40 - 260°C for geophones 0 - 100°C for sparker source and hydrophones
Life time	Replaceable

Technology Readiness Level (TRL)	Current	Planned
Basic and applied research (TRL : 1-4)		
Development (TRL : 5-7)	●	
Manufacturing (TRL : 8-9)		●

On field test or advanced test example:

Set up

Seismic experiments performed within ESDRED project aimed to monitor changes occurring to a one meter diameter microtunnel due to water saturation and pressurisation. For that purpose two boreholes were drilled perpendicular to the microtunnel. Seismic signal was generated with a sparker source in the lower borehole and was detected with a hydrophone streamer in the upper borehole and with eight vertical component geophones planted around the interior wall of the microtunnel at roughly equal distances (Figure 110 a).

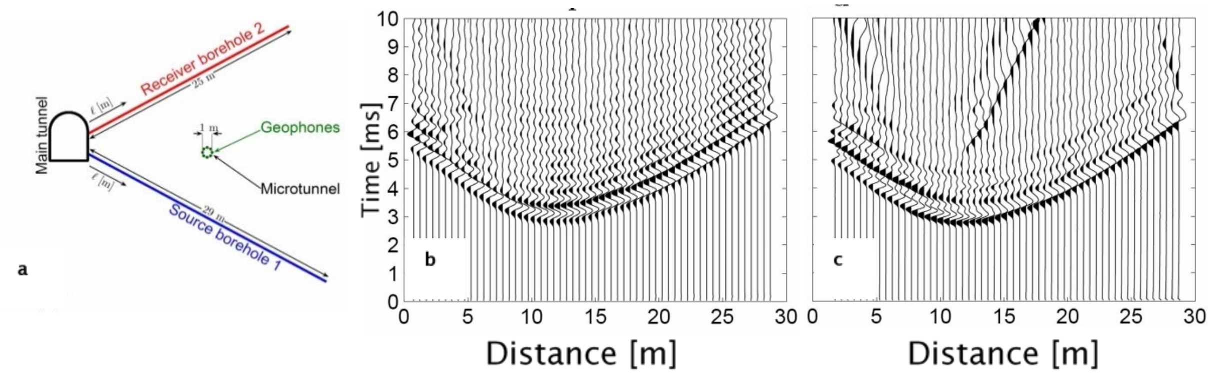

Figure 110: (a) Experimental setup of seismic experiments performed at Mont Terri rock laboratory. Seismograms of a single geophone and all sources for (b) microtunnel filled with dry sand and (c) microtunnel filled with water saturated sand.

Results

Field experiments showed that seismograms recorded by the geophones change significantly due to the water saturation of the microtunnel (Figure 110 b and c). However, due to variable hydrophone coupling between experiments, anisotropic waveform inversion is required to assess the feasibility of radioactive waste repository monitoring with cross-hole source receiver configuration.

Existing alternatives to this technique:

- Earth resistivity tomography (ERT) and induced polarity tomography (IPT)
- FWI of ground penetrating radar (GPR)

Advantages

Compared to ERT and IPT, seismic FWI is not sensitive to metallic object in the subsurface and hence can properly function also with the presence of the waste canisters. Nevertheless ERT and IPT are also investigated within the scope of MODETN2020. Compared to GPR seismic waves can propagate long distances in clayey environment which is the host for radioactive waste in many countries.

References:

Marelli, S., E. Manukyan, H. Maurer, S.A. Greenhalgh and A.G. Green, 2010, Appraisal of waveform repeatability and reliability for crosshole and hole-to-tunnel seismic monitoring of radioactive waste repositories. Geophysics 75, Q21- Q34.

Anomaly detection algorithms

Partners involved: ETH

Rationale:

The interpretation of the geophysical data is a sophisticated task requiring a deep knowledge in both geophysical and mathematical theory. To extract a full model of subsurface from acquired data always requires sophisticated software with a lot of numerical computing as well as a highly qualified geophysical specialist. Our approach is dedicated to a few special cases in geophysical research, when the subsurface model is already known and the aim of geophysical measurement is to detect any temporal changes in subsurface or to detect an appearance of predefined anomaly. Such a concept allows to run the detection in automated or semi-automated mode with no or limited human interaction. Described concept fits to the monitoring for geological disposal. Our anomaly detection algorithm will be developed as a supplementary technology to the full inversion techniques developed by our partners.

Description of the technology:

Proposed technology is a software working on in the field acquired geophysical data. The principal idea of the algorithm is depicted in the Figure 111. The algorithm can work, if at the beginning an *anomaly* or *set of anomalies* to be detected in the data. First step requires to define typical appearance of the anomaly in the data. Because the computer vision technology is later used to detect structures in the data, the typical appearance means to detect typical shapes in data vectors or matrices. When this anomaly appearance is done, the data can be processed: sampled to a set of black and white images, where typical structures can be recognized.

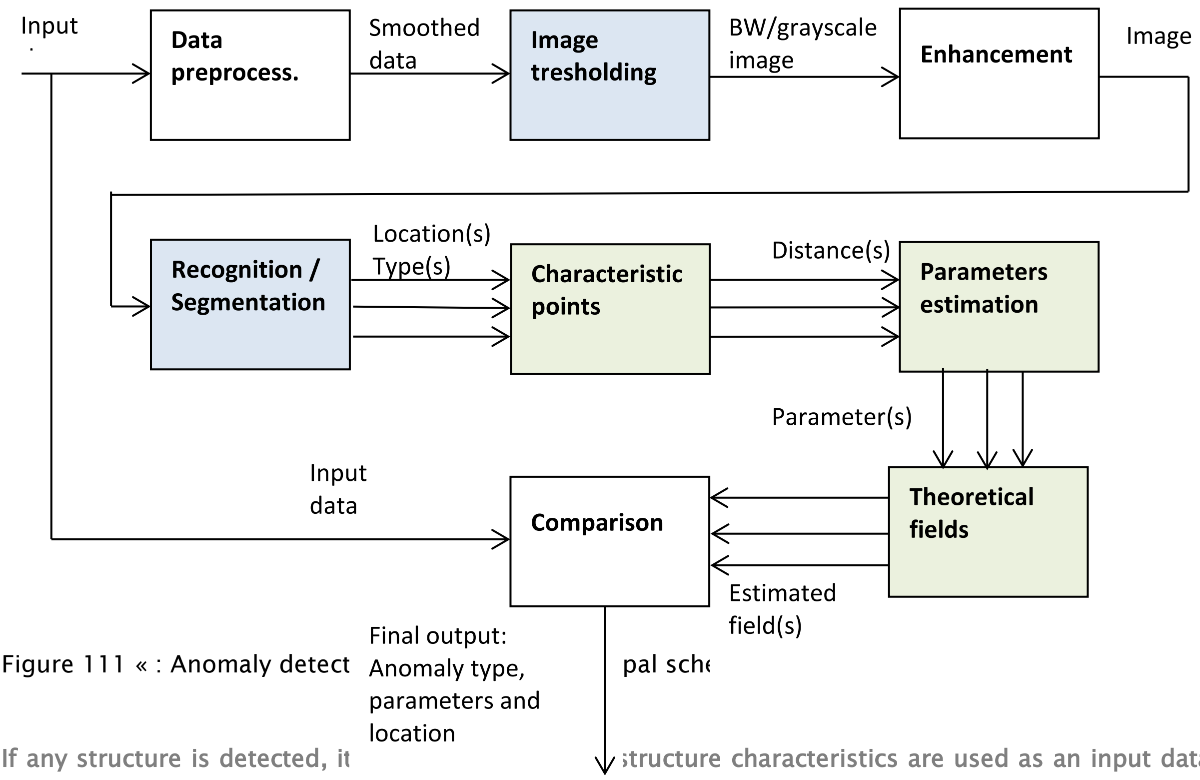

Figure 111 « : Anomaly detect pal sche

If any structure is detected, it structure characteristics are used as an input data for a module computing synthetic data with such an anomaly. Synthetic data are compared with the field data and if the data similarity reaches preselected threshold, the field data are marked as containing the anomaly with defined parameters.

As it was mentioned in the initial summary, the algorithm is being designed to run in automated or semi-automated mode. According to the geology disposal monitoring, an “anomaly” to be detected can be any unwanted configuration of the disposal regarding the temperature, water saturation or any other disposal condition. The algorithm than can be used to detect such a temporal modification in the disposal. For example, we can model several water saturations in the disposal, extract its data characteristics and train the algorithm to detect such anomalies. This way the algorithm could be used as an automated watchdog for time series data during the disposal monitoring.

Objectives/Specifications:

The algorithm should be able to detect predefined anomalies in the data. The final fully working algorithm is to be implemented in Java to be platform independent software.

Technology Readiness Level (TRL)	Current	Planned
Basic and applied research (TRL : 1-4)	🔴	⚫
Development (TRL : 5-7)	⚫	🔴
Manufacturing (TRL : 8-9)	⚫	⚫

Development steps:

Step	Start time	Completion time

Algorithm working in Matlab environment	September 2015	November 2017
Fully working algorithm implementation	May 2016	September 2018

Existing alternatives to this technique:

One option are standard geophysical inversion methods with an advantage of more general application but a need of manual evaluation. Another option are contact sensors producing temporal evolution data, but representing an invasive solution contrary to the geophysics.

Advantages

The algorithm can be a fast, sharply fitted part of the disposal monitoring.

Combined ERT/IPT imaging of 3D/4D water saturation in the buffer-backfill-bedrock systems

MODERN 2020

Development and Demonstration of monitoring strategies and technologies for geological disposal

Partners involved: USTRAT

With the combined, tomographic electrical resistivity and induced polarization (ERT/IPT) imaging it is possible to monitor more uniquely geotechnical, geochemical and hydrological behaviour/processes and integrity of the in the canister-buffer-bedrock system volumes. The ERT and IPT can be measured simultaneously and the results complement each other. Inverted 3D resistivity and IP-parameter distributions are sensitive but in different ways to spatial and time-lapse changes in key parameters: water content, porosity, salinity and surface conduction (i.e. electrical properties of mineral surfaces).

Description of the technology:

Time-lapse, tomographic, non-destructive ERT/IPT measurements are carried out using 3D electrode chains embedded into the boreholes, bentonite-crystalline rock interfaces, tunnel floors, rock-buffer-backfill materials etc. Surveying is conducted by measuring the voltages (as a function of frequency) on a pair of metal (stainless steel or copper) electrodes in direct contact with the medium while low-frequency electrical current is passed on an adjacent pair of electrodes. The measured voltages are affected by the electrical properties of the medium and reflect an average resistivities (as a function of frequency) from half a sphere around the electrodes a sphere around the electrodes. Then the current electrode pair is changed and the cycle of voltage measurement is repeated. In order to calculate the resistivity at the exact location of the measurement, the resistances (as a function of frequency) need to be inverted to a system resistivity model. An inversion procedure is then used to calculate the electrical properties needed to match the resistance measurements (i.e. the 3D resistivity distributions and the temporal (4D) changes between different 3D distributions). These result properties are then those that are affected by the moisture content (or degree of saturation), pore water ionic strength, and material type.

Indicate the progress expected in TRL

Technology Readiness Level (TRL)	Current	Planned
Basic and applied research (TRL : 1-4)		
Development (TRL : 5-7)		
Manufacturing (TRL : 8-9)		

Development steps:

1) Development of optimal numerical conceptualization, monitoring protocol and inversion processes for the combined ERT/IPT in the canister-buffer-bedrock system (this subtask will include the comparisons of different alternatives and options for conceptualizations as well as development of monitoring protocols and inversion processes for the combined ERT/IPT in the canister-buffer-bedrock system)

2) Development of 3D/4D ERT/IPT inversion process with possibility to include thermo-hydro-chemical (THC) constraints (information from point-sensor time-series, from petrophysical dependences as well as from dynamic THC behaviour/knowhow. These constraints include petrophysical and THC constraints (the dependences between resistivities, IP-parameters, water-contents, electrolytes and temperatures in the buffer-backfill-bedrock environment will be obtained from laboratory tests and theoretical knowhow

as well as from the thermo-hydro-chemical modelling considerations that can explain temporal and spatial dependences between water-content, electrolyte and temperature changes in the canister-buffer-backfill-bedrock systems)

3) Reporting

Results (so far)

Optimal numerical conceptualizations, monitoring protocols and inversion processes for the combined ERT/IPT in the canister-buffer-bedrock system have been developed (figure)

The experimental knowhow (from laboratory tests and theoretical knowhow) on dependences between resistivities, IP-parameters, water-contents, electrolytes and temperatures in the buffer-backfill-bedrock is possible to embed as constraints into the 3d/4D inversion framework

Example Sketches for the Electrode Coverage